Membrane cleaning: cleaning-in-place of a microfiltration membrane fouled during yeast harvesting

Shorrock, Chris

Award date:
1999

Awarding institution:
University of Bath

Membrane Cleaning: Cleaning-in-Place of a Microfiltration Membrane Fouled During Yeast Harvesting

Submitted by Chris Shorrock
for the degree of PhD
of the University of Bath
1999

ProQuest LLC
789 East Eisenhower Parkway
P.O. Box 1346
Ann Arbor, MI 48106-1346

Declaration

The following dissertation describes experimental research carried out between October 1994 and October 1997 at the University of Bath, Department of Chemical Engineering. The work presented is entirely the authors own original work except where stated otherwise in this text. Neither the present dissertation, nor any part thereof, has been submitted at any other university.

Signed: _____ C. J. Shorrock (candidate)

Date: 25/6/99.

Signed: _____ Dr. M.R. Bird (supervisor)

Date: 25/6/99

This thesis may be made available for consultation within the university library and may be photocopied or lent to other libraries for the purposes of consultation.

Signed: _____ C. J. Shorrock (candidate)

Acknowledgements

During the course of my studies, I have been fortunate to have mixed with some extremely knowledgeable and talented people. I would like to take this opportunity to gratefully acknowledge their contribution to my professional and personal development.

Of the many people who have in some way contributed to the production of this thesis, two in particular stand out as being the most influential. Firstly, my daily supervisor, Dr. Michael Bird who provided great motivation, enthusiasm and insight on a day-to-day basis. Secondly, Professor John Howell who, despite his busy schedule, always had time to answer my questions or offer his advice.

On a practical note, my thanks are extended to the Technical Support team, led by Mac Forsyth. Thanks Merv, Tony, Robert, Fernando, Suzanne, Ann and Richard. Your humour, help and advice are much appreciated. Thanks are also due to Les Steele and colleagues in the workshop for construction of the membrane modules and numerous other jobs, for which they always managed to find time. Thanks also to Ursula Potter and Hugh Perrera, in the Electron Optics Department, for SEM training, negative developing and help with the cryogenic microscopy work.

I would also like to thank those researchers and lecturers at the University of Bath who were kind enough to offer their assistance in areas of their own expertise or just an educated opinion.

Last, but not least, the financial support of the BBSRC and the loan of equipment from Wessex Water are gratefully acknowledged, without which this project would not have started.

Summary

This thesis contributes novel experimental research to the relatively under-developed science of chemical membrane cleaning.

Cleaning strategies have been evaluated for the removal of deposits from a microfiltration membrane fouled during yeast cell harvesting. The membrane used was a flat sheet of hydrophilic polyethersulphone with a nominal pore size of 0.1 μm (Gelman Sciences, *Supor 100*). Bakers yeast was selected as a model micro-organism. During microfiltration, a constant transmembrane pressure of 2 bar, cross-flow velocity of 1 m s^{-1} and suspension temperature of 34°C produced a steady state flux within ninety minutes. Rinsing with water removed the majority of the cellular cake revealing a tenacious non-cellular matrix and cellular deposits. Following unsuccessful attempts to restore membrane permeability by rinsing, chemically-enhanced cleaning of the rinsed deposit was investigated using dilute solutions of sodium hydroxide, nitric acid and *P3 Ultrasil 11*. Cleaning temperature effects were investigated over the range 30°C to 60°C and laminar and turbulent flow regimes were compared. A combination of water flux recovery, microscopic visualisation and X-ray diffraction was used to assess cleaning efficiency.

Two methods of restoring the clean membrane permeability were found for this system. Firstly, two-stage cleaning was achieved with sequential alkali and acid treatments; the order of application being of prime importance. Secondly, single-stage cleaning was achieved using the formulated detergent *P3 Ultrasil 11*.

With respect to cleaning, the deposit was characterised as part organic and part inorganic. Modelled removal rates were based on the assumption that resistance removal of the two species deposit was simultaneous and independent. The removal of the organic species being much faster than the inorganic. The rate expressions that best described the removal of deposit resistance were first order for both species.

Results have confirmed many earlier discoveries when cleaning surfaces fouled with food products and have important consequences for industry. It is hoped that the results will be accepted by industry leading to more economical and environmentally friendly cleaning protocols.

Contents

CHAPTER 1 - INTRODUCTION 1

1.1 THE CLEANING CHALLENGE 2

1.2 MEMBRANE SEPARATION INDUSTRY 4

1.2.1 Membrane Cleaning 5

1.3 AIMS AND SCOPE OF THIS STUDY 6

1.4 THESIS STRUCTURE 6

CHAPTER 2 - YEAST-FOULED MEMBRANE CLEANING 9

2.1 BIOSEPARATION 10

2.1.1 The Yeasts 10

1.1.2 Separation Techniques 13

1.1.2.1 Sedimentation 13

1.1.1.2 Centrifugation 14

1.1.1.3 Phase Partitioning 14

1.1.1.4 Ultrasound 15

1.1.1.5 Hydrocyclones 15

1.1.1.6 Cross-flow Membrane Separation 15

1.2 MEMBRANE SEPARATION PROCESSES 16

1.2.1 Classification 16

1.2.2 Pressure-Driven Processes 17

1.2.3 Membrane Modules 18

1.2.3.1 Flat Sheet Modules 19

1.2.3.2 Spiral Wound Modules 19

1.2.3.3 Hollow Fibre Modules 19

1.2.3.4 Tubular Modules 19

1.2.4 Microfiltration 20

1.2.4.1 Cross-flow 20

1.2.4.2 Applications 20

1.2.4.3 Membrane Characterisation and Preparation 21

1.1.1.4 General Flux Equation 24

1.3 FOULING PHENOMENA 26

1.3.1 Concentration Polarisation 26

1.1.2 Mechanisms of Back-Transport 27

1.1.1.1 Common Basis 27

1.1.1.2 Brownian Diffusion 28

1.1.1.3 Shear-Induced Diffusion 28

1.1.1.4 Inertial Lift 29

1.1.3 Fouling Implications on the MF Design Equation 29

1.1.4 Reversible Fouling 30

1.1.5 Irreversible Fouling *30*
1.1.5.1 Pore Blinding 30
1.1.5.2 Adhesion and Adsorption 30
1.1.6 Effect of Fouling on Transmission and Selectivity *35*
1.1.7 Analysis of Fouling Curves *35*
1.1.8 Flux Modelling *36*
1.1.9 Fouling Prevention *37*
1.1.9.1 Critical Flux 37
1.1.9.2 Membrane Selection 37
1.1.9.3 Pretreatment 38
1.4 CLEANING: REMOVAL OF FOULING DEPOSITS 39
1.4.1 Definition of Membrane Cleaning *39*
1.4.2 Hydraulic Cleaning *39*
1.4.2.1 Back Flushing 40
1.4.2.2 Cross Flushing 40
1.4.2.3 Rotating Disk Membrane Modules 40
1.4.2.4 Secondary Vortex Flows 41
1.4.3 Mechanical Cleaning *41*
1.4.4 Electrical Cleaning *41*
1.4.5 Chemical Cleaning *42*
1.4.6 Measurement of Cleaning Efficiency *42*
1.4.6.1 Flux Recovery 43
1.1.1.2 In situ. Surface Visualisation 43
1.1.1.3 Ex situ. surface visualisation 43
1.5 CHEMICAL MEMBRANE CLEANING 44
1.5.1 Detergents: Definition and Properties *44*
1.5.1.1 Alkalis 45
1.5.1.2 Acids 45
1.5.1.3 Surface Active Agents 46
1.5.1.4 Sequestrants 46
1.5.1.5 Enzymes 47
1.5.1.6 Disinfectants 47
1.5.2 Rinsing *48*
1.5.3 Cleaning Reactions *48*
1.5.4 Industrial Chemical Cleaning *50*
1.5.4.1 Cleaning Out-of-Place (COP) 50
1.5.4.2 Cleaning In-Place (CIP) 50
1.5.5 Characterisation of the Fouling Layer *50*
1.5.6 Yeast-Fouled Membrane Cleaning Examples *51*
1.5.7 Protein Cleaning *53*

CHAPTER 3 - MATERIALS AND METHODS 55

3.1 MATERIALS 56
3.1.1 Experimental Apparatus *56*
3.1.1.1 Membrane Module 59
3.1.1.2 Permeate Flow Measurement 60
1.1.1.3 Feed Flow Meter 61
1.1.1.4 Temperature Control 61
1.1.1.5 Transmembrane Pressure 62
1.1.1.6 Experimental Data Collection 62
1.1.1.7 Materials of Construction 63
1.1.2 Membrane Selection *63*
1.1.3 Water *64*
1.1.4 Yeast Suspension *65*
1.1.5 Chemical Cleaning Agents *66*
1.1.5.1 Sodium Hydroxide 66
1.1.5.2 Nitric Acid 66
1.1.5.3 P3 Ultrasil 11 66
1.1.5.4 Terg-A-Zyme 67
1.2 METHODS 68
1.2.1 Membrane Conditioning *68*
1.2.2 Clean Water Flux *69*
1.2.3 Membrane Fouling *69*
1.2.3.1 Effect of Yeast Concentration 69
1.2.3.2 Effect of Transmembrane Pressure 71
1.2.3.3 Effect of Salt Presence 72
1.2.4 System Flushing and Membrane Rinsing *73*
1.2.5 Membrane Cleaning *74*
1.2.6 Waste Disposal *75*
1.2.7 Yeast Culture *75*
1.2.8 Deposit Visualisation Techniques *76*
1.2.8.1 Scanning Electron Microscopy 76
1.2.8.2 Transparent Membrane Module 76
1.2.9 Titration *76*
1.2.10 Light Microscopy *77*
1.2.10.1 Cell Counts 77
1.2.10.2 Differential Staining of Viable and Non-viable Cells 77

CHAPTER 4 - RESULTS AND DISCUSSION 79

4.1 FOULING ANALYSIS 80
4.1.1 Experimental Flux Decline and Fouling Resistance *80*
4.1.2 Theoretical Fouling Mechanism *81*
1.1.3 Estimation of Cell Deposition *84*
1.1.4 Visualisation *86*

1.1.5 Fouling Summary *87*
1.2 RINSING 88
1.2.1 Fouling Resistance *88*
1.2.2 Visualisation *88*
1.1.3 Composition of Surface Deposit *89*
1.1.1.1 Fourier Transform InfraRed Microscopy 89
1.1.4 Rinsing Summary *90*
1.3 MEMBRANE CLEANING 92
1.3.1 Water Cleaning *92*
1.3.1.1 Effect of Temperature 92
1.3.1.2 Effect of Shear Stress 93
1.3.2 Sodium Hydroxide Cleaning *94*
1.3.2.1 Effect of Concentration 94
1.3.2.2 Effect of Temperature 96
1.3.2.3 Effect of Cross-flow Velocity 96
1.3.2.4 Effect of Time 97
1.3.2.5 Residual Deposit Appearance and Composition 97
1.3.2.6 Effect of Salt Presence on Sodium Hydroxide Cleaning 98
1.3.3 Nitric Acid Cleaning *98*
1.3.4 P3 Ultrasil 11 Cleaning *100*
1.3.4.1 Effect of Concentration 101
1.3.4.2 Effect of Temperature 102
1.3.4.3 Sodium hydroxide, Surfactant and EDTA Contributions 103
1.3.5 Terg-A-Zyme Cleaning *104*
1.3.6 Chemical Cleaning Summary *105*

CHAPTER 5 - MATHEMATICAL MODELLING 106

5.1 CLEANING MODELS: A REVIEW 107
5.1.1 Introduction *107*
5.1.2 Simple Models *108*
5.1.2.1 Zero order in deposit amount 108
5.1.2.2 First Order kinetics 109
5.1.2.3 Two Species Removal 109
5.1.3 Mechanistic Models *110*
5.1.3.1 Gallot-Lavallée and Lalande [1985] 110
5.1.3.2 Bird [1993] 111
5.1.3.3 Bird and Bartlett [1997] 112
1.1.4 Factors Affecting the removal rate constant k *114*
1.2 MODEL SELECTION AND APPLICATION 115
1.2.1 Two Species: Simultaneous First Order Removal *116*
1.2.2 Mathematical Derivation *116*
1.1.3 Initial Fouling Resistance *117*

1.1.4 Results & Discussion *118*
1.1.4.1 Comparison of Model to Experimental 118
1.1.4.2 Removal Rate Constants k_1 and k_2 126
1.1.4.3 Activation Energies 127

CHAPTER 6 - CONCLUSIONS AND FUTURE WORK 131

6.1 CONCLUSIONS 132
6.1.1 Experimental Apparatus and Cleaning Measurement Technique *132*
6.1.2 Fouling *132*
6.1.3 Cleaning Strategies *132*
6.1.4 Mathematical Modelling of the Cleaning Process *133*
6.2 FUTURE WORK 134
6.2.1 Fouling *134*
6.2.2 Multiple Fouling and Cleaning Cycles *134*
6.2.3 Development of Analytical Techniques *134*
6.2.4 Modelling Techniques *134*

CHAPTER 7 - REFERENCES 136

APPENDIX A - SUPOR 100 PROPERTIES 144

A.I CHEMICAL RESISTANCE (HENKEL-ECOLAB LTD SALES BROCHURE, 1997) 144

APPENDIX B - PHYSICAL AND CHEMICAL PROPERTIES 146

B.I YEAST SIZE DISTRIBUTION 146
B.II WATER VISCOSITY V TEMPERATURE 146

APPENDIX C - CALIBRATION CURVES 147

C.I PERMEATE FLOW METER 147
C.II PRESSURE TRANSDUCERS 147
C.III SPECTROPHOTOMETER CELL COUNTS 149

APPENDIX D - EXPERIMENTAL DESIGN 150

D.I EXPERIMENTAL PROCEDURES 150

APPENDIX E - NOMENCLATURE 155

E.I LATIN SYMBOLS 155
E.II GREEK SYMBOLS 155
E.III SUBSCRIPTS 156
E.IV ABBREVIATIONS 156

APPENDIX F - PUBLICATIONS 158

F.I Refereed Journal Papers and Conference Proceedings 158
F.II Non-Refereed Conference Proceedings 158
F.III Other Presentations 158

List of Figures

Figure 2-1: Cross-section through a typical yeast cell showing the main features of the cell and their distribution (reproduced from Berry [1982]).... 11

Figure 2-2: The yeast cell surface (reproduced from Schekman and Novick [1983]). (G) Glucan; (M) Mannoprotein; (PE) periplasmic enzymes; (PM) plasma membrane; (IP) integral membrane protein; (PP) peripheral membrane protein.... 12

Figure 2-3: Classification of membrane separation processes with respect to driving force.... 16

Figure 2-4: Schematic illustration of pressure-driven membrane separation principle. P1, P2 and P3 represent the feed, retentate and permeate pressures, respectively.... 17

Figure 2-5: Classification of pressure-driven process with respect to pore size.... 22

Figure 2-6: Balance of interfacial tensions for a drop of liquid on a flat surface in the presence of vapour.... 23

Figure 2-7: Schematic diagrams of yeast interaction with surfaces. The electrical double layer at a planar surface and around a spherical particle (a) and (b) polymer aspects (reproduced from Norde [1981]).... 33

Figure 3-1: Schematic representation of the purpose-built fouling, rinsing and cleaning apparatus.... 56

Figure 3-2: Front view photograph of the experimental fouling, rinsing and cleaning apparatus.... 57

Figure 3-3: Side view photograph of the experimental fouling, rinsing and cleaning apparatus.... 58

Figure 3-4: Photograph of the experimental flat sheet microfiltration module.... 59

Figure 3-5: Gelman Supor 100 microfiltration membrane top surface and bulk appearance.... 64

Figure 3-6: SEM showing the yeast cells before filtration. Budding and bud scars can be seen.... 65

Figure 3-7: CFMF of 0.25, 1.00 and 4.00 wt% isotonic yeast suspensions at the same standard fouling conditions. Note that the percentages quoted in the legend refer to the percentage water flux recovery after standard rinsing conditions.... 70

Figure 3-8: Filtration of 1 wt% isotonic yeast at a steady state transmembrane pressure of 0.75, 1.40 and 1.95 bar. Standard fouling temperature and cross-flow velocity. Note that the percentages quoted in the legend refer to the measured flux recovery after rinsing.... 71

Figure 3-9: Transmembrane pressure during fouling of 1 wt% isotonic yeast suspension.... 72

Figure 3-10: Filtration of water, salt solution (8.5g NaCl per litre of RO water), non-isotonic yeast and isotonic yeast. Hydrodynamic conditions are the same as those for fouling. 73

Figure 4-1: Permeate flux J and fouling resistance R_f versus filtration time during CFMF of the standard isotonic yeast suspension. 80

Figure 4-2: Comparison of theoretical fouling mechanism models to experimental data from 0 to 15 minutes 82

Figure 4-3: Comparison of theoretical fouling mechanism models to experimental data from 15 to 90 minutes 82

Figure 4-4: Comparison of theoretical fouling mechanism models to experimental data during the period 0 to 1.5 minutes only. 84

Figure 4-5: Cell concentration of retentate during standard fouling conditions. Cell counts via calibrated spectrophotometer at 540 nm wavelength. The conversion from absorbance to cell concentration is via a calibration curve (see Figure C-5) 85

Figure 4-6: Cross sectional view of the fouled Supor 100 membrane (x5000). 86

Figure 4-7: LTSEM visualisation of fouled Supor 100 surface after rinsing and prior to cleaning. 89

Figure 4-8: FT-IR analysis of the fouled deposit. Note that percentage transmission T = (100 - %absorbance). Chart shown is in its original form as supplied by Reading Scientific Services Ltd. 90

Figure 4-9: Plot of fouling resistance versus water cleaning time at temperatures of 30, 40, 50 and 60°C and a cross-flow velocity of 0.75 m s^{-1} (Re = 3450, 4200, 5000 and 5840 respectively) 92

Figure 4-10: Effect of sodium hydroxide concentration on fouling resistance at 40°C and 60°C (Re = 3160 and 4380, respectively). 95

Figure 4-11: Effect of sodium hydroxide temperature on flux recovery 96

Figure 4-12: Residual deposits after cleaning with sodium hydroxide 97

Figure 4-13: Effect of nitric acid concentration (50°C) on flux recovery following initial application of sodium hydroxide 99

Figure 4-14: P3 Ultrasil 11 efficiency as a function of concentration after sixty minutes cleaning 101

Figure 4-15: Cleaning with P3 Ultrasil 11 at 30°C 102

Figure 4-16: Cleaning with P3 Ultrasil 11 at 60°C 102

Figure 4-17: Cleaning for sixty minutes with P3 Ultrasil 11 as a function of temperature. 103

Figure 5-1: Modelling cleaning with 0.002 wt% P3 Ultrasil 11 @ 30°C as a function of time. 119

Figure 5-2: Modelling cleaning with 0.002 wt% P3 Ultrasil 11 @ 40°C as a function of time. 120

Figure 5-3: Modelling cleaning with 0.002 wt% P3 Ultrasil 11 @ 60°C as a function of time. 120

Figure 5-4: Modelling cleaning with 0.02 wt% P3 Ultrasil 11 @ 30°C as a function of time. 121

Figure 5-5: Modelling cleaning with 0.02 wt% P3 Ultrasil 11 @ 40°C as a function of time. 121

Figure 5-6: Modelling cleaning with 0.02 wt% P3 Ultrasil 11 @ 50°C as a function of time. 122

Figure 5-7: Modelling cleaning with 0.02 wt% P3 Ultrasil 11 @ 60°C as a function of time. 122

Figure 5-8: Modelling cleaning with 0.05 wt% P3 Ultrasil 11 @ 30°C as a function of time. 123

Figure 5-9: Modelling cleaning with 0.05 wt% P3 Ultrasil 11 @ 40°C as a function of time. 123

Figure 5-10: Modelling cleaning with 0.05 wt% P3 Ultrasil 11 @ 60°C as a function of time. 124

Figure 5-11: Modelling cleaning with 0.1 wt% P3 Ultrasil 11 @ 30°C as a function of time. 124

Figure 5-12: Modelling cleaning with 0.1 wt% P3 Ultrasil 11 @ 40°C as a function of time. 125

Figure 5-13: Modelling cleaning with 0.1 wt% P3 Ultrasil 11 @ 50°C as a function of time. 125

Figure 5-14: Modelling cleaning with 0.1 wt% P3 Ultrasil 11 @ 60°C as a function of time. 126

Figure 5-15: Arrhenius plot for removal of species 1 with 0.002 wt% P3 Ultrasil 11. 127

Figure 5-16: Arrhenius plot for removal of species 1 with 0.02 wt% P3 Ultrasil 11. 128

Figure 5-17: Arrhenius plot for removal of species 1 with 0.1 wt% P3 Ultrasil 11. 128

Figure 5-18: Arrhenius plot for removal of species 2 with 0.02 wt% P3 Ultrasil 11. 129

Figure 5-19: Arrhenius plot for removal of species 2 with 0.05 wt% P3 Ultrasil 11. 129

Figure 5-20: Arrhenius plot for removal of species 2 with 0.1 wt% P3 Ultrasil 11. 130

Figure B-1: Size distribution of baker's yeast determined by laser MasterSizer (Malvern Instruments Ltd.). 146

Figure B-2: Water viscosity as a function of temperature 146

Figure C-1: Calibration of Triton flow meter 147

Figure C-2: Inlet pressure transducer calibration 148

Figure C-3: Retentate pressure transducer calibration 148

Figure C-4: Permeate pressure transducer calibration 149

Figure C-5: Spectrophotometer cell count calibration at 540 nm wavelength 149

List of Tables

Table 1-1: Microfiltration market value comprising industrial, commercial and public use; domestic use has been excluded. Exchange rate fluctuations and inflation have been neglected. The microfiltration percentage share of the total membrane market is fixed each year for all countries showing a small decrease followed by a period of constant size (61% in 1995, 59% in 1996, 58% in 1997, and 56% for 1998-2000). 4

Table 2-1: Qualitative comparison of various membrane configurations (reproduced from Mulder [1991]). 18

Table 2-2: Relative merits of membrane preparation techniques (adapted from Mulder [1991]). 22

Table 2-3: Soil characteristics (Harper [1972]) 51

Table 2-4: Cleaning strategies for the removal of deposits formed during the cross-flow microfiltration of yeast suspensions. 52

Table 3-1: Chemical composition of the formulated cleaning agent P3 Ultrasil 11 (reproduced from Henkel-Ecolab Ltd. data sheet) 67

Table 5-1: Relative merits of mathematical model approaches. 116

Table 5-2: Theoretical values of k_1 from the two-species first order model. 126

Table 5-3: Theoretical values of k_2 from the two-species first order model. 127

Table 5-4: Summary of calculated activation energies for removal of species 1 and 2. 130

CHAPTER 1 - INTRODUCTION

1.1 THE CLEANING CHALLENGE

Process plant often suffers from fouling, which can take many forms in a wide range of processes but can broadly be defined as the accumulation of unwanted matter. Fouling is considered undesirable for two main reasons:

(i) *Health risks.* Fouled layers can be rich in nutrients, acting as potential breeding grounds for microbes. In the food industry, microbial contamination of product can have fatal consequences.

(ii) *Negative effects on performance.* Partial blocking of pipework and equipment demands higher energy input to overcome the increase in resistance to heat or mass transfer. For membrane systems, resistance occurring in both the tangential and perpendicular planes is relevant.

As a result of the common occurrence of fouling and its potential impact, cleaning is a process in common use and thus warrants scientific investigation. However, the sayings 'prevention is better than cure' and 'prevention is profit' apply. Hence, the majority of research rightly focuses upon fouling reduction rather than cleaning, despite its practical importance. Through understanding fouling mechanisms, it is hoped one day to eliminate the need to clean. However, while cleaning remains a necessary part of processing, it should be recognised that it is a costly process. Typical cleaning costs, which must be balanced against process improvements, are:

(i) *Lost Production cost.* Potential revenue lost from the necessity to stop production during cleaning.

(ii) *Consumable costs.* Chemicals and water are required for the detergent solutions. Utilities are required for heating and cooling, pH adjustment, etc.

(iii) *Capital costs.* Extra equipment to store and pump detergent solutions plus the necessary control fittings.

(iv) *Operating costs.* Although often automated, cleaning adds complexity to processes, making them more labour intensive.

(v) *Environmental costs.* Unless the effluent undergoes treatment, which can be costly, effluent from cleaning processes can be damaging to the environment.

(vi) *Energy costs.* Extra energy is required for heating, pumping, mixing, etc. In addition to the economic cost of increased energy consumption, in a global sense, there is also an indirect environmental impact at the source of power generation.

In general, industrial cleaning is automated, using cleaning in-place (CIP) procedures, which involve the circulation of detergent solutions without the dismantling of equipment (Romney [1990]). CIP offers greater reproducibility than cleaning out-of-place (COP) procedures, which involve the dismantling of the plants and manual cleaning of the components. For industrial CIP processes, choice of cleaning conditions can be an art as much as a science. For example, in the dairy industry, a CIP cross-flow velocity has been empirically fixed at not less than 1.5 m s^{-1} (Romney [1990]). Although automatic cleaning procedures are in existence, cycles used are not selected based on knowledge of the required cleaning mechanisms and kinetics, but rather through wastefully excessive procedures that are known to work (Plett [1985]). In industrial CIP operations, it is possible to find different cleaning programs for specific equipment, but nearly none regarding the difference of fouled layers due to different products and/or process conditions. Successful cleaning therefore requires the use of large safety factors; consequently, a general-purpose CIP programme must result in excess. Besides the higher than optimal costs incurred, cleaning operations of this type will also contribute greatly to waste emissions. It is therefore concluded that industrial cleaning procedures are generally automated but not optimised.

Optimisation of cleaning procedures has the potential to minimise their economic and environmental impact. However, this is only possible through elucidation of the mechanisms and kinetics of cleaning. Understanding the cleaning process at this level allows predictive models to be formulated that take existing knowledge as a basis rather than rules-of-thumb and can be applied to specific deposits and conditions.

1.2 MEMBRANE SEPARATION INDUSTRY

Membrane separation is a growth industry. In 1995 the world-wide membrane separations market had a value of around US$2.7 billion (Elsevier Advanced Technology [1996]). By the year 2000, Elsevier forecast a rise to nearly US$3.9 billion, a compound average growth rate (CAGR) of 6%. In 1995 the world-wide filtration and separation market value was estimated at US$6.1 billion (Elsevier Advanced Technology [1994], based on 6% CAGR of 1994 figure of US$5.8 billion). The membrane separation market value was therefore 44% of the total filtration and separation market value in 1995. *Table 1-1* shows the actual market value (constant US$ Millions) of microfiltration (a subset of the membrane separation market relevant to this study) in 1995 and its projected market value from 1996 through to the year 2000.

	1995	1996	1997	1998	1999	2000
USA	459.0	470.6	495.0	511.4	544.7	577.3
Japan	288.6	297.3	314.2	324.6	347.3	369.8
Germany	189.3	194.0	201.2	205.0	217.3	230.3
France	131.1	134.4	140.0	143.3	151.9	161.0
UK	100.2	102.7	107.5	111.1	118.8	127.2
Italy	86.0	88.2	91.9	93.6	98.8	103.7
Spain	34.4	35.9	38.3	40.2	43.4	46.6
Benelux	59.7	60.9	63.1	64.6	67.8	71.6
Nordic	62.4	63.7	66.0	67.0	70.3	73.8
Rest of Europe	17.2	18.0	19.2	20.2	22.1	24.2
South Korea	74.3	79.0	86.3	92.4	101.7	111.3
Taiwan	71.6	77.5	85.3	91.5	101.1	111.7
Singapore	24.1	25.6	28.0	29.7	32.7	35.9
Rest of World	70.0	79.2	89.6	99.5	117.4	138.5
Total	1667.8	1727.1	1825.7	1894.0	2035.2	2183.1

Table 1-1: Microfiltration market value comprising industrial, commercial and public use; domestic use has been excluded. Exchange rate fluctuations and inflation have been neglected. The microfiltration percentage share of the total membrane market is fixed each year for all countries showing a small decrease followed by a period of constant size (61% in 1995, 59% in 1996, 58% in 1997, and 56% for 1998-2000).

Elsevier Advanced Technology [1996] forecasts that the majority of value growth will be derived from qualitative improvements of systems and materials rather than quantitative expansion. Although volume growth is predicted strongest within microfiltration applications, decreasing unit prices and a commoditisation of certain products in this segment will mean that value growth in ultrafiltration and molecular membrane filtration will outstrip it. High growth markets include biotechnology, water treatment, emission control, food processing, pharmaceuticals, medical applications and general environmental technology markets.

1.2.1 Membrane Cleaning

Although membrane separation is a growth industry, the rate of growth has been limited by fouling phenomena. Consequently, membrane cleaning is an essential but costly and complex component of nearly all membrane processes (Zeman and Zydney [1996]). Unfortunately, the current level of understanding of chemical cleaning mechanisms is relatively poor. Cleaning protocols are often based upon the general recommendations of chemical suppliers; very much an art based on trial and error (Zeman and Zydney [1996]). Although the basic principles underlying the different cleaning procedures have been identified, there have been relatively few quantitative studies comparing the effectiveness of different cleaning protocols for different membrane systems.

In the membrane separation industry, improvements in material formulations, module designs, pretreatment of feeds and processing strategies have significantly advanced the search for an economic system that is free from fouling. A highly significant processing phenomenon is critical flux (Field *et al.* [1995b]); the 'strong' form of which does not initiate fouling. Unfortunately, critical flux occurs at relatively low transmembrane pressure, resulting in low throughput per unit area of membrane. Therefore, despite the benefits of zero fouling, higher average flux can often be achieved by operating at conditions above the critical flux, where fouling is initiated but periodically cleaned. Therefore, at present, and for the near future at least, cleaning is predicted to remain an integral part of membrane separations; chemical cleaning being the most extensively used method (Scott [1995]). Cleaning has even been considered by some to be of equal importance to processing (Hauser and Sommer [1990]).

Elucidation of the mechanisms and kinetics involved in cleaning would potentially allow optimisation of current procedures. Milder conditions could be used over shorter time periods. However, without an understanding of the cleaning mechanisms and kinetics, savings may prove to be a false economy due to a decrease in the cleaning efficiency.

Environmental and monetary benefits that can result from optimisation of industrial cleaning cycles are considerable (Bird and Espig [1994]). Due to the value of the membrane separation industry being in the order of US$ Billions, even small percentage savings through cleaning optimisation offer a potentially large absolute contribution. System improvements are predicted to be a source of economic growth for membrane separations, optimisation of cleaning procedures is one such possibility.

1.3 AIMS AND SCOPE OF THIS STUDY

The aim of this thesis is to advance the fundamental knowledge of membrane cleaning with a view to future optimisation. To this effect, an experimental study of the removal rates and mechanisms of cleaning yeast deposits from a membrane system was completed. It is hoped that the experimental results and subsequent mathematical modelling shown here will contribute to more economical and environmentally friendly cleaning protocols for industrial membrane users.

The subject matter of this thesis is presented from a chemical engineering perspective. The global effects of cleaning solution type, concentration, temperature, turbulence and operating protocols on cleaning efficiency are reported. However, it is recognised that, at the molecular level, chemical membrane cleaning of biological deposits is a complex process, which incorporates many sciences including detergent chemistry, biochemistry and material science. A detailed account of all the relevant sciences is beyond the scope of this study. However, references are provided for further reading and future research collaboration possibilities are discussed.

1.4 THESIS STRUCTURE

Starting with a review of relevant literature and ending with the conclusions, the reader is taken through the subject matter in the order in which it was approached by the author. Chapters have been designed to present the major topics as stand-alone sections but there is an inevitable amount of overlap. Therefore, where appropriate,

cross-references between sections within this dissertation are included in addition to external references. The Harvard reference system, which is the preference of the University of Bath library, has been used for all citations. For references to materials, the format is company name followed by model number.

Chapter 2 - Yeast-Fouled Membrane Cleaning contains a review of membrane fouling and cleaning with respect to bioseparation. The review aims to aid the understanding and interpretation of experimental results presented in subsequent chapters. Information is presented in a progressive order. The problems encountered using conventional separation methods for bioseparation are illustrated first. Membrane separations are then discussed as a possible alternative. There then follows a definition of the inherent membrane separation problem of fouling and its removal via cleaning. Although many related topics are discussed, particular emphasis has been placed upon keywords relevant to the title of this thesis, namely: *bioseparation, yeast, microfiltration, irreversible fouling* and *chemical cleaning.*

Chapter 3 - Materials and Methods details the apparatus, procedures and consumables selected for experimental work. The design and commissioning of the combined fouling and cleaning apparatus is described and discussed. This includes design options and assumptions. The basis taken for protocols and required materials is described. Relevant analytical techniques are also detailed.

Chapter 4 - Results and Discussion presents the key experimental data generated using the equipment and protocols described in *Chapter 3*. An analysis of fouling is first presented, which considers the resistance and flux changes during cleaning combined with microscopic visualisation. Rinsing follows, ultimately describing the appearance and composition of the deposit prior to chemical cleaning. Cleaning experiments are shown using dilute solutions of sodium hydroxide, nitric acid and *P3 Ultrasil 11* (a sodium hydroxide-based formulated cleaning agent including surfactants and EDTA). Mechanisms of removal and the modelling implications are discussed.

Chapter 5 - Mathematical Modelling shows the development and application of a model to theoretically describe the single-stage *P3 Ultrasil 11* cleaning data. A review of past cleaning models is presented first, followed by a discussion of their relative

applicability to the experimental observations. The derivation of the model appropriate to this study is then described with assumptions clearly stated. Theoretical and observational results are compared and discussed.

Chapter 6 - Conclusions and Future Work draws together experimental and modelling results. Future implications and recommendations are considered. The degree of relevance of the work to industry is considered.

Chapter 7 - References contains an alphabetical (with respect to primary author name) list of information quoted from external sources. Following each reference, page numbers for each appearance of the citation within this thesis are given. Within the main body of text, references are shown as the primary authors and year of publication. Cross-references are provided where appropriate. Page numbers have been given for cross-references found in chapters other than the current.

The *Appendices* contain technical information regarding details of membranes, yeast, calibration curves, etc. Nomenclature used within the thesis is given. Publications resulting from this study that have appeared prior to this publication in the public domain are given.

CHAPTER 2 - YEAST-FOULED MEMBRANE CLEANING

2.1 BIOSEPARATION

Product separation is a fundamental operation within the process industries involving the extraction of one or more components from a multi-component mixture. Although there are many varied separation techniques, the fundamental principle of product separation is universal. Product separation is facilitated by exploitation of differences in physical or chemical properties of key species.

Bioseparation, the separation of micro-organisms (in whole or part) from aqueous media or intracellular products, is a particularly difficult problem. This is due to the unique properties associated with micro-organisms, which are sensitive to their physical and chemical environment; have similar density to the surrounding medium; are small; form stable colloids; are highly hydrated; and are cohesive (Hanisch [1986]).

Micro-organisms have a wide taxonomic distribution; they include some metazoan animals, protozoa, many algae and fungi, bacteria and viruses. This study focuses on a model micro-organism, yeast, a species of fungus.

2.1.1 The Yeasts

Although many genera and species of yeast exist in nature and many are used commercially, the commonest yeasts are strains of *Saccharomyces cerevisiae* (Stanier *et al.* [1977]). The genus *Saccharomyces cerevisiae* contains some forty species, some of which are highly utilised raw materials for industrial processes such as brewing, distilling, wine making, baking and culturing. However, there are approximately six hundred known yeast species (Berry [1982]).

The cells of *Saccharomyces cerevisiae* are round, ovoid or ellipsoidal in shape and vary from 2.5 - 10 μm in width and 4.5 - 21 μm in length (Berry [1982]). Inside the yeast cell are many of the features of a typical cell, as shown in *Figure 2-1*.

The distinguishing feature of a growing population of yeast cells is the presence of the buds that are produced when the cell divides. The daughter cell is initiated as a small bud that increases in size throughout most of the cell cycle, until it is the same size as the mother cell, at which point separation occurs. The site of cell separation is marked on the mother cell by a structure referred to as the bud scar and on the daughter cell

by the birth scar. These scars cannot be seen under a light microscope but they do show up as very distinct structures in scanning electron micrographs, as can be seen in *Figure 3-6 (p.65)*.

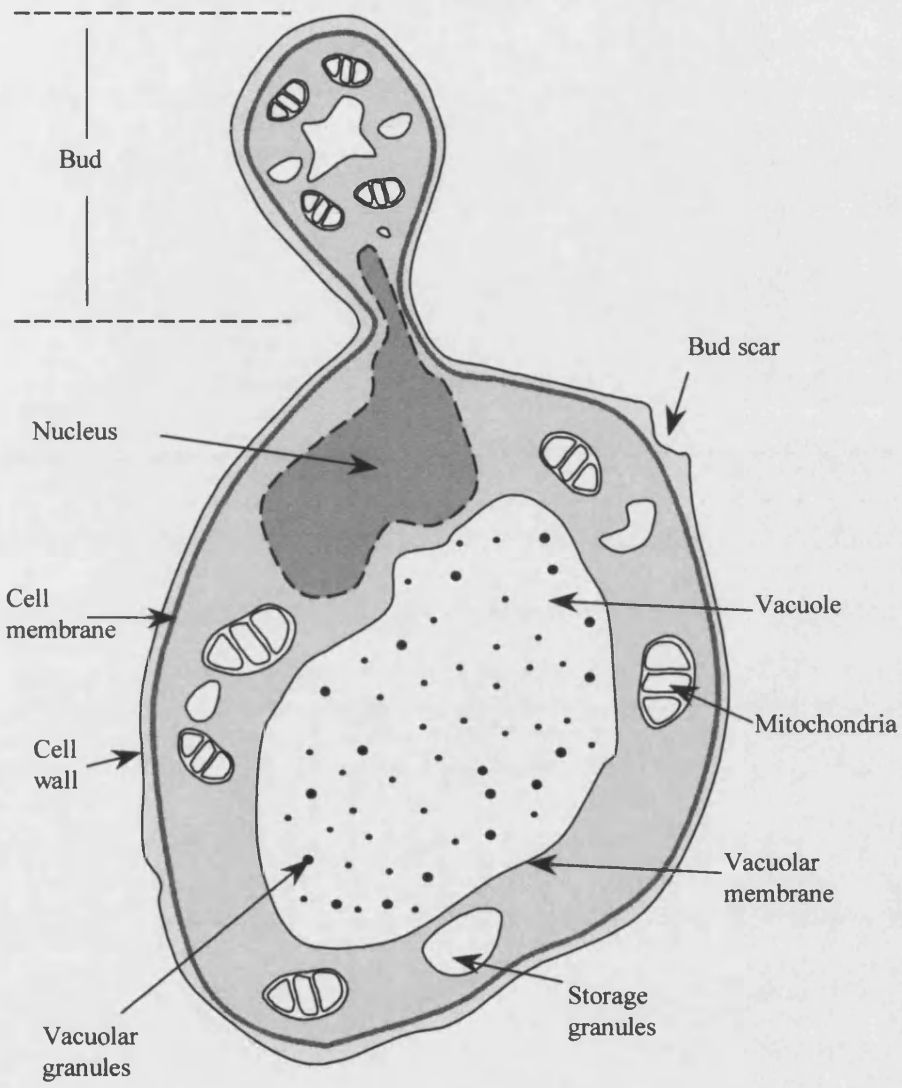

Figure 2-1: Cross-section through a typical yeast cell showing the main features of the cell and their distribution (reproduced from Berry [1982]).

Yeast cells are bounded by a cell wall. In the case of *Saccharomyces cerevisiae* it is approximately 25 nm-thick and constitutes 15 - 25% of the dry weight of the cell (Berry [1982], Fleet [1991]). The cell wall consists of several macromolecular components; namely, polysaccharides (glucan, mannan and chitin), proteins and lipids (Fleet [1991]). Mannan has been found to be covalently bound to protein so that the term mannoprotein more correctly describes their macromolecular status. The major macromolecular components of the *Saccharomyces cerevisiae* cell wall are the

glucans and mannoproteins (Berry [1982]). A representation of the cell surface is shown below in *Figure 2-2*.

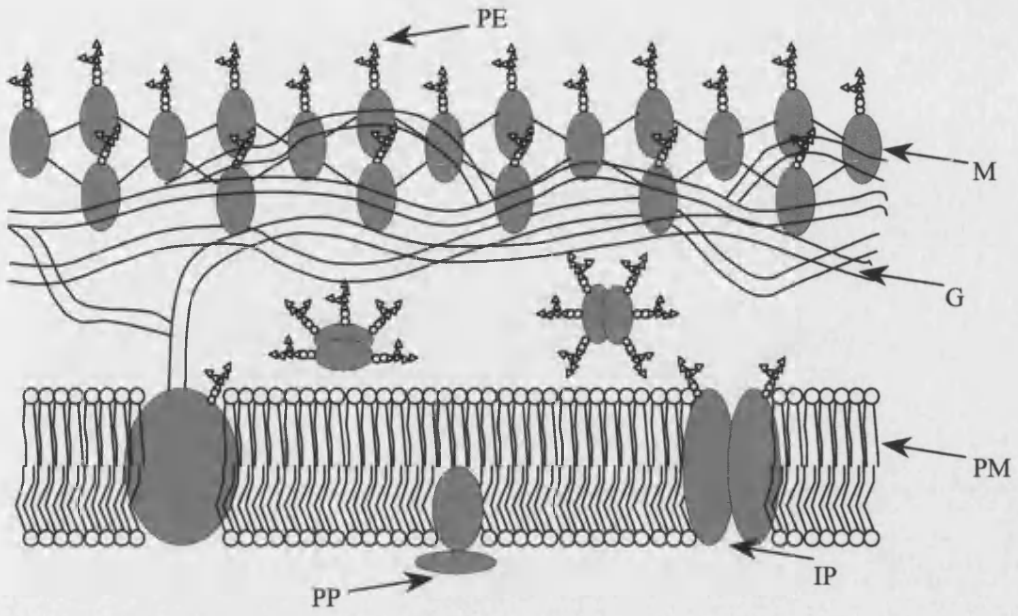

Figure 2-2: The yeast cell surface (reproduced from Schekman and Novick [1983]). (G) Glucan; (M) Mannoprotein; (PE) periplasmic enzymes; (PM) plasma membrane; (IP) integral membrane protein; (PP) peripheral membrane protein.

Glucans are complex branched polymers of glucose units only partly soluble in water and appear to be the major structural component of the cell wall, since their removal results in total disruption. Mannoprotein does not appear essential to the integrity of the cell wall, since it is possible to remove the mannoprotein without altering the general shape of the cell. The main cell wall components have different degrees of solubility and various reagents and treatments are required to extract the individual components. Mannoproteins can be extracted by relatively mild treatments, but the general insolubility of glucan and chitin has required sequential alkali and acid treatments to effect their extraction (Fleet [1991]).

Most yeasts are safe to handle, requiring good microbiological practice (GMP) rather than aseptic technique and so can be obtained in bulk. Bakers yeast, as a commercial product, knows several formulations that can be grouped into two main types; compressed yeast, also known as 'fresh yeast'; and dried yeast (Beudeker *et al.* [1989]). Compressed yeast is the traditional formulation of bakers yeast. It is commonly sold in 1 kg blocks wrapped in wax paper. Compressed yeast has a

moisture content of 27-34 wt% and a protein content of 42-56 wt%. It is ready for immediate use. However, this type of yeast is perishable and should be stored at low temperatures, preferably between 0 and 4°C. At these temperatures, a shelf life of between three and four weeks is possible with only a slight decrease in leavening capacity. Active dry yeast (ADY) is sold in pellet form stored in airtight bags filled with nitrogen. The shelf life of ADY is at least one year at room temperature. A problem inherent to ADY is the leakage of yeast solids from the cells during rehydration, especially at low temperatures (Herrera *et al.* [1956]). Therefore, ADY should be rehydrated at 35-45°C before use to minimise leakage.

2.1.2 Separation Techniques

Technically, whole cell harvesting is possible using many unit operations including sedimentation, centrifugation, phase partitioning, ultrasound, hydrocyclones and membrane separations. Removal of cell debris from intra-cellular products is also possible but the relatively small particulate size increases separation difficulty for all methods.

In the past, centrifugation has been the most widespread option for cell harvesting. Although through recent improvements in production capacity, cross-flow micro-filtration is rapidly becoming dominant (Mackay and Salusbury [1988], Scott [1995], Zeman and Zydney [1996]).

2.1.2.1 Sedimentation

Sedimentation has the advantages of being the simplest and gentlest process but is relatively slow and requires large-scale process equipment (Coulson and Richardson [1991]). Essentially, cells fall under gravity at terminal velocity eventually forming a separate solid phase. The small density difference between the cells and medium facilitates separation. Cell diameter is also an important limiting factor of the process. For sub-micron particles, Brownian diffusion becomes significant and opposes settling. Whole cells are thus more suitable than cell debris.

The velocity of sedimentation u_o is proportional to the square of the particle diameter d_p and density difference $\Delta\rho$, and inversely proportional to the medium viscosity μ. For a Reynolds number (Re) of the falling particulates of less than 0.1, Stokes law can be applied to predict the settling velocity, as shown in *Equation 2-1*.

$$u_o = \frac{d_p^2 . \Delta\rho . g}{18\mu} \qquad \textit{Equation 2-1}$$

Due to the small density difference between the cells and medium, gravity-settling times are generally long; of the order of hours rather than minutes. Settling times can be shortened by inducing cell flocculation, which increases the effective particle diameter (Weeks *et al.* [1983]). However, the use of chemical flocculating agents adds to the complexity of the broth.

2.1.2.2 Centrifugation

Centrifugation is a relatively more compact process and significantly reduces settling times but the capital cost and complexity of the process are greater. Enhanced gravitational acceleration is achieved by spinning the broth about a vertical axis at very high speed. The instantaneous velocity ($^{dr}/_{dt}$) is equal to the terminal velocity u_o in the gravitational field increased by a factor of rw^2/g, which is often expressed as Σ. The volumetric feed rate to the centrifuge Q is predicted by *Equation 2-2*.

$$\frac{dr}{dt} = u_o \frac{r\varpi^2}{g}$$

$$Q = u_o \Sigma \qquad \textit{Equation 2-2}$$

Centrifugation incurs significant running costs. Heat generated during the process must be removed giving rise to the expense of cooling. Potentially dangerous aerosol production is also a hazard. Cells experience much higher stress through high shear rates. However, centrifugation is typically preferred to sedimentation, the benefits of short settling times outweighing the additional problems.

2.1.2.3 Phase Partitioning

Phase partitioning is a surface affinity method for cell separation first developed by Walter [1977]. Separation is facilitated by the affinity of the cells for one of two immiscible polymer phases. The most extensively used polymers are polyethylene-glycol (PEG) and dextran. Separation is a two-step process with each having different characteristic times. The first step is the partition of the particles or solute into drops of one of the phases. This step is rapid. The second step is the separation of the droplets into two bulk phases to allow collection of the particles, which can take a

considerable time if gravity alone is relied upon and is thus the rate limiting step. Allman and Coakley [1994] significantly reduced the separation time to one minute for *S. cerevisiae* using an ultrasound enhanced technique.

2.1.2.4 Ultrasound

Continuous, high efficiency filtration of *Saccharomyces cerevisiae* using ultrasound has been demonstrated by Hawkes and Coakley [1996]. Cells in aqueous suspensions in a plane ultrasound standing-wave field concentrate into bands, which form clumps that settle, and can then be harvested. However, relatively low processing flow rates of only 300 mL hr^{-1} were reported.

2.1.2.5 Hydrocyclones

Hydrocyclones, like centrifuges, function on the principle of enhanced gravitational settling. Traditionally, hydrocyclones function at lower centrifugal fields than centrifuges. However, by decreasing the diameter of the hydrocyclone, known as a mini-hydrocyclone, the centrifugal fields produced can be increased. The diameter of the cylindrical section of the cyclone is also a major variable determining the size of particle that can be separated. The application of mini-hydrocyclones has been used to separate yeast suspensions (Cilliers and Harrison [1994]). The efficiency of a single unit was reported low compared to filtration and centrifugation. However, the use of multiple units in series is being investigated as a possible solution to increasing separation efficiency.

2.1.2.6 Cross-flow Membrane Separation

Rather than exploiting a small difference in density between cells and media as with centrifugation, membrane separation exploits a relatively large difference in diameter between cells and microscopic pores (*see 2.2*). In theory, a larger driving force should simplify separation. Cross-flow membrane separation also offers the potential advantages of ambient temperature operation, relatively low running and capital costs, modular construction and higher product purity. Membrane filtration offers relative simplicity of operation and low costs in comparison to centrifugation (Scott [1995]). Specifically, techniques known as microfiltration and ultrafiltration have found common usage in the biotechnology industry. Microfiltration is the focus of this study and will now be presented in greater detail.

2.2 MEMBRANE SEPARATION PROCESSES

Although membrane separation processes have numerous and varied applications, as the name suggests, their common link is the presence of a membrane. A general definition of a membrane has been suggested by Strathman [1981]:

> *"[A membrane is] an interphase separating two phases and selectively controlling the transport of materials between those phases"*

Membranes are defined as interphases rather than interfaces because, although generally very thin, the internal membrane structure can play a crucial role in effecting separation.

2.2.1 Classification

Transport of species through a membrane takes place when a driving force, i.e. a chemical potential or electrical potential difference, acts on the individual components in the system (Mulder [1991]).

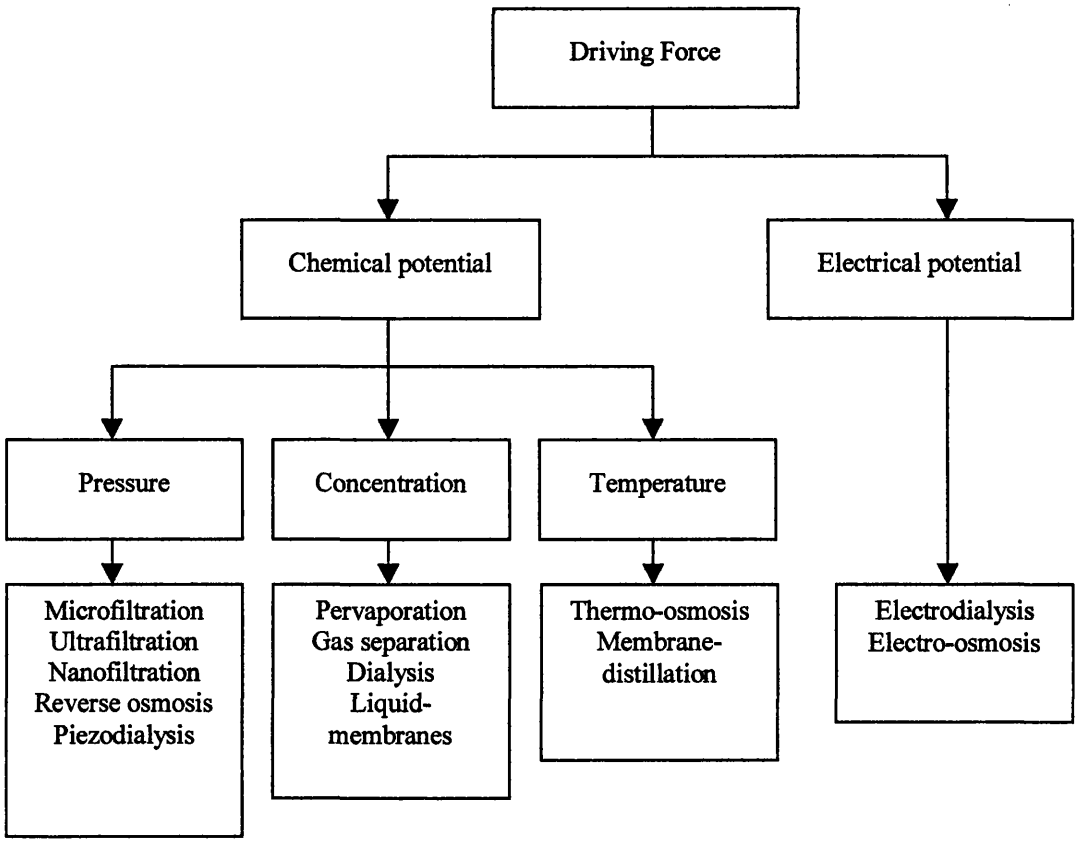

Figure 2-3: Classification of membrane separation processes with respect to driving force.

The majority of transport processes are driven by a chemical potential difference, which encompasses parameters such as pressure, concentration (activity) and temperature. Driving force provides a convenient system of classification for membrane separation processes. As shown in *Figure 2-3*, microfiltration is classified as a pressure-driven process.

2.2.2 Pressure-Driven Processes

Pressure-driven membrane separation processes generally operate on the assumption that there is a significant difference in size between *key* components. *Figure 2-4* shows a schematic representation of pressure-driven membrane separation. The fundamental principle behind product separation is analogous to sieving. Particles of greater diameter than the pores are retained while the medium, or any material smaller than the membrane pores, readily permeates through.

An ideal membrane process is characterised by high throughput (or flux) and one hundred percent transmission of a desired component. Unfortunately, reality is often far from ideality due to fouling; an inherent problem that affects flux and transmission. Fouling is covered later in this chapter (*see 2.3*).

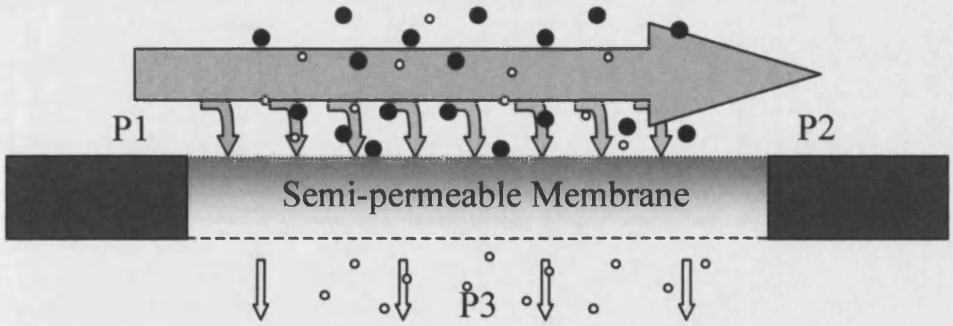

Figure 2-4: Schematic illustration of pressure-driven membrane separation principle. P1, P2 and P3 represent the feed, retentate and permeate pressures, respectively.

Figure 2-3 shows that the category of pressure-driven processes comprises microfiltration (MF), ultrafiltration (UF), nanofiltration (NF) and reverse osmosis (RO). MF, UF and NF can be considered open porous and can be classified by their respectively decreasing nominal pore size, as shown in *Figure 2-5*.

RO, often used to deionize water, is sometimes referred to as hyperfiltration; the latter

name implying that the membrane simply has smaller pores than NF. This can be very misleading. RO is not a simple filtration process but rather a solution-diffusion process. Applied hydrostatic pressure reverses the normal osmotic flow of the solvent. The normal direction of solvent flow is down its concentration gradient, i.e. from a solution of lower solute concentration to a solution of higher solute concentration. When the applied hydrostatic pressure exceeds the osmotic pressure, the solvent flow is reversed, from the concentrated to the dilute solution.

2.2.3 Membrane Modules

Pressure-driven processes utilise solid phase membranes, which can be housed in a variety of modules. Large-scale processes require large membrane areas; yet industry demands compact units. With respect to production, the module hydrodynamics are equally important. Hence, module design is challenging and always a compromise. Successful designs therefore incorporate a high membrane surface area to volume ratio whilst minimising fouling and/or concentration polarisation (*see 2.3*). The four most commonly used module designs have flat sheet, spiral wound, tubular, or hollow fibre membrane configurations. The relative merits of the configurations are summarised in *Table 2-1*.

	Tubular	Flat sheet	Spiral wound	Hollow fibre
Packing density	Low	→		High
Investment	High	→		Low
Fouling tendency	Low	→		Very high
Cleaning	Good	→		Poor
Operating cost	High	→		Low
Membrane replacement	Yes/No	Yes	No	No

Table 2-1: Qualitative comparison of various membrane configurations (reproduced from Mulder [1991]).

Although the capital costs of the various modules may vary considerably, each one has operating characteristics that suit them to specific fields of application.

In recent years, more dynamic modules with self-cleaning properties have been developed. Their relative merits are discussed later, in section *2.4.2*.

2.2.3.1 Flat Sheet Modules

The flat sheet (or plate and frame) module configuration is the simplest. It consists of one, or more, flat membrane sheets mounted between support plates. The support plates often contain moulded grooves to promote turbulence and channel the flow past the membrane. Flat sheet modules are commonly used in laboratories as they allow membrane replacement. For small-scale laboratory use, flat sheet membranes are often considered disposable. This is not the case in large industrial processes due to the large number of membrane sheets per module (Mulder [1991]). A disadvantage of flat sheet membranes is that they do not have the mechanical strength required to be compatible with back-flushing; a popular *in situ.* cleaning method (*see 2.4.2.1*).

2.2.3.2 Spiral Wound Modules

Spiral wound modules consist of several flat sheets of membrane separated by turbulence-promoting mesh separators formed into a 'Swiss roll'. The edges of the membranes are sealed to each other and to a central perforated tube. This produces a cylindrical module that can be installed within a pressure tube. The process feed enters at one end of the pressure tube and encounters a number of narrow, parallel feed channels formed between adjacent sheets of membrane. Permeate spirals toward the perforated central tube for collection. A limiting factor in terms of bioseparation is the likelihood of blockage (Howell [1993]).

2.2.3.3 Hollow Fibre Modules

Hollow fibre modules contain bundles of fine fibres, 0.1 - 2 mm in diameter, sealed in a tube. A relatively large surface area of membrane can be accommodated into a small volume. For UF and MF, the fibres have large diameter and the membrane feed is on the interior. For RO and gas separation, the fibres are relatively fine and sometimes the separating surface of the membrane is on the outer surface. High pressure is best tolerated from the outside to the inside. The membrane is weak when the feed is on the inside relative to processing being on the outside.

2.2.3.4 Tubular Modules

Tubular modules are widely used where it is advantageous to have a turbulent flow regime, for example, in the concentration of high solids-content feeds. They often consist of ceramic membrane cast on the inside of a porous support tube, which is housed in a perforated stainless steel pipe. Individual modules contain a cluster of

tubes in series held within a stainless steel permeate shroud. For microfiltration, it is often found that high cross-flow velocities are desirable, and with very viscous pastes being produced, tubes of approximately five millimetre internal diameter are used.

2.2.4 Microfiltration

Despite being the first commercialised membrane separation process, microfiltration (MF) is considered the least understood with respect to suspensions and macromolecules (Belfort *et al.* [1994]). In general, MF membranes retain particulates but allow passage of macromolecules, salts and water. The process is characterised by operation at low pressures, by high permeation fluxes, and by cross-flow mode in a flat or cylindrical geometry. MF membranes are often susceptible to intra-pore fouling.

2.2.4.1 Cross-flow

In order to obtain high rates of mass transfer suitable for large-scale operation, it is beneficial to operate at high tangential velocity and/or turbulence in the immediate vicinity of the membrane. A scouring feed action can be introduced by operating in a cross-flow geometry, in which the feed flow is parallel to the membrane surface, as shown in *Figure 2-4*. Rejected matter can potentially be scoured form the surface and transported back to the bulk flow. Cross-flow is widely used in nearly all commercial large-scale pressure-driven membrane plants (Belfort *et al.* [1994]).

At laboratory scale, processes exist where flow is perpendicular to the membrane surface, referred to as dead-end filtration. In this configuration, all material rejected by the membrane remains at the surface, which maximises the rate of apparent membrane porosity reduction. Thus, dead-end filtration is suitable only for dilute suspensions. However, an advantage of dead-end flow is its relative simplicity.

2.2.4.2 Applications

Microfiltration has become increasingly popular in a wide range of applications including heavy metal effluent treatment, semiconductor manufacture, clarification of beverages and wastewater treatment (Scott [1995], Zeman and Zydney [1996]). With respect to bioseparation, cross-flow microfiltration (CFMF) is competing in the market place with conventional course filtration and centrifugation. Three main

applications of CFMF predominate with respect to bioseparation (Defrise and Gekas [1988]):

(i) *Whole cell harvesting.* Concentration and washing of cells is important when extracellular products are obtained or when the purpose of a culture is to obtain biomass.

(ii) *Cell debris removal.* Separation of intracellular products from the cell residuals following cell wall rupture. The cell wall can be removed with enzyme action or mechanical shear.

(iii) *Cell recycling.* Achieved through a MF step coupled to a fermenter. In this case, the cells play the role of biocatalyst. A fermentation or culture broth is continuously replaced with fresh feed and the cells recycled (Warren *et al.* [1994]).

Whole cell harvesting and cell recycling are best suited to MF. Filtration of cell debris presents a greater challenge. Fragments of cell debris could be of similar diameter to MF pores possibly resulting in less than one hundred percent selectivity. In this scenario, UF would be considered more suitable for cell debris filtration despite the lower fluxes associated with a greater hydrodynamic resistance. MF gives higher throughput than UF but transmission criteria are crucial in producing a product to desired specifications. However, Wu *et al.* [1993] have successfully used a MF membrane to affect separation of cell debris from intra-cellular products.

2.2.4.3 Membrane Characterisation and Preparation

MF membranes are distinguishable from the other pressure driven membranes: UF, NF and RO in terms of pore diameter. The pore sizes associated with each process are shown in *Figure 2-5*. MF membranes have the largest pores of the pressure-driven processes, ranging from 0.1 - 10 μm, making the process suitable for retaining suspensions.

MF membranes are classified as solid-phase open-porous and can be prepared from such diverse materials as synthetic polymers, natural cellulose, ceramics and metals (Scott [1995], Mulder [1991]). Manufacturing methods include sintering, stretching, phase inversion (or solvent casting) and track etching. Each process has a

characteristic effect upon the morphology of the membrane. Ideally, membranes should have high porosity to ensure high fluxes, and a narrow size distribution to ensure good selectivity. Some of the preparation techniques and their relative pore size and distributions are shown in *Table 2-2*.

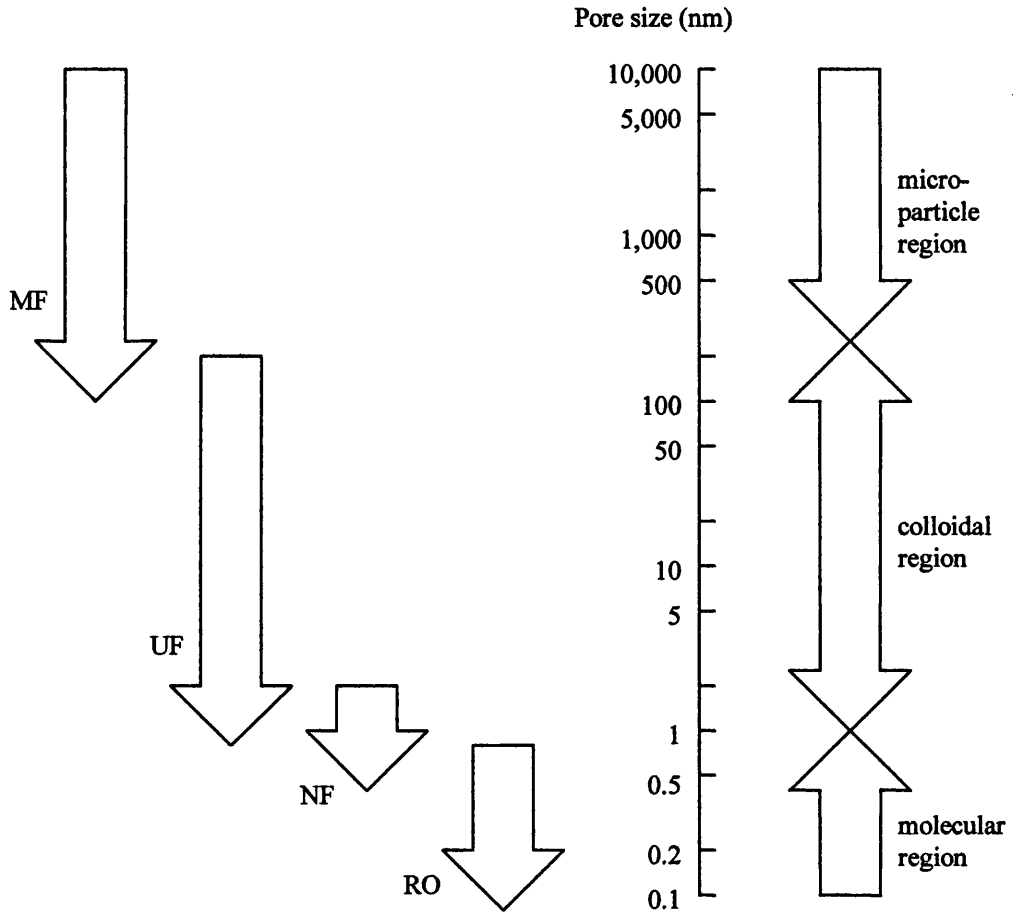

Figure 2-5: Classification of pressure-driven process with respect to pore size.

Preparation Method	Porosity	Pore size distribution
Sintering	Low/Medium	Narrow/Wide
Stretching	Medium/High	Narrow/Wide
Track-etching	Low	Narrow
Phase inversion	High	Narrow/Wide

Table 2-2: Relative merits of membrane preparation techniques (adapted from Mulder [1991]).

The membrane used throughout this study (Gelman Sciences, *Supor 100*) was a synthetic polymer manufactured using a phase inversion process (*3.1.2, p.63*). Phase

inversion is the commonest polymeric membrane preparation technique. The process typically produces an asymmetric membrane with a foam-like substructure and a nodular top layer.

Recent advances in polymer technology have led to the development of membranes with excellent thermal and chemical resistance. Indeed the *Supor 100* membrane is autoclavable and resistant to a wide range of chemicals (*Appendix A.1*).

Hydrophilicity is an important consideration in membrane selection, expressed most conveniently in terms of the water contact angle θ (Zeman and Zydney [1996]). Hydrophilic surfaces have a contact angle less than 90°, while hydrophobic materials exhibit a contact angle greater than 90°, as shown in *Figure 2-6*.

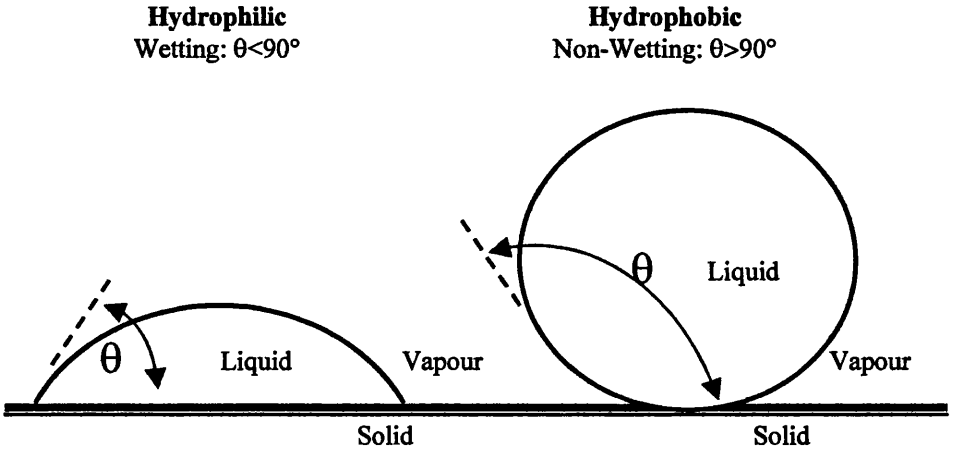

Figure 2-6: Balance of interfacial tensions for a drop of liquid on a flat surface in the presence of vapour.

Although membrane selection is process-specific, hydrophilic membranes generally have greater compatibility with biological suspensions. Macromolecular adsorption, an important mechanism that generally initiates cellular adhesion, is reduced with hydrophilic membranes compared to hydrophobic membranes. Protein is reported to have a greater affinity for hydrophobic surfaces due to molecular unfolding. However, it has been observed that surfaces can be too hydrophilic (Defrise and Gekas [1988]). Therefore, it can be summarised that the optimum membrane hydrophilicity would be weakly hydrophilic for application to suspensions with significant protein content.

2.2.4.4 General Flux Equation

The volumetric flow of permeate (flux) through a MF membrane is described by Darcy's law (Mulder [1991]). The flux J is directly proportional to the driving force ΔP_{TM} - Π_{TM}, and inversely proportional to the permeate viscosity μ_p and total hydrodynamic resistance R_T, as shown in *Equation 2-3*. ΔP_{TM} denotes the transmembrane pressure and $\Delta\Pi_{TM}$ the transmembrane osmotic pressure.

$$J = \frac{\Delta P_{TM} - \Delta\Pi_{TM}}{\mu_p (R_T)} \qquad \textit{Equation 2-3}$$

$$\Delta P_{TM} = \left(\frac{P1 + P2}{2}\right) - P3 \qquad \textit{(see Figure 2-4)}$$

During MF of yeast suspensions, there is an imbalance of yeast cells across the membrane with an associated osmotic pressure of $\approx 10^{-12}$ bar, which is considered negligible (Mulder [1991], Belfort *et al.* [1994]).

The total hydrodynamic resistance to flow R_T often varies with time, due to the accumulation of rejected material at or near the membrane surface, and comprises a number of resistances in series, which can be divided into two main categories; membrane resistance R_m and fouling resistance R_f. Fouling is discussed in the following section.

$$\Delta\Pi_{TM} \approx 0; R_T = R_m + R_f$$

$$J = \frac{\Delta P_{TM}}{\mu_p (R_m + R_f)} \qquad \textit{Equation 2-4}$$

The hydrodynamic membrane resistance R_m is a function of the membrane permeability, which is dependant on the method of manufacture and material used. R_m can be determined experimentally during clean water filtration at fixed temperature and pressure, i.e. when fouling is zero.

$$R_f = 0 \Rightarrow J = \frac{\Delta P_{TM}}{\mu_p (R_m)}$$

$$R_m = \frac{\Delta P_{TM}}{\mu_p J} \qquad \textit{Equation 2-5}$$

The physical properties of the membrane, and hence R_m, can be considered constant if the effects of compaction and corrosion are negligible with time.

Compaction is a one-off phenomena resolved during conditioning of the membrane before first use. Conditioning should be at a pressure driving force at least equal to the operating pressure in order to simulate real compression conditions. MF operates at relatively low pressure and so is the least affected by compaction. Compaction of RO membranes, which operate at much higher pressures has been reported. However, there does not appear to be a clear distinction between compaction and fouling (Zeman and Zydney [1996]).

Polymeric membranes have excellent thermal and chemical stability. Therefore, the hydrodynamic membrane resistance R_m of conditioned polymeric membranes is constant and additional to the fouling resistance R_f.

2.3 FOULING PHENOMENA

Fouling phenomena are widely regarded as being the limiting factor to the more widespread use of CFMF (van der Horst and Hanemaaijer [1990], Belfort *et al.* [1994]). In general, membrane fouling phenomena result from the accumulation of rejected material. This is due to an imbalance between transport towards and away from the membrane surface. Fouling behaviour is membrane and process specific and can take many forms, but generally manifests itself as a decline in permeate flux accompanied by a decrease in transmission (Howell and Nyström [1993]).

If the permeate produced during membrane separation is recycled, ensuring a constant volume system, the flux decline profile is exponential, as shown in *Figure 4-1 (p.80)*. However, if the permeate is removed, decreasing the volume and increasing the system concentration with time, the resultant flux profile is sigmoidal rather than exponential (Lojkine *et al.* [1992], Belfort *et al.* [1994]).

In terms of transmission, fouling prevents the passage of species with dimensions that would be expected to pass through the membrane pores. When transmission is affected product quality is compromised, which can have greater consequences than low production rates. In some cases, fouled MF membranes are reported to operate with the characteristics of UF membranes (Glimenius [1985]).

2.3.1 Concentration Polarisation

Dissolved or suspended material is transported from the bulk flow towards the membrane surface via convection. Initially, membrane permeability and therefore permeate flux is high relative to the slow, diffusive, mechanisms of back-transport (*see 2.3.2*). Thus, material accumulates near the membrane-solution interface. This reversible phenomenon is termed concentration polarisation but is not classified as fouling as there is no interaction with the membrane surface.

The presence of concentration polarisation results in reduced permeate flux by increasing the osmotic pressure Π at the upstream surface of the membrane and hence reducing the net driving force. Combined with high permeate flux, the effects can be highly significant. Concentration polarisation is therefore most significant for membranes capable of retaining macromolecules at high fluxes. Although MF membranes are associated with high flux, they should not retain macromolecules.

2.3.2 Mechanisms of Back-Transport

Several models have been developed in an attempt to predict the observed non-zero steady state flux for suspensions. All models agree that the convective transport of material to the membrane surface is balanced by back-transport. Several mechanisms of back-transport have been proposed, some more applicable than others, and are discussed in an excellent review by Belfort *et al.* [1994]. Proposed mechanisms of back-transport have included Brownian motion, shear-induced diffusion and inertial lift. These mechanisms are sensitive to particle size and shear rate. For sub-micron particles at low shear rates, Brownian diffusion is the dominant mechanism. For particle sizes from 1 to 40 μm at moderate shear, shear-induced diffusion dominates. For particles greater than 40 μm at high shear rates, inertial lift dominates. Thus, shear-induced diffusion is considered to provide the best description of observed fluxes during yeast filtration. However, in reality there are many unique contributing factors which the model does not take into account such as the effects of particle adhesion, compressibility, shape and size distribution (Lojkine *et al.* [1992]).

2.3.2.1 Common Basis

The mechanisms of Brownian diffusion and shear-induced diffusion have a common mathematical form, the application of the traditional UF 'film theory' for macromolecules, which states that the permeate flux J is proportional to the natural log of the quotient of the fractional particle concentration of the cake layer Φ_w and the bulk suspension Φ_b, as shown in *Equation 2-6*.

$$J = K \ln\left(\frac{\Phi_w}{\Phi_b}\right) \qquad \textit{Equation 2-6}$$

For laminar flow, the length-averaged mass transfer coefficient K is determined by the Leveque solution for thin boundary layers:

$$K = 0.81\left(\frac{\gamma_o D^2}{L}\right)^{1/3}$$

Where, γ_o is the nominal shear rate at the membrane surface, D is the particle diffusivity and L is the tube or channel length. Trettin and Doshi [1980] showed that, for a dilute suspension ($\Phi_w - \Phi_b << \Phi_\omega$), flux is described by *Equation 2-7*.

$$J = 1.31\left(\frac{\gamma_o D^2 \Phi_w}{\Phi_b L}\right)^{1/3} \qquad \textit{Equation 2-7}$$

2.3.2.2 Brownian Diffusion

The particle diffusivity for Brownian diffusion is denoted by D_{BO} and can be estimated at infinite dilution by the Einstein-Sutherland equation, as shown below.

$$D_{BO} = \frac{kT}{f} = \frac{kT}{6\pi\eta aF}$$

Where, k is the Boltzmann constant (1.380×10^{-23} J mol^{-1} K^{-1}), T is the suspension temperature, and f is the frictional coefficient. For rigid colloidal particles of dimension much larger than the hydrated layer, f can be obtained from the classical Stokes law, where η is the suspension viscosity, a is the particle diameter, and F is the Perrin shape factor ($F = 1$ for spherical particles).

Predicted fluxes for micron-sized particles using the Brownian diffusivity were found to be one or more orders of magnitude less than those observed in practice. Green and Belfort [1980] refer to this discrepancy as the 'flux paradox for colloidal suspensions'. The paradox being that the diffusivities of micron-sized particles in water are three orders of magnitude less than molecular diffusivities of macromolecules (yielding lower predicted flux), whereas the membrane and cake permeabilities for MF are higher than those for UF (yielding higher observed fluxes).

2.3.2.3 Shear-Induced Diffusion

As a possible resolution to the 'flux paradox', different authors proposed a shear-induced hydrodynamic diffusivity instead of the Brownian diffusivity (Zydney and Colton [1986], Romero and Davis [1988]). Shear-induced hydrodynamic diffusion was first measured by Eckstein *et al.* [1977]. and occurs because individual particles undergo random displacements from the streamlines in a shear flow as they interact with and tumble over other particles. The shear-induced hydrodynamic diffusivity is proportional to the square of the particle size a multiplied by the shear rate γ_o, whereas the Brownian diffusivity is independent of shear rate and inversely proportional to particle size. As a result, Brownian diffusion is important for sub-micron particles and low shear rates, whereas it is dominated by shear-induced hydrodynamic diffusion in typical cross-flow MF applications involving micron-sized and larger particles.

$$D_S = 0.3\gamma_o a^2$$

The back-transport mechanism during yeast filtration is best described by shear-induced diffusion, which is thought to be dominant for micron to forty micron-sized particles (Lojkine *et al.* [1992], Romero and Davis [1991], Redkar and Davis [1995]).

2.3.2.4 Inertial Lift

Other workers have proposed a mechanism of particle back transport from the membrane surface based on the inertial lift of the particles (Green and Belfort [1980], Belfort [1989]). This mechanism is thought to dominate for particles of greater than 40 μm diameter in high shear fields (Belfort *et al.* [1994]).

Inertial lift arises from non-linear interactions of particles with their surrounding field flow under conditions where the Reynolds number, based on the particle size, is significant. The inertial lift velocity of spherical particles under laminar flow conditions in dilute suspensions, where particle-particle interactions are neglected, is of the form:

$$v_{L,o} = \frac{b\rho_o a^3 \gamma_o^2}{16\eta_o}$$

The inertial lift velocity for fast laminar flows increases with the cube of the particle size, and the square of the tangential shear rate, and so is expected to be significant for large particles and high flow rates.

2.3.3 Fouling Implications on the MF Design Equation

The general microfiltration equation predicts that the flux is inversely proportional to the fouling resistance R_f, as shown in *Equation 2-4*.

The fouling resistance R_f is the sum total resistance of many potential fouling phenomena, which are generally sub-divided into reversible (*r*) or irreversible (*ir*) categories.

$$J = \frac{\Delta P_{TM}}{\mu(R_m + R_r + R_{ir})}$$

Reversibility is defined as the tendency of a deposit to be removed by the shear action of *in situ.* hydraulic cleaning techniques. Reversible fouling is shear removable, irreversible fouling is not. There are no standards of rinsing to define these regimes. The terms are relative to individual procedures and systems.

2.3.4 Reversible Fouling

Reversible fouling is defined as surface deposition resulting in decreased flux and/or transmission removable at conditions of zero transmembrane pressure. The degree of reversibility is therefore process specific, dependent upon the fouling and rinsing conditions.

Loosely bound cake formation is often found to be reversible. However, a fouling cake layer can have greater selectivity than the membrane itself, acting as a secondary filter retaining macromolecular particles with binding properties. However, it would be commonly expected that rinsing at zero transmembrane pressure should increase system permeability significantly.

2.3.5 Irreversible Fouling

Although cake formation can often be removed easily, its existence promotes favourable conditions for such irreversible phenomena as pore blinding and adhesion at the interface between the membrane and foulant.

2.3.5.1 Pore Blinding

Pore blinding is the physical entrapment (or immobilisation) of a particle within the membrane structure. This definition includes particles trapped at pore entrances and within the main support structure. For pore blinding to initiate, the pore diameter will be similar to that of the particle. Yeasts are approximately two orders of magnitude larger than microfiltration membrane pores and so pore blinding is unlikely for such a system.

2.3.5.2 Adhesion and Adsorption

The interfacial accumulation of micro-organisms and macromolecules are referred to as adhesion and adsorption respectively (Norde [1981]). The distinction is important due to the mechanisms of microbial fouling. Micro-organisms rarely adhere directly to clean surfaces but rather to biopolymers adsorbed on the inert surface.

Even in fast-flowing streams, micro-organisms are known to adhere to surfaces. For example, on rocks in rivers or on boat hulls. Immobilised micro-organisms in a flowing stream enjoy an environment conducive to growth; benefiting from a steady source of nutrients, vigorous aeration, and excellent waste removal (Costerton *et al.* [1978], Ho [1986]).

Studies of adhesion of micro-organisms to inert surfaces has focussed upon bacteria as a result of their ecological, medical and economic significance. For example, the adhesion mechanisms of bacteria to teeth and boat hulls are well documented (Defrise and Gekas [1988]). In contrast to the wealth of data now available on bacterial adhesion, relatively little is known about the mechanisms by which yeasts attach to inert surfaces (Douglas [1987]). Of the few examples available the majority of data concentrates on the pathogenic yeasts (Douglas [1987]). Particular attention has been focussed on the yeast *Candida albicans*, the most versatile of the yeast pathogens, and its adhesion to human epithelial cells (Hurley *et al.* [1987]). The mechanisms of *Saccharomyces cerevisiae* adhesion to microfiltration membranes unfortunately are not well documented. However, analogies to colloidal and bacterial adhesion systems can be made to understand the potential interactions between *Saccharomyces cerevisiae* and the inert surface of a polymeric microfiltration membrane.

The colloidal approach to understanding the mechanisms of yeast adhesion is to consider the interaction between a rigid sphere and a flat, clean, inert surface. A colloidal sphere will adhere to a surface if the free energy of interaction between the colloid and the surface is negative (Harbron and Kent [1988]). This free energy results from the equilibrium between the four types of forces that may act between surfaces in aqueous solutions: electrostatic interactions, van der Waals forces, hydration forces, and steric forces (Defrise and Gekas [1988], Ho [1986]).

Electrostatic interactions result from the charges carried by the two interacting surfaces. Micro-organisms generally carry a net-negative charge at normal pH values. These charges may arise from the ionisation or dissociation of surface groups (mainly COO^-, NH_3^+ and PO_4^{3-}) or from the adsorption of ions from the bulk solution onto the surface. Most surfaces immersed in an aqueous medium also possess a net negative charge. To maintain neutrality, surface charges are balanced by counter-charge made

up of ions that are diffusely distributed in solution. This gives rise to a repulsive electrostatic double-layer, which is schematically represented in *Figure 2-7*.

The *van der Waals interaction* is the second term of the total interaction energy and is the result of electromagnetic fluctuations of the molecules composing both the micro-organism and the surface. These forces are attractive.

Hydration forces (also referred to as structural or hydrophilic forces) are short-range, repulsive forces, arising from the binding of water molecules to surfaces containing hydrophilic groups. Their strength depends on the energy needed to disrupt the ordered water structure resulting from the hydrogen bonds and to dehydrate the two surfaces as they approach each other. These forces can be regulated by exchanging ions of different hydration on the surfaces.

Steric interactions lead to repulsive forces due to the unfavourable free energy associated with different polymeric segments composing the cell surface.

Two models have been proposed to resolve the physical forces involved in cellular adhesion (Defrise and Gekas [1988]). Firstly, the Derjaguin-Landau-Verwey-Overbeek (DLVO) theory and secondly, the thermodynamic approach. DLVO theory considers the electrostatic mechanisms to be dominant and disregards hydration and steric effects. The opposite is true for the thermodynamic approach. There is no global model that takes all mechanisms into account. A further weakness of the models is the idealisation of the yeast cell. A large number of features which characterise micro-organisms have been neglected. Indeed, micro-organisms in general do not behave as inert colloids but rather are soft, non-spherical bodies surrounded by a diffuse layer of not very well-defined polymeric material, generally called glycocalyx. They are capable of metabolism, growth and possibly independent motion.

It has been suggested that micro-organism adhesion is preceded by a spontaneous adsorption of a macromolecular film on the surface. These films consist of polymeric material either secreted by the micro-organisms or found in the medium. The presence of polymers is of great significance to adhesion. Polymers are amphiphilic, having both positively and negatively charged sites on a single molecule. Ionic strength of solution affects molecule configuration through the degree of folding, determining

how many sites are available for adhesion. Polymers can be considered either flexible (sugars, non-globular proteins) or rigid (globular proteins).

As a result of their amphiphilic nature, protein molecules show a strong tendency to adsorb at interfaces. The affinity between a given protein and a surface usually increases with increasing hydrophobicity of that surface. This is due to the entropy gain resulting from hydrophobic dehydration. Water is displaced from the surface by protein, or dehydrated, which is obviously easier if the surface is hydrophobic.

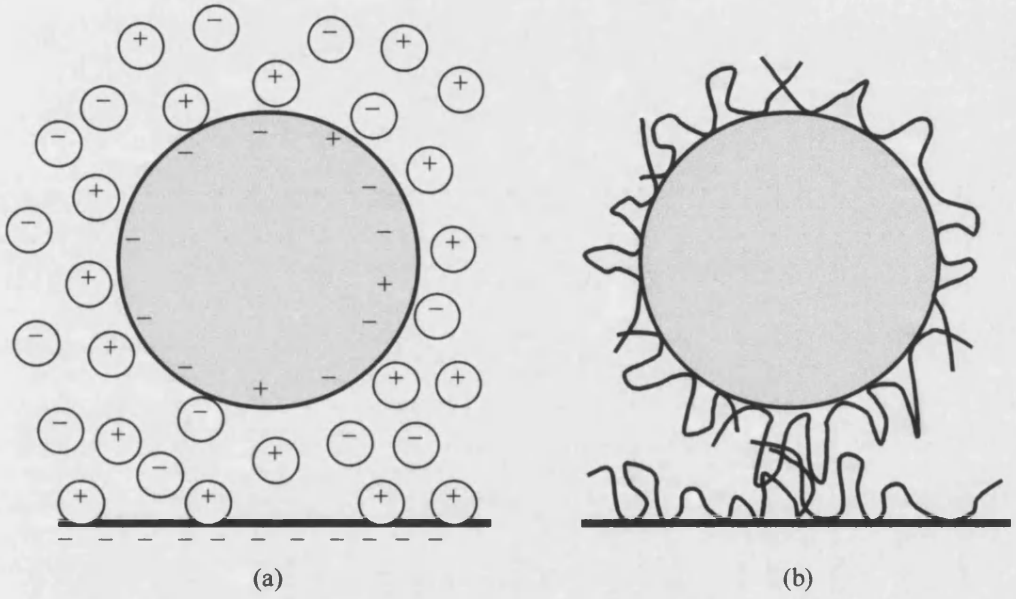

Figure 2-7: Schematic diagrams of yeast interaction with surfaces. The electrical double layer at a planar surface and around a spherical particle (a) and (b) polymer aspects (reproduced from Norde [1981]).

In summary, the interaction of micro-organisms with surfaces can be considered a three-stage process (Ho [1986]). The first stage is weak reversible adhesion due to long-range forces. The second stage is a firmer and non-specific adhesion by fimbriae and pili, involving formation of some hydrogen and ionic bonds. The third stage would be the formation of extracellular material such as polysaccharides either by the cell or by the bacterium. The first two stages would happen in very rapid succession of the order of milli- or even micro-seconds, while the third would be expected to happen more slowly depending on biosynthetic processes of the cells and micro-organisms.

It would be impossible or erroneous to conclude that one single mechanism dictates the adhesive or aggregating tendency of micro-organisms. In addition, different micro-organisms may use various means for adhesion under different culture conditions. At present, the situation is too complex for a global mechanism (Ho [1986]).

Interestingly, it has been discovered that the mechanism of bacterial adhesion to teeth enamel is due to the presence of glucans in the medium (Costerton *et al.* [1978]). Enzymes in the glycocalyx polymerise glucose into glucan, a long polysaccharide, which is insoluble in water. The important finding was that the glucan was able to adhere to the inert enamel surface of a tooth and subsequently attach the bacterial cell to the tooth. Once adhered, the polysaccharides can withstand large shear forces (not quantified by the author). The nature of the cell glycocalyx changes with age. This phenomenon may relate to observations of cleaning difficulty related to deposit residence times.

The yeast cell wall consists of a large number of secreted proteins, many of which are mannoproteins, and the structural polysaccharides glucan and chitin. The outer surface of the wall contains a cross-linked network of mannoprotein, the average composition of which is about 10% protein and 90% carbohydrate. It is therefore conceivable that the presence of glucan in the cell wall could play a major part in overcoming short range repulsive forces (*see Figure 2-2*).

In some applications, yeasts have been deliberately immobilised, for example in the vinegar and brewing industries. However, the binding forces of cells immobilised with the carrier-binding technique are reported to be weak and there is an inherent problem of autolysis and cell leakage (Nakanishi [1989]). Carrier-binding immobilisation includes physical, ionic and covalent bonding. Membrane yeast-fouling is analogous to carrier-binding immobilisation. It is therefore possible that yeast-fouling of membranes will be weakly bound and suffer from cell autolysis and leakage.

Yeast cell flocculation is dependent on an intricate interplay between electrostatic interactions, long distance van der Waals forces and also short distance interactions (Mozes *et al.* [1987]). The role of the latter is revealed by the influence of

hydrophobicity and, in the case of *Saccharomyces cerevisiae* flocculation, of molecular recognition phenomena.

2.3.6 Effect of Fouling on Transmission and Selectivity

Theoretically, an ideal MF process will retain particulates but allow the passage of solutes and macromolecules. However, the accumulation of a fouling layer presents an additional challenge to that of increased flow resistance. Cake layers above the membrane surface effectively act as a second membrane, often with greater selectivity than the membrane itself. Such cake layers have been reported to behave as ultrafiltration membranes, retaining proteins and other extracellular material (Glimenius [1985]). This is very significant. Product quality will alter and key components may no longer pass through the membrane. In the case of beer filtration for example, selectivity changes due to fouling are vital. Retention of aromatic and flavour compounds during beer clarification is highly undesirable. Membrane selection and operating conditions must be such that the beer is clarified through retention of yeast but the aromas and flavours pass through (Gan *et al.* [1997]).

MF membranes operating ideally should not retain proteins, which are orders of magnitude smaller than the pores. However, workers have shown that after preparation of a yeast-fouled membrane surface under static conditions, proteins were readily retained (Arora and Davis [1994]).

2.3.7 Analysis of Fouling Curves

It is widely accepted that the typical fouling curve, shown in *Figure 4-1 (p. 80)*, can be described in terms of multiple periods of single fouling mechanisms (Belfort *et al.* [1994]). Up to three significant periods have been postulated for the constant volume system (Schleup and Widmer [1996]). Initially, membrane porosity is high and every cell dragged to the membrane surface plugs a pore, leading to the steep linear gradient of flux decline. This is analogous to dead-end operation, comparisons to which have been the basis for modelling in this period (Romero and Davis [1994]).

Once all the available pore sites have been occupied, the rate of flux reduction decreases. Cells dragged to the cake surface subsequently may be partially compressed or re-organised, forming a more compact and less permeable cake.

Finally, there exists a period of steady state where the flux remains constant at a non-zero value. For permeate flux greater than the critical flux, cells are still being dragged towards the cake but with zero net flux reduction. Thus, at steady state, there is an equilibrium established between cells dragged to the surface and those returning to the bulk stream.

2.3.8 Flux Modelling

A model to predict flux based on knowledge of theoretical fouling mechanisms was first developed for constant pressure dead-end filtration by Hermia [1982]. This was later modified by Field and Arnot [1995] to incorporate cross-flow terms where appropriate. Four fouling mechanisms were postulated: cake, intermediate, standard and complete (n = 0, 1, 1½ and 2 respectively). The four equations associated with the four mechanisms were neatly unified by Field and Arnot as shown in *Equation 2-8*.

The model may be applied to any part or whole of the filtration data. However, for each application of the model a single dominant fouling mechanism is assumed. Therefore, to identify multiple fouling mechanisms, experimental data should be sectioned and the model applied to each in turn.

$$-\frac{dJ}{dt} = k\left(J - J^*\right)J^{(2-n)} \qquad \textit{Equation 2-8}$$

Complete blocking (n = 2) describes systems where each particle that reaches the membrane participates in pore sealing, which includes the assumption that particles are not superimposed upon one another. Intermediate blocking (n = 1) also assumes that any particle reaching a pore will seal it but is a less specific model in that particles are also assumed to settle on other particles to form cakes. The probability of pore blocking is evaluated. Standard blocking (n = 1.5) is much different, it assumes that the reduction in flux corresponds to an effective reduction of pore diameter due to progressive deposition on the pore walls. The filter is assumed to consist of capillary pores of constant diameter, as displayed by track-etched membranes. Cake filtration (n = 0) assumes that the porosity of the filter is unaffected but that the resistance to flow is a function of the packing depth and density.

2.3.9 Fouling Prevention

Before considering cleaning as the solution to membrane fouling, it is right that methods of fouling prevention should be highlighted. In industry, cleaning is a costly process. Thus, operating conditions should be optimised to ensure that fouling is minimal. Important considerations are the choice of membrane, feed pretreatment and the system hydraulics.

2.3.9.1 Critical Flux

An anomalous case, where fouling is not initiated, is the *strong* form of the critical flux (Field *et al.* [1995b]). Critical flux occurs at relatively low transmembrane pressure, when the drag forces acting on the cells are insufficient to overcome the drag initiation and/or repulsive forces between cell and membrane. Consequently fouling is not initiated. The *weak* form of the critical flux is thought to briefly initiate fouling, which quickly reaches a maximum.

Many hydraulic strategies minimise the net rate of fouling but critical flux minimises the absolute rate of fouling, and in the case of the strong form eliminates fouling. However, the benefits of zero fouling must be balanced against the low flux, which demands large membrane areas to achieve sufficiently high production rates; membrane cost is often the single highest capital cost, and is therefore a limiting factor to economical membrane plant production at critical flux.

2.3.9.2 Membrane Selection

Membrane material may greatly affect the performance of microfiltration processes. For example, hydrophobic membranes are known to have greater affinity for protein based media than hydrophilic membranes (Mulder [1991]). Therefore, selection of an appropriate membrane is a crucial, and process specific, consideration.

Hydrophilic and hydrophobic microfiltration membranes have been applied simultaneously by Stratton and Meagher [1994] for *Saccharomyces cerevisiae* harvesting. Hydrophilicity was found crucial with respect to membrane selection; even more so than pore size because the medium contained significant quantities of protein. Mulder [1991] also states that proteins generally adsorb tenaciously at hydrophobic surfaces and are less readily removed than at hydrophilic surfaces.

Another disadvantage of hydrophobic membranes is that water will not generally flow through them at low pressure unless they are pre-treated with a polar organic solvent, for example, isopropanol.

2.3.9.3 Pretreatment

Pretreatment methods employed industrially include heat treatment, pH adjustment, the addition of complexing agents, chlorination, adsorption onto active carbon, chemical clarification, and pre-microfiltration (Mulder [1991], Scott [1995]). Fouling reduction often starts with developing a suitable pretreatment method. Unfortunately, considerable time and effort is often spent on membrane cleaning when pretreatment has been overlooked.

2.4 CLEANING: REMOVAL OF FOULING DEPOSITS

Fouling is clearly a limitation to the wider application of membrane separation processes. In the absence of an economic process that produces high flux without initiating fouling, cleaning is found necessary to periodically regenerate membrane permeability.

Both cleaning and fouling can be characterised in terms of the energy involved. Jennings [1965] was the first worker to recognise the importance of the energy phenomena involved in the process of soil deposition and cleaning. He concluded that the cleanliness of a surface was an unnatural state, that the fouling process is a spontaneous phenomenon corresponding to a decrease of the free energy of the system and that soil removal requires a sufficiently large energy supply to break the surface-soil bond. Cleaning must reduce the free energy further in order to replace the foulant. Energy must therefore be input to the system for cleaning to take place, which can be supplied in any or all of the following three forms:

(i) *Kinetic energy*: in the form of turbulence.

(ii) *Thermal energy*: in the form of solution temperature.

(iii) *Chemical energy*: chemical reactions between the detergent components and the soil.

2.4.1 Definition of Membrane Cleaning

Trägårdh [1989] has defined membrane cleaning as:

> "*a process where the membrane is relieved of materials which are not an integral part of the membrane.*"

This definition neatly unifies the four possible methods of foulant removal: hydraulic, mechanical, electrical and chemical cleaning.

2.4.2 Hydraulic Cleaning

Hydraulic cleaning comprises all methods of foulant removal resulting from turbulence or reversal of transmembrane pressure. Methods of hydraulic cleaning include the use of back flushing, cross flushing, membrane rotation and secondary

vortex flows. Hydraulic cleaning can operate in parallel to processing, rather than in series as is necessary for chemical cleaning. As mentioned previously (see *2.2.4.1*), the fundamental operation of cross-flow is also a method of turbulence generation and hence hydraulic cleaning.

2.4.2.1 Back Flushing

Back flushing involves periodic reversal of the transmembrane pressure. Permeate is forced in the reverse direction with the effect of removing foulant accumulated on the retentate side. The resulting flux profile is a 'saw-tooth' type; periods of flux loss followed by sharp gains (Mulder [1991]). Cross-flow microfiltration with high frequency reverse filtration has been reported by Redkar and Davis [1995] to be beneficial for yeast cell harvesting. Under favourable reverse transmembrane pressure, complete flux recovery was reported. However, it is far more common for the average flux to gradually decay with time (Scott [1995]).

Improvements in productivity are at the expense of increased power consumption and limits the choice of membrane configuration. Flat sheet and spiral wound modules do not have the required mechanical strength to be compatible with back flushing, tubular and hollow fibre modules do.

2.4.2.2 Cross Flushing

Occasionally, processing at zero transmembrane pressure for relatively long periods (termed cross flushing) has been reported to be capable of good flux recovery during yeast microfiltration (Kuruzovich and Piergiovanni [1996]). Cross flushing is carried out between short harvesting periods of between thirty seconds and six minutes for cleaning times of between five and ninety seconds. However, potential production is lost during cross flushing, which is a significant percentage of the harvesting time. Therefore, economics may determine that cross flushing for long periods is impractical.

2.4.2.3 Rotating Disk Membrane Modules

Rotation of a flat sheet membrane within a purpose-built module creates high shear at the membrane surface without incurring a high transmembrane pressure. Yeast cell harvesting improvements have been reported by Lee *et al.* [1995] and Kroner and Nissinen [1988]). This was presumably due to reduced fouling as a direct result of the

high surface shear. However, rotating disk membrane modules have the disadvantage of increased power consumption and heat dissipation. The packing density of a rotating disk module accommodating a single flat sheet is significantly the lowest of all configurations (Zeman and Zydney [1996]).

2.4.2.4 Secondary Vortex Flows

Secondary vortex flows aim to provide good fluid mixing in a direction perpendicular to the membrane surface, which minimises concentration polarisation and fouling. Improved mixing arises from generated turbulence, even at low Reynolds numbers.

Improved flux has been reported using helical flows (Field *et al.* [1995a]), pulsed flows (Finnigan and Howell [1989], and Howell *et al.* [1993]) and oscillatory flows (Bellhouse and Millward [1995]) in baffled systems. The idea of vortex mixing arose from the vortices generated during each heartbeat (Bellhouse *et al.* [1968]). Enhanced performance has also been reported for flow around curved channels (Mallubhotla *et al.* [1995]). At a sufficient rate of flow, centrifugal instabilities (called Dean vortices) at the membrane surface depolarise the build-up of suspended particles.

2.4.3 Mechanical Cleaning

Mechanical cleaning involves scouring a fouled surface with abrasive material. *In situ.* mechanical cleaning is limited by the mechanical strength and accessibility of the membrane surface (Scott [1995]). A mechanical cleaning method currently in use is to pass slightly under-size sponge balls through tubular systems at high velocity (Mulder [1991]).

2.4.4 Electrical Cleaning

Bowen *et al.* [1989] described two innovative techniques for reducing fouling during cross-flow microfiltration. The first technique, termed '*in situ.* intermittent electrolytic membrane cleaning' (IIEMC), makes use of brief intermittent electric field pulses during processing to clean membranes without the interruption of the separation process. The second technique, termed '*in situ.* electrolytic membrane restoration' (IEMR), restores membrane permeability under mild chemical conditions. The fundamental cleaning mechanism is simple. Bowen [1993] describes that voltage applied across the membrane causes the formation of micro-bubbles at the membrane surface which push foulant material out into the feed stream. The foulant materials are

then carried along by the cross-flow, and negatively charged materials can be electrophoretically transported away from the membrane surface.

Special module designs are required to introduce the charge to the membrane, which limits selection. Membranes must be sufficiently conductive, generally metallic.

2.4.5 Chemical Cleaning

Chemical cleaning is usually performed as cleaning in-place (CIP) by filling the retentate channel with a cleaning solution (or detergent) from a separate tank (Romney [1990]).

Chemical cleaning is the most important and extensively used method for controlling fouling in membrane separations (Scott [1995], Sandu *et al.* [1985]). Chemical cleaning involves replacing the process stream with a chemical stream that reacts with, and removes, the foulant from the membrane. Chemical cleaning can potentially remove unwanted heat and/or mass transfer resistance and microbial contamination. The details of chemical cleaning are discussed further in section *2.5*.

2.4.6 Measurement of Cleaning Efficiency

Membrane cleaning efficiency is commonly assessed by comparing the clean water fluxes from before and after cleaning. However, a good water flux does not guarantee a good operational flux (Trägårdh [1989]). Neither does a good water flux guarantee cleanliness. Membrane porosity is usually low, the pores accounting for a fraction of the surface. However, a low water flux is an indication that cleaning was not sufficient.

Food surfaces are often swabbed and the samples incubated to determine the presence of viable cells. Such tests unfortunately take days to complete and so are not suitable for placing *in situ.* to monitor membrane cleaning.

Visual inspection of cleaned surfaces can give a good indication of their state of cleanliness. Contaminants too small to be observed with the naked eye may well be apparent when studied with microscopy. However, some foulants, such as surface-active agents, can not be viewed, even using electron microscopy, which is suitable for particulates and agglomerated macrosolutes.

2.4.6.1 Flux Recovery

Cleaning, with respect to permeate flux, is essentially the reduction of the membrane fouling resistance, R_f. As the permeate flux J decreases at constant transmembrane pressure ΔP_{TM} and viscosity μ_p the fouling resistance increases.

$$R_f = \frac{\Delta P_{TM}}{\mu_p J} - R_m \qquad \textit{Equation 2-9}$$

At any moment in time, fouling resistance is therefore expressed by *Equation 2-9*. All required parameters are measurable experimentally. Therefore, resistance analysis is well suited to cleaning studies. However, to fulfil the earlier definition of cleaning, there must not even be a trace of foulant. Resistance alone can not ascertain this. It is possible for material to adhere to areas between the pores, which by definition requires cleaning, but does not affect porosity.

2.4.6.2 In situ. Surface Visualisation

Techniques to determine surface cleanliness that are more rigorous than resistance calculations are known but difficult to place *in situ.* and can be destructive, such as scanning electron microscopy. Some non-destructive methods of *in situ.* measurement of surface cleanliness are presently under development. Karlsson *et al.* [1997] have reported encouraging results using ellipsometry accurately measure surface foulant depth. The system at present is unfortunately applicable only to small areas of homogeneous deposit. Takahashi *et al.* [1991] reported the use of an ultrasonic polymer concave transducer to also calculate surface foulant depth. The challenge of calibrating the equipment for the changing fluid rheology was overcome to give accurate data verified by microscopic visualisation.

2.4.6.3 Ex situ. surface visualisation

An alternative to *in situ.* analysis is *ex situ.* visualisation, such as microscopy, which is well defined and readily accessible. Samples can be taken over a range of cleaning periods, analysed and combined to create a dynamic model.

Microfiltration can be stopped and the module carefully opened to reveal the membrane. With care, a sample can be removed from the membrane, pre-treated and observed under an electron microscope.

2.5 CHEMICAL MEMBRANE CLEANING

Chemical cleaning involves contacting the fouled membrane with appropriate aqueous agents. In time the adhesive bonds between foulant and membrane are weakened, or broken, and the scouring action of the cross-flow feed completes removal. Industrial chemical cleaning is usually performed using 'cleaning in-place' (CIP) techniques by filling the retentate channels of the membrane module with cleaning solution from a separate cleaning tank. The flow of cleaning solutions is generally provided by the feed or circulation pumps, rather than by dedicated cleaning pumps (Romney [1990]).

A system comparable to membrane cleaning is hard surface cleaning, which has been analysed extensively in the dairy and textile industries. However, in addition to surface fouling, membranes can suffer from depth fouling. A simplifying approach may be to consider internal membrane fouling as hard surface fouling but in a different plane. The flow of aqueous cleaners is also significantly different. Flow can be parallel and perpendicular to the membrane surface rather than just parallel for hard surface cleaning.

2.5.1 Detergents: Definition and Properties

The word 'detergent' can often be interpreted very differently. In an attempt to resolve the confusion, Bourne and Jennings [1963a] proposed the following unifying definition:

> *"A detergent is any substance that, either alone or in a mixture, reduces the work requirement of a cleaning process."*

This definition is based on the premise that the common factor of detergency is a work requirement. The principal function of a detergent is therefore to reduce the work requirement. In other words, detergents are used to make cleaning easier.

The definition proposed by Bourne and Jennings [1963a] is consistent with the meaning of the word 'detergency'. It does not specify any special chemical group of compounds. It includes soaps. It includes the surface-active compounds that have some power of detergency, and excludes those that do not. It includes substances with strong powers of detergency (such as sodium hydroxide or nitric acid) that are not surface-active; it includes substances that may have a synergistic effect (such as the

polyphosphates); and substances that restrict re-deposition of removed soil (such as EDTA). It is a broad enough definition to include detergents that are used in non-aqueous systems. It includes solvents and cleaners that function by chemical degradation (such as strong acids), since these reduce the work requirement to zero. It does not include abrasives, which do not reduce work requirement but increase efficiency with which work is applied to the soil.

In present day terminology, 'detergent' is interchangeable with 'cleaning agent' (Wright [1990]). Therefore, the original definition given by Bourne and Jennings [1963a] applies equally to cleaning agents and detergents.

Detergent products are often formulated from a wide range of raw materials, each with specific properties suitable for cleaning. The choice of detergent(s) should be process and foulant specific, depending upon the type of membrane, the type and severity of fouling. However, there are several types of detergent that are commonly used including acids, alkalis, surface-active agents, complexing agents, enzymes and disinfectants.

2.5.1.1 Alkalis

Alkalis are effective cleaning agents for biological/organic foulants (Zeman and Zydney [1996]). There are a large number of available alkaline cleaners including hydroxides, carbonates and phosphates. Alkalis generally have the ability to saponificate fats and solubilise proteins to some extent.

Sodium hydroxide is a relatively simple and cheap alkaline cleaner, which is also the most alkaline due to its complete dissociation into Na^+ and OH^-. Sodium hydroxide has good powers of detergency for fatty-type soils and protein deposits by virtue of its ability to form water-soluble chemical products (Wright [1990]). It is also a relatively good and inexpensive disinfectant, which is the reason for its common use as the basis of many commercial detergent formulations. Disinfectants are shown later in *2.5.1.6*. However, sodium hydroxide is a relatively poor wetting agent.

2.5.1.2 Acids

Acids are typically used to dissolve precipitations of inorganic salts or oxide films, for which alkalis have very little power of detergency. Nitric acid or phosphoric acid are often used for membrane cleaning (Trägårdh [1989]). The disadvantage of acid

detergents is their inability to remove protein and fat as effectively as alkaline detergents (Kane and Middlemiss [1985]). Acids may also have a subsidiary role as sanitising agents.

Concentrated acids can be a great corrosion threat. Nitric acid has found favour for CIP in the dairy industry due to its compatibility with stainless steel, unlike hydrochloric acid.

2.5.1.3 Surface Active Agents

Surface active agents (or surfactants) typically improve wetting, by lowering the surface tension, they increase contact between the soil and the detergent solution (Wright [1990]). If the soil particle is an aggregate of small particles, the surface active agent will penetrate the interstices and cause disintegration, so yielding smaller particles, which are more easily dispersed. Surfactants have a split solubility characteristic, with one portion of the molecule being hydrophilic and the other portion being hydrophobic. Surfactants are available with a wide range of chemical structures, and they can possess neutral (non-ionic), negatively charged (anionic), positively charged (cationic) and amphoteric hydrophilic groups, depending on how they dissociate in aqueous solutions (Ottewill [1984]).

Microfiltration of anionic and non-ionic surfactants through ceramic and PVDF membranes has been reported with respect to the water flux (Field *et al.* [1994]). All surfactants tested interacted with the membrane, causing significant flux reduction over a twenty minute period.

Humphries *et al.* [1987] found that most non-ionic surfactants tested had an anti-adhesive effect on hydrophobic but not hydrophilic surfaces for bacteria. If adsorption is a minimum for low-energy solids, the treatment of surfaces with chemicals, which reduce the free energy of the solid, should decrease micro-organism adhesion.

2.5.1.4 Sequestrants

Sequestrants (or chelating agents) form stable complexes with metal cations, such as Ca^{2+} and Mg^{2+}, which are soluble in water. Therefore, they are effective in removing inorganic scale, and preventing redeposition. The most effective organic sequestrant is EDTA (ethylenediamine tetraacetic acid).

2.5.1.5 Enzymes

Enzymes are highly specific catalysts that assist in the breakdown and removal of organic matter. Although enzymatic cleaners tend to be relatively expensive, they can be important components of formulated cleaning solutions for membranes that are unable to withstand elevated temperatures, strong chemicals, or pH extremes, such as cellulose acetate. Enzymes are available that degrade proteins (proteases), fats and oils (lipases) and starches (amylase).

Proteases are the most commonly used enzymes in membrane cleaning applications, due to the importance of protein fouling in many membrane systems and the inherent difficulty of removing these proteins from the membrane surface (Zeman and Zydney [1996]).

Today, progress in membrane technology has significantly increased tolerance to extremes of pH and temperature, reducing the demand for enzyme-based detergents.

Enzymes are best used at a temperature that corresponds to optimum activity. In general the optimum enzyme temperature is below the recommended cleaning temperatures of other components of detergent formulations. Ideally enzymes could be used at higher temperatures without compromising activity or denaturation. To this aim, work is presently studying the enzymes isolated from sea dwelling worms that can tolerate temperatures up to 80°C (Bruggeman [1998]). Heat-tolerant enzymes have exciting biocatalyst possibilities for the future advancement of detergents.

2.5.1.6 Disinfectants

Disinfectants destroy all living pathogenic micro-organisms and reduce the numbers of other micro-organisms. Membrane systems in the dairy and potable water industries are typically disinfected on a daily basis, while systems in the pharmaceutical industry must be sterilised prior to each use.

Sodium hypochlorite (NaOCl) is probably used most extensively for the chemical disinfection of membrane systems, although it cannot be used even in dilute solutions for polyamide membranes (Zeman and Zydney [1996]).

It is important to note that disinfection is defined as the destruction of pathogenic micro-organisms but does not specify their removal. In contrast, cleaning of micro-

organism based deposits focuses on the quantities removed but does not specify the required viability. This is not to say that disinfection is unimportant, it is vital, but should not be confused with the term cleaning.

2.5.2 Rinsing

Often the first step of a CIP procedure is to rinse away loosely bound or unbound material with water (Scott [1995], Romney [1990]). If the degree of fouling is high, a large proportion of the cleaning agent can be consumed in the bulk, if the detergent has no buffering capacity such as sodium hydroxide (Zeman and Zydney [1996]), which would subsequently be unavailable for cleaning. Thus, it is important that as much as possible of the loose deposit is rinsed from the membrane before application of detergents.

Rinsing is also the final step of the cleaning process. Following chemical cleaning, all traces of the detergent must be removed, or they too would be regarded as foulants.

2.5.3 Cleaning Reactions

At the heart of any cleaning process is the chemical reaction. Without an input of energy from the detergent, the foulant-membrane bonds will not be broken. The cleaning reaction is heterogeneous, taking place between the liquid phase detergent solution and the solid phase deposit. As a heterogeneous reaction it can be divided into mass transport and reaction processes. According to Plett [1985], cleaning reactions can be divided into the following six stages:

1. *Bulk reaction of detergents*. Consumption of detergents through reaction with foulant in the bulk phase. As mentioned previously, rinsing is essential to minimise the mass of the initial deposit, minimising detergent consumption.

2. *Transport of detergents to the fouled surface*. The mass transport of detergents from the bulk flow through the boundary layer at the solution-membrane interface. Laminar sub-layer thickness is a function of the bulk turbulence.

3. *Transport into the fouled layer*. Detergents can be transported into the fouled layer by capillary or molecular diffusion. Due to their lower surface tension, surface-active agents have the ability to penetrate through pores and crevices.

Due to their adsorption characteristics, they can be adsorbed onto the surface, thereby weakening the foulant-membrane bond.

4. *Cleaning reaction.* The process that takes place when the detergent is exposed to the fouled layer can be subdivided into physico-chemical transformations and chemical reactions. The physical and physico-chemical transformations which take place can include melting, mechanical and thermal stress, wetting, soaking, swelling, shrinking, solvation (e.g. the solution of soluble substances), emulsification, deflocculation and desorption. The chemical reactions that can occur include hydrolysis, peptisation, saponification (to a lesser extent), solubilisation (by the formation of soluble salts through chemical reactions), dispersion, chelation, sequestering and suspending. These reactions always produce some soluble products or, at least, disperse some products. These reactions will help to overcome the cohesive forces between foulant particles and adhesion forces between fouling particles and the membrane surface.

5. *Transport of cleaning reaction products back to the interface.* Mechanisms are as for transport into the fouled layer.

6. *Transport of products back to the bulk solution.* The cleaning reaction products will be transferred through the boundary layer due to concentration gradients (back diffusion) or turbulence. When the mechanical, thermal stress and other physical, physico-chemical and/or chemical processes have weakened the foulant-surface and foulant-foulant bonds, larger sections of the fouled layer can be detached. The flow of the cleaning solution under turbulent conditions will cause erosion of the fouled layer. This mechanical cleaning mechanism will be enhanced if the foulant-foulant bonds are weakened through physical changes or chemical reactions.

These six stages do not necessarily always occur. In specific cases, some stages will be by-passed. When cleaning equipment with fatty fouling for example, it may be necessary to melt the fat (there after the oil could simply be eroded away by hot water), or detergent may be added to emulsify the oil, or it may be dissolved using a suitable solvent.

2.5.4 Industrial Chemical Cleaning

Before examining the details of foulant removal, it is important to first have an appreciation of the overall process. The two available industrial cleaning practices are cleaning out-of-place (COP) and cleaning in-place (CIP). CIP being by far the most commonly used method (Romney [1990]).

2.5.4.1 Cleaning Out-of-Place (COP)

Cleaning out-of-place (COP) involves the dismantling of fouled process equipment, which is then manually cleaned. Being labour intensive, the process is slow, costly and subject to human error. In the past, COP was standard industrial practice but has now been superseded by cleaning in-place.

2.5.4.2 Cleaning In-Place (CIP)

Cleaning in-place (CIP) takes place *in situ.* eliminating the need for dismantling. During CIP, processing is temporarily halted and suitable aqueous cleaning agents are recirculated around the system. The system is then rinsed to remove traces of the cleaner and then processing is resumed. It has become apparent that CIP of industrial equipment by means of chemical solutions is, in many cases, safer and more economical than the older, labour intensive, mechanical methods (McCoy [1984]).

CIP cleaning strategies must be robust, as deposits remain unreachable within the process equipment. Visualisation and analysis of the deposits is not possible. A protocol must be in place that is sufficiently robust to be effective when the foulant varies slightly from the model.

A typical CIP cycle in the dairy industry consists of an initial rinse, to remove loose bound material; a caustic clean; a rinse; an acid clean; and a final rinse (Romney [1990]).

2.5.5 Characterisation of the Fouling Layer

In order to clean a membrane (or substrate), it must be assumed that the foulant (or soil) is irreversibly bonded to it. If no bond exists, then it must be assumed that the dirt will fall off, or at worst, it can be rinsed off. Unless there is the possibility that unbound dirt can block narrow flow channels, it does not present a serious cleaning problem. Several bonding mechanisms can exist between a substrate and the soil. In

most cases there is more than one bonding mechanism present, but in all cases it is necessary to weaken or break the bonds.

Components of an isotonic yeast suspension include sugars, lipids and proteins at the cell wall and minerals in the media. *Table 2-3* indicates some soil characteristics of these components, according to their relative ease of removal as found within the dairy industry.

Component on surface	Solubility characteristics	Ease of removal	Changes induced by heating
Sugar	Water: soluble	Easy	Caramelisation
Lipid	Water: insoluble	Difficult (Good with surfactants)	Polymerisation
	Alkali: Poor		
	Acid: Poor		
Protein	Water: Poor	Difficult	Denaturation
	Alkali: Good	Good	
	Acid: Medium	Difficult	
Mineral Salts - monovalent	Water: soluble	Easy to difficult	Interactions with other constituents
	Acid: soluble		
Mineral salts - polyvalent	Water: insoluble	Easy to difficult	Interactions with other constituents
	Acid: soluble		

Table 2-3: Soil characteristics (Harper [1972])

In the dairy industry, soils can be categorised into two broad headings with respect to cleaning, as defined by Romney [1990]:

Organic soil, mainly of plant or animal origin, which is often susceptible to chemical reaction with alkaline detergents.

Inorganic soil, mainly of mineral origin, which is often susceptible to chemical reaction with acidic detergents.

2.5.6 Yeast-Fouled Membrane Cleaning Examples

At the time of writing, to the authors knowledge, there are no other published chemical cleaning studies dedicated to the systematic cleaning of deposits formed during yeast harvesting using membrane separation. Yeast fouling studies are relatively well published, as yeast is often chosen as a model micro-organism.

Table 2-4: Cleaning strategies for the removal of deposits formed during the cross-flow microfiltration of yeast suspensions.

Reference	Filtrate	Module	Membrane	Cleaning Procedure
Russotti *et al* [1995]	Recombinant yeast	Flat sheet	PVDF	Primary rinse with alternating direction of flow followed by ten secondary rinses. Cleaned with 500 ppm sodium hypo-chlorite solution recirculation for 20 minutes at 25°C.
Bell and Davies [1987]	Oleaginous yeast (*A. curvatum)*	Cartridge Hollow fibre	Acrylic PS	Rinsed with water at 40°C then cleaned with 0.5 wt% sodium hydroxide.
Taddei *et al* [1990]	Cider broth	Flat sheet	PVDF	First clean with 0.2% *Terg-A-Zyme* at 50°C for 60 min. Second clean with 50 ppm sodium hypochlorite 35°C for 30 min. Third clean with 0.1% nitric acid at 35°C for 30 min.
Stratton and Meagher [1994]	Culture broth	Multiple flat sheet	PVDF, NYL, PES, PS	Slow primary water rinse. Clean with 0.5% *P53 Ultrasil* 45 min at 45°C. Final water rinse at 45°C

However, in rare cases, yeast fouling studies have included the cleaning protocols used for membrane regeneration. Summaries of example protocols are presented in *Table 2-4*. The protocols used were not the result of an optimised cleaning study but those found to reliably restore membrane permeability. It is highly likely that extreme conditions were used to ensure cleanliness with a great likelihood of excess. The small number and variety of cleaning approaches is testament to the current lack of published cleaning data.

To date, chemical membrane cleaning in general has received much less attention than hydraulic cleaning or membrane fouling. In addition, recent cleaning research has been focussed almost exclusively on challenges within the dairy industry. However, knowledge from such systems has started to be transferred to membrane systems. For example, the removal mechanisms of whey proteins from hard surfaces (Bird [1993], and Gallot-Lavallée and Lalande [1985]) has recently been transferred to membrane systems (Bartlett *et al.* [1995], and Bird and Bartlett [1997]).

The lack of fundamental membrane cleaning data does not reflect its importance. In the absence of a foulant-free system, cleaning in-place is a common feature of most membrane separations, which is an expensive process and can occur daily (Zeman and Zydney [1996]). Although advances in membrane technology perhaps increase the periods between cleans; the need to clean has not yet been eliminated. It should also be noted that regular disinfection is a requirement of hygienic workplaces, regardless of process efficiency. Therefore, it remains to be seen whether standards of hygiene will dictate that cleaning should still be applied to systems with little or no fouling.

In the absence of fundamental data regarding the cleaning mechanisms of yeast-fouled membranes, analogies may be drawn with similar systems, such as protein deposit cleaning. In fact, yeast suspension contains proteins both in the media and in the cell wall. As has already been seen, protein is the most tenacious of deposits in the dairy industry. Therefore, protein fouling may be a key to yeast fouling.

2.5.7 Protein Cleaning

Removal of whey proteins (a model foulant for milk) from a stainless steel hard surface has been characterised by Gallot-Lavallée and Lalande [1985] and Bird [1993]. They reported that whey protein removal was not proportional to sodium

hydroxide concentration as would be expected, but that a sodium hydroxide concentration of 0.5 wt% corresponded to optimal removal. Visualisation of the whey protein morphology change on contact with the sodium hydroxide was central to understanding of this phenomenon. As sodium hydroxide concentration increased up to 0.5 wt%, the whey protein deposit voidage increased up to a maximum. Above the optimal concentration, the whey protein voidage began to decrease. Hence, at an optimal sodium hydroxide concentration, the whey protein deposit had minimum mechanical strength. The same optimal behaviour has also been reported for a whey protein-fouled membrane system (Bird and Bartlett [1997], Bartlett *et al.* [1995]). The analogy between hard surface and membrane cleaning was particularly close if the permeate side was closed, i.e. producing no permeate.

Chemical cleaning of a polysulphone membrane fouled with bovine serum albumin (BSA) and whey proteins has also been reported by another worker to display some optimal behaviour (Muñoz-Aguado *et al.* [1996]). The detergents used were a commercial enzyme cleaner (*Terg-A-Zyme*), a model enzyme (α-chymotrypsin) and a cationic surfactant (cetyl-trimethyl-ammonium bromide [CTAB]). Removal of BSA with *Terg-A-Zyme* displayed a maximum at 0.4 wt%, significantly lower than the concentration of 0.75 wt% recommended by the supplier. Cleaning efficiency with the other cleaners increased with temperature and concentration up to the maximum tolerated by the membrane.

In another study, it was found that cleaning of BSA deposits fouled at pH 5 was best with hydrochloric acid and sodium hydroxide, but when BSA was fouled at pH 7 it was best removed with CTAB (Kim *et al.* [1993]). This was thought due to the electrostatic interactions between the fouled layer and the detergents.

CHAPTER 3 - MATERIALS AND METHODS

3.1 MATERIALS

Materials used have been classified into the following categories: experimental apparatus, membranes, consumables and utilities.

3.1.1 Experimental Apparatus

A purpose-built experimental apparatus was designed, constructed and commissioned as shown schematically in *Figure 3-1*. To aid visualisation of the apparatus, colour photographs can be seen in *Figure 3-2* and *Figure 3-3*.

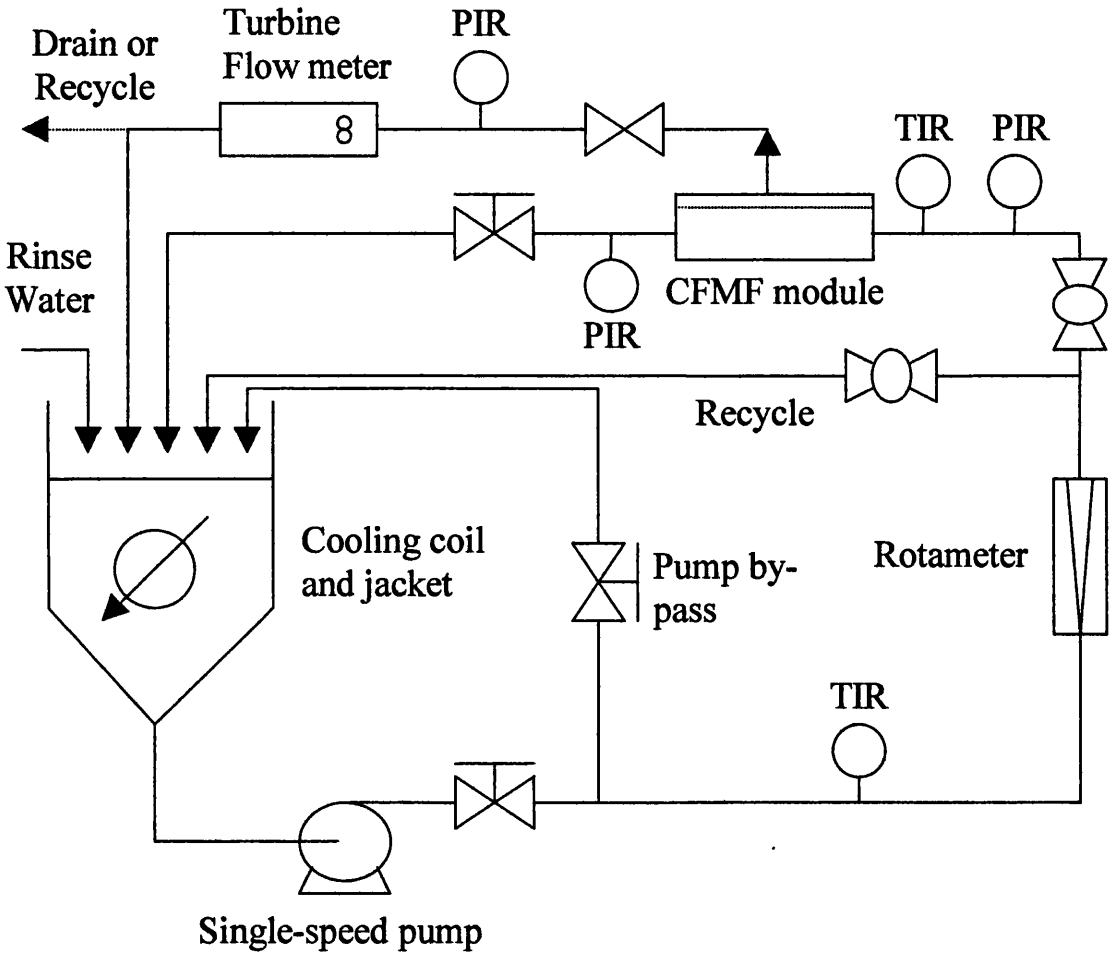

Figure 3-1: Schematic representation of the purpose-built fouling, rinsing and cleaning apparatus.

Fouling, rinsing and cleaning operations were all carried out on the same versatile apparatus. The apparatus was designed to achieve process conditions that would be used in an equivalent full-scale process. The equipment achieves typical full-scale velocities, temperatures and pressures but on pilot-scale equipment.

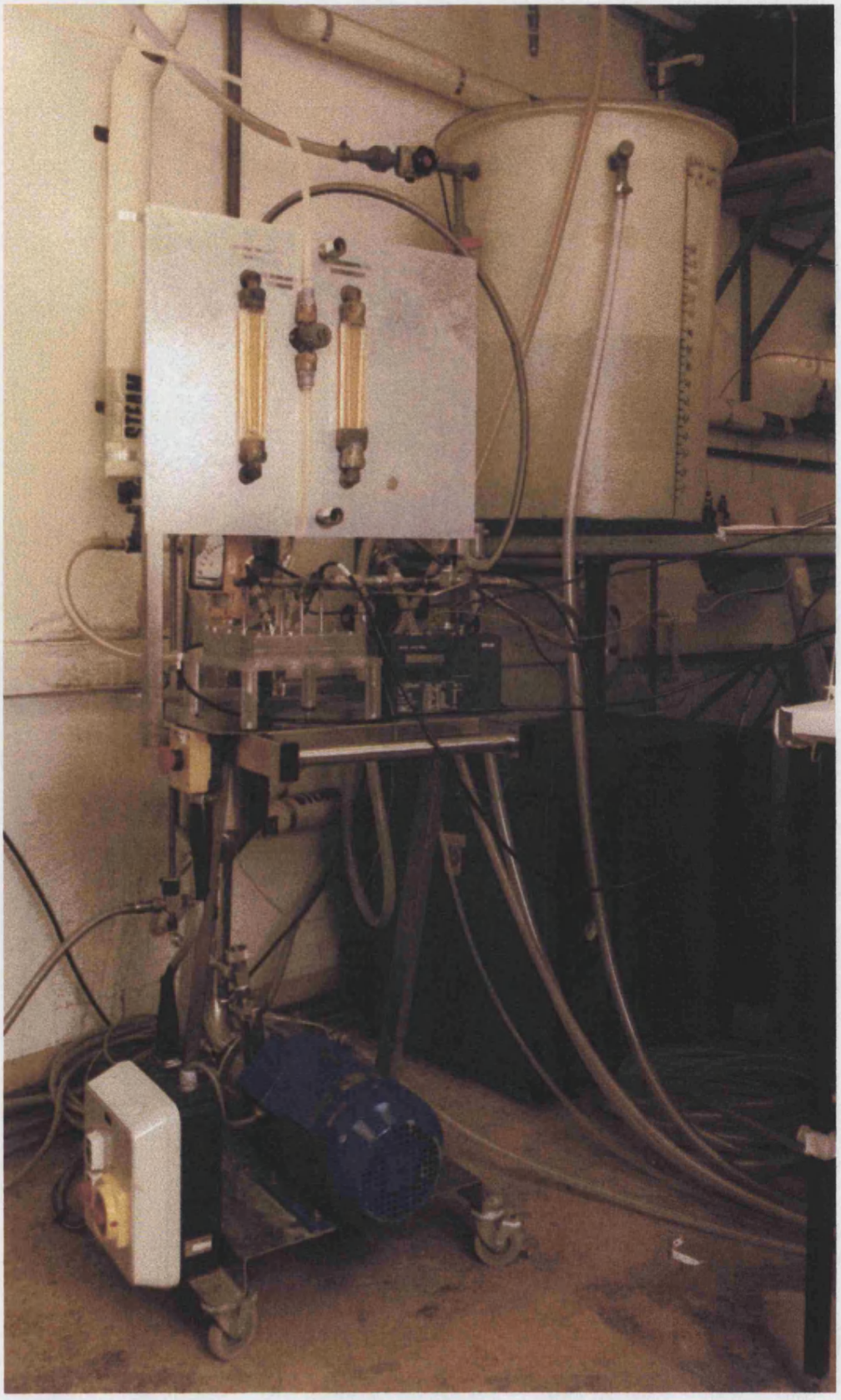

Figure 3-2: Front view photograph of the experimental fouling, rinsing and cleaning apparatus.

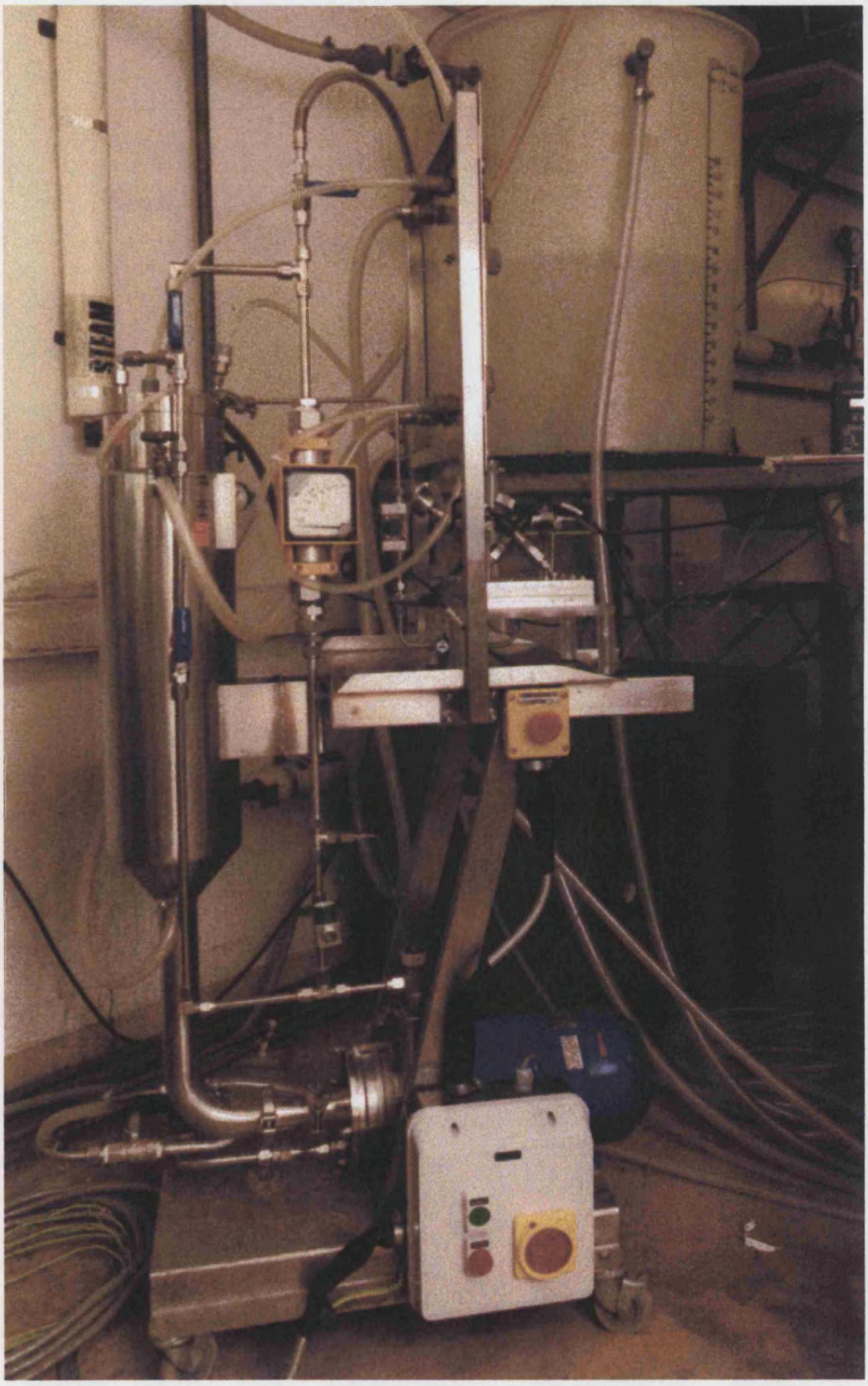

Figure 3-3: Side view photograph of the experimental fouling, rinsing and cleaning apparatus.

3.1.1.1 Membrane Module

In any MF process, the membrane module lies at the heart of the apparatus. Therefore, selection of an appropriate module assessed the relative advantages and disadvantages of all module configurations; flat sheet, tubular, spiral wound and hollow fibre (*see 2.2.3*). The critical selection criteria was the ease of membrane removal. In the absence of an *in situ.* visualisation technique, membrane removal from the module was essential for *ex situ.* scanning electron microscopy, which could be compared with the corresponding flux data. Other selection criteria were the industrial relevance and hydrodynamic compatibility of modules. Ultimately, a flat sheet module was selected, as it is the only module where the membrane is considered truly removable. In fact at the laboratory scale, single membranes can be considered disposable.

The flat sheet module used in this study is shown in *Figure 3-4*. The design was first introduced by Aimar *et al.* [1989] who validated the flow distribution between channels using a high-speed video camera and a Perspex module.

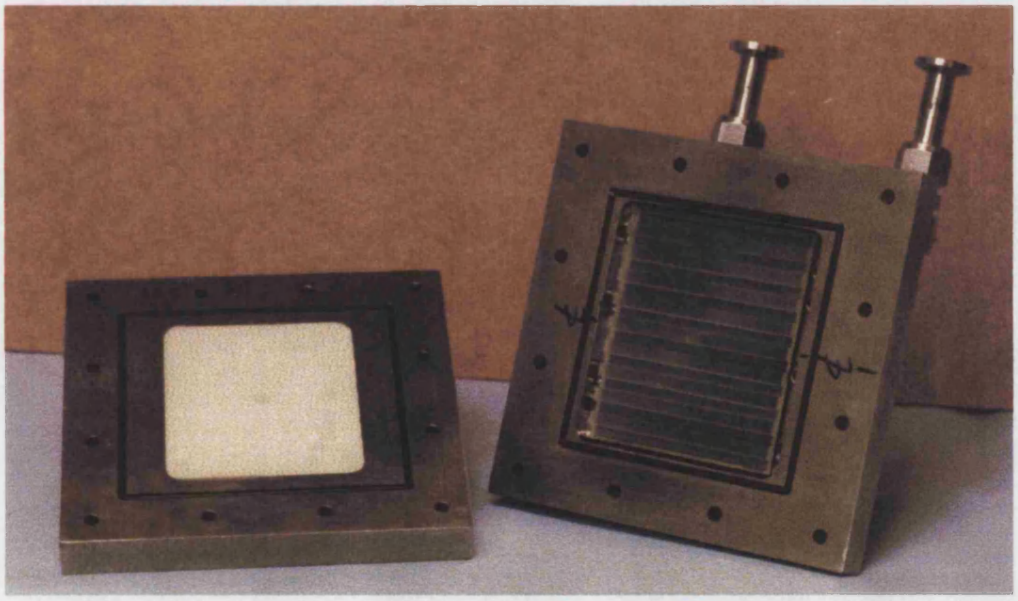

Figure 3-4: Photograph of the experimental flat sheet microfiltration module.

The module accommodates a single flat sheet of membrane. Replaceable Perspex inserts within the module allow channel dimensions to be altered, giving great flexibility. However, to allow comparison, all experiments used a module insert with ten channels, each of 3 mm height and 5 mm width. Typical industrial channel dimensions lie in the range 0.3 - 10 mm (Zeman and Zydney [1996]). When the Perspex insert is in place the membrane area available for permeation is 4.2×10^{-3} m^2.

The lid and base of the membrane module are bolted together in twelve places. A double layer of rubber seals between the lid and base prevents leakage. Care was taken when replacing and tightening the module lid due to the risk of membrane rupture, which can result from over-tightening and uneven distribution of force.

3.1.1.2 Permeate Flow Measurement

MF is typically associated with relatively high permeate flow rates suitable for measurement with an in-line flow meter or by direct weighing. An alternative technique for measuring relatively low permeate flux is the bubble flow meter developed by Bishop and Sanders [1989].

In this study, permeate flux was measured with a small turbine flow meter (Titan Enterprises Ltd., 203-231). The listed flow range is 100-5000 L m^{-2} hr^{-1} with a linearity of ±1.5%. In practice, it is possible to measure flows of less than 100 L m^{-2} hr^{-1} but the turbine movement is erratic and subject to increasing error of up to 30%. Below a minimum of 50 L m^{-2} hr^{-1} the flow meter displays no flow, as there is not enough momentum to spin the turbine. Thus, steady state flows during fouling are treated with care. However, the main emphasis of this work is to study cleaning. Permeate flow rates measured after cleaning are in the region of minimum error, ±1.5%.

The principle of the turbine flow meter operation is simple. A jet of permeate is directed at a free running turbine in a specially shaped chamber. As it spins, the turbine blade cuts a beam of infrared light, which triggers a single pulse output. The frequency of these pulses is proportional to the flow rate and the total number of pulses to the total volume of fluid passed. Digital pulses were accumulated for five seconds and logged continuously during processing.

The flow meter was calibrated with deionized water at 37°C; the temperature of the clean water flux. The flow meter was mounted in series with a computer-interfaced balance and the two sets of data compared. The calibration chart is shown in *Figure C-1*. To convert the digital pulse signal from the data logger to normal engineering units of flux (L m^{-2} hr^{-1}), *Equation 3-1* was used, where A is the membrane area and ρ_{pf} is the permeate density.

$$J\left(L\,m^{-2}\,hr^{-1}\right)=\frac{J\left(Pulses.5s^{-1}\right)\times 7200}{348.4124\times A\times \rho_{pf}} \qquad \textit{Equation 3-1}$$

The flow meter responds erratically to the presence of air or particulates within the flow chamber. To avoid this, the flow meter was mounted vertically and when the membrane was placed in the module all air was evacuated from the module and pipework before permeate was collected. Fortunately, air entrainment resulted in major flux disruptions and so was easily identifiable. The turbine flow meter is required to measure permeate, which is upstream of the membrane, therefore the possibility of particulate interference was avoided.

3.1.1.3 Feed Flow Meter

Feed flow is measured with a rotameter type flow meter with a gauge display of 160-1600 L hr^{-1} (Platon). The flow meter was mounted vertically and calibrated with deionized water at 23°C. For all experiments, the quoted flow was set while the temperature was ambient at 23°C and then the temperature increased. The variation in viscosity with temperature was therefore compensated. As temperature increased the gauge readout fell, however, this was already compensated for by setting the flow at the same temperature.

3.1.1.4 Temperature Control

Heating requirements were achieved by recycling process fluids through the single-speed centrifugal feed pump (Hilge Pumps Ltd., B 22 3.0), which was throttled and thus imparted significant sensible heat to the circulating fluids. Cooling of the bulk solutions and suspensions was subsequently required to achieve the desired temperature. Temperature was maintained within ±0.4°C of the set-point during processing using manual control of needle valves controlling flow through the cooling coil and jacket. Mains water was used as the coolant.

Recycle and process fluid temperatures were measured using two identical thermistors with a working range of -10 to 90°C and a resolution of ±0.4°C.

Shear effects of the pump impeller were investigated with respect to cell viability. It was a concern that the cell wall may be ruptured altering the composition of the suspension. Methylene blue staining (*see 3.2.10.2*) of cells before and after ninety

minutes of recycle flow with no permeate produced, revealed that change in cell viability was negligible.

Limitations of the mains water flow rate and temperature fixed the minimum operating recycle temperature at 25°C. The maximum operating temperature was limited to 70°C by the poor thermo-tolerance of various plastic fittings. The membrane itself is autoclavable and so extremely heat resistant.

3.1.1.5 Transmembrane Pressure

MF membranes typically operate at transmembrane pressures of less than 2 bar (Mulder [1991]). At higher pressures the membrane becomes vulnerable to rupturing. Therefore, on feed pump start-up, the membrane was isolated to avoid exposure to pressure surges.

Pressure within the system is significant, even without applying back-pressure, due to the small channels within the membrane module and the relatively high average rate of cross-flow. Back-pressure is only required to achieve the transmembrane pressure during fouling. A needle valve located at the membrane outlet on the retentate side allowed the back-pressure to be controlled.

Fluctuations of transmembrane pressure were observed due to the slightly pulsing flow from the throttled pump. This became more pronounced at higher flow rates.

The system had a minimum transmembrane pressure of 0.3 bar at cross-flow velocity of 0.56 m s^{-1}. The maximum transmembrane pressure was unknown due to the physical limitations of the membrane, but certainly in excess of 2 bar.

3.1.1.6 Experimental Data Collection

Permeate flux and temperature data were stored at five-second intervals on a data logger (Wessex Power Technology Ltd., Eltek). Pressure data was simultaneously recorded on an IBM compatible 80286 PC via an interface card (Advantech Co. Ltd., PCL-711B) and software developed personally in-house.

Measurements of pH and conductivity were displayed on hand-held displays and recorded with pen and paper.

Negatives resulting from electron microscopy were printed to A4 size development paper, which have been scanned to produce digital images.

3.1.1.7 Materials of Construction

Use of high-temperature alkaline and acidic chemicals during cleaning required careful selection of wettable materials, which should be resistant to the combined effects of thermal stress and chemical attack. All wettable process materials are stainless steel (316) with the exception of the Perspex insert within the membrane module. In the case of the permeate flow meter, the spindle and body materials are stainless steel while the turbine and cover moulding materials are PVDF.

The original carbon seals supplied with the feed pump were replaced with silicon carbide. After pump operation using carbon seals, significant carbon deposits were deposited on the membrane surface, significantly contributing to flux decline with time. The carbon deposits were identified using atomic absorption. Silicon carbide seals have much greater durability yielding a much improved water flux.

An alternative to changing the seals was to use a pre-filter. However, gradual fouling of the pre-filter would affect the back-pressure and thus the cross-flow velocity, so was rejected.

3.1.2 Membrane Selection

A polyethersulphone membrane with a nominal pore size of 0.1 μm (Gelman Sciences, *Supor 100*) was used for all experiments. Both sides of the asymmetric membrane are shown in *Figure 3-5*.

The membrane has a thickness of 154 μm with a top surface (skin layer) consisting of a porous flat sheet while the support layer has a spongy appearance. To the naked eye, the top surface appears shiny while the underneath is dull. The configuration of a skin layer supported by a more porous layer minimises the hydrodynamic resistance of the membrane.

The *Supor 100* membrane is hydrophilic. Stratton and Meagher [1994] observed that membrane hydrophilicity was more important for *Saccharomyces cerevisiae* harvesting than pore size. They base this conclusion on experimental comparisons

between the water fluxes resulting from various membranes when simultaneously harvesting a yeast suspension. They observed that hydrophilicity was especially influential when the media contained significant quantities of protein. Sheldon *et al.* [1991] had previously reported that hydrophobicity caused proteins to unfold at the membrane surface. Adsorption of biopolymers initiating the adhesion of micro-organisms has been discussed previously (*see 2.3.5.2 p.30*).

Top surface of *Supor 100* **Underside of *Supor 100***

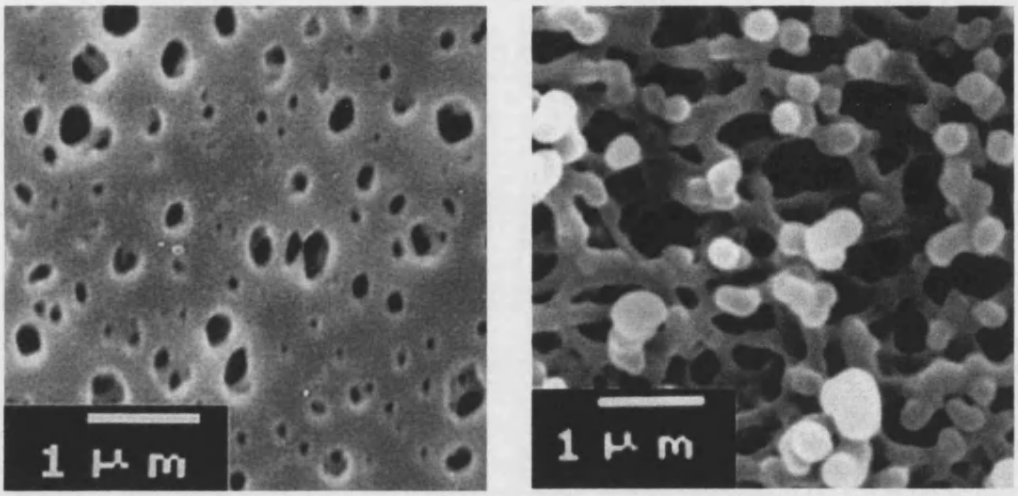

Figure 3-5: Gelman Supor 100 microfiltration membrane top surface and bulk appearance.

The *Supor 100* membrane is highly resistant to temperature and chemical effects making it highly compatible with cleaning studies. The chemical resistance of the membrane with some known cleaning agents is shown in *Appendix A.I.*

Although regeneration of used membranes was possible, each experiment used a new, conditioned membrane. Regeneration has unknown effects on long-term membrane properties and so was avoided. To allow comparisons to be drawn between experiments, reproducibility was maximised by starting with a new membrane to ensure a steady base line. However, it is understood that industrial processes regenerate membranes many times.

3.1.3 Water

Water was prepared using a reverse osmosis (RO) unit (Elga Ltd., Intercept RO-S) with a low salt content, having a measured conductivity of 12 - 22 µS cm^{-1}. RO water

was used to make all experimental solutions, suspensions and for rinsing. Processing conditions are described in the relevant sections.

3.1.4 Yeast Suspension

Reconstitution of commercially available fresh bakers yeast (British Fermentation Products Ltd., *Saccharomyces cerevisiae*) was preferred to the more time-consuming option of culturing. Baker's yeast was bought in 12 kg batches and stored in a refrigerator to ensure a storage temperature in the range 0°C to 4°C. Each yeast batch was stored for a maximum of ten days.

A 1 wt% baker's yeast suspension ($7x10^7$ cells mL^{-1}) was used for all experiments. Two bench-scale yeast cultures (*see 3.2.7*) independently yielded an average of $4x10^7$ cells mL^{-1}. The culture yield was scaled up to 1 wt% with the assumption that industrial scale processes would have higher yield than bench scale.

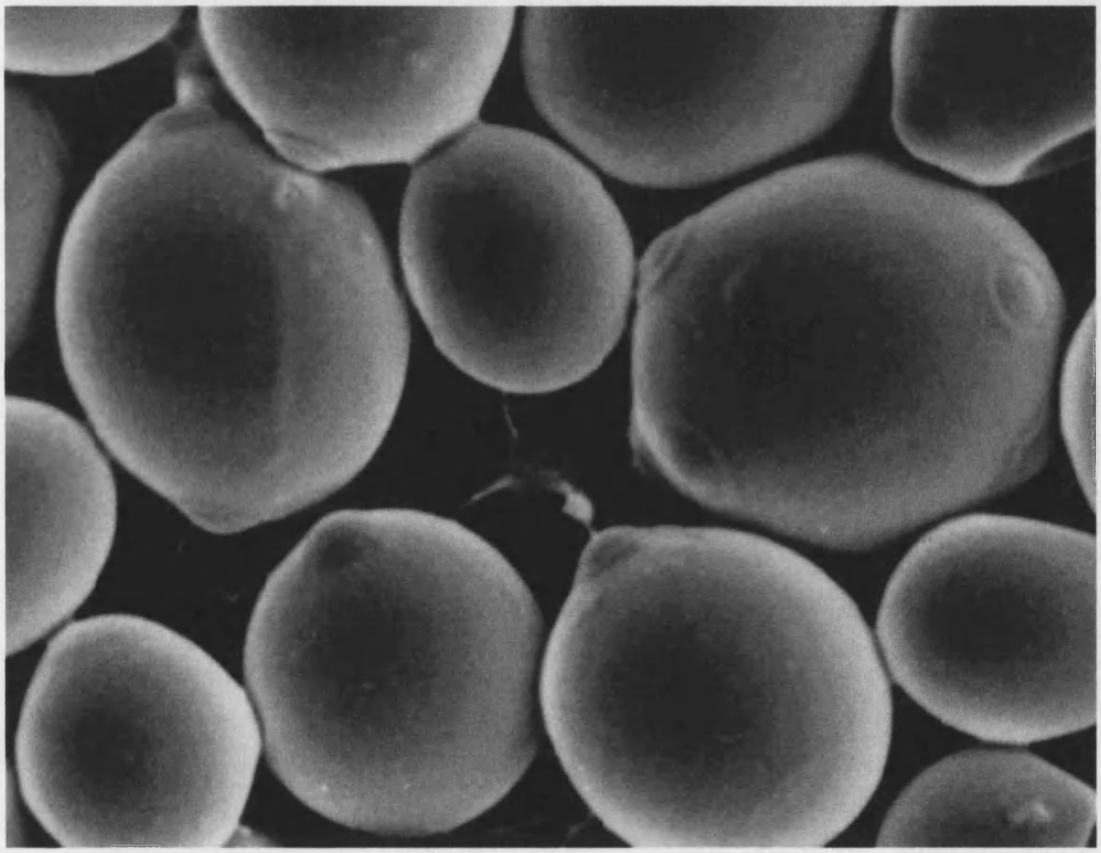

Figure 3-6: SEM showing the yeast cells before filtration. Budding and bud scars can be seen.

Before processing, the yeast was suspended in a saline solution (8.5 g NaCl L^{-1}) and stirred thoroughly for fifteen minutes. The sodium chloride (Sigma Chemical Co., S-

7653) balances the osmotic pressure across the cell wall, which if omitted would eventually result in cell rupture.

Yeast viability was 96±2%. A laser MasterSizer (Malvern Instruments Ltd.) was used to measure a normal yeast size distribution of 2 - 12 μm with an average cell diameter of 5.5 μm (*see Figure B-1*). Figure 3-6 shows that there is range in size but the presence of buds can clearly be seen. The MasterSizer calculates cell diameters using the assumption that the cells are spherical and individual. However, budding of the cells produces an irregular shape that may account for a size distribution wider than that observed in the SEM picture.

3.1.5 Chemical Cleaning Agents

Cleaning effects have been investigated to varying levels of detail for a range of industrially relevant chemicals, namely sodium hydroxide, nitric acid, *P3 Ultrasil 11*, *Terg-A-Zyme* and EDTA.

3.1.5.1 Sodium Hydroxide

Sodium hydroxide (Sigma Chemical Co., S-5881) was chosen for first inspection due to its relatively low cost, common industrial use and past applications to a number of deposits. In addition, sodium hydroxide forms the basis of many cleaning formulations, including *P3 Ultrasil 11*. It has the ability to saponify fats and solubilise proteins to a certain extent. However, it is generally ineffective when applied to mineral deposits. Sodium hydroxide was bought in solid pellet form and pre-mixed in a beaker of water before addition to the feed reservoir.

3.1.5.2 Nitric Acid

Mineral-based deposits are commonly targeted for removal with acids. The cleaning effects of nitric acid (Fisons Scientific Equipment, N/2300/PB17) have been assessed. Nitric acid was preferred to hydrochloric acid due to its compatibility with stainless steel. Nitric acid was bought in concentrated liquid form and was diluted in a beaker of water before addition to the feed reservoir.

3.1.5.3 P3 Ultrasil 11

P3 Ultrasil 11 (Henkel-Ecolab Ltd.), a free-flowing white powder, is a caustic-based formulated cleaning agent. The formulation of *P3 Ultrasil 11* is shown in Table 3-1. It

has been designed by Henkel to remove foulants commonly found in UF plants in the food industry, e.g. proteins, fats, blood and similar foulants.

Ingredient	Percentage (wt%)
Sodium hydroxide	43.6%
EDTA	>30%
Anionic surfactants	<5%
Non-ionic surfactants	<5%

Table 3-1: Chemical composition of the formulated cleaning agent P3 Ultrasil 11 (reproduced from Henkel-Ecolab Ltd. data sheet)

Ethylenediaminetetraacetic acid (EDTA) is a commonly used chelating agent, which can prevent re-deposition of removed foulant. A question mark hangs over EDTA with respect to its environmental impact as it is not biodegradable (Graßhoff [1989]). In sewage treatment plants it has been observed that heavy metal ions bound to the sedimented sewage sludge were remobilized by EDTA. It has been shown though to improve the cleaning efficiency of caustic-based cleaners.

The relative alkalinity of *P3 Ultrasil 11* and sodium hydroxide have been measured using titration. Results agreed well with the manufacturers literature on the relative alkalinity of *P3 Ultrasil 11* and sodium hydroxide. *P3 Ultrasil 11* was found to be less alkaline in solution than sodium hydroxide to the ratio of 1.96:1.

3.1.5.4 Terg-A-Zyme

Terg-A-Zyme is a formulated cleaner comprised of enzymes and wetting agents. It has found popularity for use in cleaning of sensitive membranes in RO and UF units within the dairy, food and water industries. The manufacturers recommend a 1 - 1½% solution at 50°C, which is the optimal temperature for enzymatic activity.

3.2 METHODS

Following design and construction of the experimental equipment, a detailed commissioning programme was carried out with the aim of formulating and perfecting experimental protocols. The commissioning programme involved a trial and error approach to improving experimental methods to increase reproducibility. Protocols exist for all practical work, for all stages of the cleaning experiments and all analytical techniques. These experimental protocols were strictly adhered to in order to minimise potential systematic errors.

Essentially, all of the membrane cleaning experiments comprised six stages: initial clean water flux, fouling, first water rinse, cleaning, second water rinse, and a final clean water flux. The protocol for operation of the apparatus for a complete experiment is listed in *Appendix D.I.*

3.2.1 Membrane Conditioning

Conditioning involved recycling clean water at 37°C for 15 minutes at a cross-flow velocity of 1 m s^{-1}.

It was found that the *Supor 100* membrane was very resistant to compression after conditioning. A plot of transmembrane pressure versus water flux shows a linear relationship over the range 0 to 1.55 bar. Thus, compaction after conditioning was not significant.

Another reason for conditioning can be the removal of residues inherent from the manufacturing process. This is not necessary for the *Supor 100* membrane, which is supplied ready for use by Gelman Sciences.

Even after conditioning, the water flux slowly decreased linearly with time. This is not due to compaction but thought to be a fouling phenomenon. Although the water is of high quality the small membrane area effectively magnifies the foulant content of the water. Although the water appears to be clean, only a small quantity of microscopic foulant is required in the water to produce significant coverage of the membrane area, and hence flux reduction. The slow decrease in flux is testament to the relatively small foulant content of the water

3.2.2 Clean Water Flux

Clean water fluxes, both initial and final, were measured at a temperature of 37°C, a cross-flow velocity of 1 m s^{-1} and a transmembrane pressure of 0.55 bar. This corresponds to a Reynolds number of 5460.

A combination of temperature and transmembrane pressure ensures that the flow meter is operating in the centre of its range, and so at its most accurate. The cross-flow velocity ensured turbulence within the membrane channels to keep bulk suspended. The transmembrane pressure is a function of the system hydraulics, as determined by the cross-flow velocity.

3.2.3 Membrane Fouling

Fouling cycles involved recycling the isotonic bakers yeast suspension at a constant temperature of 34°C for 90 minutes. A cross-flow velocity of 1 m s^{-1} and a steady state transmembrane pressure of 2.0 bar were fixed during filtration. The initial transmembrane pressure was 1.55 bar, which linearly approached the steady state pressure within 10 minutes. Permeate and retentate were returned to the feed tank, maintaining a constant system volume. However, the bulk cell concentration reduced during filtration due to fouling, the accumulation of cells and non-cellular material at the membrane surface.

The yeast culturing process used by British Fermentation Products Limited is reported to be fixed at 34°C (verbal communication). At temperatures in excess of approximately 45°C, yeast cell viability is reduced, while low temperatures reduce cell activity.

Cell viability and pH of the bulk yeast suspension showed little variation during filtration. The pH of the yeast suspension during filtration was 4.7 - 4.3±0.1. While the total cell concentration reduced during filtration, as cells accumulated at the membrane surface, the cell viability in the bulk remained approximately constant at 96±2%.

3.2.3.1 Effect of Yeast Concentration

The yeast concentration used for this study was based on the average experimental biomass yield from laboratory scale cultures. Two simultaneous 10 L yeast cultures

produced an average biomass yield of $7.4x10^7$ cells mL^{-1}. This compares closely to a 1 wt% (100g L^{-1}) bakers yeast suspension with $7.7x10^7$ cells mL^{-1}.

The chosen yeast concentration was fixed at 1 wt%. However, the consequences of fouling at different concentrations have been estimated. *Figure 3-7* shows that for yeast concentrations in the range 0.25 - 4 wt%, initially the degree of permeate flux reduction increases with concentration, while the final steady state fluxes are similar.

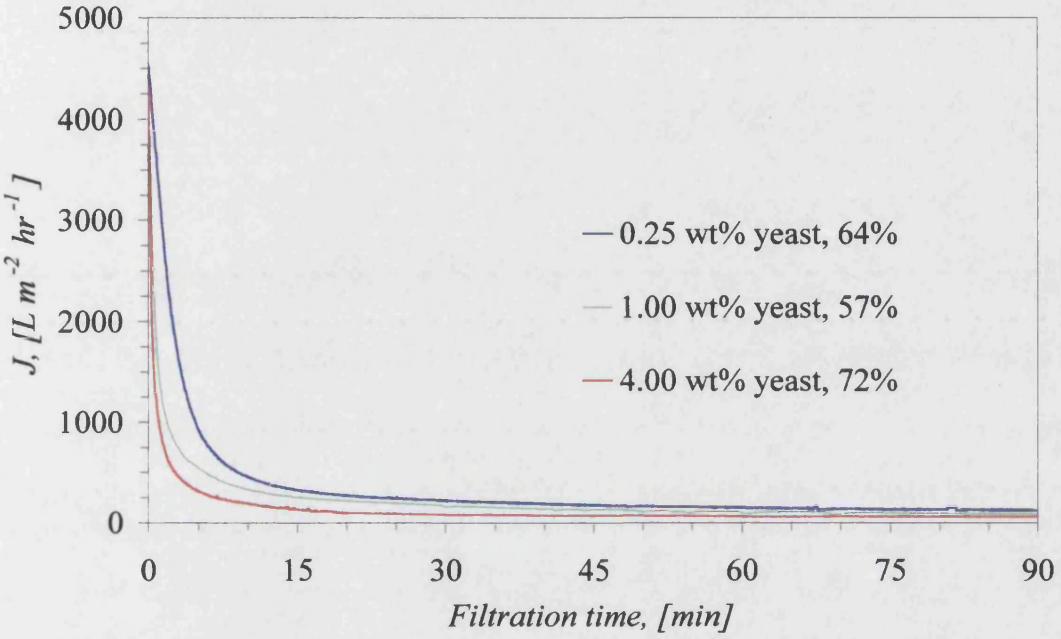

Figure 3-7: CFMF of 0.25, 1.00 and 4.00 wt% isotonic yeast suspensions at the same standard fouling conditions. Note that the percentages quoted in the legend refer to the percentage water flux recovery after standard rinsing conditions.

With respect to cleaning, the degree of irreversible fouling has been estimated by measuring the subsequent rinsability of the respective deposits. In this case it has been seen that at 1 wt% rinsing has the least effect on the deposit, yielding an average water flux of 57±5%. At concentrations of 0.25 and 4 wt% the average water fluxes after rinsing were 64±5% and 72±5% respectively. Within experimental error, the rinsing effect at concentrations of 0.25 and 1.0 wt% are insignificant. However, at 4 wt% the rinsing effect is significantly greater than when fouled at 1 wt%. This suggests that although the initial rate of fouling is rapid, and the final flux is similar to other concentrations, the tenacity of the fouling deposit is less. Therefore, a 1 wt% yeast suspension represents a potential worst case in terms of fouling deposit tenacity.

3.2.3.2 Effect of Transmembrane Pressure

Although MF membranes can be operated at transmembrane pressures of up to approximately 2 bar, commercial operation is often at lower transmembrane pressures. However, *Figure 3-8* shows that the deposit formed after CFMF at a transmembrane pressure of 0.75 bar produced less fouling resistance after rinsing than when fouled at the greater transmembrane pressures of 1.40 and 1.95 bar.

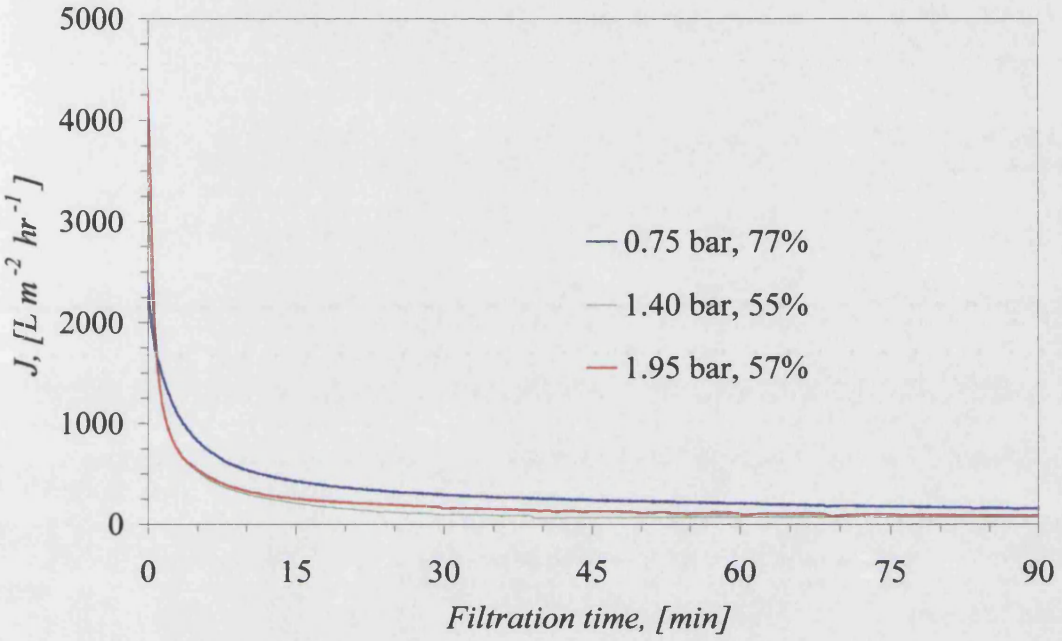

Figure 3-8: Filtration of 1 wt% isotonic yeast at a steady state transmembrane pressure of 0.75, 1.40 and 1.95 bar. Standard fouling temperature and cross-flow velocity. Note that the percentages quoted in the legend refer to the measured flux recovery after rinsing.

Flux reduction and rinseability at 0.75 bar were significantly less severe than those observed at 1.40 and 1.95 bar. While great importance is placed on industrial relevance in this study, a transmembrane pressure of 1.95 bar was chosen to produce a 'worst case' deposit, worthy of analysis. In addition to reduced transmembrane pressure, industrial CFMF would commonly employ fouling prevention techniques such as pre-treatment and back-flushing. When these valid and beneficial steps are employed, the time required to produce a tenacious deposit is increased significantly. CFMF using a transmembrane pressure of 1.95 bar and no fouling prevention allowed a rapid turnaround of experiments and produced a tenacious deposit.

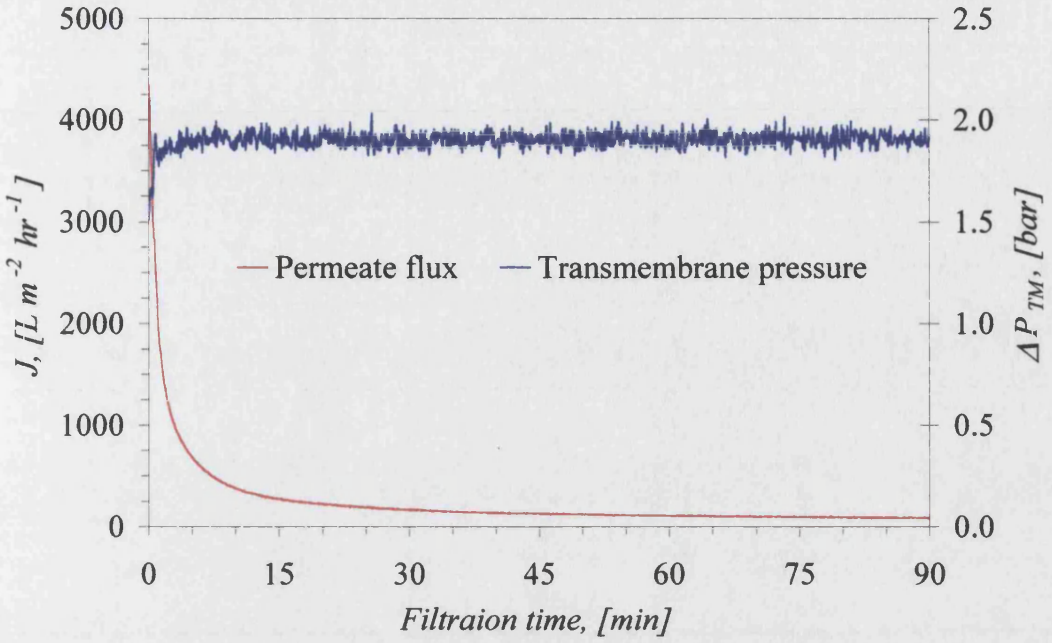

Figure 3-9: Transmembrane pressure during fouling of 1 wt% isotonic yeast suspension

It should be noted that the quoted transmembrane pressure of 1.95 bar refers to the steady state condition. During CFMF, the transmembrane pressure actually increases from 1.5 to 1.95 within two minutes, as shown in *Figure 3-9*. This corresponds to the rapid reduction in permeate flux.

3.2.3.3 Effect of Salt Presence

A summary of the fouling effects of the components of the fouling suspension is shown in *Figure 3-10*. CFMF of the isotonic medium at normal conditions showed a steady, approximately linear flux decrease with time. When the salt was omitted from the yeast suspension, the fouling curve shifted significantly in the transitional phase between initial rapid decline and the approach to steady flux. Although the isotonic and non-isotonic yeast suspension curves started and finished with similar flux, the paths taken are significantly different. The salt medium serves to regulate the osmotic transport of water through the cell wall. In the presence of salt, fouling is more dynamic. This could be due to the relative hydration of the yeast cells. In the absence of salt in the medium, the yeast cells become highly hydrated and therefore firmer. In the presence of salt, the cells have a lower water content and so are more flaccid and compressible, which may result in a more compact cake layer and reduced permeability.

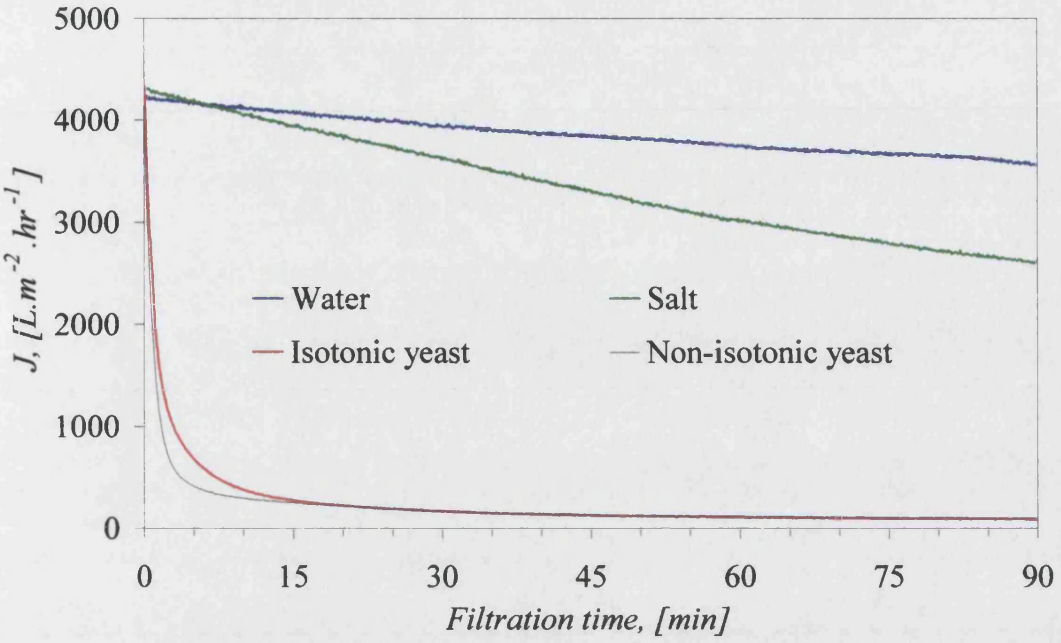

Figure 3-10: Filtration of water, salt solution (8.5g NaCl per litre of RO water), non-isotonic yeast and isotonic yeast. Hydrodynamic conditions are the same as those for fouling.

It was suspected that salt also played a role in the tenacity of the fouling deposit. Evidence came later when the effect of cleaning with sodium hydroxide was studied. The water flux after cleaning the non-isotonic yeast deposit with sodium hydroxide was recovered completely, unlike isotonic yeast which proved more stubborn (*see 4.3.2, p.94*).

3.2.4 System Flushing and Membrane Rinsing

After fouling, the membrane was given a primary rinse to remove loose cake, concentration polarisation and all traces of the yeast suspension from the bulk flow. After chemical cleaning, a secondary rinse was required to rinse the process line membrane surface.

In both cases, rinsing was carried out at a temperature of 23°C and a cross-flow velocity of 0.75 m s^{-1} for one minute. Water alone was not capable of cleaning the fouled yeast deposit. Therefore, it was considered wasteful of energy to use a temperature higher than ambient. In addition, the desire to minimise pumping energy fixed the cross-flow rate. The cross-flow rate of 0.75 m s^{-1} was calculated to coincide with a Reynolds number of 2960, sufficiently high to create turbulence in the bulk flow.

Validation of rinsing techniques is difficult to assess at the microscopic level. Detection of adsorbed chemical species is beyond the range of even electron microscopy. However, a rinsing period of one minute was fixed by results gained from monitoring the conductivity of the effluent during rinsing. A conductivity meter (Jenway, TDS 4076) was placed in-line in a purpose-built glass housing. The meter was placed in the retentate line immediately before going to drain. Deionized rinse water had a conductivity of 0.01 - 0.02 mS cm^{-1}, much less than the chemical solutions, in excess of the meter range. The range of the conductivity meter was 0 - 19.99±0.01 mS cm^{-1}. For all of the experimental cleaning conditions, the conductivity of the effluent rinse water returned to the base value of 0.01 - 0.02 mS cm^{-1} within one minute. The possibility of chemical adsorption to the membrane surface was expected to manifest itself in terms of permeate flux if significant, and will be discussed later.

To avoid cross contamination, the permeate line, pump bypass and recycle lines were closed during rinsing. To aid rinsing, the process line was first isolated and the reservoir emptied. Two litres of water were added and the pump started. This purged the system dislodging stubborn deposits. The by-pass and recycle lines were then closed and the process line opened and the reservoir filled with water. The flow meter was set at the rinsing flow rate and the pump stopped, ready for rinsing when required.

3.2.5 Membrane Cleaning

Four possible methods of operation during chemical cleaning were considered:

(i) Permeate line open with single pass of the detergent(s).

(ii) Permeate line open with recycle of the detergent(s).

(iii) Permeate line closed with single pass of the detergent(s).

(iv) Permeate line closed with recycle of the detergent(s).

Methods (i) and (ii) generate copious information regarding the change of fouling resistance during cleaning. However, cleaning efficiency with the permeate line open was relatively poor. Cleaning efficiency with the permeate line open was as much as 30% less than when closed, at the same cleaning conditions.

Method (iii) was found unnecessary when compared to method (iv). Under recycle at cleaning conditions with the permeate line closed, the detergents used had no measurable effect on the permeability of clean membranes. In addition, recycle of removed foulant also resulted in no measurable change in membrane permeability, showing the lack of re-deposition with the permeate line closed.

Method (iv) economically achieved the highest cleaning efficiency but provided a problem of data collection. Single experimental runs, with no permeate collected during cleaning, provide only the overall flux recovery. In order to determine the fouling resistance change as a function of time it was necessary to carry out several experiments to take 'snap shots' of the permeability. This was achieved by cleaning for a short period with the permeate line closed and then measuring the clean water flux. Repeating this process for a range of cleaning times with the same membrane completed the profile of fouling resistance.

Under single pass conditions with the permeate line open, membrane-detergent interactions were observed, complicating the interpretation of permeability data following cleaning of fouled membranes. As expected, method (ii) was the worst case where removed material was presumably re-deposited explaining the lowest recovery of permeability.

Method (iv) was most efficient and industrially relevant, and so was adopted as the cleaning procedure in this study. It should be noted that cleaning with the permeate line closed is process sensitive. Spiral wound membrane configurations can suffer damage when cleaned with back-pressure on the permeate.

3.2.6 Waste Disposal

The dilute concentrations of caustic and acid cleaners used did not warrant neutralisation before disposal. The working fluids were diluted with copious water and sent to drain.

3.2.7 Yeast Culture

A 25L glass bell jar was primed with 20 L of distilled water and 20 g L^{-1} of malt extract broth (Oxoid, CM 57). Air inlet and outlet filters were fitted to the lid of the bell jar and a flexible hose added for sample extraction. Inside the jar, the air inlet

filter was connected to a stainless steel sparger, to reduce bubble size, enhancing mass transfer. The complete system was then autoclaved at 121°C for 13 minutes. The lid was sealed to the base and cooled in a water bath at 24°C. A 5g sachet of brewing yeast (Young's Homebrew Ltd.) was then added to the media and mixed. An air line was attached to the inlet filter and a constant air supply of 1 L min^{-1} was passed through a rotameter (Platon). A 5 ml sample was removed from the vessel at regular intervals and the total cell count and viability were calculated.

The culture was harvested using centrifugation after 3 days. The final concentration of yeast was approximately $4x10^7$ cells mL^{-1}.

3.2.8 Deposit Visualisation Techniques

To complement the permeate flux data visual techniques were used, microscopy being the predominant method.

3.2.8.1 Scanning Electron Microscopy

Low temperature scanning electron microscopy (LTSEM) was used to view the hydrated, biological samples in a pseudo natural state. LTSEM ensured that possible artefacts of drying procedures such as shrinkage and collapse were avoided (Hermann and Müller [1993]).

Sample preparation involved three steps; immersion of samples in liquid nitrogen slush at -180°C, removal of surface frost in the viewing chamber to -90°C and finally gold sputtering at -180°C for three minutes, all under vacuum.

3.2.8.2 Transparent Membrane Module

A transparent Perspex membrane module was constructed to allow visualisation of the fouling and cleaning procedures. Although the module only allows visualisation at the optic level (greater than 0.1 mm), it yields important corroborating evidence. Video playback of captured footage has shown that the yellow colour associated with the yeast deposit was removed in the same time scale as flux increased. Also, the depth of the yeast cake layer could be viewed, though not measured.

3.2.9 Titration

Alkaline strength of the sodium hydroxide and *P3 Ultrasil 11* solutions were determined by titration with known molar nitric acid and a phenol phthalein indicator.

Two drops of the indicator were added to a flask containing 100 mL of the detergent solution and mixed well. A burette filled with known molarity of nitric acid was used to gradually neutralise the detergent solution. At the point of neutralisation the indicator changed from pink to transparent. The molarity of the acid and volume used was known, therefore, through knowledge of the stoichiometry, the number of moles of OH^- were deduced.

3.2.10 Light Microscopy

A light microscope (Olympus, CH-2) was used to determine sample cell concentration and viability. Yeast was best viewed at a magnification of x400 (x40 lens and x10 eyepiece). Light microscopy does not show surface detail of yeast, which are seen as thick-walled disks.

3.2.10.1 Cell Counts

Yeast suspensions were diluted before counting to ensure the number of cells per grid lay between 30 and 300. Dilution included the addition of both water and methylene blue stain (used to determine viability). Samples were pipetted onto the counting chambers of a haemocytometer, which fill via capillary action, occupying 10^{-4} cm^3. Each counting chamber is divided into 25 smaller squares. Cells within the 25 squares of three chambers were accumulated and averaged. The cell concentration is equal to the number of cells counted multiplied by the dilution factor. The concentration of cells per mL is calculated as follows:

$$\text{Cells mL}^{-1} = \text{average count per square} \times \text{dilution factor} \times 10^4$$

The number of cells in the 1 wt% fresh yeast suspension was $\approx 10^8$.

The light microscope also revealed rod-shaped bacteria (between one in a hundred and one in a thousand) and crystalline deposits, sugars from the growth medium.

3.2.10.2 Differential Staining of Viable and Non-viable Cells

The preparation for determining cell viability is the same as for cell counting. Methylene blue is a basic dye of the thiazine group and acts in this instance as an oxidation-reduction indicator. After staining, it was possible to differentiate between the transparent viable cells and the blue non-viable cells. Both viable and non-viable cells take up the blue stain but only the viable cells are able to expel the stain at the

rate of uptake. Cell counts of the viable and non-viable cells reveals the percentage viability. After taking triplicated averages of observed cell numbers, the average cell viability of the yeast suspension before CFMF was ≈96%.

Although staining is not as rigorous a method as some alternatives for determining cell viability, such as plating, it has sufficient accuracy for the purposes of this study.

CHAPTER 4 - RESULTS AND DISCUSSION

4.1 FOULING ANALYSIS

4.1.1 Experimental Flux Decline and Fouling Resistance

Using the experimental protocol described in section *3.2.3* (*p.69*), CFMF of the isotonic yeast suspension resulted in exponential decay of flux as a function of time. The average percentage flux decline over the ninety minute period was 95±3%. After an initial start-up period of rapid decline, the flux gradually approached a non-zero value of 95±50 L m^{-2} hr^{-1} (LMH). As discussed earlier (*3.1.1.2, p.60*), systematic errors of the flow meter at fluxes less than 100 LMH were significant, therefore the high percentage error in the steady state flux was expected.

A typical flux decline profile during fouling is shown in *Figure 4-1*, which also shows the calculated fouling resistance corresponding to the accumulation of the fouling layer.

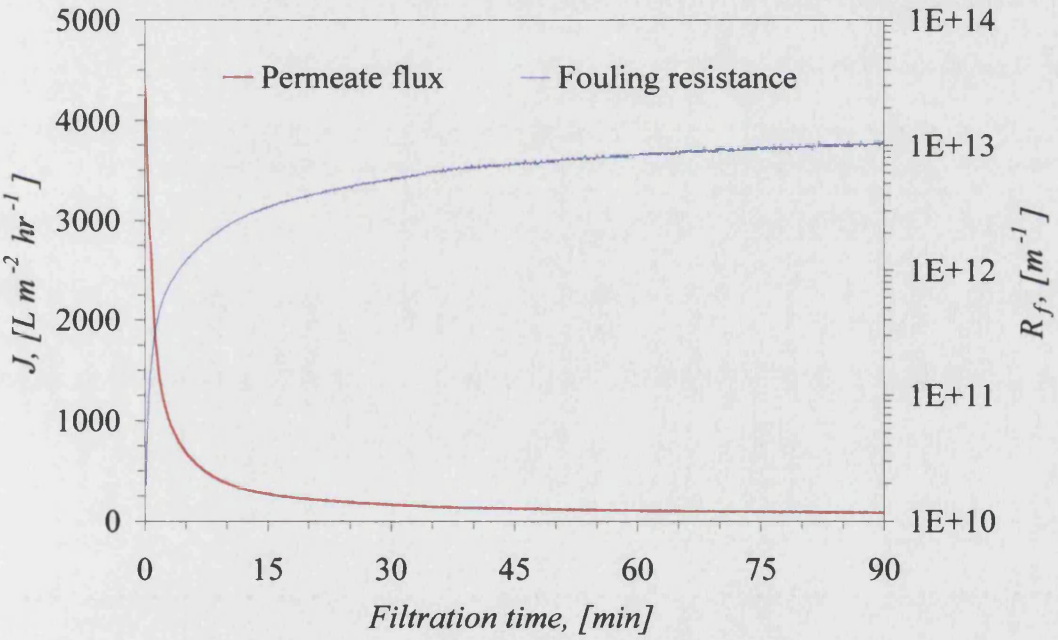

Figure 4-1: Permeate flux J and fouling resistance R_f versus filtration time during CFMF of the standard isotonic yeast suspension.

Due to the initial rapid rate of flux decline combined with the relatively long data logging frequency of five seconds, the first flux measurement was subject to great variability. Therefore, the value of the initial flux plotted in *Figure 4-1* is the water flux through the clean, conditioned membrane at identical conditions used for fouling. The measured average initial clean water flux was 4260±310 L m^{-2} hr^{-1}. The 7%

variability of the measured clean water flux at fouling conditions is attributed to the unique physical properties of each membrane used.

The average flux after ninety minutes equated to a fouling resistance of $1.0\pm0.4\text{x}10^{13}$ m^{-1}; approximately two orders of magnitude greater than the average membrane resistance of $1.3\pm0.1\text{x}10^{11}$ m^{-1}.

Throughout fouling, the permeate was visibly colourless compared to the dark yellow feed. Using a light microscope, it was established that transmission of yeast cells was zero. This was expected as yeast cells are approximately two orders of magnitude larger than the membrane pores.

Permeate and bulk conductivity were equal and constant during fouling, indicating that, as expected, the *Supor 100* microfiltration membrane freely allowed the salt ions to permeate readily through the fouling layer and membrane structure. Microfiltration membranes have been compared to ultrafiltration membranes when fouled, therefore increasing selectivity. However, an ultrafiltration membrane would be expected to retain large macromolecules such as proteins but not salts.

A micro-assay detected trace amounts of protein in the bulk and permeate streams during fouling. Unfortunately, it was not possible to accurately measure quantities due to the limits of the assay technique. Therefore, changes of protein transmission during fouling are unknown.

For several experiments during CFMF, the pH of the retentate was measured at 5 minute intervals and found to fall from 4.7±0.1 to 4.3±0.1. Viability of the bulk yeast during fouling remained constant at 96±2%.

4.1.2 Theoretical Fouling Mechanism

The typical fouling flux curve shown in *Figure 4-1* has been analysed to identify the likely theoretical fouling mechanism (*see 2.3.8, p.36*). Flux predictions based on the four theoretical mechanisms of cake, intermediate, standard and complete fouling are plotted alongside the experimental values in *Figure 4-2* and *Figure 4-3*, which show plots from zero to fifteen and fifteen to ninety minutes respectively. A single mechanism was assumed for the period zero to ninety minutes. The optimal values of

k for the n values 0, 1, 1.5 and 2 were $2.38x10^{-7}$, $2.61x10^{-4}$, $9.87x10^{-3}$ and $5.29x10^{-1}$ respectively.

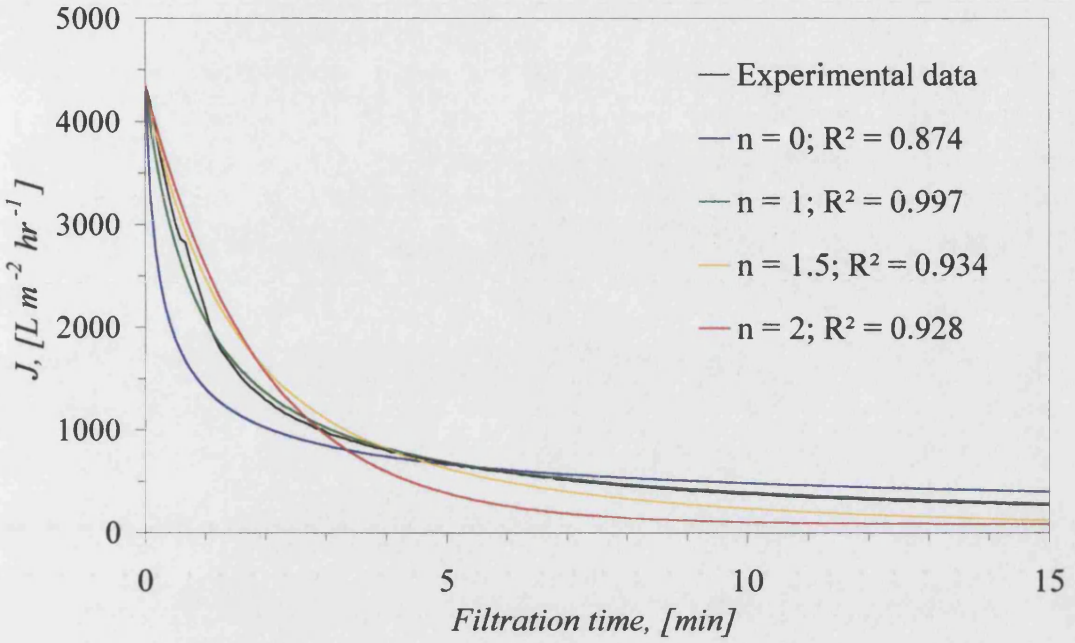

Figure 4-2: Comparison of theoretical fouling mechanism models to experimental data from 0 to 15 minutes.

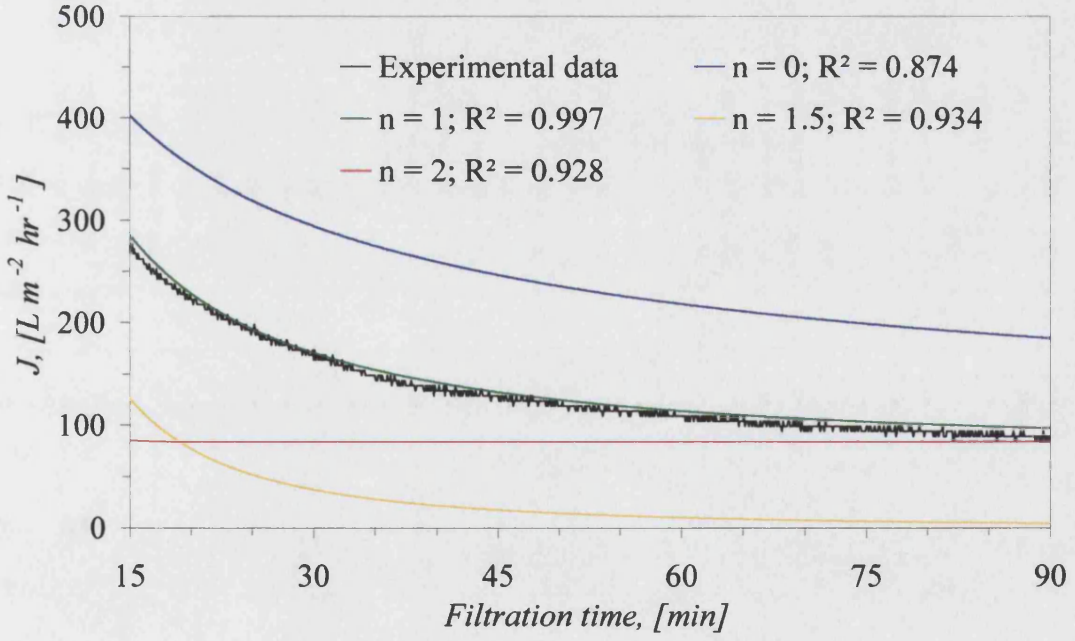

Figure 4-3: Comparison of theoretical fouling mechanism models to experimental data from 15 to 90 minutes.

When applied to the whole of the experimental data, the single fouling mechanism which best described the observed experimental flux decline was intermediate

blocking (n = 1). Intermediate blocking alone is defined as a surface accumulation of cells, some of which block pores. Therefore, flux reduces as a consequence of reduced porosity. Thus, n = 1 mode might be apparent as n = 2 complete pore blocking followed by n = 0 cake formation which might give similar fouling dynamics.

Theoretical fluxes shown were calculated by assuming a mechanism, to fix the value of n, and inputting the experimental value of J^* to *Equation 2-8 (p.36)*. An optimal value of k was calculated that minimised the overall sum of the differences between each theoretical and experimental flux value. This was achieved with a mathematical software package (MicroMath® Scientist® 2.0 for Windows™). For values of n = 0, 1 and 2 the value of J^* was fixed at 84 L m^{-2} hr^{-1}, the experimental steady state value for the fouling curve chosen. However, the mechanism corresponding to n = 1.5 by definition fixes J^* at 0. The value of k was adjusted until a minimum total of error squared values was found. The error is defined as the square of the difference between the predicted value and the experimental value.

Results suggest that internal fouling was not a dominant mechanism. Further evidence for this is that visualisation of the membrane internal structure after fouling did not show fouling deposits, which could clearly be seen on the surface (*see Figure 4-6*). Yeast cells are between one and two orders of magnitude greater than the membrane pores, hence the intermediate blocking fouling mechanism is physically plausible. Although theory suggests that internal blocking is not the overall dominant mechanism it is not assumed to be irrelevant. Proteins have been shown to foul internally in many other studies but do not have as great an affect on flux due to the relatively massive proportions of yeast cells. However, in studies where the proteins are known to foul internally, the membranes used were ultrafilters in order to separate two protein species.

For the period 0 to 1.5 minutes an excellent fit was achieved with the complete blocking model (n = 2), as shown in *Figure 4-4*. Physically, this is not surprising. Initially, the membrane has high porosity and the high flux convectively drags cells to the pores. Therefore, it is possible that each cell dragged to the surface could block a pore as predicted by the complete blocking model. However, there are a limited number of pore sites and so as time increases the probability of complete blocking decreases. It is therefore likely that after the initial period of complete blocking the

fouling mechanism switches either to intermediate or cake blocking, or a combination of both.

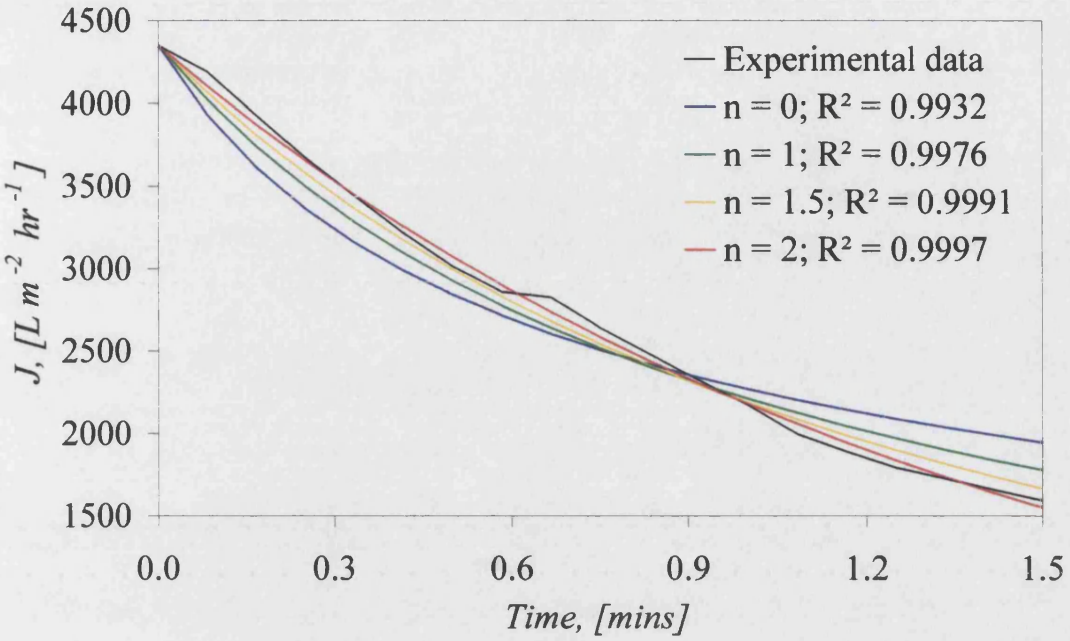

Figure 4-4: Comparison of theoretical fouling mechanism models to experimental data during the period 0 to 1.5 minutes only.

4.1.3 Estimation of Cell Deposition

Through measurement of the bulk cell concentration during fouling, the number of cells accumulated at the membrane surface as a function of time has been estimated. Using assumptions for the yeast cell arrangement, the height of the fouling layer was estimated.

Fouling operates in a closed system under recycle conditions, therefore accumulation at the membrane surface manifests itself as a reduction in permeate flux and bulk cell concentration. As a control, the yeast suspension was recycled with the permeate side closed under otherwise identical fouling conditions. As expected, the measured retentate cell concentration was constant with time due to there being no fouling.

The accumulation of cells at the membrane surface corresponded to a decrease in the bulk cell concentration as shown in *Figure 4-5*. Although there is a degree of scatter due to the high bulk concentration relative to membrane area, a trend of reduced cell concentration is apparent. This is the same trend seen for the flux reduction.

Therefore, as expected, it was confirmed that the accumulation of cells at the membrane surface resulted in reduced permeate flux.

Assuming the yeast cells are approximately spherical with constant diameter and rigid, the empty space within the fouling layer can be represented by the voidage *e*. For a cubic arrangement of cells $e = 0.476$. By further assuming that the cells form a uniform deposit thickness, the height of the cake *h* can be calculated from *Equation 4-1*. Assumptions are necessary to simplify the problem because in reality yeast cell diameter is variable and budding distorts the shape from spherical. The fouling layer is often dependent upon channel length, deposit thickness increasing with channel length.

The height of the cellular deposit *h* is equal to its volume *V* divided by the area of deposition *A*. The volume of the cells V_c is equal to $V(1- e)$, which is equal to the number of accumulated cells N_y multiplied by the volume of one cell $^4/_3\pi r^3$. The average cell diameter d_y is equal to twice the length of its radius $2r$.

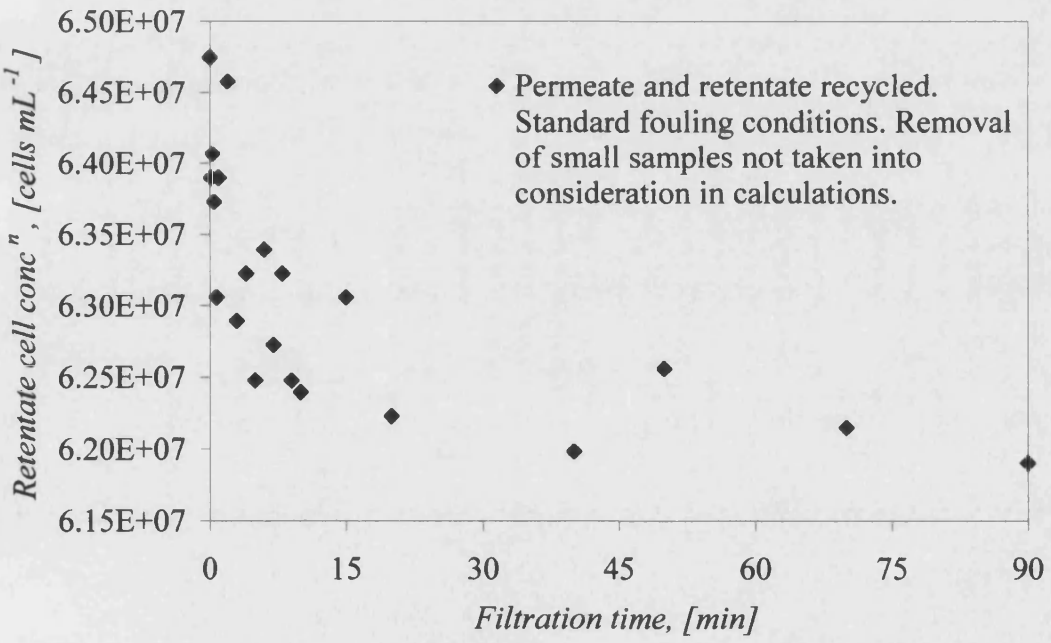

Figure 4-5: Cell concentration of retentate during standard fouling conditions. Cell counts via calibrated spectrophotometer at 540 nm wavelength. The conversion from absorbance to cell concentration is via a calibration curve (see Figure C-5)

$$h = \frac{4N_y \pi r^3}{3A(1-e)}$$ *Equation 4-1*

Assuming that the voidage lies between 0 and 0.476, h lies between 0.59 and 1.13 mm. The relationship between voidage and height is described by *Equation 4-2*.

$$h = 0.5895 + 0.645e + 0.0357e^2 + 2.0502e^3 \qquad \textit{Equation 4-2}$$

The height of the Perspex channels is 3 mm. Therefore, voidage aside, the height of the cellular layer was significant.

Quantifying the number of cells present initially has allowed the affect of rinsing to be quantified.

4.1.4 Visualisation

The membrane surface after fouling was obscured by the abundance of deposited yeast cells. However, after removing the membrane and rinsing lightly with distilled water, the yeast-membrane interface was observable with scanning electron microscopy. The sample shown in *Figure 4-6* was cross sectioned using a sharp scalpel blade.

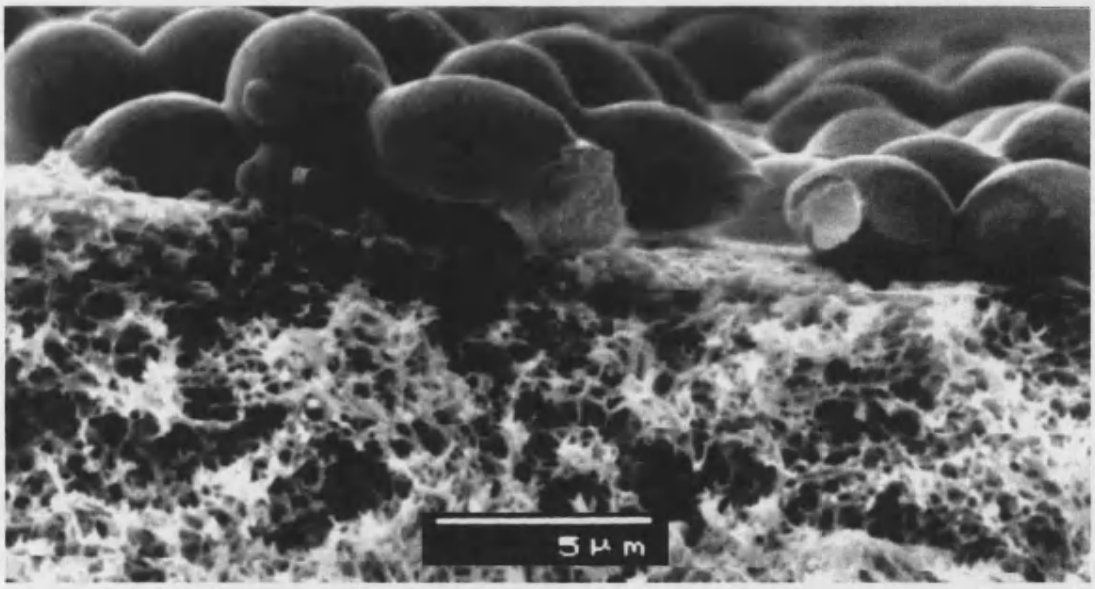

Figure 4-6: Cross sectional view of the fouled Supor 100 membrane (x5000).

Electron microscopy showed no evidence of interior fouling. Yeast cells or debris and agglomerated macromolecules should be observable at electron microscopy resolution. The membrane was also viewed from the underside, as it is more porous and so increases visibility of the structure, but also failed to show internal fouling.

4.1.5 Fouling Summary

During microfiltration of the isotonic yeast suspension, an exponential flux decline was observed with time. Analysis of a typical fouling curve has predicted that the dominant theoretical fouling mechanism was intermediate blocking, which states that the yeast cell layer at the membrane surface partially blocks pores while a thick cake builds above introducing hydrodynamic resistance, which is a function of the cake depth. The exponential flux decline has been shown to coincide with an accumulation of cells at the membrane surface. The height of the yeast cake has been estimated at between 0.6 and 1.2 mm at the end of the fouling process.

Visualisation of the membrane structure has failed to identify cellular or macromolecular internal fouling.

4.2 RINSING

The effects of rinsing the yeast-fouled membrane, under the conditions described in *3.2.4 (p.73)*, have been evaluated with respect to the change in fouling resistance and visualised using scanning electron microscopy. Rinsing is often the first step of a cleaning protocol, ensuring that loose material is removed, which minimises the bulk consumption of detergent species.

4.2.1 Fouling Resistance

A clean water flux was taken after the primary rinse and the fouling resistance calculated. This was compared to the fouling resistance calculated from the flux after fouling for ninety minutes. Rinsing had the effect of reducing the fouling resistance by approximately two orders of magnitude, from $1.0\pm0.4\text{x}10^{13}$ to $6.0\pm0.5\text{x}10^{10}$ m^{-1}. During fouling, the convective drag force created by the permeate flow is therefore significant. In the absence of convective drag force during rinsing, the fouling resistance is significantly reduced as the fouling layer is partly removed.

4.2.2 Visualisation

After a primary rinse, membrane samples were removed from the module, prepared and viewed using LTSEM (*see 3.2.8.1, p.76*). Comparisons between images of the membrane surface before and after rinsing revealed that indeed the majority of the cellular cake was removed during rinsing. This is consistent with the calculated reduction in fouling resistance due to the increase in the measured water flux. Prior to rinsing, a thick cake of cellular material was apparent, even to the naked eye. Previous calculations estimated the thickness of the fouling deposit to be between 0.6 and 1.2 mm, compared to the measured average diameter of a single cell of 5.5 μm. After rinsing, the residual deposit comprised of scattered cells and an intact non-cellular matrix, as shown in *Figure 4-7*. Impressions of the cell sites, prior to rinsing, have been well preserved. The remaining cellular deposits are not thought to have a regular pattern but to be randomly scattered about the surface. In rare cases cells were seen to exist in groups of up to ten, but were more often found to be alone. From the known average yeast cell diameter, the non-cellular matrix height is estimated at 1 μm. The healthy, hydrated cells seen under the microscope are testimony to the applicability of the LTSEM technique used.

4.2.3 Composition of Surface Deposit

A FT-IR microscopic analysis technique was used to assess the chemical composition of the rinsed deposit shown in *Figure 4-7*.

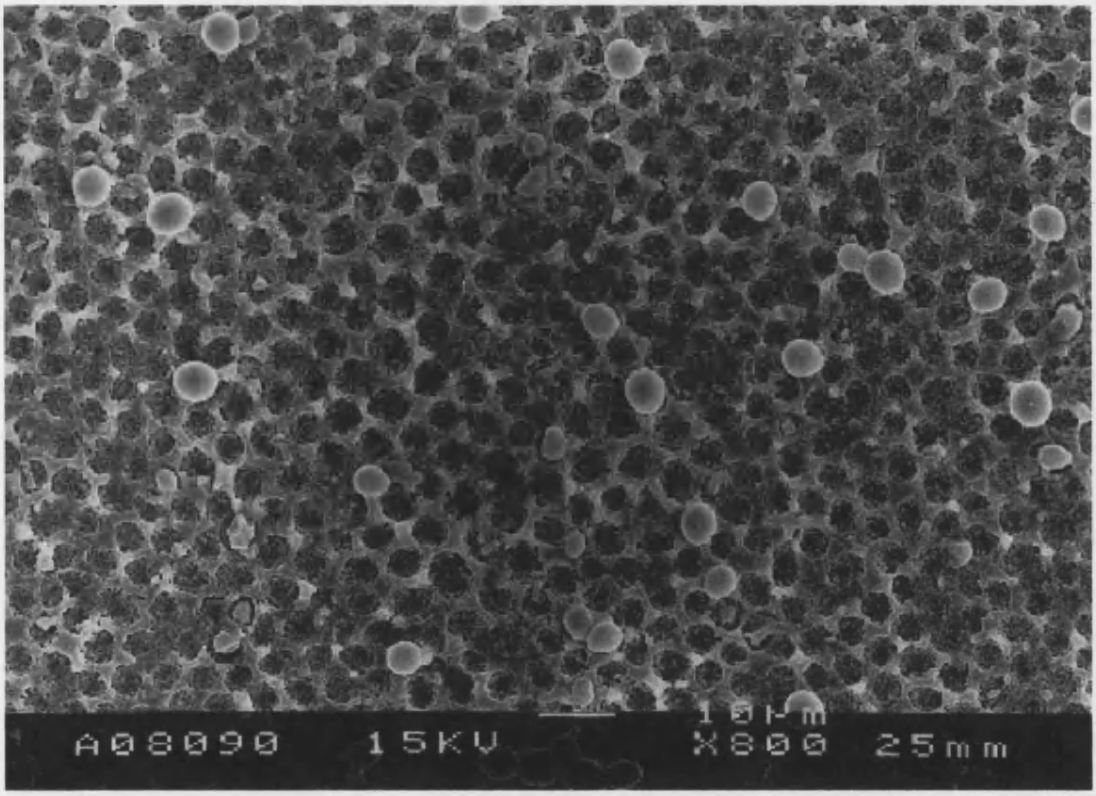

Figure 4-7: LTSEM visualisation of fouled Supor 100 surface after rinsing and prior to cleaning.

4.2.3.1 Fourier Transform InfraRed Microscopy

The chemical composition of the irreversibly fouled layer has been analysed independently by Reading Scientific Services Ltd using Fourier Transform InfraRed (FT-IR) microspectroscopy. The apparatus used was a Perkin-Elmer 1725 X FT-IR spectrometer with a Spectra-Tech IR-PLAN™ research microscope attachment. The wavelength range was 600 - 4000 cm^{-1} with a resolution of 8 cm^{-1}. Samples were flattened between two diamonds in an anvil before analysis. Fouled samples and yeast controls were analysed and compared. The transmission profile for a representative sample is shown in *Figure 4-8*.

Significant peaks exist at 1652 and 1536 cm^{-1}, which correspond well to the amide I and II peaks assigned to proteins. The majority of the other wavelengths were assigned to the presence of hydrocarbon chains. In conclusion, Reading Scientific

Services Ltd reported that spectra of the deposited material closely matched that of the reference yeast, and was predominantly proteinaceous. It was also thought possible that fractionation of proteins had occurred during fouling.

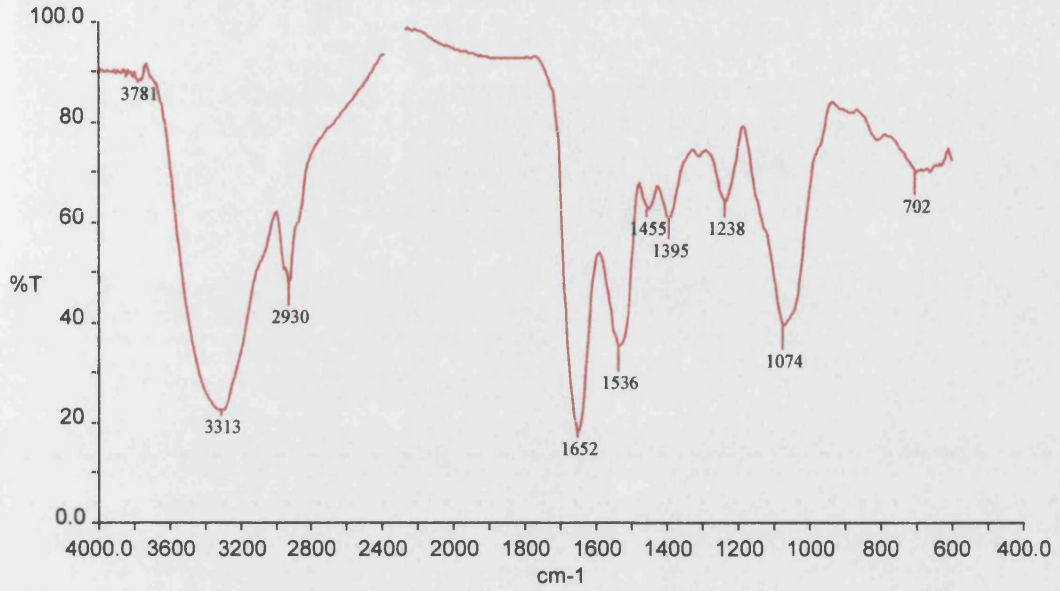

Figure 4-8: FT-IR analysis of the fouled deposit. Note that percentage transmission T = (100 - %absorbance). Chart shown is in its original form as supplied by Reading Scientific Services Ltd.

Under conditions of zero fouling, macromolecules, and specifically proteins, would be expected to permeate through a microfiltration membrane. However, fouling has the effect of increasing selectivity by acting as a depth filter with a nominal pore size less than the membrane supporting it. Indeed yeast cake layers have been deliberately utilised as an active barrier to filter proteins (Arora and Davis [1994]). For this system, it is evident that protein selectivity was more comparable to ultrafiltration than microfiltration.

4.2.4 Rinsing Summary

Rinsing was very effective in reducing fouling resistance, which resulted from shear removal of the majority of the deposited yeast cells. However, rinsing alone did not restore membrane porosity. Scanning electron microscopy revealed a tenacious non-cellular deposit with randomly distributed single cells. Analysis of membrane samples using FT-IR by Reading Scientific Services Ltd suggested that the tenacious deposit was predominantly proteinaceous. The non-cellular deposit appears to have formed around the well-preserved cell sites. Increased selectivity, due to the presence of the

yeast cell layer, may account for the observed retention of macromolecules from the supernatant.

4.3 MEMBRANE CLEANING

4.3.1 Water Cleaning

The water temperature used for rinsing was maintained at an ambient value of 23°C to minimise energy consumption. Therefore, the effectiveness of water as a cleaning agent at higher temperatures was investigated. In addition, water was the medium for all the cleaning solutions and so its contribution to cleaning must be defined.

Neither thermal or kinetic energy were able to restore the membrane permeability. However, the thermal energy associated with water temperature was more effective at reducing fouling resistance than the kinetic energy associated with turbulence.

4.3.1.1 Effect of Temperature

The cleaning effect of water was investigated at temperatures of 30, 40, 50 and 60°C. A plot of fouling resistance versus cleaning time for each temperature is shown in *Figure 4-9.*

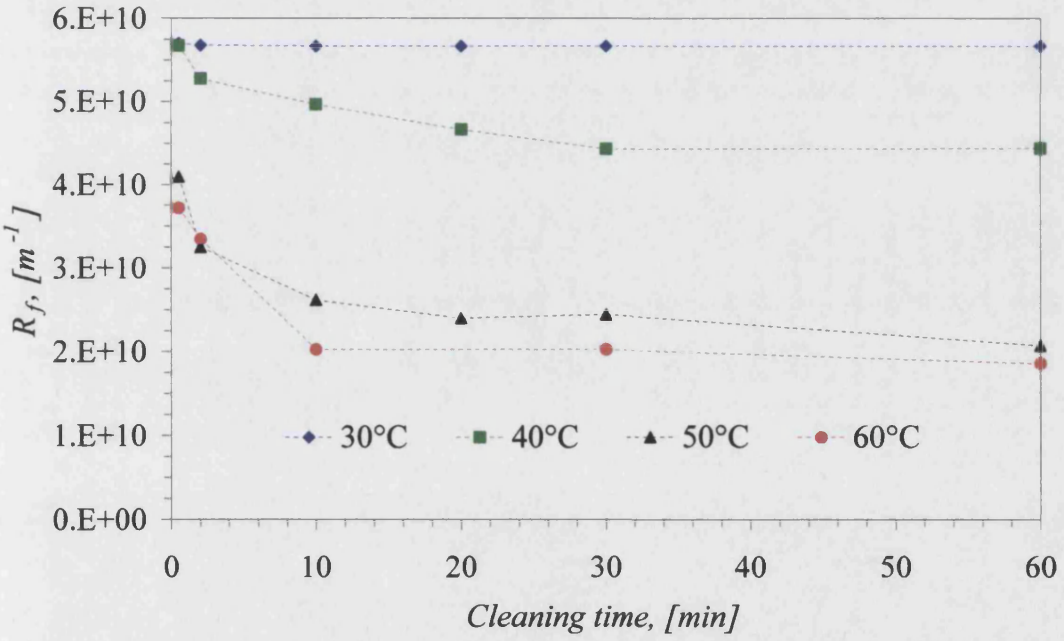

Figure 4-9: Plot of fouling resistance versus water cleaning time at temperatures of 30, 40, 50 and 60°C and a cross-flow velocity of 0.75 m s^{-1} (Re = 3450, 4200, 5000 and 5840 respectively)

At 30°C, no measurable decrease in fouling resistance was observed. At 40°C, the fouling resistance was progressively reduced over a thirty minute period. A significant energy barrier appears to have been overcome by increasing the water temperature

from 40 to 50°C. Fouling resistance was reduced more rapidly at temperatures of 50°C and 60°C, reaching a minimum of $2x10^{10}$ m^{-1} after approximately ten minutes. Triplicated averages of randomly chosen experimental data points shows that no significant distinction can be made between cleaning at temperatures of 50°C and 60°C.

Variability was lowest for cleaning at 30°C. Thus, the deposit was relatively stable at low temperature. This further strengthens the decision to rinse at low temperature in this study, as the fouling deposit reproducibility is maximised. However, this is based on theoretical reasons. In reality, industrial cleaning protocols would benefit from a rinse at elevated temperature if possible, as the main concern is the reduction of fouling resistance and not deposit reproducibility.

4.3.1.2 Effect of Shear Stress

Repetitions of the experiments shown in *Figure 4-9* at higher and lower cross-flow velocities of 0.30 and 1.85 m s^{-1} did not significant enhance cleaning efficiency. At 0.30 m s^{-1}, the Reynolds numbers at 30, 40, 50 and 60°C were laminar to intermediate; 1380, 1680, 2000 and 2340 respectively. At 1.85 m s^{-1}, the Reynolds numbers at 30, 40, 50 and 60°C were turbulent; 8625, 10500, 12500 and 14585 respectively. Stepping from a laminar to turbulent bulk flow regime has the effect of reducing the laminar sub-layer but did not result in a measurable change in fouling resistance. Thus, shear force resulting from bulk turbulence did not enhance fouling resistance removal.

When the affects of shear force are compared to temperature it is clear that temperature dominates. Although it is recognised that the Reynolds number increased from 3450 to 5840, due to the water temperature increase of 30°C, the associated increase in shear is not thought to be responsible for the observed increase in reduction of fouling resistance as temperature increases. It is therefore thought likely that the increase in thermal energy, rather than kinetic energy, was responsible for deposit removal.

To investigate very high, artificial shear rates, manual shear was applied by scouring the surface of the fouled membrane with an abrasive sponge. The membrane module lid was then replaced and the water flux taken. Surprisingly, the subsequent water flux was only equivalent to water cleaning at a temperature of 40°C. However, the

possibility exists that the action of wiping the surface can push deposits into the pores. Therefore, the post-wiped deposit was viewed under the electron microscope. There was still no evidence of intra-pore fouling. Thus, the overall conclusion was that while high temperature alone was not successful in restoring membrane permeability, thermal energy was far more efficient than kinetic energy with respect to reducing fouling resistance for the conditions tested.

4.3.2 Sodium Hydroxide Cleaning

The cleaning effect of water alone was unsuccessful in restoring the membrane permeability. Therefore, the next step taken was to assess the effect of chemical cleaning. Sodium hydroxide was the first chemical selected as it is commonly used in the food industry for protein removal and forms the basis of many cleaning formulations.

Sodium hydroxide was found to greatly improve fouling resistance removal, even at low temperatures, but was unable to fully restore permeability. An optimal sodium hydroxide concentration of 0.01 wt% produced a flux recovery of 93±3% independent of cleaning temperature (30°C - 60°C) and the bulk flow regime ($1380 \leq Re \leq 8070$). Visualisation of the fouled surface provided an explanation for this phenomenon. At the optimal sodium hydroxide concentration, non-cellular matrix removal was complete.

4.3.2.1 Effect of Concentration

Optimal flux recovery was observed as a function of sodium hydroxide concentration (*Figure 4-10*). A sodium hydroxide concentration of 0.01 wt% [0.002M] resulted in a minimum fouling resistance of approximately $1x10^{10}$ m^{-1}.

Optimal cleaning of whey proteins with sodium hydroxide has been reported recently by Bird [1993] and Bartlett *et al.* [1995]. The existence of the optimal concentration was related to the visualised morphological changes to proteins on contact with sodium hydroxide. The optimal sodium hydroxide concentration caused whey protein deposits to swell by up to two and a half times their original thickness. Maximum swelling resulted in a structurally weak deposit that was susceptible to removal by fluid mechanical shear. Above and below the optimal concentration the deposit was more compact and less susceptible to shear removal.

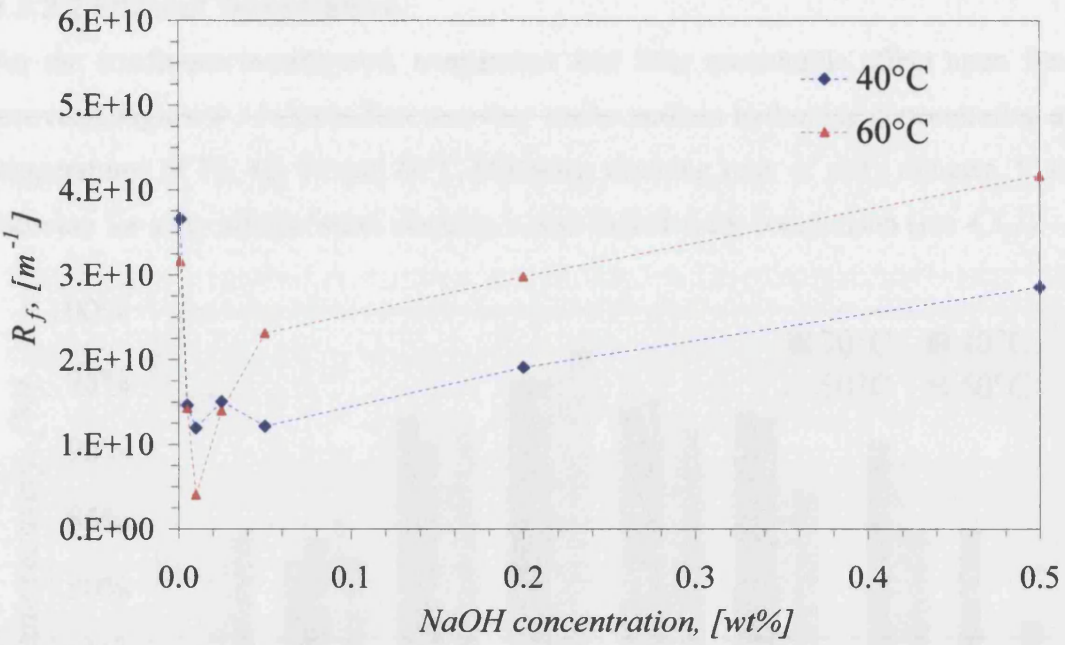

Figure 4-10: Effect of sodium hydroxide concentration on fouling resistance at 40°C and 60°C (Re = 3160 and 4380, respectively).

Bird [1993] and Bartlett *et al.* [1995] reported an optimal sodium hydroxide concentration of 0.5 wt% for removal of whey proteins from stainless steel hard surfaces and membranes with the permeate line closed. However, with the permeate line open Bartlett *et al.* [1995] reported reduced optimal sodium hydroxide concentrations of 0.2 and 0.4 wt% for stainless steel and ceramic membrane cleaning respectively. Thus, with respect to cleaning, membranes with the permeate line closed were analogous to hard surfaces. However, with the permeate line open the comparison of membranes with hard surfaces was not applicable. Although membrane cleaning with the permeate line open resulted in relatively low optimal sodium hydroxide concentrations, overall recovery was reduced due to foulant re-deposition and internal swelling leading to pore blocking. Therefore, membrane cleaning can be a compromise between flux recovery and the quantity of chemicals used.

In this study the permeate line was closed during membrane cleaning, analogous to hard surface cleaning. However, the observed optimal sodium hydroxide concentration of 0.01 wt% for yeast deposit removal was far less than the 0.5 wt% reported for whey proteins. Relevant differences between the systems are the different sources of fouling and the relative thickness of deposits, microns in this study and millimetres in the whey protein studies.

4.3.2.2 Effect of Temperature

For the conditions investigated, temperature had little measurable effect upon flux recovery. *Figure 4-11* shows flux recovery versus sodium hydroxide concentration at temperatures of 30, 40, 50 and 60°C following cleaning runs of sixty minutes. Flux recovery for sixty minute water cleaning is also included for comparison (*see 4.3.1*).

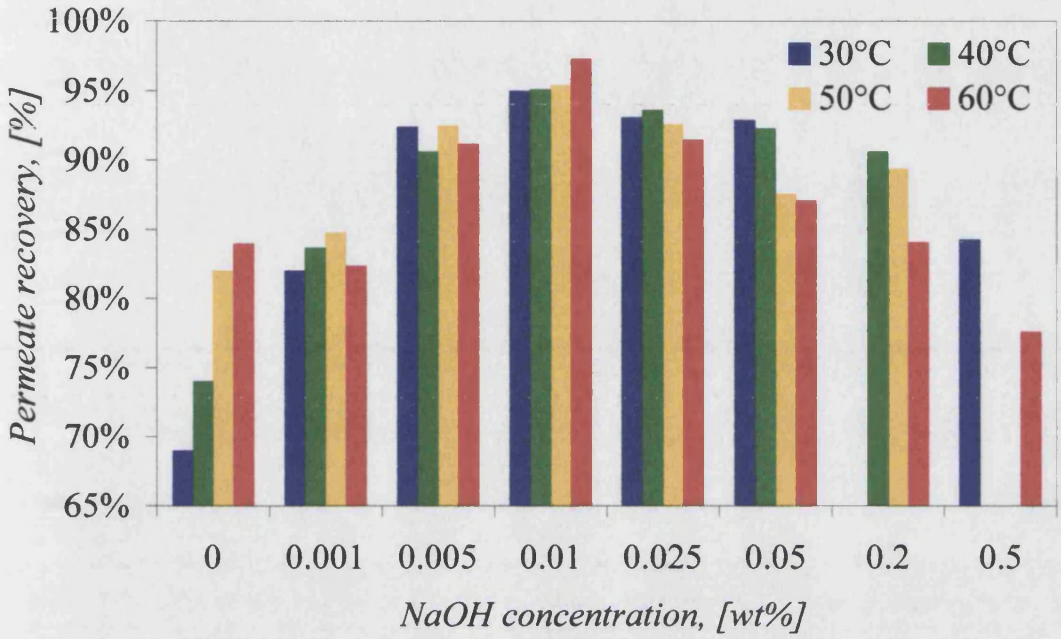

Figure 4-11: Effect of sodium hydroxide temperature on flux recovery

The optimal concentration profile is apparent for each temperature. At concentrations less than 0.025 wt%, temperature effects are not significant. However, at concentrations above 0.025 wt%, a temperature of 60°C resulted in significantly reduced membrane permeability. The residual deposit after cleaning at higher temperatures and concentrations was also very resistant to further cleaning. Jennings [1965] and Romney [1990] have described this observation during fouling as a burning effect. Deposits formed at high temperatures being more tenacious.

4.3.2.3 Effect of Cross-flow Velocity

The effects of four cross-flow velocities were investigated at a mild cleaning temperature of 40°C. The cross-flow velocities investigated were 0.30, 0.56, 1.02 and 1.85 m s^{-1}, which approximate to Reynolds numbers of 1680, 3150, 5775 and 10500. For this range of cross-flow velocity, no measurable change from the recovery shown in *Figure 4-10* was found. As for hydraulic cleaning with water only, the increase in

Reynolds number from a laminar to turbulent flow regime did not produce a significant increase in flux recovery.

4.3.2.4 Effect of Time

Deposit removal with sodium hydroxide was a very weak function of time. The shortest cleaning time possible, including static flow time, was thirty seconds, by which time cleaning had reached a maximum. Removal kinetics in the period before thirty seconds were unmeasureable. The relative speed of removal was surprising as the majority of other cleaning studies report cleaning times in the order of minutes rather than seconds for protein removal with sodium hydroxide. Again, the relatively thin deposit is thought to be the reason for the relatively small cleaning energy requirement.

4.3.2.5 Residual Deposit Appearance and Composition

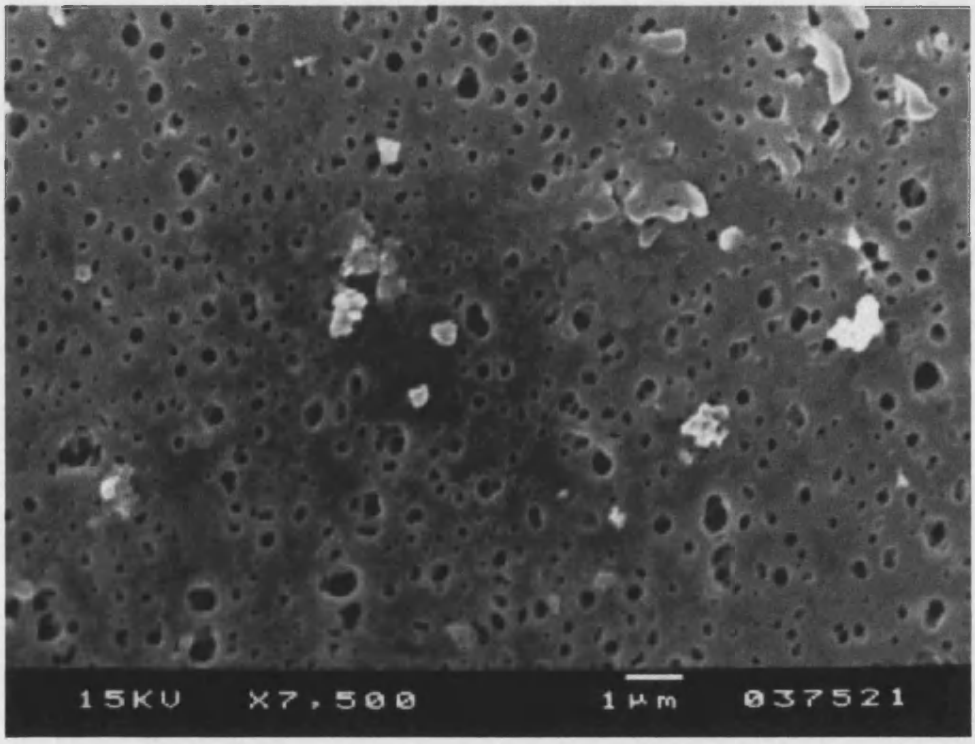

Figure 4-12: Residual deposits after cleaning with sodium hydroxide

Electron microscopy was used to visualise the residual foulant following cleaning with the optimal sodium hydroxide concentration. The appearance and chemical composition of the deposits were significantly different to the post-rinse data. Scattered cells were still visible but the non-cellular matrix had been completely removed, which revealed a previously hidden deposit. On close inspection of the post-

clean deposits, shown in *Figure 4-12*, they resemble fragments within the non-cellular matrix of the post-rinse deposit, shown in *Figure 4-7*.

X-ray analysis of the partially cleaned membrane surface identified the existence of elements not previously detected. Small peaks were identified for magnesium, sodium, potassium and silicon with a single large peak corresponding to chlorine. Absolute quantities of the elements are unknown though the peaks indicate relative quantities. Magnesium, sodium, potassium and silicon were associated with the new deposits, while the higher concentration of chlorine was associated with the cells.

The new deposits are small relative to the remaining cells. The remaining flux resistance would predominantly be due to the cells.

4.3.2.6 Effect of Salt Presence on Sodium Hydroxide Cleaning

It was postulated that the presence of sodium and chlorine in the deposit was directly related to the presence of salt in the suspension medium. Therefore, the fouling and cleaning process was repeated with the sodium chloride omitted from the medium. For each of three repetitions, membrane fouling resistance was successfully removed with a 0.01 wt% sodium hydroxide clean.

Thus, the required presence of salt in the yeast suspension to avoid cell rupture is thought to greatly complicate the cleaning process.

Results suggest that the omission of salt in the filtrate medium decreases the tenacity of the yeast deposit. In the absence of salt, yeast cells become highly hydrated and therefore less compressible. *Figure 3-10* shows that the profile of flux with time is altered by the omission of salt. The respective deposits are likely to have different characteristics with unique selectivities. Equally the dissociated sodium and chlorine ions may play an active role in the bonding process. It is unlikely that salt deposits onto the membrane surface first, thus occupying available sites. Flux reduction is a slow function of time for salt filtration relative to flux reduction due to cell deposition.

4.3.3 Nitric Acid Cleaning

It was likely that the inability of sodium hydroxide to completely restore membrane permeability was due to its ineffectiveness against inorganic species. Other workers have reported that sequential alkali and acid washes successfully remove soils in the

dairy industry, which essentially comprise a thin inorganic phosphate layer beneath a thick protein layer (Romney [1990]). Therefore, the effectiveness of nitric acid was investigated as a detergent; on its own and as the second stage of an alkali-acid clean.

Nitric acid was found to be a poor detergent when applied to the rinsed deposit. An 88% flux recovery was obtained at a temperature of 50°C and was independent of acid concentration. This is comparable to the effect of water cleaning at the same temperature. However, when the membrane was first cleaned with 0.01 wt% sodium hydroxide at 40°C, a subsequent clean with 0.064 M nitric acid at 50°C completed flux recovery, as shown in *Figure 4-13*. At temperatures of 30°C and 40°C flux recovery was incomplete for the conditions tested.

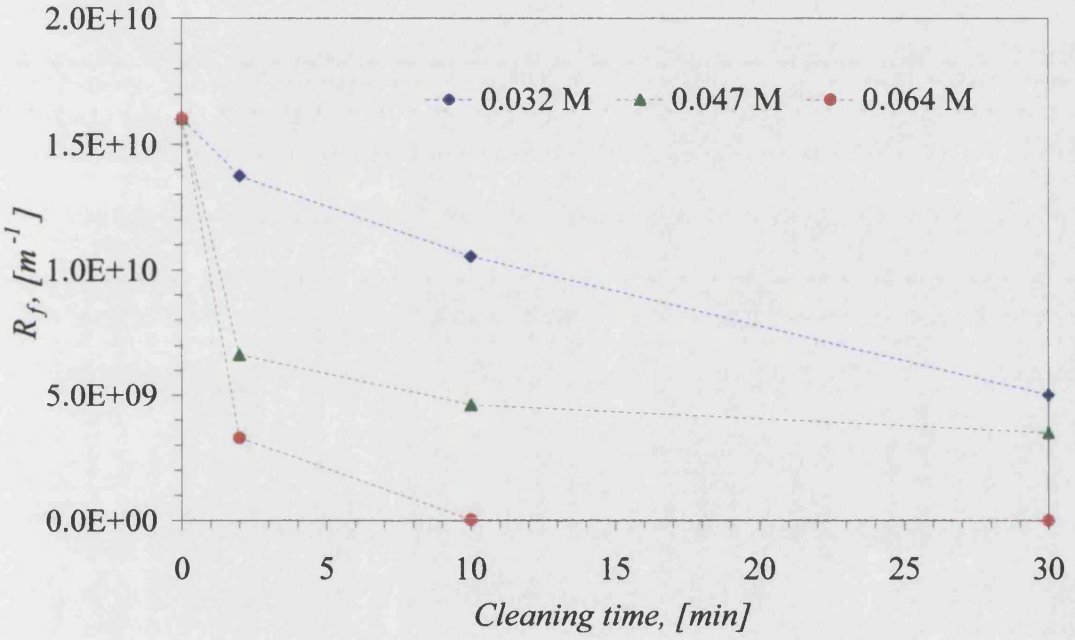

Figure 4-13: Effect of nitric acid concentration (50°C) on flux recovery following initial application of sodium hydroxide

Sodium hydroxide was responsible for removal of the organic non-cellular matrix, which was masking the inorganic deposit. This is analogous to milk or whey protein deposits. The inorganic residual layer remaining after sodium hydroxide cleaning is readily removed with nitric acid. However, when applied to the rinsed deposit, nitric acid was ineffective against the organic layer, the inorganic fraction remained and measured removal was due only to thermal energy effects.

Nagata *et al* [1989] have reported that cleaning with 1 M sodium hydroxide for 4 hours followed by 1 M nitric acid for 1 hour was effective for the removal of *Bacillus*

polymyxa deposits from ceramic, stainless steel and polypropylene membranes. For yeast deposit removal in this system, the required sodium hydroxide and nitric acid concentrations are far less, 0.002 M and 0.064 M respectively. Either *Bacillus polymyxa* form a more tenacious deposit than *Saccharomyces cerevisiae*, which could be related to the bacterial extracellular matrix (Hodgson *et al* [1993]), or there is further scope for optimisation within that study.

The application of the alkaline and acid detergents was reversed but at the same temperature, cross-flow velocity and concentration as previously. A 0.064 M nitric acid clean at 50°C for 20 min was therefore followed by a 0.01 wt% sodium hydroxide clean at 40°C. In the order of acid first alkali second, fouling resistance was not removed. In fact recovery was poor. The nitric acid clean recovered the flux to just 83%, while the sodium hydroxide clean increased the flux to 88%. Water at 50°C for twenty minutes achieved a flux recovery of 84%, very comparable to the nitric acid clean. Thus, it must be concluded that cleaning was not necessarily due to chemical interaction but could be attributable to thermal energy effects. Interestingly, the overall flux recovery achieved with the acid and alkali clean was equivalent to results using sodium hydroxide cleaning only.

The observed results may be explained in terms of reaction rather than mass transfer. Although the bond between the foulant and the membrane lies underneath the cell, relatively sheltered from chemical penetration, following a sodium hydroxide clean, nitric acid was able to restore membrane permeability in a matter of minutes. Sodium hydroxide was not. Therefore, the nature of the foulant bond must be the key to removal. Sodium hydroxide and nitric acid have similar diffusivities therefore the fact that one was successful where the other was not suggests that compatibility of detergent to foulant was an issue for successful cleaning.

4.3.4 *P3 Ultrasil 11* Cleaning

P3 Ultrasil 11 was able to completely restore membrane permeability in a single-stage clean. LTSEM confirmed that no measurable traces of foulant remained.

Increasing time, temperature and concentration all had a favourable effect upon recovery; temperature and concentration being the critical factors. Although sodium

hydroxide removed the non-cellular material within seconds, *P3 Ultrasil 11* completed recovery over a period of approximately thirty minutes.

The fouling resistance prior to cleaning was $6\pm0.5x10^{10}$ m^{-1}. Concentrations of *P3 Ultrasil 11* were selected to give equivalent sodium hydroxide alkalinity. Titration with hydrochloric acid and phenolphthalein indicator showed the ratio of alkaline strength between sodium hydroxide and *P3 Ultrasil 11* to be in the ratio 1.96:1.

4.3.4.1 Effect of Concentration

Figure 4-14 shows fouling resistance versus *P3 Ultrasil 11* concentration after cleaning for sixty minutes. At 30°C and 40°C, the investigated treatment combinations did not fully restore fouling resistance. However, at 60°C concentrations of 0.05 wt% and 0.1 wt% did achieve complete flux recovery, removing the fouling resistance completely.

In all cases, increasing the *P3 Ultrasil 11* concentration had a positive effect upon cleaning. However, at concentrations above 0.02 wt%, fouling resistance removal was not a strong function of *P3 Ultrasil 11* concentration. Although increasing temperature reduced fouling resistance in conjunction with concentration, a trend of decreasing removal rate can be seen as a function of concentration.

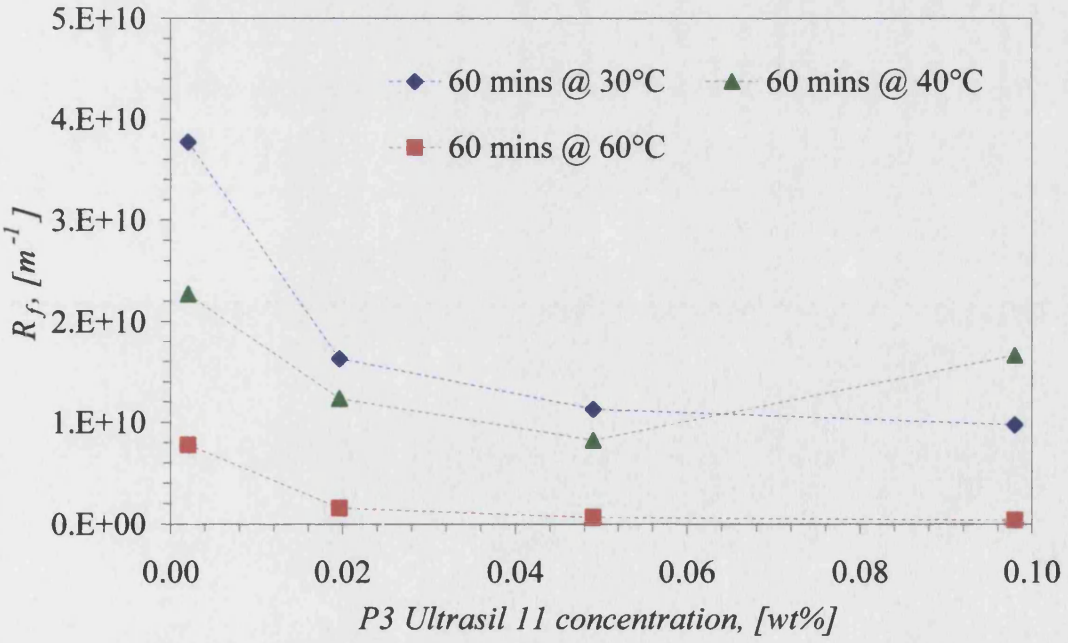

Figure 4-14: P3 Ultrasil 11 efficiency as a function of concentration after sixty minutes cleaning

4.3.4.2 Effect of Temperature

Figure 4-15 and *Figure 4-16* show fouling resistance as a function of time for *P3 Ultrasil 11* cleaning temperatures of 30°C and 60°C respectively.

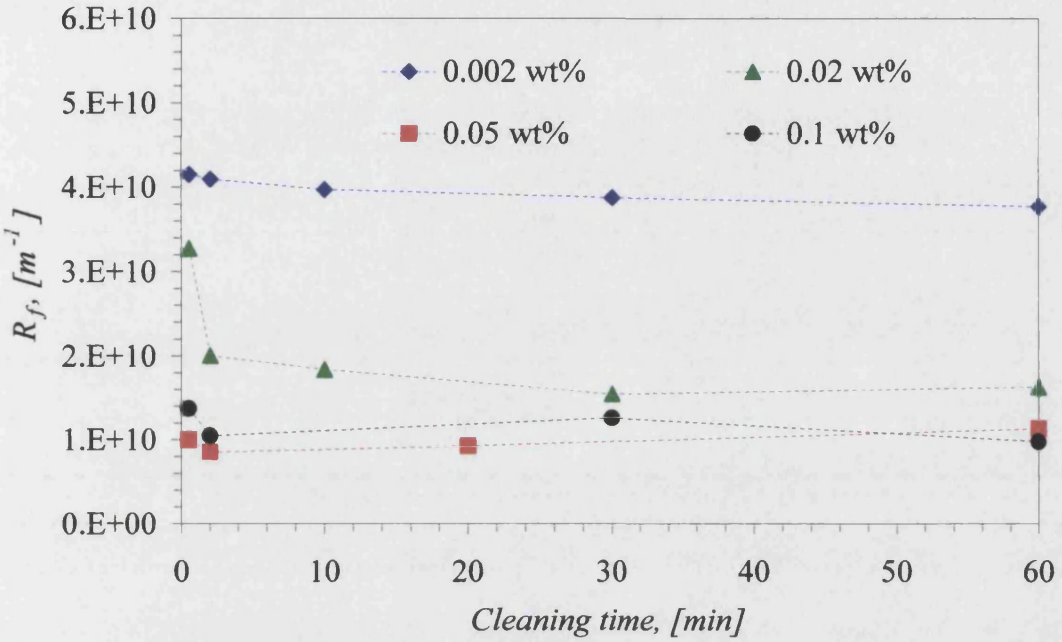

Figure 4-15: Cleaning with P3 Ultrasil 11 at 30°C

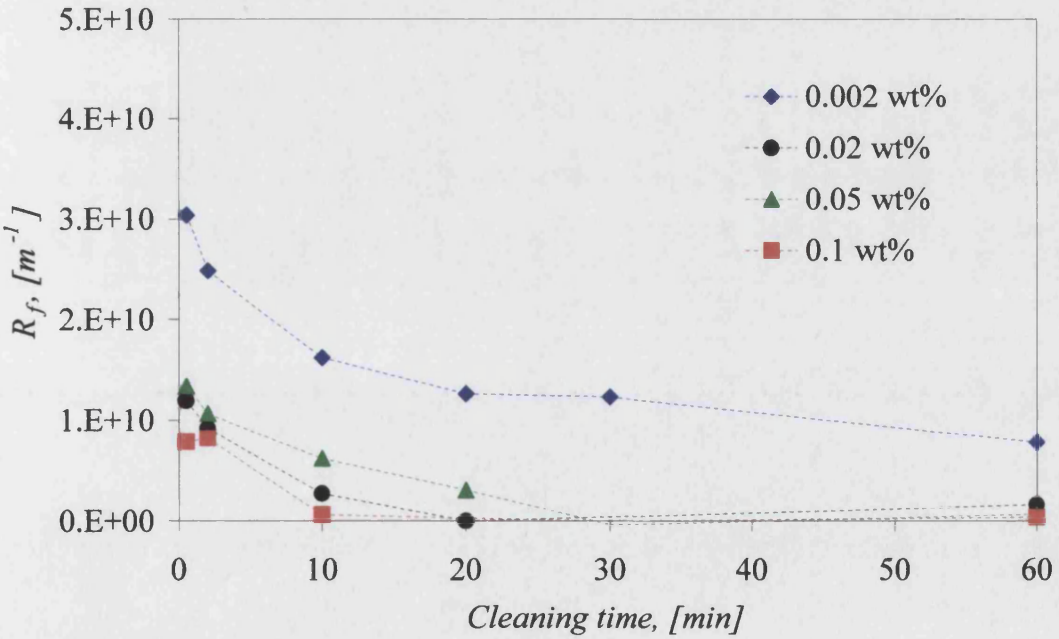

Figure 4-16: Cleaning with P3 Ultrasil 11 at 60°C

Cleaning at 30°C was less dynamic than at the relatively high temperature of 60°C. At 30°C, fouling resistance changes were only a very weak function of time. For all of

the *P3 Ultrasil 11* concentrations applied, fouling resistance removal was not completed. However, at 60°C fouling resistance reduced significantly with time and complete removal was achieved within thirty minutes for concentrations of 0.02, 0.05 and 0.1 wt%.

Figure 4-17 shows fouling resistance removal as a function of temperature, which summarises that increasing temperature has a positive effect upon fouling resistance removal. The profile seen for 0.002 wt% is similar to the profile seen when cleaning with water only, suggesting that there is minimal benefit from chemical energy compared to thermal energy. At higher concentrations of 0.02, 0.05 wt% and 0.1 wt% fouling resistance was successfully removed at 60°C, which was not the case with water, but not at the lower temperature of 30°C. Therefore, fouling resistance removal is attributed to the combined contributions of chemical and thermal energy from the *P3 Ultrasil 11* solution.

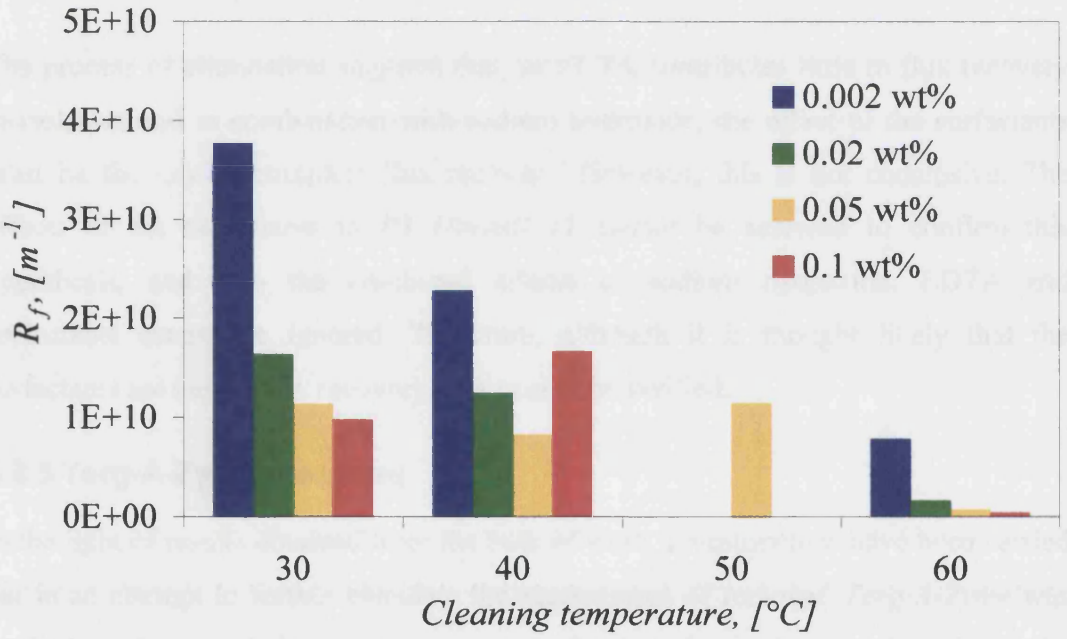

Figure 4-17: Cleaning for sixty minutes with P3 Ultrasil 11 as a function of temperature.

4.3.4.3 Sodium hydroxide, Surfactant and EDTA Contributions

The ingredients of *P3 Ultrasil 11* are sodium hydroxide, anionic and non-ionic surfactants, and EDTA. The individual cleaning characteristic of sodium hydroxide has been defined. Therefore, consider the contributions of EDTA and surfactants.

Knowledge of the exact surfactants within *P3 Ultrasil 11* is not in the public domain. Therefore, their detergent or wetting contribution to cleaning is speculation only. Thus, only the effects of EDTA and sodium hydroxide can be studied in isolation.

The exact amount of EDTA in *P3 Ultrasil 11* is not in the public domain but it is known to be between 30 wt% and 50%. Thus, the fraction of EDTA in *P3 Ultrasil 11* can be estimated at approximately 40%. Thus, for a 0.1 wt% *P3 Ultrasil 11* solution, the EDTA contribution is equivalent to a 0.04 wt% solution.

When 0.04 wt% EDTA at 50°C was applied to the rinsed deposit for thirty minutes, flux recovery was equivalent to that of water only, 84%. Little measurable effect due to the EDTA was seen. Also, when 0.04 wt% EDTA was applied in combination with the optimal sodium hydroxide concentration of 0.01 wt%, flux recovery was 93%, equivalent to sodium hydroxide only. Therefore, the individual effect of EDTA and its combined effect with sodium hydroxide was negligible.

The process of elimination suggests that, as EDTA contributes little to flux recovery in isolation and in combination with sodium hydroxide, the effect of the surfactants must be the key to complete flux recovery. However, this is not conclusive. The effects of the surfactants in *P3 Ultrasil 11* cannot be assessed to confirm this hypothesis, and also the combined effects of sodium hydroxide, EDTA and surfactants cannot be ignored. Therefore, although it is thought likely that the surfactants are key to flux recovery, this cannot be verified.

4.3.5 Terg-A-Zyme Cleaning

In the light of results obtained from the bulk of work, investigations have been carried out in an attempt to further elucidate the mechanisms of removal. *Terg-A-Zyme* was applied to the rinsed deposit to investigate the hypothesis that the deposit can be characterised as part organic and part inorganic.

Terg-A-Zyme (TAZ) is an enzyme-based commercial cleaner with an optimal operating temperature, corresponding to maximum enzyme activity, of 50°C. TAZ was applied to the original, rinsed deposit at the manufacturers recommended concentration and temperature of 0.3 wt% and 50°C, respectively. At temperatures greater than 50°C, the enzyme can be denatured, while at temperatures lower than

50°C, enzyme activity reduces. The flux recovery achieved with TAZ was equivalent to optimal cleaning with sodium hydroxide only. This proved very interesting. It has been stated that sodium hydroxide is thought to be effective against organic deposits, and specifically the predominantly proteinaceous part of the deposit. TAZ, being a protease based enzyme, is specifically targeted for protein deposits. If both TAZ and sodium hydroxide were capable of removing the proteinaceous deposit fraction, they would be expected to achieve similar flux recovery. Although this did not constitute absolute proof of the deposit nature, it was very encouraging.

4.3.6 Chemical Cleaning Summary

Cleaning in-place of the rinsed deposit with water could not remove the fouling resistance, although water at 50°C and 60°C performed significantly better than at 30°C and 40°C.

Sodium hydroxide greatly improved cleaning but could not recover the membrane permeability under the conditions used. A sodium hydroxide concentration of 0.01 wt% was found optimal for flux recovery. The optimal concentration was independent of temperature and time.

Nitric acid was a poor detergent when applied to the rinsed deposit. However, when used as the second stage of a sequential clean with sodium hydroxide, flux recovery was completed. Order of application was crucial. Nitric acid first followed by sodium hydroxide was inferior, recovery being equivalent to using sodium hydroxide only.

P3 Ultrasil 11 was also able to recover membrane permeability but in a single-stage clean. However, overall cleaning time was greater than the sequential alkali and acid clean.

CHAPTER 5 - MATHEMATICAL MODELLING

5.1 CLEANING MODELS: A REVIEW

5.1.1 Introduction

Mathematical modelling can be defined as the activity of translating observations into mathematics for subsequent analysis. A mathematical model will be created and its solution will usually provide information useful in solving current problems or predicting future trends.

The interest of mathematical modelling lies not so much in solving equations, as being able to make the most effective translation from the original problem into mathematics (Edwards and Hamson [1996]). This ensures that the resulting model is of some practical use in solving the real problem. Powerful modern computer software has made the process of solving derived mathematical models relatively easy. The main difficulty therefore lies in understanding the problem and its subsequent conversion into a mathematical form.

Modelling a cleaning process involves calculating precisely the deposit removal rate, the total time taken to clean and the amount of cleaning agent required. If possible, this would result in the non-empirical design of cleaning systems and an optimisation of industrial cleaning operations, resulting in a reduction of the costs incurred by cleaning. In addition, the environment would benefit from reduced waste emissions from milder cleaning processes.

A number of mathematical models have been used previously to describe the removal of fats, proteins and sugar deposits from hard surfaces. Despite the undoubted complexity of the cleaning processes, all have commonly been described by either simple zero or first order removal rates. However, recent advances in deposit analysis have allowed more mechanistic models to be developed, describing observed morphological changes of whey protein deposits when contacted with sodium hydroxide.

Membrane cleaning models have evolved from hard surface cleaning knowledge. In the case of the permeate line being closed during cleaning, membrane systems can be regarded as hard surfaces, especially if in-pore fouling is absent. However, in the case of cleaning with the permeate line open, system parameters of membrane cleaning models are unique.

5.1.2 Simple Models

Despite the undoubted complexity of the cleaning process at the molecular level, it is perhaps surprising that many experimental cleaning observations have been described well with simple mathematical expressions.

When formulating models, all workers agree that cleaning is a function of the system (temperature and flow rate) and the cleaning solution (formulation and concentration). The most common modelling approach adopted by workers is to consider the removal of deposit mass from unit surface area with time. Models vary though in their assumed kinetic dependence on deposit mass.

Physically, simple cleaning models predict that the tenacious deposit X undergoes a transformation via reaction, yielding a product Z. The product is readily solubilised or dispersed and transported away from the site of reaction. In the case of membranes, the shearing action of cross-flow provides an aid to the relatively small diffusive driving force, due to the large size of the removed product.

$$X \xrightarrow{reaction} Z$$

5.1.2.1 Zero order in deposit amount

Zero order kinetics state that the rate of removal is proportional to the deposit mass X to zero power i.e. unity. Therefore, the rate of removal at any time is constant, and independent of deposit mass, as shown in *Equation 5-1*.

$$-\frac{dX}{dt} = kX^0 \Rightarrow \int_{X_0}^{X} dX = -k\int_{0}^{t} dt \Rightarrow X = X_0 - kt \qquad \textit{Equation 5-1}$$

Schlüssler [1970] studied the removal of milk protein from steel and glass surfaces using sodium hydroxide. He found that removal rates were zero order with respect to both the amount of deposit and detergent concentration for caustic solutions above 1 w%.

Physically, a zero-order removal rate in mass states that deposit depth has no effect on the removal rate from the surface. This implies that detergent transport into the deposit does not occur. Mass transfer from the bulk flow into the deposit thickness is therefore the rate limiting step of the cleaning process. For a zero order removal, the reaction of detergent and deposit occurs only at the solid-liquid interface. As time

continues, a reaction front moves through the depth of the deposit at a constant rate. The relatively few occurrences of zero order kinetics reported in the literature suggests that detergent penetration of deposits is not commonly the rate limiting step.

5.1.2.2 First Order kinetics

First order kinetics state that the rate of removal is proportional to the deposit mass X to the first power, as shown in *Equation 5-2*.

$$-\frac{dX}{dt} = kX^1 \Rightarrow \int_{X_0}^{X} \frac{dX}{X} = -k\int_{0}^{t} dt \Rightarrow X = X_0\, exp(-kt) \qquad \textit{Equation 5-2}$$

First order reaction kinetics have been the most widely used to model cleaning observations, especially in the textile and dairy industries (Plett [1985]). First order reaction kinetics have described the removal of fats, proteins and sugars. Jennings [1965] showed that the removal of milk deposits from stainless steel with sodium hydroxide was first order in both deposit mass and sodium hydroxide concentration.

Physically, a removal rate that is first order in deposit mass implies that penetration of the deposit by the detergent is instantaneous (Corrieu [1981]). Thus, the reverse of zero order is true, removal is reaction controlled rather than mass transfer controlled. Unlike zero order kinetics, it must be assumed that for first order kinetics the detergent is exposed to all parts of the deposit instantaneously, i.e. detergent diffusion into the deposit is complete and fast.

5.1.2.3 Two Species Removal

For some observations, the assumption of a single reaction kinetic could not describe the observed cleaning data. An approach to solving these anomalies was to consider that the deposit contained two species, each with independent removal rates. Simple, simultaneous reaction kinetics describe the removal of each deposit species. The total rate of removal, the sum of the individual rates, can then be compared to cleaning observation.

$$X_1 \xrightarrow{reaction} Z$$
$$X_2 \xrightarrow{reaction} Z$$

The observed removal of the fat tristearin from stainless steel has been modelled as two simultaneous first order reaction kinetics (Bourne and Jennings [1961], Bourne

and Jennings [1963b], Bourne and Jennings [1963c], Bourne and Jennings [1963d]). Bourne and Jennings labelled pure synthetic tristearin with the radioactive carbon isotope ^{14}C. A 0.03 M sodium hydroxide solution was used as the detergent. Further experimentation sought to provide physical evidence for the existence of two species. Bourne and Jennings have also successfully applied the two-species model to previous works; previously described less accurately with single-species models.

5.1.3 Mechanistic Models

Mechanistic models take a more theoretical approach to modelling the removal kinetics. Such models have thus far been formulated to describe the cleaning of deposits that change morphology on contact with detergents.

A mechanistic approach to modelling the cleaning process was first applied to the removal of milk deposits from a hard surface by Harper [1972] who described the cleaning process as several distinct steps. This approach has since been applied to the removal of whey protein concentrate from both hard and membrane surfaces.

5.1.3.1 Gallot-Lavallée and Lalande [1985]

The qualitative multi-stage model of Harper [1972] was greatly improved upon by Gallot-Lavallée and Lalande who developed a quantitative model to describe the observed removal of pasteurised milk when cleaned in-place with sodium hydroxide.

Gallot-Lavallée and Lalande found that, in contrast to the cleaning observations of previous workers, their experimental observations were that the initial rate of removal was zero, followed by an increase up to a maximum, followed by a decrease back to zero.

The fact that the initial cleaning rate was zero supported the theoretical mechanism proposed by Harper [1972]. He proposed that solid deposits should be considered either porous or non-porous. Porous deposits were defined as being penetrated instantaneously and non-porous as not penetrated. In this case, cleaning was found to be proportional to the amount of detergent used and the amount of soil remaining. However, for porous deposits, the water and detergent absorption in the mass of the deposit can provoke swelling followed by detachment. In the case of Gallot-Lavallée and Lalande, the initial compound adhering to the wall X underwent a morphological

change becoming intermediate *Y* before being washed away with the cleaning solution bulk flow as product *Z*. The model comprises four successive cleaning steps:

(1). External mass transfer of hydroxyl ions from the bulk of the cleaning solution to the solid-liquid interface at the surface of the deposit.

(2). Internal diffusion of hydroxyl ions through the layers of intermediate Y already formed.

(3). Reaction of the initial deposit X with the hydroxyl ions at a reaction interface. As a result, the structure of the deposit changes from the initial X to the intermediate Y.

(4). The elimination of intermediate Y from the surface by mass transfer of material back into the bulk solution.

Each step of the process is represented by one of four first order differential equations:

$$-\frac{dX}{dt} = nfk_r C_{OH.I} \qquad \textit{Equation 5-3}$$

$$-\frac{dY}{dt} = \frac{Yk_D}{v} - nfk_r C_{OH.I} \qquad \textit{Equation 5-4}$$

$$-\frac{dZ}{dt} = \frac{Yk_D}{v} \qquad \textit{Equation 5-5}$$

$$-\frac{dC_{OH.I}}{dt} = k_r C_{OH.I} - \frac{(C_{OH.B} - C_{OH.I})}{f\left(\frac{1}{k_{OH}} + \frac{Y}{\rho_y D_{OH}}\right)} \qquad \textit{Equation 5-6}$$

$$X \xrightarrow{swelling} Y \xrightarrow{removal} Z$$

5.1.3.2 Bird [1993]

Bird used the work of Gallot-Lavallée and Lalande [1985] as a basis for the cleaning in-place of whey protein concentrate from a hard stainless steel surface using sodium hydroxide. Observed recovery rates were compatible with the path proposed by

Gallot-Lavallée and Lalande [1985]. The initial removal rate was zero, followed by an increase up to a maximum, followed by a decrease back to zero. Swelling of the whey protein was visualised using scanning electron microscopy. Maximum swelling was found to coincide with optimal recovery corresponding to the optimal sodium hydroxide concentration. Bird's conclusion was that the deposit had minimum mechanical strength at the point of maximum swelling.

A significant advancement of the model of Gallot-Lavallée and Lalande was the introduction of a pseudo steady state approximation for $C_{OH,I}$. The number of variables in the model was reduced from eight to four; those being the rate constants k_x and k_y, the hydroxyl ion diffusion D_{OH} and stoichiometric coefficient s. Of these parameters D_{OH} and s can be estimated with a degree of confidence from literature values.

5.1.3.3 Bird and Bartlett [1997]

Bird and Bartlett have applied hard surface cleaning knowledge to a membrane system. They have formulated a model to describe the reduction of resistance occurring when a 2.0 μm sintered stainless steel flat sheet membrane fouled with reconstituted whey protein concentrate is cleaned using aqueous sodium hydroxide. The change in morphology of the whey proteins in the presence of sodium hydroxide was central to their modelling approach. The model relies on simultaneous removal and swelling processes occurring to the surface and in-pore deposits respectively.

Bartlett *et al.* [1995] have demonstrated that flux recovery curves determined experimentally showed a characteristic shape. From an initial flux recovery of zero, there was a rapid increase of flux recovery upon contact of the deposit with the sodium hydroxide up to a maximum value. The magnitude of the optimal flux recovery observed was dependent upon both detergent concentration and temperature. There followed a relatively long period where flux recovery fell gradually, and in some instances reached a non-zero steady state value. Bird [1993] observed that whey protein deposits fouled on hard surfaces swell to form a structure that has greatest voidage at the optimum sodium hydroxide concentration.

Cleaning was carried out with the permeate line open allowing flux data to be collected during the cleaning process. X-ray diffraction confirmed the presence of intra-pore deposits.

The flow through a microfiltration membrane is described by Darcy's law, as shown in *Equation 2-4* (*p.24*). In the presence of fouling, the variation of fouling resistance R_f is responsible for the flux reduction form the ideal. Bird and Bartlett considered the fouling resistance as the sum of three resistances; the resistance due to concentration polarisation R_{cp}, the cake resistance R_c, and the in-pore deposit resistance R_i, as shown in *Equation 5-7*. R_{cp} was negligible during cleaning.

$$R_f = R_{cp} + R_c + R_i \qquad \textit{Equation 5-7}$$

The rate of removal of R_c was modelled with a second order kinetic in surface deposit resistance, as shown in *Equation 5-8*. The in-pore deposit resistance was considered to affect flux in terms of reducing the effective pore diameter as the deposit swells. The effective diameter change d_e was described by second order swelling. The link between effective pore diameter and resistance was modelled using a modified Carman-Kozeny relationship.

$$-\frac{dR_c}{dt} = k_\alpha R_c^2 \Rightarrow \int_{R_{c(0)}}^{R_c} \frac{dR_c}{R_c^2} = -k_\alpha \int_0^t dt \Rightarrow R_c = \frac{R_{c(0)}}{1 + R_{c(0)} k_\alpha t} \qquad \textit{Equation 5-8}$$

$$R_i = \frac{36 h_k (1-\varepsilon)^2 l}{\varepsilon^3 d_e^2} \text{ where, } d_e = \left(d_0 - 2\left[\left(\frac{\delta}{k_2 t + \delta} \right) (\eta k_2 t + \delta) \right] \right) \qquad \textit{Equation 5-9}$$

$$R_f = \frac{R_{c(0)}}{1 + R_{c(0)} k_\alpha t} + \frac{36 h_k (1-\varepsilon)^2 l}{\varepsilon^3 \left(d_o - 2\left[\left(\frac{\delta}{k_2 t + \delta} \right) (\eta k_2 t + \delta) \right] \right)^2} \qquad \textit{Equation 5-10}$$

Where, d_o is the nominal pore diameter, k_2 a second order rate constant, δ the original unswollen in-pore deposit thickness, η the ratio of the swollen to unswollen deposit thickness, and t is the time of cleaning.

The variation of R_f with time is described by *Equation 5-10*. The equation allows optimisation of the rate constants k_α and k_2. The other parameters are measurable or known. Good correlation with observed data was found. Further improvements to the

model are planned. For example, several parameters are presented as being constant but are actually time dependent.

5.1.4 Factors Affecting the removal rate constant k

Depending on the model used, the dimensions of the removal rate constant k can vary greatly. Many factors can potentially affect k, including detergent temperature, detergent concentration, nature of the foulant, age of the deposit, etc.

Experimentally, the influence of temperature on the rate constant of a reaction is well represented by the Arrhenius equation:

$$k = k_0 \exp\left(\frac{-E}{RT}\right) \qquad \textit{Equation 5-11}$$

$$\ln k = \ln k_0 - \frac{E}{R}\frac{1}{T}$$

E is termed the activation energy because it is associated with an energy barrier, which the reactants must surmount to form a cleaned product Similarly, k_0 is associated with frequency with which the activated complex breaks down into products; or, in terms of simple collision theory, it is associated with the probability of reaction related to the frequency of collision.

For many reactions E lies in the range 50 - 250 kJ mol^{-1} (Coulson and Richardson [1979]). Bird [1993] specifically states that diffusion controlled cleaning processes would display an activation energy of approximately 20 kJ $kmol^{-1}$, whereas reaction controlled cleaning processes would typically display an activation energy of 150 - 300 kJ mol^{-1}.

5.2 MODEL SELECTION AND APPLICATION

According to Plett [1985], mathematical models in general should be kept 'as simple as possible and as complex as necessary'. Thus, while the six steps described by Plett [1985] in the general chemical cleaning scheme must be taken into consideration, it may not be necessary to involve all of them in a model. The engineering approach to considering the selection process is to determine the controlling or rate-limiting step, or steps, among the diverse mechanisms in each particular situation.

Experimental flux results when cleaning with sodium hydroxide and nitric acid, alone and in combination, have suggested that two species exist with respect to cleaning. Microscopic visualisation has provided further evidence for this. The first species is readily removed with sodium hydroxide and is presumably organic. The second is removable with acid and is presumably inorganic. This is consistent with fouling deposits found in the dairy industry, which contain multiple organic and inorganic foulants (Zeman and Zydney [1996]). However, it was not possible to model and then compare the dynamics of cleaning for sodium hydroxide solutions because the cleaning was too rapid for the experimental set-up used.

P3 Ultrasil 11 was able to remove both deposit species. On the basis of the experimental evidence, it would therefore seem likely that two-species removal kinetics should be investigated. The mechanistic models of Bird [1993], Bird and Bartlett [1997], and Gallot-Lavallée and Lalande [1985] are not applicable due to the lack of experimental evidence for morphological changes in the deposit. A maximum removal rate was not observed. The removal rate either decreased or was constant with time. Thus, the mechanistic models are not applicable to this study.

The cleaning dynamics with the *P3 Ultrasil 11* were sufficiently slow to allow comparison between experimental data and model to be made, as shown below. Zero and first order removal kinetics have been applied with varying degrees of success, singly and in combination, to the single-stage removal experiments, as shown in *Table 5-1*.

Hard surface cleaning is modelled as the rate of deposit mass removal as a function of time. However, in membrane studies it is more realistic to model the decrease of fouling resistance as a function of time. If the deposit is homogeneous with respect to

mass then the corresponding resistance is proportional. However, in reality, deposits are rarely homogeneous. Therefore, converting resistance values to approximate deposit masses would be unwise. Bird and Bartlett [1997] have also taken the option of modelling fouling resistance rather than estimating the deposit mass. Thus, in the following derivation, the deposit mass M is replaced with resistance R.

Model (in deposit resistance)	Total Error Squared
Zero order	7.51E+22
First order	7.89E+21
Zero - Zero order	7.51E+22
Zero - First order	3.09E+21
First - Zero order	3.07E+21
First - First order	1.32E+21

Table 5-1: Relative merits of mathematical model approaches.

The model that best described the *P3 Ultrasil 11* cleaning data was a two-species removal type, with both organic and inorganic species displaying first order removal with respect to fouling resistance. Although the removal orders were not initially apparent, the model is derived directly from experimental observations. The models relationship to the data and its simplicity are its strengths.

5.2.1 Two Species: Simultaneous First Order Removal

A simultaneous two-species removal model is described with each deposit species displaying a first order resistance decrease with time. First order kinetics imply that the deposit is penetrated instantaneously by the detergent. Therefore, it is considered that in this instance the cleaning process is not diffusion controlled. Therefore, it is concluded that the process must be reaction controlled, as transport away from the reaction site is assumed to be aided by the cross-flow of feed.

5.2.2 Mathematical Derivation

Consider the rate of removal of fouling resistance associated with organic and inorganic species. Let subscripts *1* and *2* denote the organic and inorganic layers respectively. Thus, the total resistance is comprised of two independent resistances R_1 and R_2. Upon reaction with the detergent the two resistances are transformed to

varying degrees into product Y, which is either dispersed or solubilised in the bulk flow.

$$R_1 \xrightarrow{\textit{first order resistance removal rate}} Y$$

$$R_2 \xrightarrow{\textit{first order resistance removal rate}} Y$$

If the sum of the individual removal rates is equal to the total removal rate, the rates must be simultaneous and independent, as shown in *Equation 5-12*.

$$-\frac{dR}{dt} = -\left(\frac{dR_1}{dt} + \frac{dR_2}{dt}\right) \qquad \textit{Equation 5-12}$$

The observed fouling resistance removal was best described with first order models for each species. Thus, at time *t*, the fouling resistance of each species can be solved implicitly by integrating the first order expressions. The total fouling resistance is the sum of the individual species contributions, as shown in *Equation 5-13*.

$$-\frac{dR_1}{dt} = k_1 R_1 \Rightarrow \int_{R_{1(0)}}^{R_1} \frac{dR_1}{R_1} = -k_1 \int_0^t dt \Rightarrow R_1 = R_{1(0)} exp(-k_1 t)$$

$$-\frac{dR_2}{dt} = k_2 R_2 \Rightarrow \int_{R_{2(0)}}^{R_2} \frac{dR_2}{R_2} = -k_2 \int_0^t dt \Rightarrow R_2 = R_{2(0)} exp(-k_2 t)$$

$$R = R_{1(0)} exp(-k_1 t) + R_{2(0)} exp(-k_2 t) \qquad \textit{Equation 5-13}$$

$R_{1(0)}$ and $R_{2(0)}$ denote the initial fouling resistance of species *1* and *2*, respectively. Let α denote the resistance of the initial deposit comprised of species *1*. Therefore, $R_{1(0)} = \alpha R_{(0)}$ and $R_{2(0)} = (1-\alpha)R_{(0)}$. The change of total fouling resistance with time is represented by *Equation 5-14*.

$$R = \alpha R_{(0)} exp(-k_1 t) + (1-\alpha) R_{(0)} exp(-k_2 t) \qquad \textit{Equation 5-14}$$

The model therefore requires knowledge of the total initial fouling resistance $R_{(0)}$, the fraction of species *1* in the initial deposit α, and the reaction rate constants k_1 and k_2.

5.2.3 Initial Fouling Resistance

The total initial deposit resistance $R_{(0)}$ is quantified when the permeate flux is measured after rinsing prior to cleaning. The average value was 6×10^{-10} m^{-1}, which

has been used as the starting point for all sets of data in the model. It should be noted though that variation in the resistance initially is a source of error within the model.

The fraction of the resistance due to organic species within the total deposit can be estimated from the results gained during sodium hydroxide cleaning, since it is assumed that sodium hydroxide acts only on organic deposits. Thus, the fraction of the resistance removed by sodium hydroxide can be estimated to be the organic fraction.

The average deposit resistance before cleaning was 6×10^{10} m^{-1}. After cleaning with 0.01 wt% sodium hydroxide the fouling resistance was reduced on average to 1×10^{10} m^{-1}. Thus, the percentage removal of organic deposit can be estimated at 83%.

5.2.4 Results & Discussion

The correlation between the two species model and the observed data gave an acceptable fit. The strength of the model lies in its simplicity, with relatively few variable parameters. The model also has physical applicability. In fact analysis of experimental results suggested a two-species approach before modelling was approached. It was encouraging that the model matched the physical evidence.

The model was found sensitive to the initial deposit composition. An initial organic fraction of 73.5% gave the smallest error sum of squares. Analysis of flux recovery using sodium hydroxide gave an estimated value of 83%. However, individual optimisations for each treatment combination has revealed that the optimum values for the initial organic deposit fraction, applied individually, varies between 30% and 85%.

5.2.4.1 Comparison of Model to Experimental

Plots are presented showing the model results superimposed onto the experimental observations. Individual and overall optimisations are shown. Individual optimisation reflects the optimal parameters for each individual treatment combination. Overall optimisation reflects the parameters that minimise the total sum of the individual sums of squares.

The model can be seen to best fit concentrations of *P3 Ultrasil 11* above 0.002 wt%, especially at temperatures greater than 40°C. In all plots the general experimental trend of flux decline is well represented by the model.

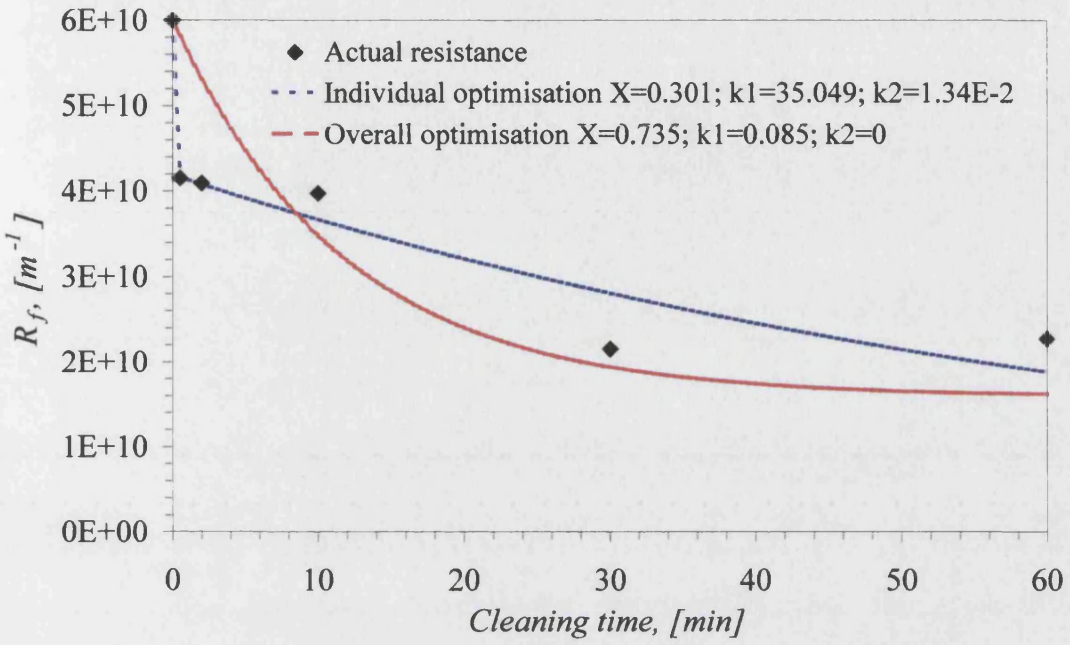

Figure 5-1: Modelling cleaning with 0.002 wt% P3 Ultrasil 11 @ 30°C as a function of time.

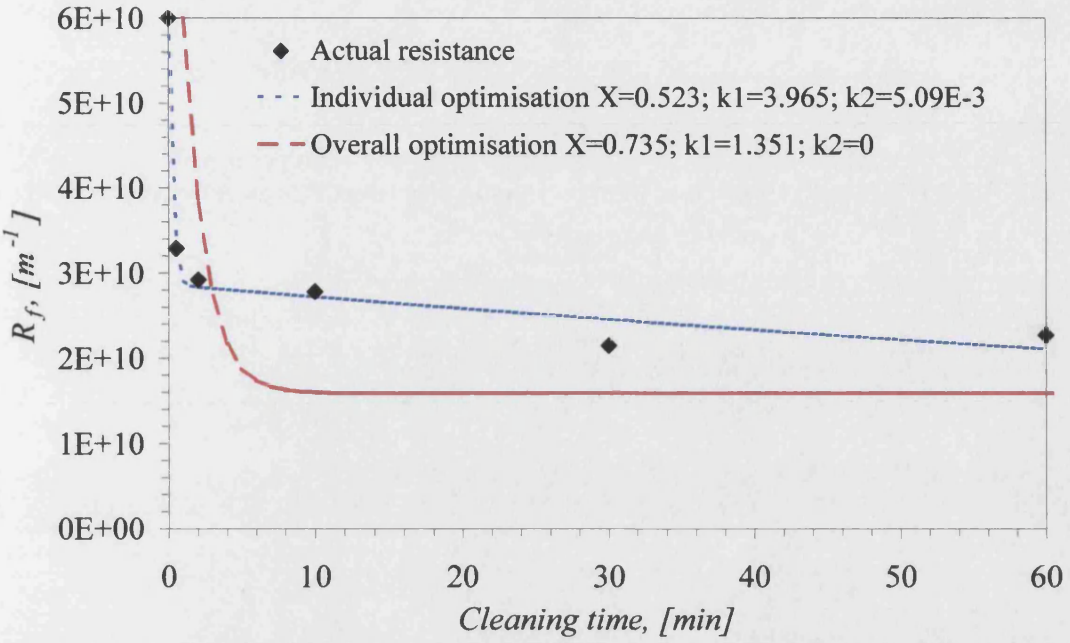

Figure 5-2: Modelling cleaning with 0.002 wt% P3 Ultrasil 11 @ 40°C as a function of time.

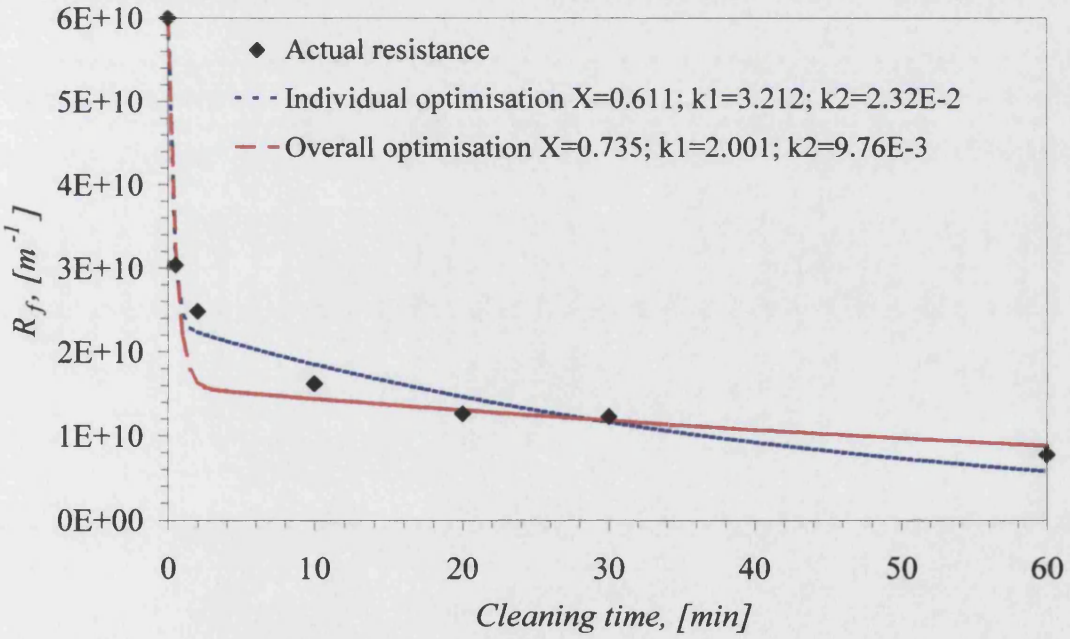

Figure 5-3: Modelling cleaning with 0.002 wt% P3 Ultrasil 11 @ 60°C as a function of time.

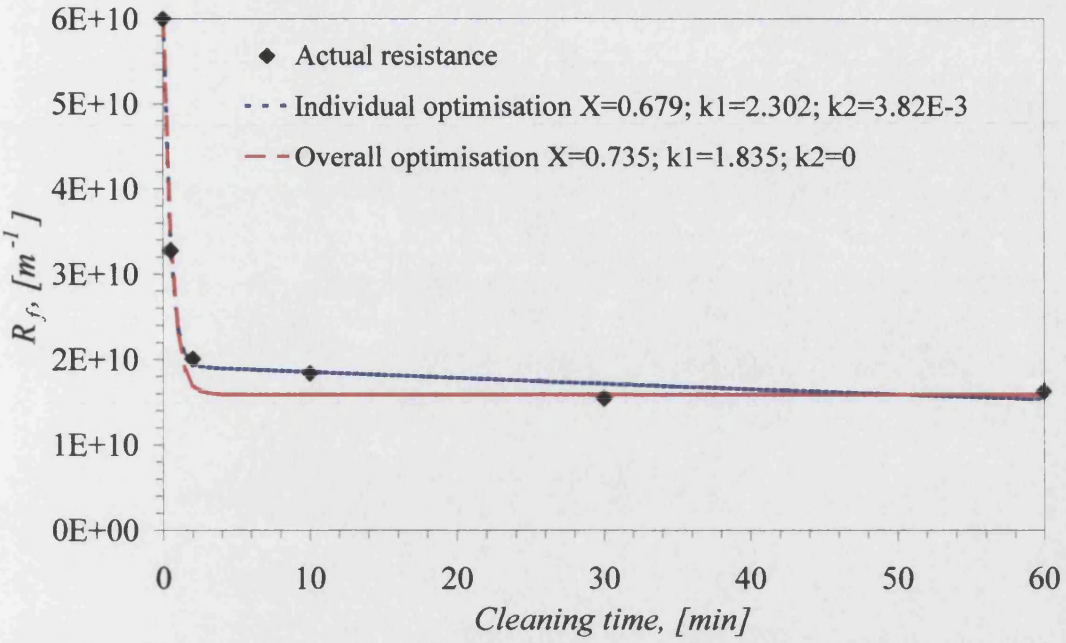

Figure 5-4: Modelling cleaning with 0.02 wt% P3 Ultrasil 11 @ 30°C as a function of time.

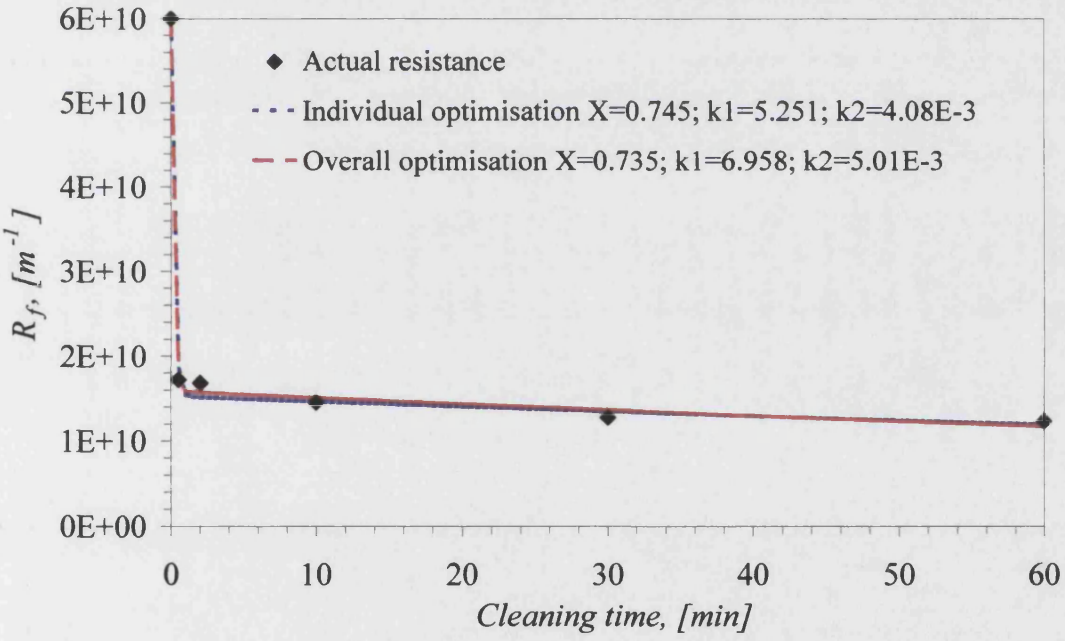

Figure 5-5: Modelling cleaning with 0.02 wt% P3 Ultrasil 11 @ 40°C as a function of time.

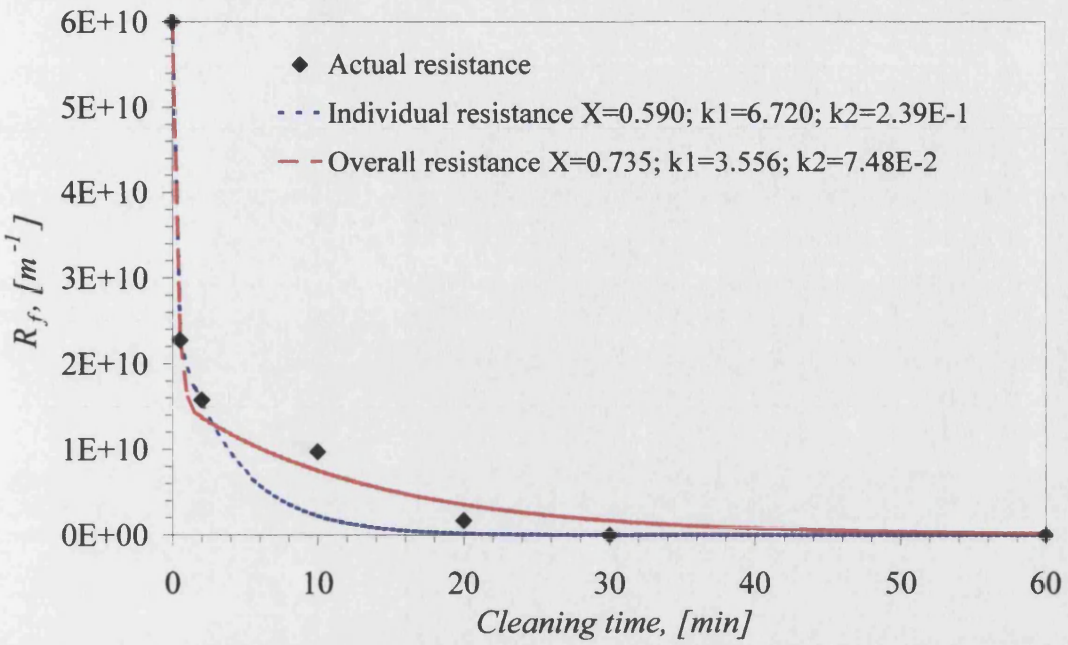

Figure 5-6: Modelling cleaning with 0.02 wt% P3 Ultrasil 11 @ 50°C as a function of time.

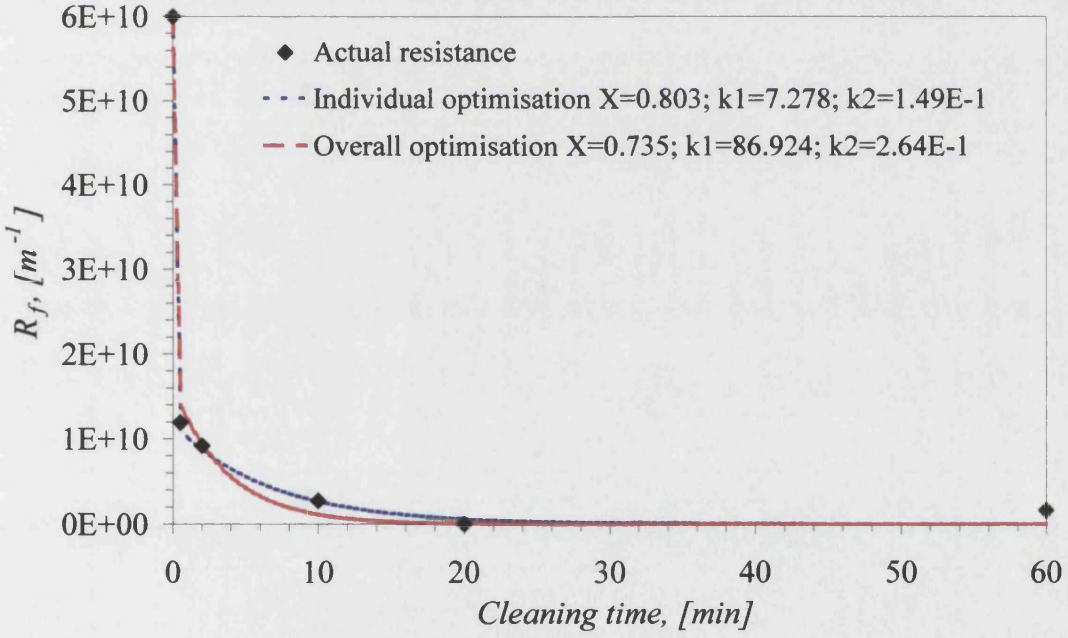

Figure 5-7: Modelling cleaning with 0.02 wt% P3 Ultrasil 11 @ 60°C as a function of time.

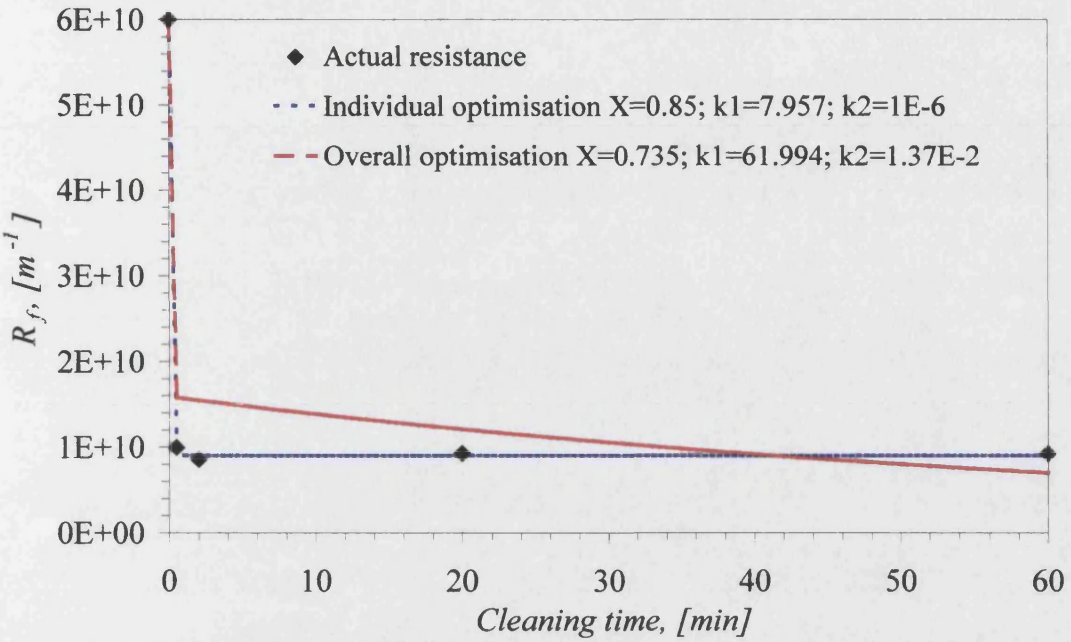

Figure 5-8: Modelling cleaning with 0.05 wt% P3 Ultrasil 11 @ 30°C as a function of time.

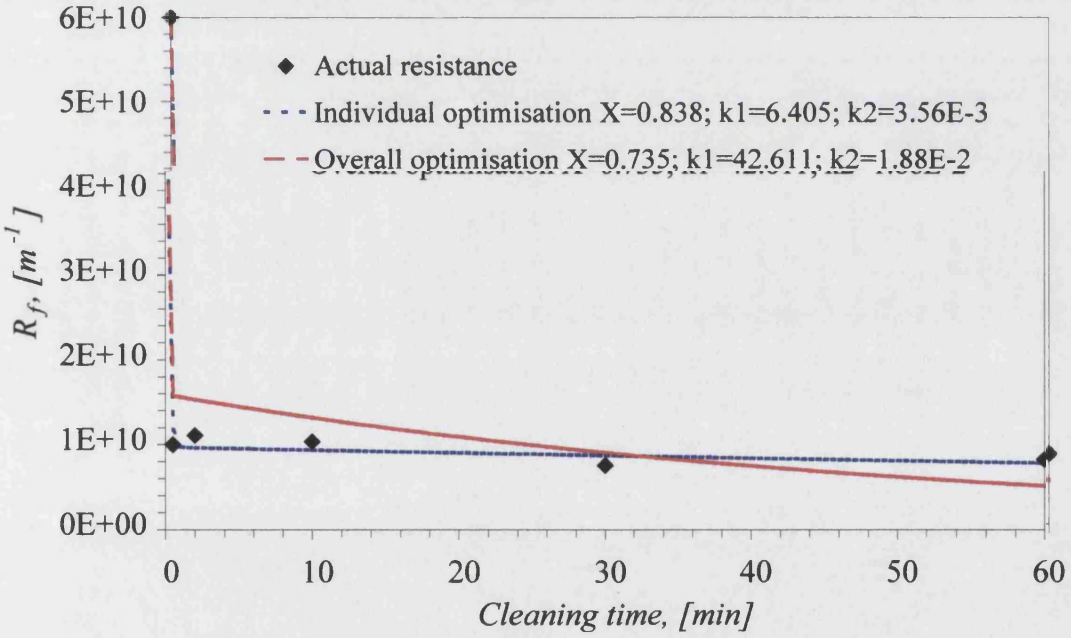

Figure 5-9: Modelling cleaning with 0.05 wt% P3 Ultrasil 11 @ 40°C as a function of time.

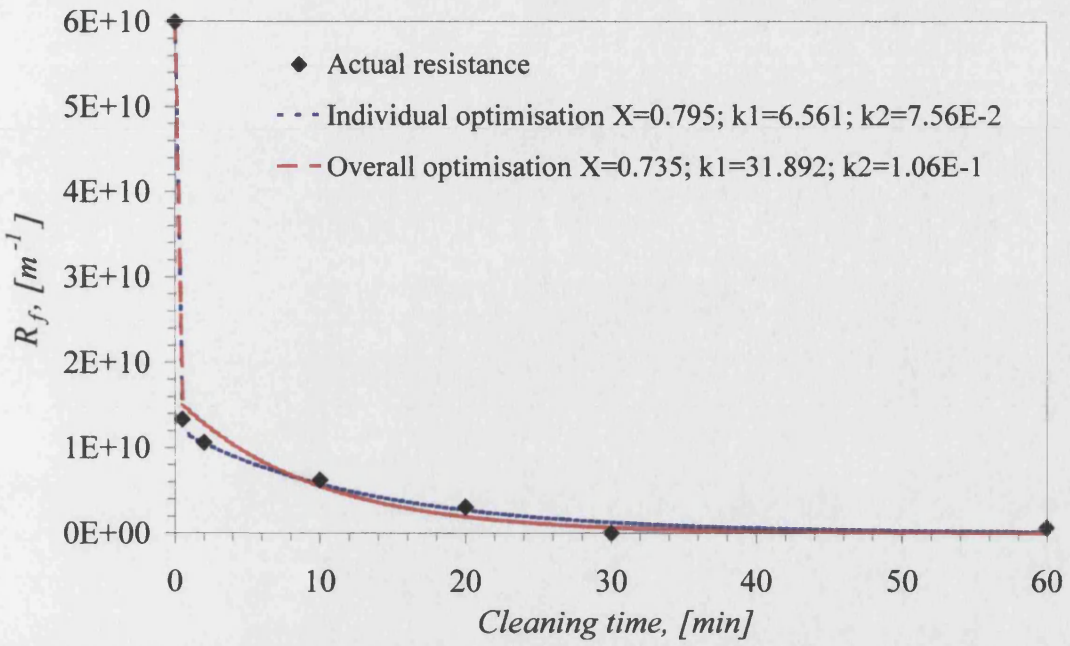

Figure 5-10: Modelling cleaning with 0.05 wt% P3 Ultrasil 11 @ 60°C as a function of time.

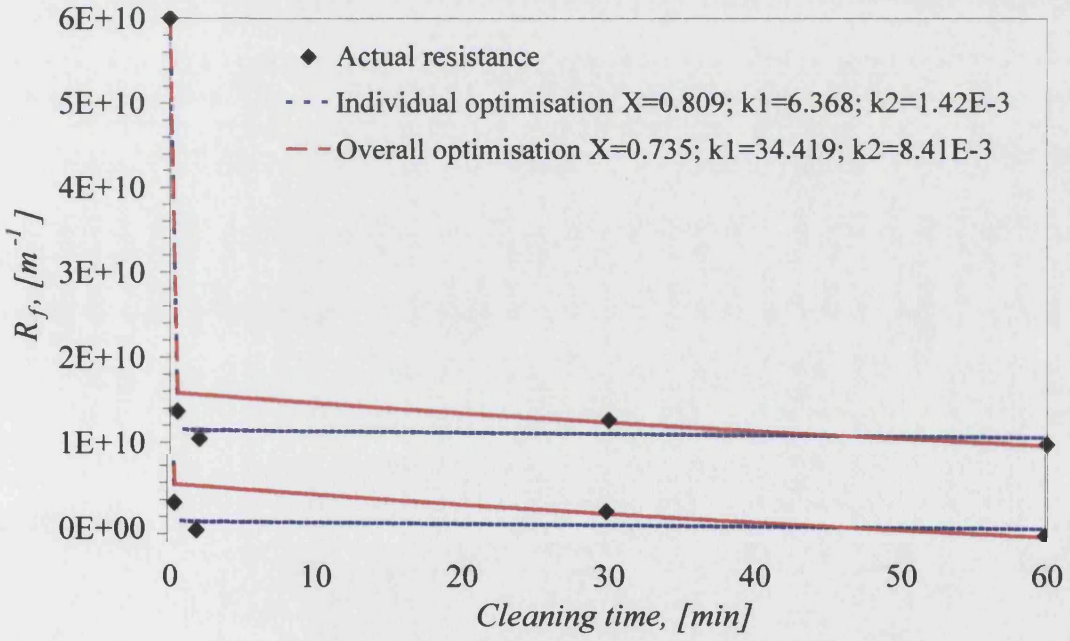

Figure 5-11: Modelling cleaning with 0.1 wt% P3 Ultrasil 11 @ 30°C as a function of time.

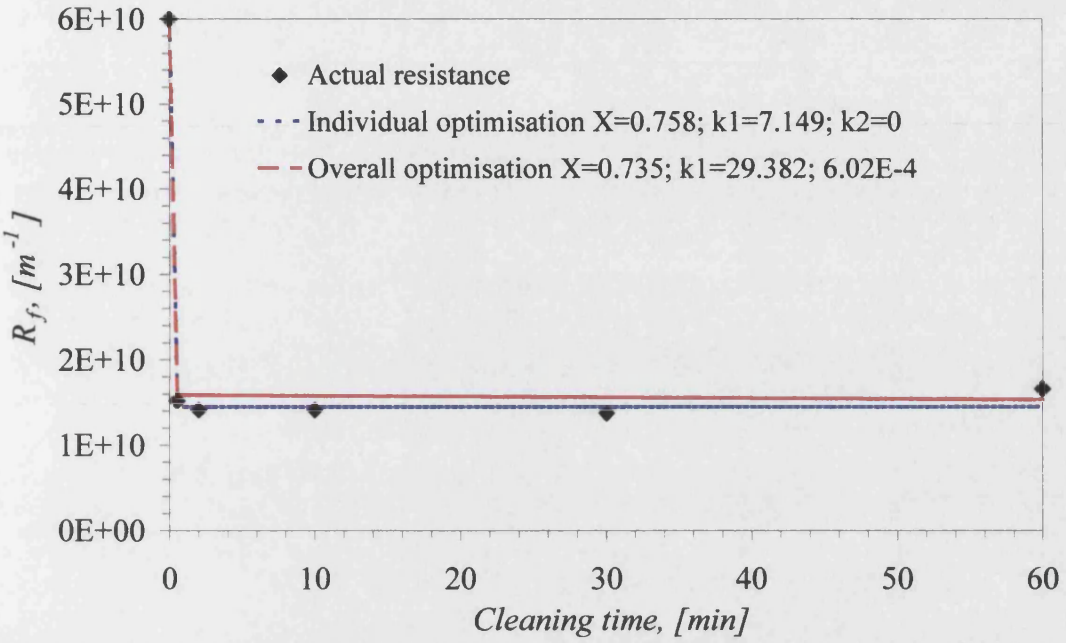

Figure 5-12: Modelling cleaning with 0.1 wt% P3 Ultrasil 11 @ 40°C as a function of time.

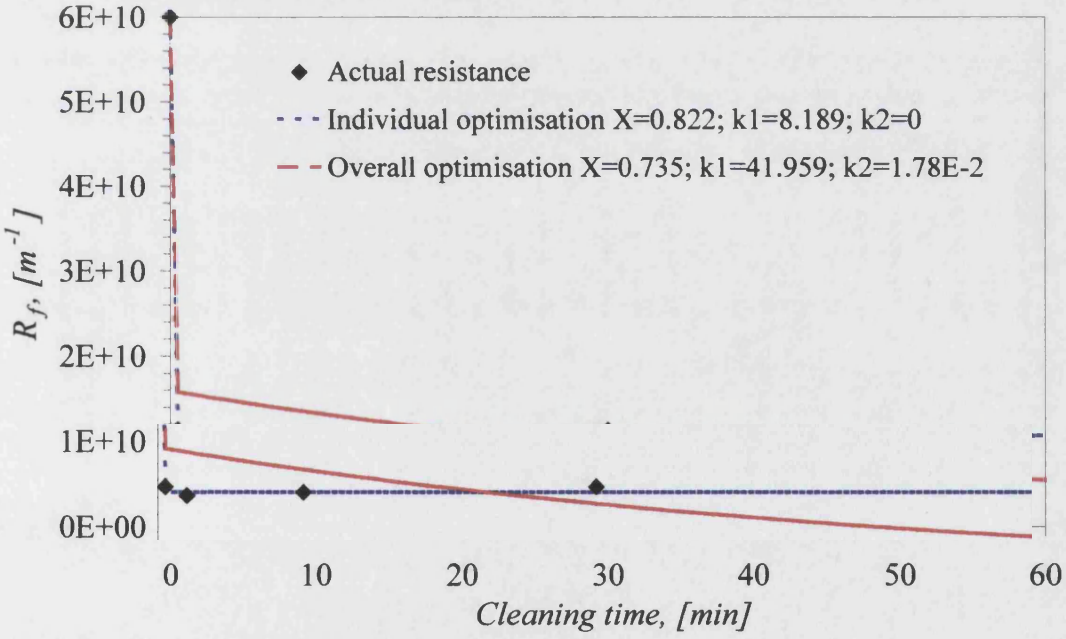

Figure 5-13: Modelling cleaning with 0.1 wt% P3 Ultrasil 11 @ 50°C as a function of time.

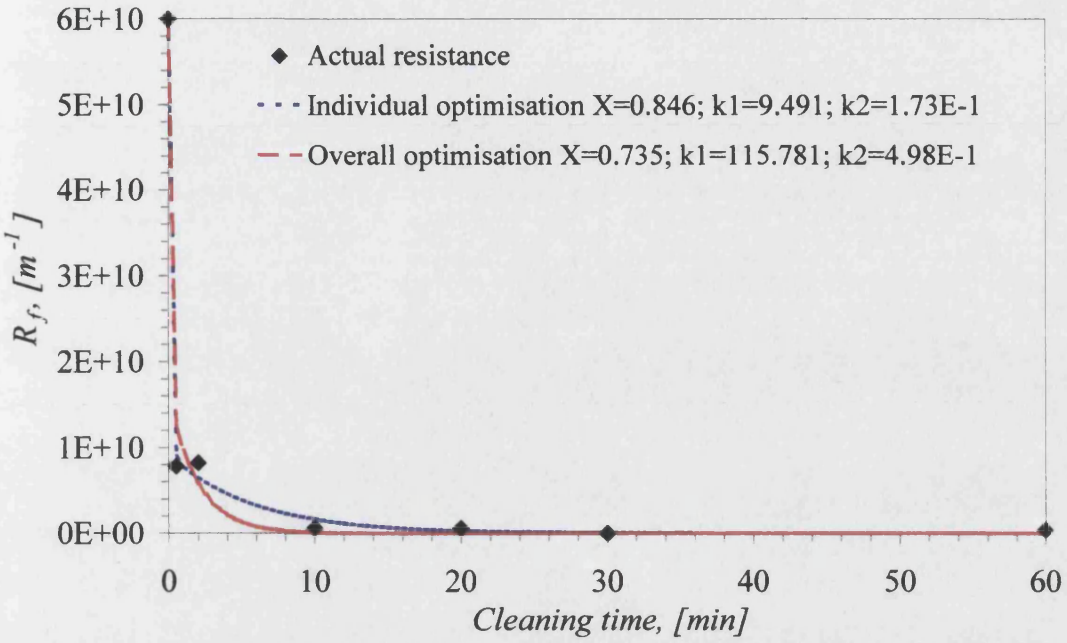

Figure 5-14: Modelling cleaning with 0.1 wt% P3 Ultrasil 11 @ 60°C as a function of time.

5.2.4.2 Removal Rate Constants k_1 and k_2

Overall optimisation yielded the following values for the removal rate constants for the organic and inorganic deposits, k_1 and k_2:

***P3 Ultrasil 11* concentration [wt%]**	**Cleaning temperature, [°C]**			
	30	**40**	**50**	**60**
0.002	0.1	1.4	-	2.0
0.02	1.8	7.0	3.4	86.9
0.05	62.0	42.6	-	31.9
0.1	34.4	29.4	42.0	115.8

Table 5-2: Theoretical values of k_1 from the two-species first order model.

***P3 Ultrasil 11* concentration [wt%]**	**Cleaning temperature, [°C]**			
	30	**40**	**50**	**60**
0.002	0	0	-	9.8E-3
0.02	0	5.0E-3	1.4E-1	2.6E-1
0.05	1.4E-2	1.9E-2	-	1.1E-1
0.1	8.4E-3	6.0E-4	1.78E-2	4.7E-1

Table 5-3: Theoretical values of k_2 from the two-species first order model.

The model rightly reflects that removal of the organic species *1* is faster than species *2*, k_1 being orders of magnitude larger than k_2. In general, k_1 and k_2 increase with cleaning temperature and concentration of *P3 Ultrasil 11*. Indicating that increasing temperature and concentration enhance cleaning. However, at 0.05 wt%, k_1 is predicted to reduce with temperature. Although the errors observed during fouling, cleaning and fitting the mathematical model were acceptable, their compounded error is displayed in the k values. Therefore, the values of k obtained from the model show only significant trends.

Arrhenius plots have been applied to the k_1 and k_2 data sets with the exception of two, which display positive gradients. The six resultant activation energies are summarised in *Table 5-4*.

5.2.4.3 Activation Energies

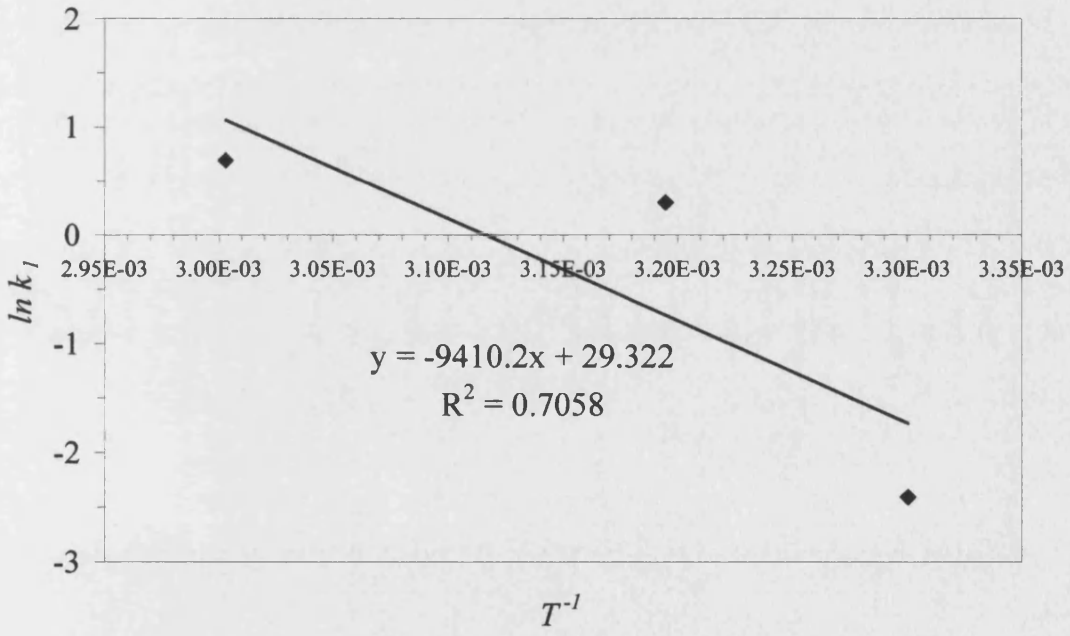

Figure 5-15: Arrhenius plot for removal of species 1 with 0.002 wt% P3 Ultrasil 11.

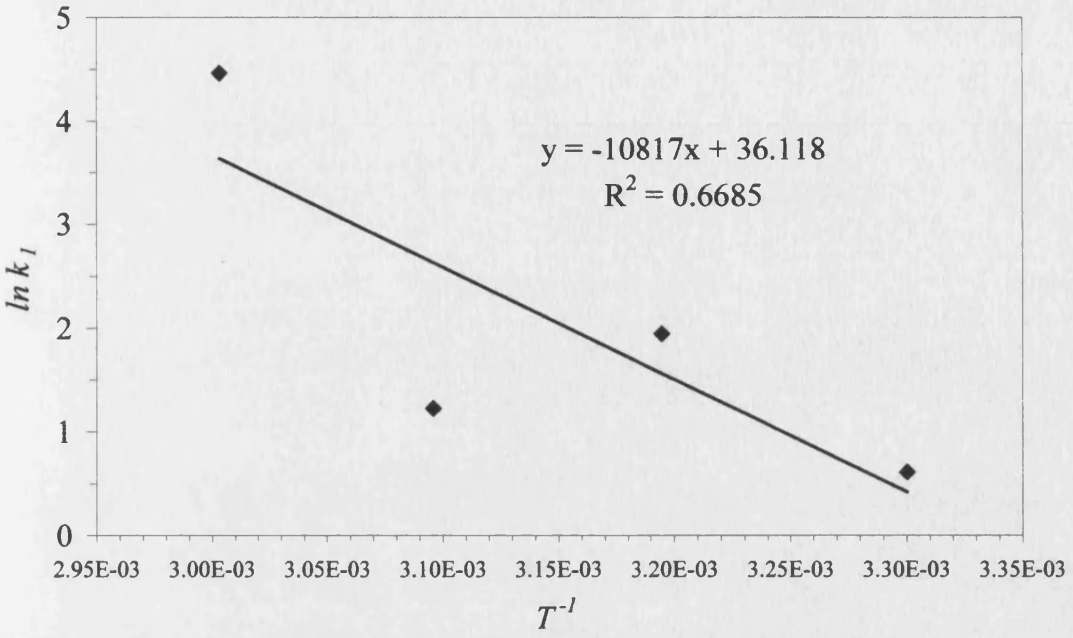

Figure 5-16: Arrhenius plot for removal of species 1 with 0.02 wt% P3 Ultrasil 11.

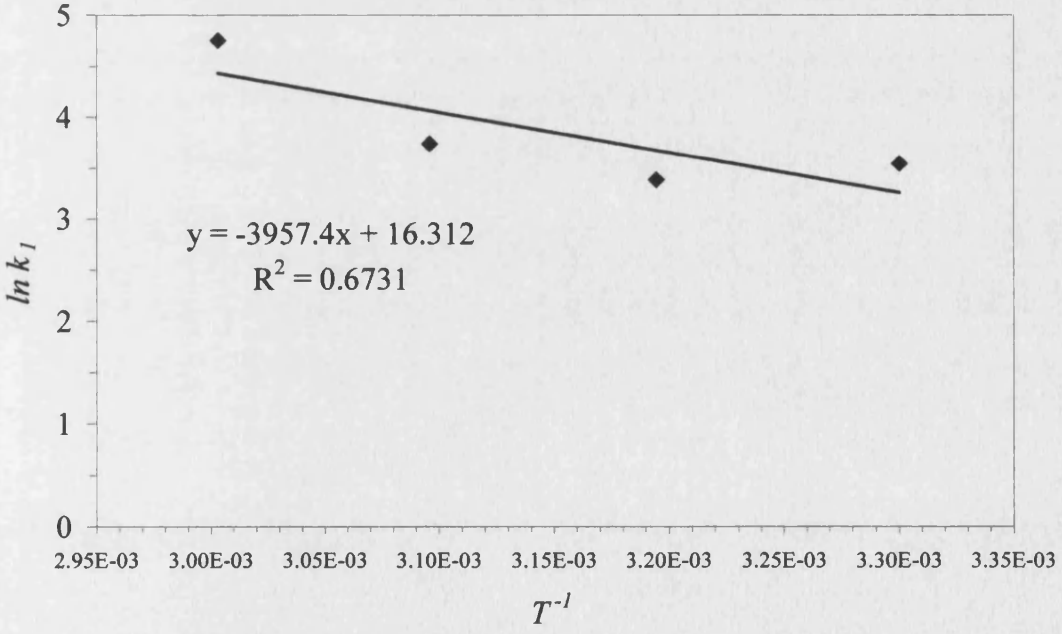

Figure 5-17: Arrhenius plot for removal of species 1 with 0.1 wt% P3 Ultrasil 11.

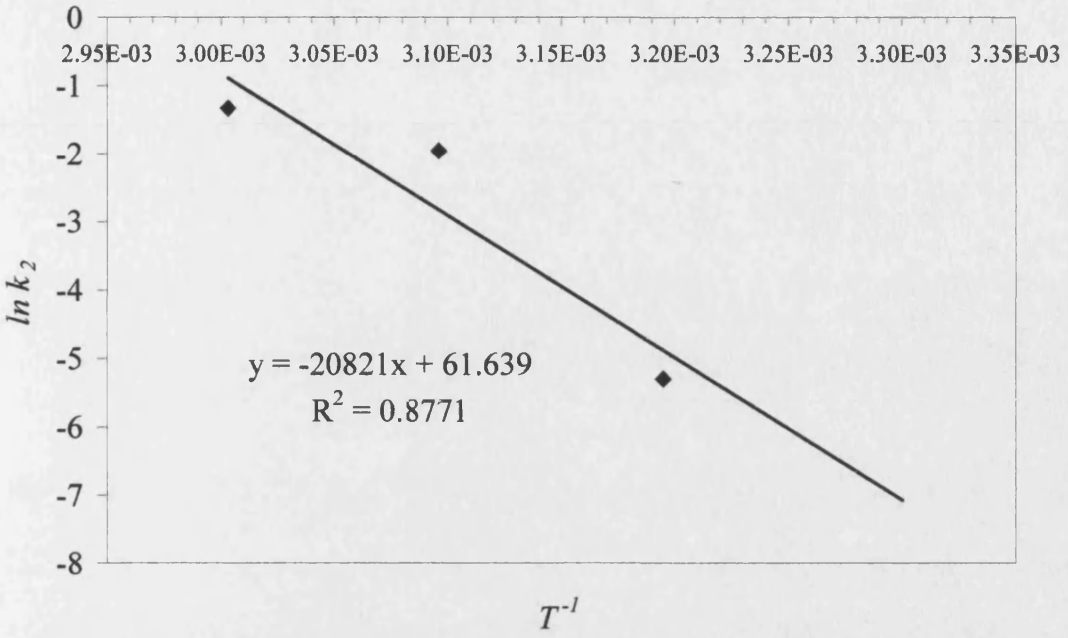

Figure 5-18: Arrhenius plot for removal of species 2 with 0.02 wt% P3 Ultrasil 11.

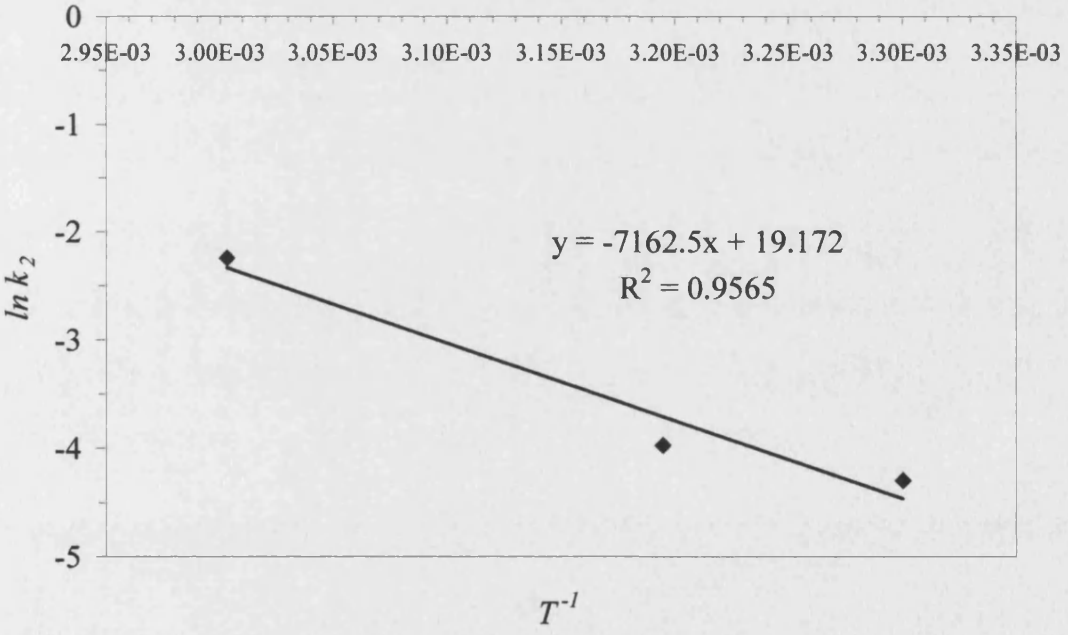

Figure 5-19: Arrhenius plot for removal of species 2 with 0.05 wt% P3 Ultrasil 11.

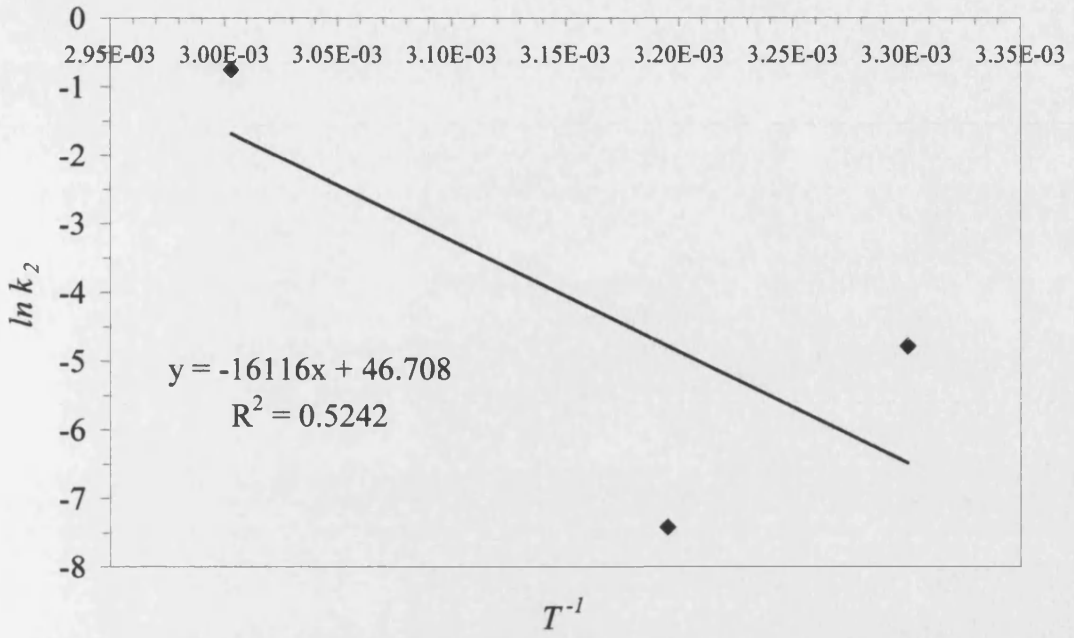

Figure 5-20: Arrhenius plot for removal of species 2 with 0.1 wt% P3 Ultrasil 11.

P3 Ultrasil 11 concentration [wt%]	E_1 [kJ mol^{-1}]	E_2 [kJ mol^{-1}]
0.002	78	-
0.02	90	173
0.05	-	60
0.1	33	134

Table 5-4: Summary of calculated activation energies for removal of species 1 and 2.

The activation energies found for this system lie in the range 33 – 173 kJ mol^{-1}. Errors do not allow trends to be hypothesised as a function of concentration. However, the activation energies found are typical of reactions found by other workers (Bird [1993], Coulson and Richardson [1979]). The activation energies calculated are relatively high, suggesting that if one mechanism dominated it was that removal was reaction controlled. This finding is in agreement with the hypothesis used to derive the mathematical model, that removal was a function of the deposit resistance (first order removal), i.e. diffusion from the bulk into the deposit was instantaneous.

CHAPTER 6 - CONCLUSIONS AND FUTURE WORK

6.1 CONCLUSIONS

6.1.1 Experimental Apparatus and Cleaning Measurement Technique

Rigorous fouling and cleaning protocols have been used in conjunction with a purpose-built experimental apparatus to successfully characterise the removal of fouling resistance as a function of time, detergent concentration, cleaning temperature and bulk flow. Flux recovery was used as a quantitative measure of cleaning efficiency while visualisation qualitatively related the observed flux recovery to the fouled state of the membrane.

6.1.2 Fouling

Mechanisms of yeast fouling in the microfiltration system studied were more complex than simple cell accumulation. Microfiltration of a bakers yeast suspension resulted in dramatic flux loss, corresponding to the accumulation of a thick cellular cake layer. Rinsing had the effect of removing the loosely bound yeast cake, revealing a tenacious non-cellular deposit, which was predominantly proteinaceous.

6.1.3 Cleaning Strategies

Hydraulic cleaning of the rinsed deposit could not restore membrane permeability. Therefore, chemical cleaning strategies were investigated.

An optimal sodium hydroxide concentration was found to exist, which minimised fouling resistance. However, sodium hydroxide alone was not sufficient to ensure complete flux recovery. Nitric acid was found to have much less cleaning effect than sodium hydroxide and was also incapable of restoring membrane permeability

However, two cleaning strategies were found to successfully restore membrane permeability following yeast harvesting. The first strategy was a two-stage cleaning protocol, which sequentially applied dilute solutions of sodium hydroxide followed by nitric acid. Order of application was crucial to complete recovery. This result was consistent with the observation that mineral deposits present a significant foulant. Nitric acid was assumed effective against the mineral deposit, which could not be removed with sodium hydroxide alone. The second strategy was a single-stage cleaning protocol, which used the commercial formulated cleaning agent *P3 Ultrasil 11*.

Cleaning of the membrane surface-based deposits had much greater effect with the permeate line closed. Up to thirty percent of the water flux was lost during cleaning with the permeate line open. However, it is acknowledged that cleaning with the permeate line closed is not suitable for all membrane module configurations, especially polymeric spiral wound, which can unwind with sufficient back-pressure.

6.1.4 Mathematical Modelling of the Cleaning Process

Observed cleaning using the formulated detergent *P3 Ultrasil 11* has been modelled successfully as two-species removal. Simultaneous first order removal rates with respect to fouling resistance gave the best fit to the data. The success of the model confirms the research of other workers, who concluded that although cleaning is a complex process, relatively simple mathematical expressions can describe observed cleaning results.

Derivation of the model was directly from the observed experimental cleaning data. Characterisation of the fouling deposit as essentially two species, organic and inorganic, was key to model selection. The relation of the model to the observed experimental data is one of its strengths, the other is its relative simplicity.

6.2 FUTURE WORK

6.2.1 Fouling

Cleaning is ultimately a consequence of fouling. In this study, a good understanding of the fouling mechanisms aided interpretation of the cleaning data. However, there is scope for future work to increase the fundamental understanding of the mechanisms of yeast fouling. As yeast is a commonly used model for micro-organisms in general this is very likely to happen. For example, the adhesion mechanisms of yeasts to specific membranes has yet to be addressed.

6.2.2 Multiple Fouling and Cleaning Cycles

In this study, membranes were replaced rather than regenerated to maximise reproducibility as the effects of multiple fouling and cleaning cycles were unknown. However, industry demands guarantees on membrane lifetime, commonly in the order of three years. Therefore, the long term effects of cleaning are important. Therefore, an understanding of the long-term effects of multiple fouling and cleaning cycles is required.

6.2.3 Development of Analytical Techniques

In situ. quantification of surface deposits would be extremely beneficial to cleaning studies. Although flux recovery is a good indication of cleaning efficiency it is not a direct measurement of surface cleanliness, which is the aim. This study would have benefited from the use of such techniques. It is hoped that future cleaning research will benefit form the on-going efforts of workers to develop direct *in situ.* measurements of surface cleanliness. Analytical techniques developed to study the kinetics of cleaning would ideally provide accurate readings in very small time increments. Also, simultaneous *in situ.* visualisation of the deposit during cleaning would identify morphological changes, which have been reported by other workers as key to the understanding of flux resulting from removal of whey proteins using sodium hydroxide.

6.2.4 Modelling Techniques

When modelling the internal membrane microstructure, workers often rely on the Carmen-Kozeny equation, which relates the physical properties of the microstructure

to spherical packing. Significant progress has recently been made on an alternative modelling approach using Voronoi tesselations. Visual comparisons between the real membrane structure and that predicted with Voronoi tesselations is a vast improvement on the spherical packing analogy. After being first applied to foams, the potential to apply Voronoi tesselations to membrane structures, amongst many other possibilities, is being realised.

CHAPTER 7 - REFERENCES

Aimar, P., Howell, J.A. and Turner, M. (1989). Effects of concentration boundary layer development on the flux limitations in ultrafiltration. *Trans. IChemE. Part A.* **67**, pp. 255-261 59

Allman, R. and Coakley, W.T. (1994). Ultrasound enhanced phase partition of microorganisms. *Bioseparation.* **4**, pp. 29-38 15

Arora, N. and Davis, R.H. (1994). Yeast cake layers as secondary membranes in dead-end microfiltration of bovine serum albumin. *J. Membrane Science.* **92**, pp. 247-256 ..... 35, 90

Bartlett, M., Bird, M.R. and Howell, J.A. (1995). Experimental study for the development of a qualitative membrane cleaning model. *J. Membrane Science.* **105**, pp. 147-151 ..... 53, 54, 94, 95, 112

Belfort, G. (1989). Fluid mechanics in membrane filtration: recent developments. *J. Membrane Science.* **40**, pp. 123-147 29

Belfort, G., Davis, R.H. and Zydney, A.L. (1994). The behaviour of suspensions and macromolecular solutions in crossflow microfiltration (review). *J. Membrane Science.* **96**, pp. 1-58 ..... 20, 24, 26, 27, 29, 35

Bell, D.J. and Davies, R.J. (1987). Cell harvesting of oleaginous yeast by cross flow filtration. *Biotechnology and Bioengineering.* **29**, pp. 1176-1178 52

Bellhouse, B.J. and Bellhouse, F.H. (1968). Mechanism of closure of the aortic valve. *Nature.* **217**, pp. 86-87 41

Bellhouse, B.J. and Millward, H.R. (1995). The role of vortices in enhancing membrane separation processes. **In:** *proceedings of Euromembrane '95*, University of Bath, UK, 18-20 Sep 1995 (W.R. Bowen, R.W. Field and J.A. Howell, eds). **1**, pp. 3-10 41

Berry, D.R.(1982). *The biology of yeast (studies in biology no. 140).* London: Edward Arnold (Publishers) Ltd 10, 11, 12

Beudeker, R.F., van Dam, H.W., van der Plaat, J.B. and Vellenga, K. (1989). Developments in baker's yeast production. **In**: *Yeast: biotechnology and biocatalysis* (H. Verachtert and R.D. Mot, eds), pp. 103-146. New York: Marcel Dekker, Inc 12

Bird, M.R. (1993). *Cleaning of food process plant.* Ph.D. thesis, University of Cambridge, UK 53, 94, 95, 111, 114, 115, 130

Bird, M.R. and Bartlett, M (1997). Modelling flux recovery during the chemical cleaning of microfiltration membranes fouled with whey protein concentrate. **In:** *Proceedings of Engineering and Food at ICEF7*, Brighton, UK, April 1997. (R. Jowitt, ed). **2**, pp. L33-36. Sheffield: Sheffield Academic Press Ltd53, 54, 112, 115, 116

Bird, M.R. and Espig, S.W.P. (1994). Cost optimisation of dairy cleaning in-place (CIP) cycles. *Trans. IChemE.* **72**(C), pp.17-20 6

Bishop, J.Y. and Sanders, N. (1989). Bubble flow meter for measurement of low permeate flows in ultrafiltration. *Biotechnol. Technol.* **3**, pp. 101-106 60

Bourne, M.C. and Jennings, W.G. (1961). Some physicochemical relationships in cleaning hard surfaces. *Food Technology.* **15**, pp. 495-499 109

Bourne, M.C. and Jennings, W.G. (1963a). Definition of the word 'detergent'. *J. American Oil Chemists' Society.* **40**, p. 212 ..... 44, 45

Bourne, M.C. and Jennings, W.G. (1963b). Kinetic studies of detergency. I. Analysis of cleaning curves. *J. American Oil Chemists' Society.* **40**, pp. 517-523 110

Bourne, M.C. and Jennings, W.G. (1963c). Kinetic studies of detergency. II. Effect of age, temperature, and cleaning time on rates of soil removal. *J. American Oil Chemists' Society.* **40**, pp. 523-531 110

Bourne, M.C. and Jennings, W.G. (1963d). Existence of two soil species in detergency investigations. *Nature.* **197**, pp. 1003-1004 110

Bowen, W.R., Kingdon, R.S. and Sabuni, H.A.M. (1989). Electrically enhanced separation processes: the basis of *in-situ* intermittent electrolytic membrane cleaning (IIEMC) and *in-situ* electrolytic membrane restoration (IEMR). *J. Membrane Science.* **40**, pp. 219-229 41

Bruggeman, T. (1998). A hot wriggle. *The Chemical Engineer.* **652**, p. 19 47

Cilliers, J.J. and Harrison, S.T.L. (1994). The application of mini-hydrocyclones in the concentration of yeast suspensions. *Chemical Engineering Journal.* **65**(1), pp. 21-26 15

Corrieu, G. (1981). State-of-the-art of cleaning surfaces. **In:** *Fundamentals and Applications of Surface Phenomena Associated with Fouling and Cleaning in Food Processing, Tylösand, Sweden April 6-9* (B. Hallström, D.B. Lund, C. Trägårdh, eds). Lund University: Sweden 109

Costerton, J.W., Geesey, G.G. and Cheng, K-J. (1978). How bacteria stick. *Scientific American.* **238**, pp. 86-95 ..... 31, 34

Coulson, J. M. and Richardson, J.F. (1979). *Chemical Engineering.* **3**. 2nd Ed. Oxford: Pergammon Press Plc. 114, 130

Coulson, J.M. and Richardson, J. F. (1991). *Chemical Engineering.* **2**. 4h Ed. Oxford: Pergammon Press Plc 13

Defrise, D. and Gekas, V. (1988). Microfiltration membranes and the problem of microbial adhesion: a literature survey. *Process Biochemistry.* **23**, pp. 105 - 116 ..... 21, 23, 31, 32

Douglas, L.J. (1987). Adhesion to surfaces. In: *The Yeasts* (A.H. Rose and J.S. Harrison, eds), 2nd Ed., **2**, pp. 239 - 280 31

Eckstein, E.C., Bailey, P.G. and Shapiro, A.H. (1977). Self-diffusion of particles in shear flow of a suspension. *J. Fluid Mech.* **79**, pp. 191-208 28

Edwards, D. and Hamson, M.J. (1996). *Mathematical modelling skills.* London: Macmillan Press Ltd 107

Elsevier Advanced Technology (1994). *Profile of the international filtration and separation industry.* 2nd ed. Oxford: Elsevier Advanced Technology 4

Elsevier Advanced Technology. (1996). *Profile of the international membrane industry: market prospects to 2000.* Oxford: Elsevier Advanced Technology.. 4, 5

Field, R.W, Hang, S. and Arnot, T. (1994). The influence of surfactant on water flux through microfiltration membranes. *J. Membrane Science.* **86**, pp. 291-304 46

Field, R.W. and Arnot, T.C. (1995). Fouling mechanisms and modelling with due allowance for cross-flow and back diffusion: testing of recent theoretical advances with data on the membrane filtration of yeast cells. **In:** *proceedings of Euromembrane '95*, University of Bath, UK, 18-20 Sep 1995 (W.R. Bowen, R.W. Field and J.A. Howell, eds). **1**, pp. 17-22 36

Field, R.W., Howell, J.A., Wu, D. and Gupta, B.B. (1995a). Helically baffled crossflow microfiltration. **102** 41

Field, R.W., Wu, D., Howell, J.A. and Gupta, B.B. (1995b). Critical flux concept for micro-filtration fouling. *J. Membrane Science*. **100**, pp. 259-272 ..... 5, 37

Finnigan, S.M. and Howell, J.A. (1989). The effect of pulsed flow on ultrafiltration fluxes in a baffled tubular membrane system. In: proceedings of *Fouling and Cleaning in Food Processing (ICFC III), 5-7 June,* (H.G. Kessler and D.B. Lund, eds), pp. 216-238. Augsburg: Druckerei Walch 41

Fleet, G.H. (1991). Cell Walls. **In**: *The Yeasts*. (A.H. Rose and Harrison, eds), 2nd Ed, **4**, pp. 199 - 277 ..... 11, 12

Gallot-Lavallée, T. and Lalande, M. (1985). A mechanistic approach of pasteurized milk deposit cleaning. **In**: *Fouling and cleaning in food processing*, University of Wisconsin-Madison. (D. Lund, E. Plett and C. Sandu, eds), pp. 374-394. Wisconsin: University of Wisconsin-Madison Extension Duplicating53, 110, 111, 112, 115

Gan, Q., Field, R.W., Bird, M.R., England, R., Howell, J.A. McKechnie, M.T. and O'Shaugnessy, C.L. (1997). Beer clarification by cross-flow microfiltration: fouling mechanisms and flux enhancement. *Trans. IChemE. Part A.* **75**(A1), pp. 3-8 35

Glimenius, R. (1985). Microfiltration - state of the art. *Desalination*. **53**, pp. 363-372 ..... 26, 35

Graßhoff, A. (1989). Environmental aspects of the use of alkaline cleaning solutions. In: proceedings of *Fouling and Cleaning in Food Processing (ICFC III), 5-7 June,* (H.G. Kessler and D.B. Lund, eds), pp. 107-115. Augsburg: Druckerei Walch 67

Green, G. and Belfort, G. (1980). Fouling of ultrafiltration membranes: lateral migration and the particle trajectory model. *Desalination*. **35**, pp. 129-147 . 28, 29

Hanisch, W. (1986). Cell harvesting. **In**: *Membrane separations in biotechnology* (W.C. McGregor, ed), pp. 61-88. New York: Marcel Dekker, Inc 10

Harbron, R.S. and Kent, C.A. (1988). Aspects of cell adhesion. **In:** *Fouling science and Technology* (L.F. Melo *et al.*, eds), pp. 125-140. London: Kluwer Academic Publishers 31

Harper, W.J. (1972). Sanitation in dairy food plants. **In**: Food sanitation, Wesport, CA (R.K. Guthrie, ed), p. 112. AVI Publishing Co. the AVI publishing Co. Inc. Westport, CA 51, 110

Hauser, G. and Sommer, K. (1990). Basic aspects on plant cleaning in the food industry. In: Additional Papers - *Engineering innovation in the food industry: it's role in quality assurance*, 9-11 Apr, Uni. Bath. 5

Hawkes, J.J. and Coakley, W.T. (1996). A continuous flow ultrasonic cell-filtering method. *Enzyme and Microbial Technology*. **19**(1), pp. 57-62 15

Hermann, R. and Müller, M. (1993). Progress in scanning electron microscopy of frozen-hydrated biological specimens. *Scanning Microscopy*. 7(1), pp. 343-35076

Hermia, J. (1982). Constant pressure blocking filtration laws - application to power law non-newtonian fluids. *Trans IChemE*. **60**, pp. 183-187 36

Herrera, T., Peterson, W.H., Cooper, E.J. and Peppler, H.J. (1956). Loss of cell constituents on reconstitution of active dry yeast. *Archives Biochem. BioPhys*. **63**, pp. 131-143 13

Ho, C.S. (1986). An understanding of the forces in the adhesion of micro-organisms to surfaces. *Process Biochemistry*. **21**(5), pp. 148-152 ..... 31, 33, 34

Hodgson, P.H., Leslie, G.L., Schneider, R.P., Fane, A.G., Fell, C.J.D. and Marshall, K.C. (1993). Cake resistance and solute rejection in bacterial microfiltration: the role of the extracellular matrix. *J. Membrane Science*. **79**, pp. 35-53 100

Howell, J.A. (1993). Design of membrane systems. In: *Membranes in bioprocessing: theory and applications* (J.A. Howell, V. Sanchez, R.W. Field, eds), pp. 141-202. Cambridge: Chapman and Hall 19

Howell, J.A. and Nyström, M. (1993). Fouling Phenomena. In: *Membranes in bioprocessing: theory and applications* (J.A. Howell, V. Sanchez, R.W. Field, eds), pp. 203-241. Cambridge: Chapman and Hall 26

Howell, J.A., Field, R.W. and Wu, D. (1993). Yeast cell microfiltration: flux enhancement in baffled and pulsatile flow systems. *J. Membrane Science*. **80**, pp. 59-71 41

Humphries, M., Jaworzyn, J.F., Cantwell, J.B. and Eakin, A. (1987). Title unknown. *FEMS Microbiol. Letters*. **42**, p. 91 46

Hurley, R., de Louvois, J. and Mulhall, A. (1987). Yeasts as human and animal pathogens. **In**: *The Yeasts* (A.H. Rose and J.S. Harrison, eds), 2nd Ed, **1**, pp. 207 - 281 31

Jennings, W.G. (1965). Theory and practice of hard-surface cleaning. *Adv. Food. Res*. **14**, pp. 325-455 ..... 39, 96, 109

Kane, D.R. and Middlemiss, N.E. (1985). Cleaning chemicals - state of the knowledge in 1985. **In**: *Fouling and cleaning in food processing*, University of Wisconsin-Madison (Plett, Lund Sandu, eds), pp. 312-335. Wisconsin: University of Wisconsin-Madison 46

Karlsson, C.C-A., Trägårdh, A.C. and Wahlgren, M.C. (1997). Fouling and cleaning of solid surfaces. In: *proceedings of Engineering and Food at ICEF 7*, Brighton, UK, April 1997 (R. Jowitt, ed). **2**, pp. J47-50 43

Kim, K.J., Sun, P. Chen, V., Wiley, D.E. and Fane, A.G. (1993). The cleaning of ultrafiltration membranes fouled by protein. *J. Membrane Science*. **80**, pp. 241-249 54

Kroner, K.H. and Nissinen, V. (1988). Dynamic filtration of microbial suspensions using an axially rotating filter. *J. Membrane Science*. **36**, pp. 85-100 40

Kuruzovich, J.N. and Piergiovanni, P.R. (1996). Yeast cell microfiltration: optimisation of backwashing for delicate membranes. *J. Membrane Science.* **112,** pp. 241-247 40

Lee, S.S., Burt, A., Russotti, G. and Buckland, B. (1995). Microfiltration of recombinant yeast cells using a rotating disk dynamic filtration system. *Biotechnology and Bioengineering.* **48,** pp. 386-400 40

Lojkine, M.H., Field, R.W. and Howell, J.A. (1992). Crossflow microfiltration of cell suspensions: a review of models with emphasis on particle size effects. *Trans. IChemE Part C.* **70,** pp. 149-164 ..... 26, 27, 29

Mackay, D. and Salusbury, T. (1988). Choosing between centrifugation and crossflow microfiltration. *The Chemical Engineer.* (477), pp. 45-50 13

Mallubhotla, H., Nunes, E. and Belfort, G. (1995). Microfiltration of yeast suspensions with self-cleaning spiral vortices: possibilities for a new module design. *Biotechnology and Bioengineering.* **48,** pp. 375-385 41

McCoy, J.W. (1984). *Industrial chemical cleaning.* New York, Chemical Publishing Co. 50

Mozes, N., Marchal, F., Hermesse, M.P., van Haecht, J.L., Reuliaux, L., Leonard, A.J. and Rouxhet, P.G. (1987). Immobilization of microorganisms by adhesion: interplay of electrostatic and nonelectrostatic interactions. *Biotechnology and Bioengineering.* **30,** pp. 439-450 34

Mulder, M (1991). *Basic principles of membrane technology.* Dordrecht: Kluwer Academic Publishers Group 16, 18, 22, 24, 37, 38, 40, 41, 62

Muñoz-Aguado, M.J., Wiley, D.E. and Fane, A.G. (1996). Enzymatic and detergent cleaning of a polysulfone ultrafiltration membrane fouled with BSA and whey. *J. Membrane Science.* **117,** pp. 175-187 54

Nagata, N., Herouvis, K.J., Dziewulski, D.M. and Belfort, G. (1989). Cross-flow membrane microfiltration of a bacterial fermentation broth. *Biotechnology and Bioengineering.* **34,** pp. 447-466 99

Nakanishi, K. (1989). Beer production with immobilized yeast cells. **In:** *Yeast: biotechnology and biocatalysis* (H. Verachtert. and R.D. Mot, eds), pp. 85-102. New York: Marcel Dekker, Inc 34

Norde, W. (1981). The behaviour of biological materials at solid/liquid surfaces: physicochemical aspects. **In:** Fundamentals and Applications of Surface Phenomena Associated with Fouling and Cleaning in Food Processing, Tylösand, Sweden April 6-9 (B. Hallström, D.B. Lund, C. Trägårdh, eds), pp. 148-167. Lund University: Sweden 33

Ottewill, R.H. (1984). Introduction. **In:** *Surfactants* (Th.F. Tadros, ed), pp. 1-18. London: Academic Press Inc 46

Plett, E. (1985). Cleaning of fouled surfaces. **In:** *Fouling and cleaning in food processing,* University of Wisconsin-Madison. (D. Lund, E. Plett and C. Sandu, eds), p. 286-311. Wisconsin: University of Wisconsin-Madison Extension Duplicating 3, 48, 109, 115

Redkar, S.G and Davis, R.H. (1995). Cross-flow microfiltration with high-frequency reverse filtration. *AIChemE Journal.* **41**(3), pp. 501-508 ..... 29, 40

Romero, C.A. and Davis, R.H. (1988). Global model of crossflow microfiltration based on hydrodynamic particle diffusion. *J. Membrane Science.* **62**, pp. 157-185 28

Romero, C.A. and Davis, R.H. (1991). Experimental verification of the shear-induced hydrodynamic diffusion model of crossflow microfiltration. *J. Membrane Science.* **92**, pp. 247-256 29

Romney, A.J.D. (1990). Principles of cleaning. **In**: *CIP: cleaning in place* (A.J.D. Romney, ed), pp. 1-6. Amersham: Halstan & Co. Ltd. 3, 42, 44, 48, 50, 51, 96, 99

Russotti, G., Osawa, A.E., Sitrin, R.D., Buckland, B.C., Adams, W.R. and Lee, S.S. (1995). Pilot-scale harvest of recombinant yeast employing microfiltration: a case study. *J. Biochemistry.* **42**, pp. 235-246 52

Sandu, C., Lund, D. and Plett, E. (1985). Fouling and cleaning of heat exchangers - a definition of terms. **In**: Fouling and cleaning in food processing, University of Wisconsin-Madison (C. Sandu, D. Lund, Plett, E. eds), pp. 3-21. Wisconsin: University of Wisconsin-Madison Extension Duplicating 42

Schekman and Novick. (1983). Unknown source. 12

Schluep, T. and Widmer, F. (1996). Initial transient effects during cross flow microfiltration of yeast suspensions. *J. Membrane Science.* **115**, pp. 133-145 ... 35

Schlüssler, H.J. (1970). Zur reinigung fester oberflächen in der lebensmittelindustrie. *Milchwissenschaft.* **25**(3), p. 133 108

Scott, K. (1995). *Handbook of industrial membranes.* 1st Ed. Oxford: Elsevier Science Publishers Ltd 5, 13, 15, 20, 38, 40, 41, 42

Sheldon, M.J., Redd, I.M. and Hawes, C.R. (1991). The fine structure of ultrafiltration membranes. II. Protein fouled membranes. *J. Membrane Science.* **62**, pp. 87-102 64

Strathman, H. (1981). Membrane separation processes (review). *J. Membrane Science.* **9**, pp. 121-189 16

Stratton, J. and Meagher, M. (1994). Effect of membrane pore size and chemistry on the cross flow filtration of Escherichia coli and Saccharomyces cerevisiae: simultaneous evaluation of different membranes using a versatile flat-sheet membrane module. *Bioseparation.* **4**, pp. 255-262 ..... 37, 52, 63

Taddei, D., Aimar, P., Howell, J.A. and Scott, J.A. (1990). Yeast cell harvesting from cider using microfiltration. *J. Chemical Technology Biotechnology.* **47**, pp. 365-376 52

Takahashi, K., Kobayashi, Y., Yokota, T. and Koyama, K. (1991). Measurement of cake thickness on membrane for microfiltration of yeast using ultrasonic polymer concave transducer. *J. Chemical Engineering Japan.* **24**(5), pp. 599-603 43

Trägårdh, G. (1989). Membrane cleaning. *Desalination.* **71**, pp. 325-335 ..... 39, 42, 45

Trettin, D.R. and Doshi, M.R. (1980). Limiting flux in ultrafiltration of macromolecular solutions. *Chem. Eng. Commun.* **4**, pp. 507-522 27

van der Horst, H.C. and Hanemaaijer, J.H. (1990). Cross-flow microfiltration in the food industry: state of the art. *Desalination.* **77**, pp. 235-258 26

Walter, H. (1977). Partition of cells in two polymer aqueous phases. A surface affinity method for cell separation. **In:** *Methods of cell separation.* (N Catsimpoolas, ed). **1**, pp. 307-354 14

Warren, R.K., Hill, G.A. and MacDonald, D.G. (1994). Continuous cell recycle fermentation to produce ethanol. *Trans. IChemE(C).* **72**, pp. 149-157..... 21

Weeks, M.G., Munro, P.A. and Spedding, P.L. (1983). New concepts for rapid yeast settling - 1. Flocculation with an inert powder. *Biotechnology and Bioengineering.* **25**(3), pp. 687-697 14

Wright, W.A. (1990). The chemistry of detergents. **In**: *CIP: cleaning in place* (A.J.D. Romney, ed), pp. 17-29. Amersham: Halstan & Co. Ltd..... 45, 46

Wu, D., Howell, J.A. and Field, R.W. (1993). Pulsatile flow filtration of yeast cell debris: influence of preincubation on performance. *Biotechnology and Bioengineering.* **41**, pp. 998-1002..... 21

Zeman, L.J. and Zydney, A.L. (1996). *Microfiltration and ultrafiltration: principles and applications.* New York: Marcel Dekker Inc.5, 13, 23, 25, 41, 45, 47, 48, 53, 59, 115

Zydney, A.L. and Colton, C.K. (1986). A concentration polarisation model for the filtration flux in crossflow microfiltration of particulate suspensions. *Chem. Eng. Communications.* **47**, pp. 1-21 28

Appendix A - Supor 100 Properties

A.I Chemical Resistance (Henkel-Ecolab Ltd sales brochure, 1997)

The following information shows the *Supor 100* resistance to a number of chemicals. A key for the data follows:

Code	Full label	Explanation
R	Resistant	No significant change was observed in flow rate or bubble point of the membrane, nor visible indications of chemical attack.
L	Limited Resistance	Moderate changes in physical properties of dimensions of the membrane were observed. The filter may be suitable for short term, non-critical use. Hardware or housing may be suitable for short-term exposure at low pressures and ambient temperatures.
N	Non Resistant	The membrane or housing is unstable, and is not recommended for use.
I	Insufficient Data	Information not available. Trial testing is recommended.

Acids

Acetic acid, glacial: **R**
Acetic acid, 90%: **R**
Acetic acid, 30%: **R**
Acetic acid, 10%: **R**
Hydrochloric acid, conc. (35%): **R**
Hydrochloric acid, 6N (20%): **R**
Hydrochloric acid, 1N (3.3%): **R**
Nitric acid, conc. (67%): **N**
Nitric acid, 6N (27%): **R**
Sulphuric acid, (95%): **N**
Sulphuric acid, 6N (16%): **N**

Alcohols

Amyl alcohol: **N**
Benzyl alcohol: **N**
Butanol: **R**
Ethanol: **R**
Isopropanol: **R**
Methanol: **R**
Propanol: **R**

Bases

Ammonium hydroxide, 3N (5.7%): **R**
Ammonium hydroxide, 6N (11.4%): **R**
Potassium hydroxide, 3N (15%): **R**
Sodium hydroxide, 3N (11%): **R**
Sodium hydroxide, 6N (22%): **I**

Esters

Amyl acetate: **R**
Butyl acetate: **R**
Cellosolve acetate: **R**
Ethyl acetate: **L**
Isopropyl acetate: **R**
Methyl acetate: **N**

Ethers

Dioxane: **I**
Ethyl ether: **R**
Isopropyl ether: **R**
Tetrahydrofuran: **N**
Tetrahydrofuran/water (50% vol.): **I**

Glycols

Ethylene glycol: **R**
Glycerol: **R**
Propylene glycol: **R**

Aromatic hydrocarbons

Benzene: **R**
Toluene: **R**
Xylene: **R**

Halogenated hydrocarbons

Carbon tetrachloride: **R**
Chloroform: **N**
Chlorothene NU: **I**
Ethylene dichloride: **N**
Dowclene WR: **I**
Freon TF: **R**
Freon TMC: **N**
Genesolv D: **R**
Methylene chloride: **N**
Perchloroethylene: **L**
Trichloroethylene: **L**

Ketones

Acetone: **N**
Cyclohexane: **N**
Methyl ethyl ketone: **N**
Methyl isobutyl ketone: **N**

Oils

Cottonseed: **R**
Lubrication MIL-L-7808: **N**
Peanut: **R**
Sesame: **R**

Photoresistance

Positive: **N**
Negative: **N**

Miscellaneous

Acetonitrile: **L**
Aniline: **N**
Dimethyl formamide: **N**
Dimethyl sulphoxide: **N**
Formaldehyde, 37%: **R**

Formaldehyde, 4%: **R**
Gasoline: **R**
Hexane, dry: **L**
Kerosene: **R**
Phenol, liquefied: **N**
Pyridine: **N**
Skydrol 500: **R**
Turpentine: **R**
Water: **R**

Appendix B - Physical and Chemical Properties

B.I Yeast Size Distribution

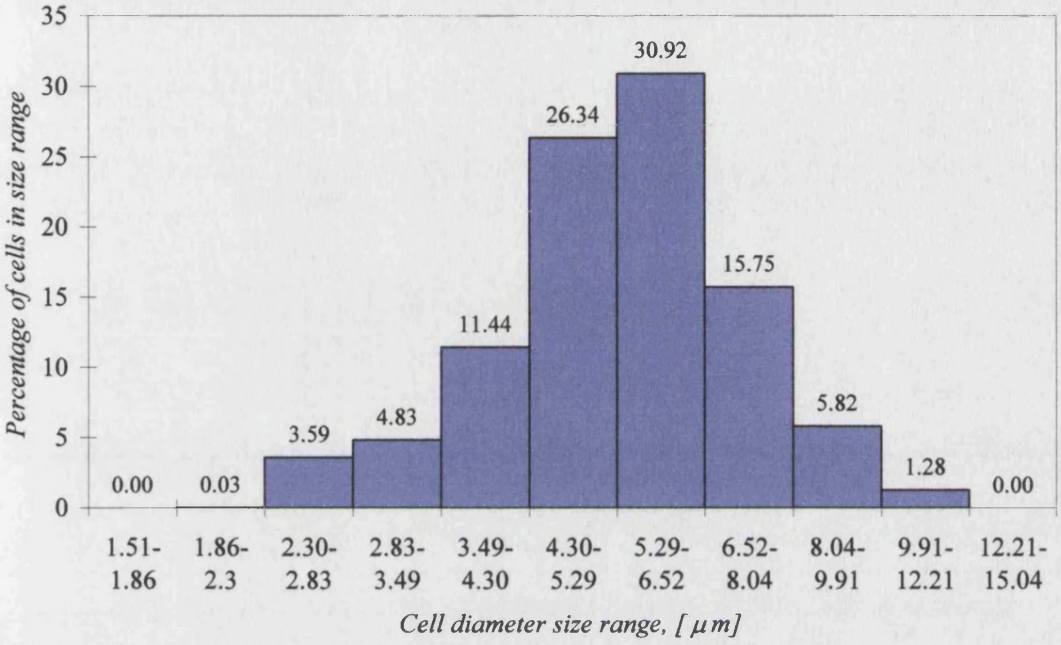

Figure B-1: Size distribution of baker's yeast determined by laser MasterSizer (Malvern Instruments Ltd.).

B.II Water Viscosity v Temperature

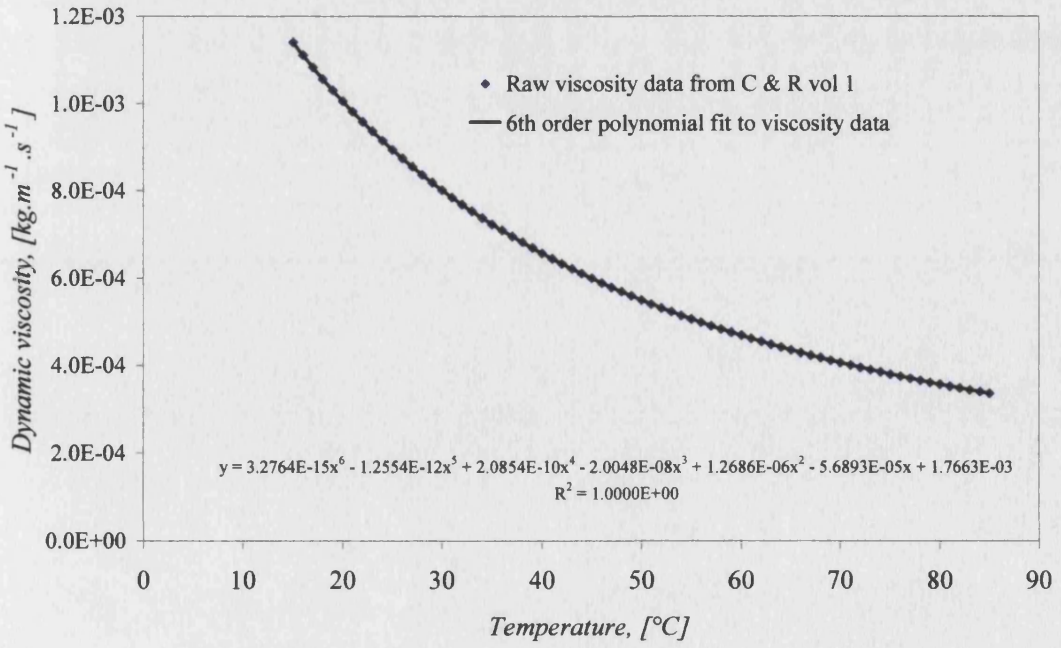

Figure B-2: Water viscosity as a function of temperature

Appendix C - Calibration Curves

C.I Permeate Flow Meter

Viscosity affects all turbine flow meters and where possible the viscosity (temperature) of the liquid should be kept constant. Before calibration, the potentiometer was adjusted until a satisfactory pulse width was attained. Using an oscilloscope, the troughs were adjusted to be roughly half the width of the peaks.

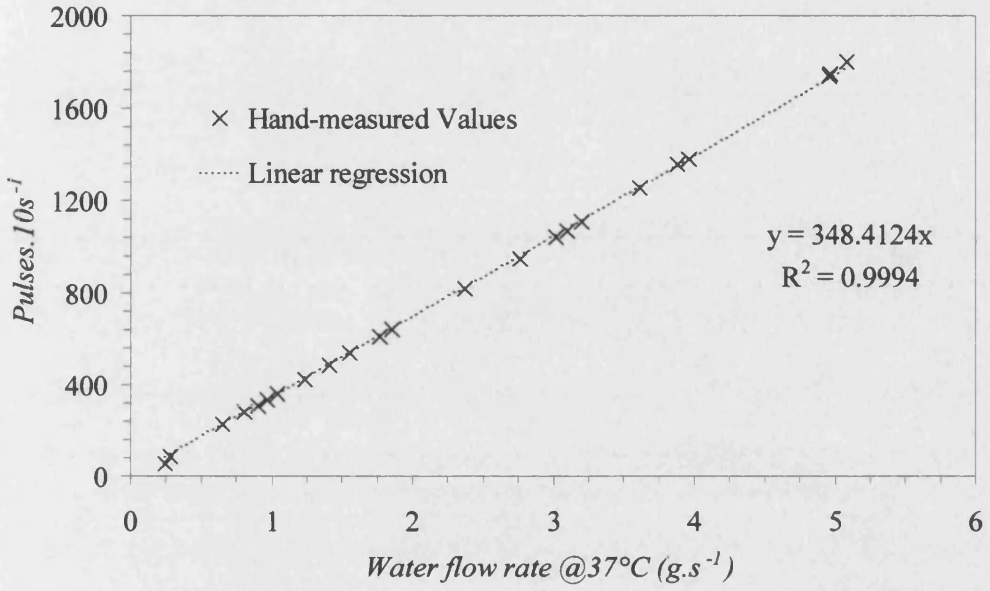

Figure C-1: Calibration of Triton flow meter

C.II Pressure transducers

Identical pressure transducers were used for inlet, retentate and permeate. However, each transducer had a unique calibration curve.

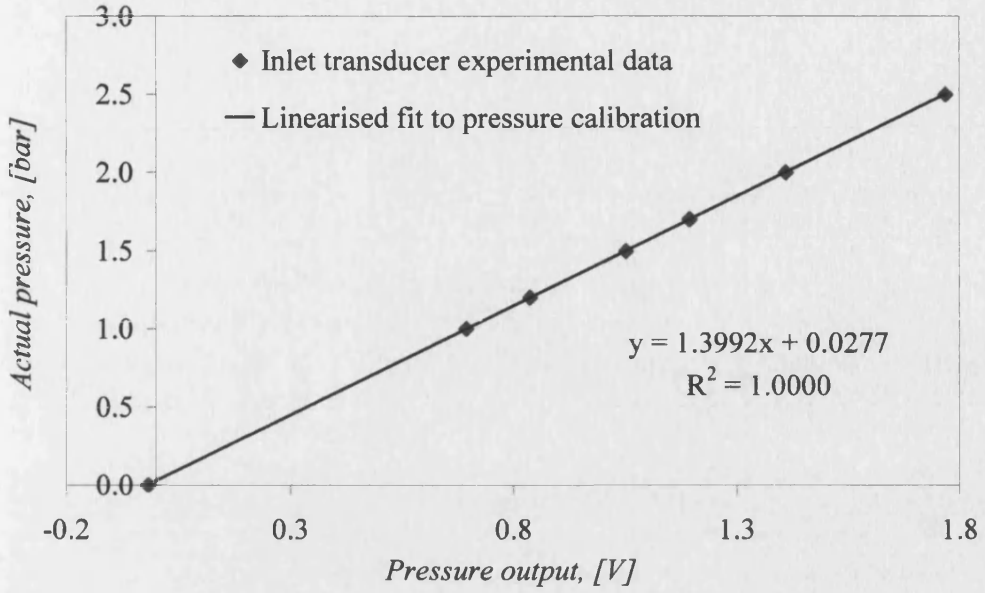

Figure C-2: Inlet pressure transducer calibration

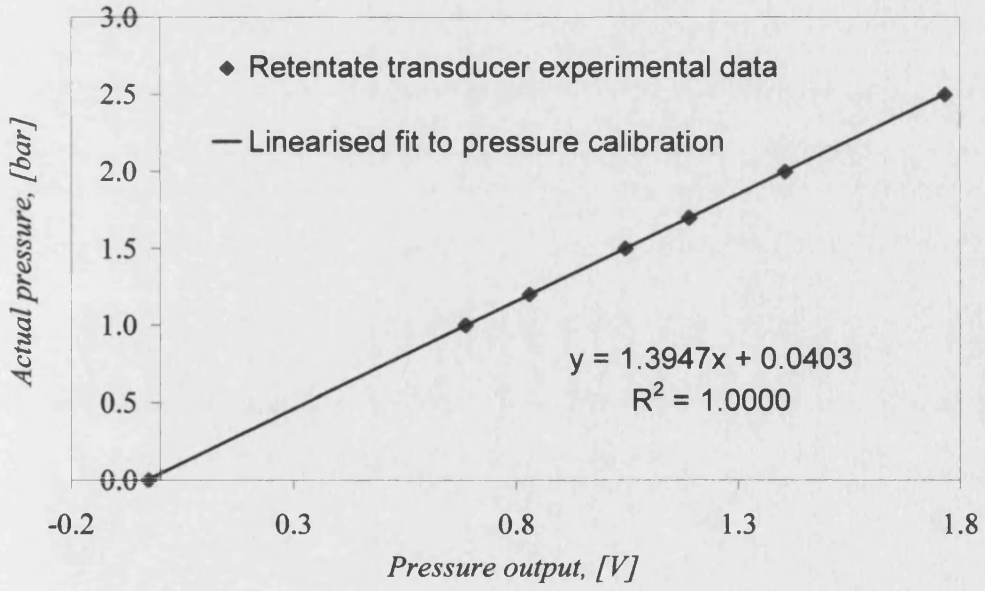

Figure C-3: Retentate pressure transducer calibration

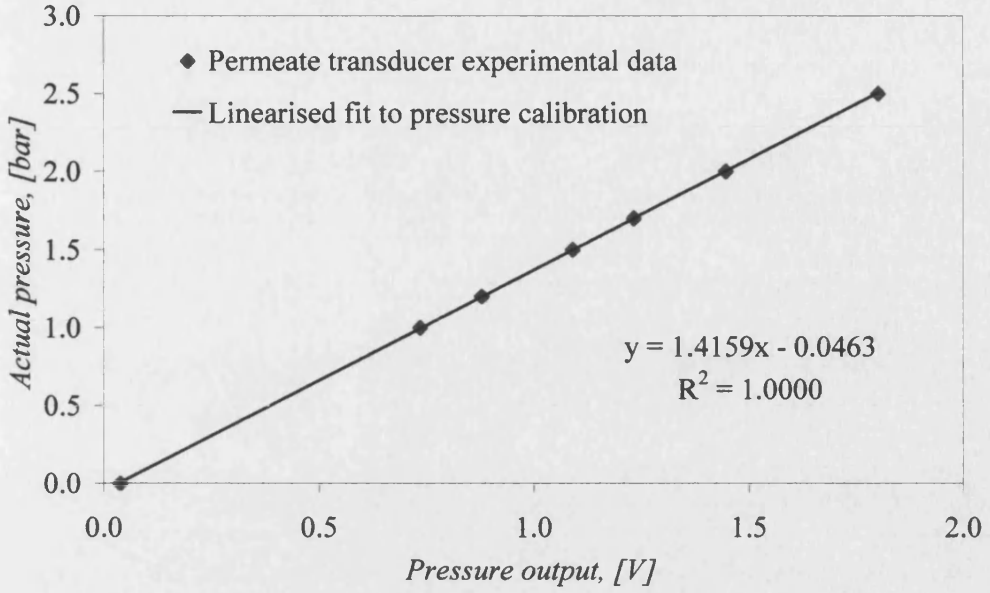

Figure C-4: Permeate pressure transducer calibration

C.III Spectrophotometer Cell Counts

A range of 350 - 700 nm was searched for evidence of maximum absorbance peek. None were found. At low wavelengths, protein interference can be strong so an arbitrary value or 540 nm was selected as this has been used by others although no scientific reason is available for this. The blank used was isotonic water only.

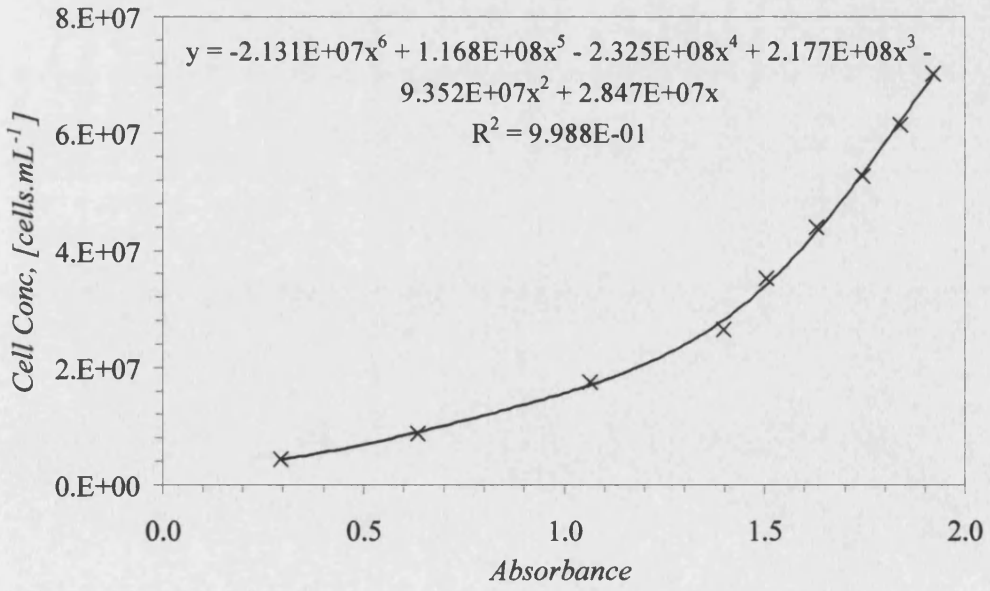

Figure C-5: Spectrophotometer cell count calibration at 540 nm wavelength

The standard deviation of the experimental results was 6.8×10^6 cells.mL^{-1}.

Appendix D - Experimental Design

D.I Experimental Procedures

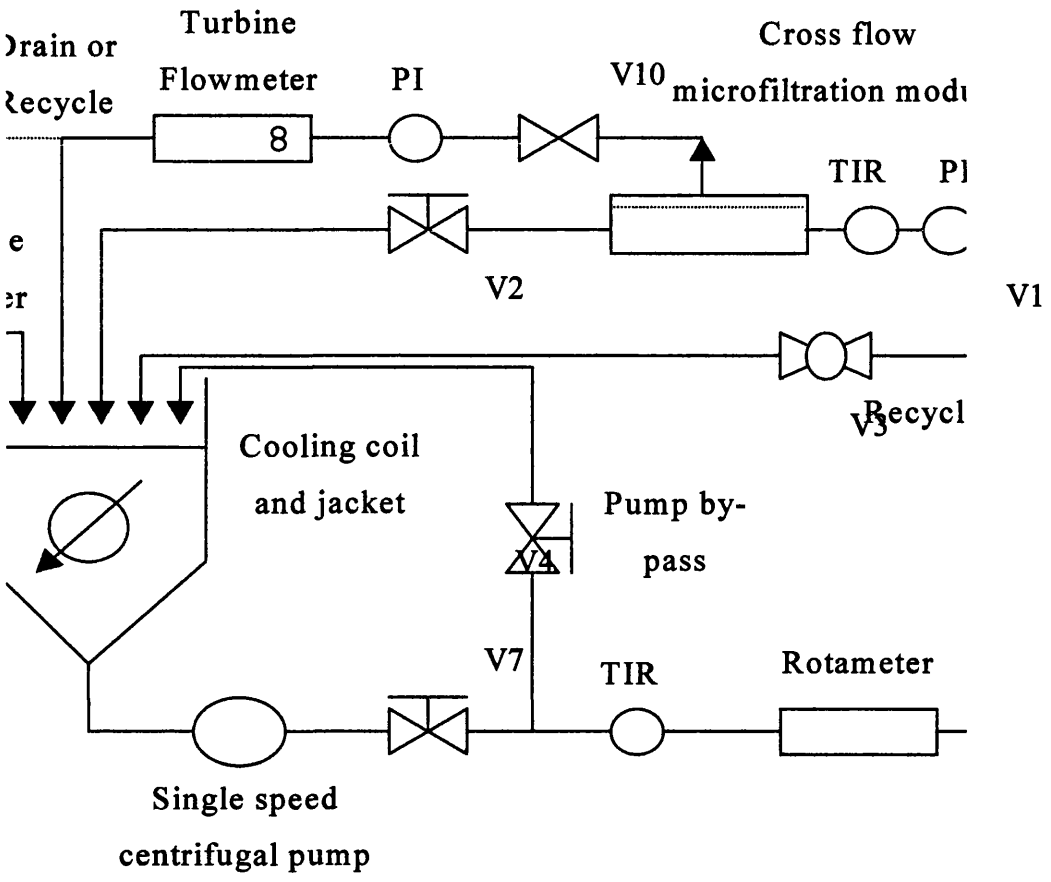

Fouling suspension

- Add 4.5 litres RO water to fouling beaker and stir.
- Add 40 g NaCl to the beaker. Place 45 g NaCl near the reservoir tank.
- Add 100 g bakers yeast to the beaker.
- Stir the yeast suspension until completely dispersed over a period of about 15 min.

Start-up check

- Put logger display to channel 1 (recycle temperature).
- Ensure that the following valves are in the correct positions. V1 closed, V2 open, V3 open, V4 open, V5 closed, V6 closed, V7 partially throttled, V8 closed, V9 closed and V10 closed.
- RO water tank should be at least 80 litres full.
- Ensure the logger is properly connected and set with sufficient battery power.
- Ensure the membrane module is secure.

Start-up

- Ensure emergency button is 'out'.
- Press green 'start' button to start pumping.
- Adjust V7 until the flow reads approximately 850 litres per hour.
- Open V1 then close V3.
- Adjust V7 until flow is 550 litres per hour.
- Allow to recycle and to approach a temperature of 35.6°C.

Initial water flux

- When temperature has reached 35.6°C open V9 until cooling water flow is 5 $L.min^{-1}$.
- Allow water to reach the equilibrium temperature of 37°C (will read either 36.8°C or 37.2°C).
- Start recording and change logger channel from 1 to 3 (flow rate).
- Open V10 for 30 seconds and close. If air is trapped in the flow meter put finger over end of permeate outlet and apply pressure rapidly.
- It is possible that flow will require regulating via V7.

Preparation for fouling

- To increase the hydrostatic pressure ready for the fouling stage partially close V4 and partially close V2 until the inlet pressure is 2.3 bar keeping the flow across the membrane at 550 litres per hour. The sequence is close V4 slightly then regulate the flow with V2 and repeat if necessary.
- Open V3 and close V1 and V9. Switch off the pump by depressing the red button and open V5 until the liquid level is approximately 5 cm above the neck of the taper in the tank and then close V5.
- Remove yeast suspension from stirrer and carefully pour into the tank ensuring the magnetic stirrer stays in the beaker. Add the remaining 4.5 g of NaCl.
- Make up the liquid level to 10 litres by adding RO water only.
- Place the used beaker in the sink with a squirt of bleach and washing up liquid filled with hot water.
- Start the pump by depressing the green button and make up the liquid level to 10 litres if necessary.
- Change logger display to channel 1.

Fouling

- When the yeast suspension reaches a temperature of 32.4°C open V9 until jacket water flow rate is 3 litres per minute and V8 until coil water flow rate is 1.0 litres per minute.
- When the temperature is at 34.0°C open V10 and quickly open V1 and close V3 together. Start the stopwatch and regulate the flow if necessary using V7.
- Leave for 90 minutes occasionally checking the temperature. Control of temperature should be with coil water only varying between 1.0 and 0.8 litres per minute depending on the ambient temperature.
- During fouling several things can be done in parallel; clean the yeast suspension beaker, fill the water tank if necessary.
- When the 90 minutes are over promptly open V3 and close V1 and V10. Open V5 and V6. Close V8 and V9. Open V4 and V2.

Rinsing preparation

- Allow the tank to drain completely. Start to pour in RO water and turn on the pump for 3 seconds. Switch off pump and stop water flow into tank.
- Remove retentate pipe and place in the drain and open V1 and allow tank to drain fully again.
- When the tank is empty start to fill the tank with water and close V5 and V6. Close V7 and then open one full turn only.
- When the tank level reaches the 9 litre mark start the pump and regulate V7 until the flow meter reads 400 litres per hour. Switch off the pump and allow air bubbles to escape.

Rinsing

- Switch the pump on and keep flow steady for 1 minute. Water should still be flowing into the tank and leaving via the drain.
- After 1 minute has elapsed open V3 and close V1 stopping the water flow to the tank when the level reaches 10 litres. Return the retentate pipe to the tank and open V7 until the flow is approximately 850 litres per hour.

Water flux

- Change the logger display to channel 1 and allow the temperature to reach 36°C.
- Open V9 until the water flow reads 5 litres per minute and allow the temperature to reach 37.2°C.

- Open V10 and simultaneously open V3 and close V1. Regulate V7 until the flow reads 550 litres per hour. Change the logger display to channel 3.
- Collect data for approximately 30 seconds - 1 minute.
- Close V10 and simultaneously open V3 and close V1 when data has been collected.

Cleaning preparation

- Prepare the chemical solution in a small beaker and when dispersed add to the tank.
- Regulate the temperature by adjusting V8 and V9 to attain the required cleaning temperature.

Cleaning

- When the required cleaning temperature has been reached open V1 and close V3.
- During the cleaning adjust V8 to control the temperature. After the required cleaning time has elapsed (usually 2 minutes) open V3 and close V1.

Rinsing preparation

- Switch off the pump and open V5 and V6.
- Allow the tank to drain completely. Start to pour in RO water and turn on the pump for 3 seconds. Switch off pump and stop water flow into tank.
- Remove retentate pipe and place in the drain and open V1 and allow tank to drain fully again.
- When the tank is empty start to fill the tank with water and close V5 and V6. Close V7 and then open one full turn only.
- When the tank level reaches the 9 litre mark start the pump and regulate V7 until the flow meter reads 400 litres per hour. Switch off the pump and allow air bubbles to escape.

Rinsing

- Switch the pump on and keep flow steady for 1 minute. Water should still be flowing into the tank and leaving via the drain.
- After 1 minute has elapsed open V3 and close V1 stopping the water flow to the tank when the level reaches 10 litres. Return the retentate pipe to the tank and open V7 until the flow is approximately 850 litres per hour.

Water flux

- Change the logger display to channel 1 and allow the temperature to reach 36°C.

- Open V9 until the water flow reads 5 litres per minute and allow the temperature to reach 37.2°C.
- Open V10 and simultaneously open V3 and close V1. Regulate V7 until the flow reads 550 litres per hour. Change the logger display to channel 3.
- Collect data until the display shows a steady output or at least for 1 minute.
- Close V10 and simultaneously open V3 and close V1 when data has been collected.

Shut down

- Open V3 and close V1. Switch off the pump and valves V8 and V9.
- Stop the logger recording.

Downloading experimental data

- Immediately after the experiment has finished double click on the data transfer icon on the computer desktop.
- Press '4' and enter a five character file name and press enter. Change logger display to 8.1 and wait for 'ready' to be displayed before pressing the space bar.
- Enter the year of experiment when prompted and press the space bar after the data file has been completed.

Appendix E - Nomenclature

E.I Latin Symbols

Symbol	Description	Units
a	Particle diameter	m
A	Membrane area available for permeation	m^{-1}
C	Concentration	$kg\ m^{-3}$
D	Diffusion coefficient	$m^2\ s^{-1}$
d_p	Particle diameter	m
f	Frictional coefficient	-
F	Perrin shape factor	-
F_t	Reaction front thickness (GLL)	m
g	Gravitational acceleration	$m\ s^{-2}$
J	Permeate flux	$m^3\ m^{-2}\ s^{-1}$
k	Boltzmann constant	$J\ mol^{-1}\ K^{-1}$
K	Length-averaged mass transfer coefficient	$m\ s^{-1}$
k_D	Deposit mass transfer coefficient (GLL)	$m\ s^{-1}$
k_r	Reaction rate constant (GLL)	s^{-1}
L	Tube or channel length	m
n	Mass of deposit reacting per unit mass of hydroxide	-
Q	Volumetric feed rate to centrifuge	$m^3\ s^{-1}$
r	Radius of rotation	m
R	Resistance to flow through membrane	m^{-1}
T	Suspension temperature	K
u_o	Terminal falling velocity of particle	$m\ s^{-1}$
v	Volume per unit area (GLL)	m
ω	Angular velocity ($rad\ s^{-1}$)	s^{-1}
X	Initial deposit mass per unit area (GLL)	$kg\ m^{-2}$
Y	Intermediate deposit mass per unit area (GLL)	$kg\ m^{-2}$
Z	Removed deposit mass per unit area	$kg\ m^{-2}$

E.II Greek Symbols

Symbol	Description	Units
α	Organic fraction of total irreversible deposit	-

$\Delta\rho$	Density difference	$kg\ m^{-3}$
Φ	Void fraction	-
η	Suspension viscosity	$kg\ m^{-1}\ s^{-1}$
γ_o	Nominal shear rate at the membrane surface	
μ	Liquid viscosity	$kg\ m^{-1}\ s^{-1}$
ρ_{pf}	Density of the permeate flow	$kg\ m^{-3}$
Σ	Capacity term for centrifuge	m^2

E.III Subscripts

Symbol	Description
0	Initial condition
1	Organic species
2	Inorganic species
b	Bulk
BO	Brownian diffusion (related to diffusivity)
f	Fouling
i	Interface
ir	Irreversible membrane fouling
m	Membrane
OH	Hydroxyl ion
r	Reversible membrane fouling

E.IV Abbreviations

Abbreviation	Description
CAGR	Compound Average Growth Rate
ADY	Active Dry Yeast
CFMF	Cross-flow Microfiltration
CIP	Cleaning in-place
COP	Cleaning out-of-place
GLL	Gallot-Lavallée and Lalande
GMP	Good Microbiological Practice
LTSEM	Low Temperature Scanning Electron Microscopy
MF	Microfiltration
NF	Nanofiltration
NYL	Nylon

PES	Polyethersulphone
PIR	Pressure Indicator and Recorder
PS	Polysulphone
PVDF	Polyvinylidenfluoride
RO	Reverse Osmosis (or hyperfiltration)
TIR	Temperature Indicator and Recorder
UF	Ultrafiltration

Appendix F - Publications

Public presentations of the work contained in this thesis are as follows:

F.I Refereed Journal Papers and Conference Proceedings

Shorrock, C.J. and Bird, M.R. (1998). Membrane cleaning: chemically enhanced removal of deposits formed during yeast cell harvesting. *Trans. IChemE Part C: Food and Bioproducts Processing.* **76**(C1), pp. 30-38.

[1]Shorrock, C.J., Bird, M.R. and Howell, J.A. (1997). 'Cleaning of microfiltration membranes fouled with yeast'. **In:** *proceedings of Engineering and Food at ICEF* 7. Brighton, UK, April 1997 (R. Jowitt, ed). **2**, pp. J29-32.

F.II Non-Refereed Conference Proceedings

[2]Shorrock, C.J., Bird, M.R. and Howell, J.A. (1998). Yeast deposit removal from a polymeric microfiltration membrane. In: proceedings of *Fouling and Cleaning in Food Processing '98.* University of Cambridge. 6-8th April 1998.

[2]Shorrock, C.J., Bird, M.R. and Howell, J.A. (1996). 'Cleaning of yeast fouled microfiltration membranes using sodium hydroxide solutions'. Presented at the *International Membrane Science and Technology Conference (IMSTEC'96),* Sydney, Australia, 12-14 Nov 1996

[2]Shorrock, C.J., Bird, M.R. and Howell, J.A. (1996). 'A protocol for determining cleaning characteristics of microfiltration membranes fouled with yeasts'. **In:** *proceedings of the 1996 IChemE Research Event.* **2**, pp. 34-36

F.III Other Presentations

[3]Shorrock, C.J., Bird, M.R. and Howell, J.A. (1995). 'Cleaning of MF membranes fouled with microbial suspensions'. Poster presentation at *Regional Courses in Membrane Processes - Module 2.* Joint European Project No. JEP 4720. Bratislava, Slovakia, July 3-14, 1995.

---

[1] Presented orally and as a poster by the candidate

[2] Presented as a poster by supervisor Dr M.R. Bird on behalf of the candidate

[3] Presented as a poster by the candidate

MEMBRANE CLEANING: CHEMICALLY ENHANCED REMOVAL OF DEPOSITS FORMED DURING YEAST CELL HARVESTING

C. J. SHORROCK (GRADUATE) and M. R. BIRD (GRADUATE)
Department of Chemical Engineering, University of Bath, Claverton Down, Bath BA2 7AY

Cleaning strategies have been evaluated for a microfiltration membrane fouled during cell harvesting. The membrane selected was a flat sheet of hydrophilic polyethersulphone with a nominal pore size of 0.1 μm. Baker's yeast was selected as a model micro-organism. During microfiltration, a constant transmembrane pressure of 2 bar, cross-flow velocity of 1 $m.s^{-1}$, and suspension temperature of 34°C produced a steady state flux within 90 minutes. A water rinse removed the majority of the cellular cake revealing tenacious non-cellular and cellular deposits. Chemically enhanced cleaning of the rinsed deposit was investigated using dilute solutions of sodium hydroxide, nitric acid and *P3 Ultrasil 11*. Cleaning temperature effects were investigated over the range 30°C to 60°C and laminar and turbulent flow regimes were compared. A combination of measured flux recovery and microscopic visualisation was used to assess cleaning performance. Effective two-stage cleaning was achieved with sequential alkali and acid treatments. Effective single-stage cleaning was achieved using the formulated detergent *P3 Ultrasil 11*.

Keywords: chemical cleaning; microfiltration; yeast; sodium hydroxide; nitric acid; P3 Ultrasil 11

INTRODUCTION

Biological materials, which are sensitive to their physical and chemical surroundings, are difficult and expensive to separate using conventional centrifugal methods[1]. Cross-flow microfiltration (CFMF) is competitive with centrifugation, offering the potential advantages of operation at ambient temperature, relatively low running and capital costs, modular construction and higher product purity[2,3]. However, the more widespread application of CFMF has been limited by fouling[4,5]. Regular cleaning (or foulant removal) is thus an integral part of membrane separations, chemical cleaning being the most extensively used method[2,6]. Current industrial methods of cleaning in-place (CIP) are generally automated but derived empirically[7]. In addition to the high costs, cleaning operations conceived in this way will be a major contributor to pollutant waste emissions. CIP has been automated but not optimised[8].

This paper describes work that increases the fundamental knowledge of chemical membrane cleaning by elucidating the mechanisms of yeast deposit removal from a polymeric flat sheet membrane. Future work will present the kinetics of removal, allowing the cleaning of such systems to be predicted.

BACKGROUND

Cross-Flow Microfiltration (CFMF)

CFMF is a pressure-driven membrane separation process analogous to sieving at the microscopic level. Yeast cells, which are between one and two orders of magnitude larger than the membrane pores, are retained while the media readily permeate through.

In order to obtain high rates of mass transfer, it is necessary to operate at high tangential velocity (or shear rate) and/or turbulence in the immediate vicinity of the membrane. This is achieved using the cross-flow geometry in which the feed flow is parallel to the membrane surface, as shown in Figure 1. Cross-flow, due to its scouring action, allows rejected cells to be transported back to the bulk flow. The alternative to cross-flow is dead-end flow, which is perpendicular to the membrane, and so is only suitable for dilute suspensions.

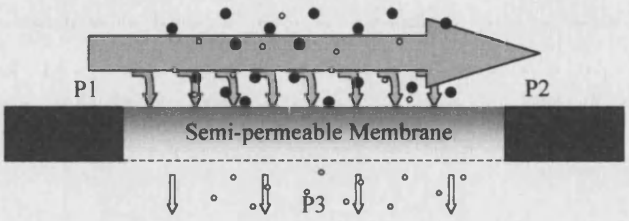

Figure 1: Schematic representation of CFMF at the microscopic level.

The volumetric flow of permeate through microfiltration membranes is directly proportional to the net applied pressure:

$$J = \frac{\Delta P_{TM} - \Delta\Pi}{\mu_p R_T}; \Delta P_{TM} = \left(\frac{P1+P2}{2}\right) - P3 \qquad (1)$$

Due to the large diameter of yeast cells relative to solutes, the osmotic pressure difference $\Delta\Pi$ is negligible[6]. The total hydrodynamic resistance to mass transfer R_T comprises the constant membrane resistance R_m and a variable fouling resistance R_f.

$$\Delta\Pi \approx 0; R_T = R_m + R_f \Rightarrow J = \frac{\Delta P_{TM}}{\mu_p (R_m + R_f)} \qquad (2)$$

Clean Water Flux

The hydrodynamic membrane resistance R_m, which reflects the physical properties of the membrane, is determined experimentally during clean water filtration. In the absence of fouling, permeate flux is measured at fixed temperature and pressure:

$$R_f = 0 \Rightarrow R_m = \frac{\Delta P_{TM}}{\mu_p J} \qquad (3)$$

Assuming that compaction is reversible and that the membrane is chemically and thermally resistant, the physical properties of the membrane (and hence R_m) are independent of operating conditions.

Membrane Fouling

Above a critical flux[9], the pressure-driven fluid flow through the membrane (or permeate flux) convectively transports cells towards the upstream surface of the membrane. Although cross-flow operation promotes back-transport of deposited cells, flux decline can still be dramatic.

Figure 4 shows an experimental plot of permeate flux versus time during CFMF of an isotonic yeast suspension. After a brief start-up period, in which a concentrated layer of cells builds up near the membrane, a non-zero steady state flux is established[5,10,11]. At the steady state flux, equilibrium exists between cells convectively transported towards the surface and those returning to the bulk stream. Proposed mechanisms of cellular back-transport include Brownian diffusion[12], inertial lift[13,14], and shear-induced diffusion[15,16]. The mechanisms are sensitive to particle diameter. Yeast filtration is best described by shear-induced diffusion, which is thought to be dominant for particles between 0.1 and 10 μm in diameter[17].

In addition to low fluxes, fouling also increases membrane selectivity. The yeast cake layer at the membrane surface effectively creates a pre-filter with greater retention capabilities than the microfiltration membrane itself[18].

It is important to recognise that fouling is a collective term for any mechanism that has a negative effect on permeate flux and/or selectivity. Fouling can be termed either reversible or irreversible. Reversible fouling is defined as being rinsable at zero transmembrane pressure such as loose cake and concentration polarisation. Irreversible fouling is defined as not being removed by rinsing such as adhesion and pore blinding. Therefore, the term irreversible is a relative one dependant upon the rinsing conditions used. Although cake formation and concentration polarisation are themselves reversible, the associated high concentrations at the membrane surface increase the probability of irreversible fouling. Microbial attachment to solid surfaces is common; the first step in the process of microbial colonisation[19]. Therefore cake formation should be avoided, as it can lead to irreversible fouling in addition to flux decline and increased selectivity.

Membrane Cleaning

Membrane cleaning can be defined as "*a process where the membrane is relieved of materials which are not an integral part of the membrane*"[20]. This definition neatly unifies the four possible cleaning strategies[2,6]; hydraulic, mechanical, electrical, and chemical cleaning. During any cleaning cycle energy can be applied to the foulant in three basic forms[7]:

Kinetic energy: in the form of solution turbulence
Thermal energy: in solution temperature
Chemical energy: chemical reactions between the foulant and the detergent components

Hydraulic cleaning includes all *in-situ* methods of foulant removal using turbulence or reversal of transmembrane pressure. Successful examples include: back flushing[21] (or back pulsing), rotating disks[22] and secondary vortex flows[23,24], though hydraulic cleaning rarely maintains maximum membrane permeability[2].

Mechanical cleaning involves scouring the fouled surface with solid abrasive material. *In-situ* mechanical cleaning is limited to tubular systems using sponge balls[6].

Electrical cleaning is achieved by applying a voltage across the membrane causing the formation of micro-bubbles at the membrane surface, which push deposited material out into the feed stream[25]. However, special module designs are required to introduce the charge to the membrane, which must be sufficiently conductive.

Chemical cleaning is usually performed as cleaning in-place (CIP) by filling the retentate channel with a cleaning solution (or detergent) form a separate tank[7]. A detergent can be defined as any substance that either alone, or in a mixture, reduces the work requirement of a cleaning process[26]. Over a period of time, the soil-substrate (foulant-membrane) bonds are weakened, or broken, and the natural scouring action generated during cross-flow completes removal. Cleaning reactions can generally be divided into six stages[8]; bulk reaction of detergents, transport of detergents to the fouled surface, transport into the fouled layer, cleaning reactions, transport of cleaning reaction products back to the interface and transport of products back to the bulk solution.

Detergent	General Properties
Acids	Dissolve inorganic salts or oxide films
Alkalis	Hydroxides generally saponificate fats and solubilise proteins
Enzymes	Compatible with sensitive membranes
Sequestrants (or chelating agents)	Prevention of re-deposition and/or removal of mineral deposits
Disinfectants	Destruction of pathogenic micro-organisms
Surfactants	Increase wettability promoting contact with the detergent and hence removal

Table 1: Common detergents and their general properties.

The choice of detergent depends upon the chemical and thermal resistance of the membrane, the nature of the foulant, and the severity of the fouling. The major detergent categories are shown in Table 1.

Table 3 shows the major foulants within the food and dairy industry and their relative ease of cleaning. However, fouling rarely occurs due to a single species. Deposits formed in the dairy and food industries often contain both organic and inorganic species necessitating the sequential use of alkali and acid[27,28].

Chemical cleaning is a complex problem, which can be an art as much as a science[27]. Cleaning is thought best at low pressure, high cross-flow velocity and at moderate temperature[2,7]. Although the basic principles have been identified, there have been relatively few quantitative studies comparing the effectiveness of different cleaning protocols for different membrane systems[27].

Reference	Filtrate	Module	Membrane	Cleaning Procedure
Russotti *et al*[29]	Recombinant yeast	Flat sheet	PVDF	Primary rinse with alternating direction of flow followed by ten secondary rinses. Cleaned with 500 ppm sodium hypochlorite solution recirculated for 20 minutes at 25°C
Bell and Davies[30]	Oleaginous yeast	Cartridge and Hollow fibre	Acrylic and PS	Rinsed with water at 40°C then cleaned with 0.5 wt% sodium hydroxide
Taddei *et al*[31]	Cider broth	Flat sheet	PVDF	First clean with 0.2% *Terg-A-Zyme* at 50°C for 60 min. Second clean with 50 ppm sodium hypochlorite 35°C for 30 min. Third clean with 0.1% nitric acid at 35°C for 30 min
Stratton and Meagher[32]	Biomass broth	Flat sheet	PVDF, NYL, PES, PS	Slow primary water rinse. Clean with 0.5% *P53 Ultrasil* for 45 min at 45°C. Final water rinse at 45°C

Table 2: Cleaning strategies for the removal of deposits formed during the cross-flow microfiltration of Saccharomyces cerevisiae suspension.

To date, chemical membrane cleaning has received much less attention than hydraulic cleaning or membrane fouling. In addition, a large proportion of cleaning research has been focussed exclusively on the dairy industry. For example, removal mechanisms of whey proteins from both hard[33] and membrane surfaces[28,34] have recently been defined. However, in rare cases, fouling studies include the cleaning protocols used for membrane regeneration. Examples are presented in Table 2.

Foulant	Solubility Characteristics	Removal
Proteins	Water insoluble	Very
	Alkali soluble	Difficult
Fats	Water insoluble	Difficult
	Alkali soluble	
Sugars	Water soluble	Easy
Mineral salts: monovalent	Water soluble	Easy
	Acid soluble	
Mineral salts: polyvalent	Water insoluble	Difficult
	Acid soluble	

Table 3: Typical components in food process fouled layers and their relative ease of cleaning[8].

With respect to flux, membrane cleaning is essentially the reduction of fouling resistance R_f. Permeate flux decreases as the fouling resistance increases.

$$R_f = \frac{\Delta P_{TM}}{\mu_p J} - R_m \qquad (4)$$

At any point in time, fouling resistance is expressed by equation (4), which can be solved at constant pressure and temperature. Membrane resistance is known and variables are maintained constant. Therefore, resistance analysis is commonly applied to cleaning studies. However, to fulfil the earlier definition of cleaning, there must be no traces of the foulant. This cannot be determined by resistance alone. Material may adhere to areas between the pores, which by definition requires cleaning, but does not affect permeability. However, techniques that are more rigorous are difficult to perform *in-situ* and are generally destructive. Non-destructive methods of *in-situ* deposit quantification are presently under development and include the use of ellipsometry[35] and ultrasound[36]. Alternatively, scanning electron microscopy is commonly used *ex-situ*. Samples taken over a range of cleaning times are analysed individually and combined to observe the mechanisms of removal as a function of time.

Economic Considerations

To maximise profitability it is desirable to avoid flux decline. This can be achieved by operating under conditions of zero fouling or by periodically returning the membrane to its original clean state using hydraulic or chemical cleaning. Hence, for the overall process to be economical, both the filtration and cleaning steps must be optimised[37].

Chemical cleaning efficiency is often a function of four primary variables: detergent concentration, temperature, cross-flow rate and contact time. Many different treatment combinations may prove practically successful, but only one will be economically optimal.

MATERIALS

Experimental Equipment

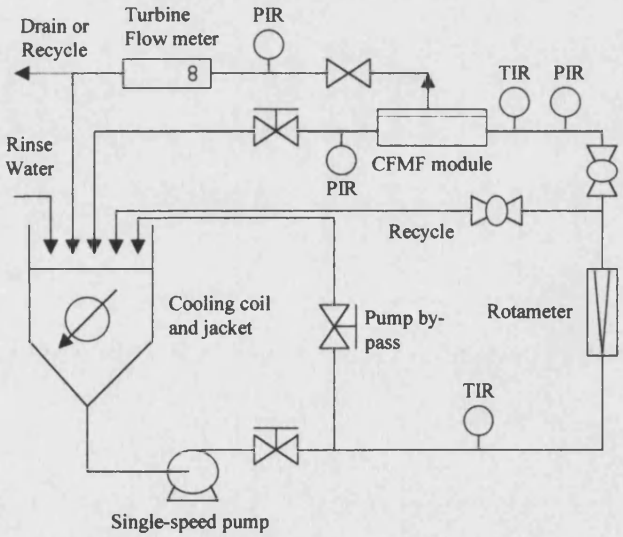

Figure 2: Schematic of experimental apparatus

A diagram of the purpose-built cleaning and fouling apparatus is shown in Figure 2. The microfiltration module accommodates a single, flat sheet membrane and allows a variety of hydrodynamic flow conditions to be fixed[38]. Replaceable Perspex inserts within the module allow channel dimensions to be altered. All experiments used a

module insert with ten channels each of 3 mm height and 5 mm width.

Recycle and process fluid temperatures were measured with two identical thermistors with a resolution of ±0.4°C. Permeate flux was measured using a turbine flow meter (Titan Enterprises Ltd., 203-231) with a flow range of ≈50-5000 $L.m^{-2}.hr^{-1}$ and linearity of ±1.5%. Inlet, retentate, and permeate pressures were measured using identical transducers (Druck, PDCR 810-0799) with a range of 0-7 bar, accurate to 2 decimal places. Permeate flux and temperature data were recorded, at five second intervals, on a data logger (Eltek Ltd., SQ32-2U/2B). Pressure data were simultaneously recorded via an interface card (Advantech Co. Ltd., PCL-711B) on a PC.

Heating requirements are achieved by recycling through a centrifugal pump (Hilge Pumps Ltd., B 22 3.0) which is throttled and thus imparts significant sensible heat to the circulating fluids. Temperature was maintained within ±0.4°C of the target during processing using manual control of the coolant flow rates. Tests have shown that pumping does not measurably alter yeast viability.

Membrane Selection

A polyethersulphone membrane with a nominal pore size of 0.1 μm (Gelman Sciences Ltd., Supor 100) was used for all experiments, and is shown in Figure 3.

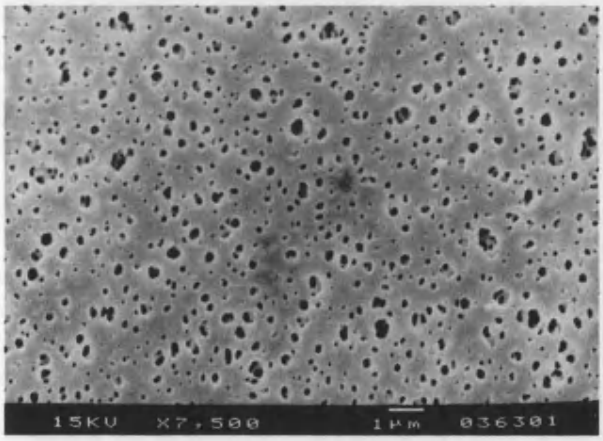

Figure 3: Clean Supor 100 membrane surface before use

The Supor 100 membrane is hydrophilic. Stratton and Meagher[32] report that hydrophilicity is more important for *Saccharomyces cerevisiae* harvesting than pore size. They found this especially true when the media contained significant quantities of protein. Sheldon *et al*[39] deduced that the hydrophobicity caused proteins to unfold at the surface of the membrane.

Chemical Cleaning Agents

Cleaning effects have been investigated for sodium hydroxide (Sigma Chemical Co., S-5881), nitric acid (Fisons Scientific Equipment, N/2300/PB17) and *P3 Ultrasil 11* (Henkel-Ecolab Ltd.). All are compatible with the Supor 100 membrane and industrially relevant.

Sodium hydroxide has the ability to saponify fats and solubilise proteins to a certain extent. However, unlike nitric acid, it is ineffective against mineral deposits.

Ingredient	Quantity (wt%)
Sodium hydroxide	43.6
EDTA	>30
Anionic surfactants	<5
Non-ionic surfactants	<5

Table 4: Chemical composition of P3 Ultrasil 11. Exact values for components other than sodium hydroxide are unknown. The balance to 100% is water.

P3 Ultrasil 11, a free flowing white powder, is a detergent specifically formulated for the removal of foulants commonly found in ultrafiltration (UF) plants in the food industry, e.g. protein, fat, blood and similar foulants. The ingredients of *P3 Ultrasil 11* are quantified in Table 4.

Surfactants are usually classified according to the charge of the head-group, anionic being positive and non-ionic neutral[40]. Surfactants are commonly found in pH neutral solutions. However, the surfactants in *P3 Ultrasil 11* are stable in an alkaline solution.

Yeast Suspension

Reconstitution of commercially available baker's yeast (British Fermentation Products Ltd., *Saccharomyces cerevisiae*) was preferred to time-consuming in-house fermentation. A 1 wt% baker's yeast suspension (≈10^8 $cells.ml^{-1}$) was used for all experiments. The yeast was suspended in a saline solution (8.5 $g.L^{-1}$ sodium chloride) and stirred thoroughly for 15 minutes. The sodium chloride (Sigma Chemical Co., S-7653) balances the osmotic pressure across the cell wall, which if omitted would result in cell rupture.

Yeast viability has been calculated using methylene blue staining agent, a haemocytometer, and a light microscope. Results show an average cell viability of 96±2%. A MasterSizer (Malvern Instruments Ltd., 0.1 μm cell) was used to measure a normal yeast size distribution of 2-12 μm with average diameter of ≈6 μm. Cell diameters were calculated using the assumption that the cells were spherical. However, budding of the cells produces an irregular shape and may account for the wide size distribution.

METHODS

Experiments were comprised of six stages; initial clean water flux, fouling, first water rinse, cleaning, second water rinse and a final clean water flux.

Clean Water Flux

The initial and final clean water fluxes were measured under recycle conditions at a temperature of 37°C, a cross-flow velocity of 1.02 $m.s^{-1}$ and a transmembrane pressure of 0.5 bar. At these conditions, the Reynolds number (Re) was 5457. The water used was prepared using reverse osmosis (RO) separation (Elga Ltd., Intercept RO-S) and

of high quality, between 17 and 22 $\mu S.cm^{-1}$. RO water was used for all solutions, suspensions and rinsing.

Fouling

Fouling cycles involved recycling the baker's yeast suspension and permeate at a constant temperature of 34°C for 90 minutes. A cross-flow velocity of 1.02 $m.s^{-1}$ and transmembrane pressure of 2 bar were kept fixed during filtration. The relatively high transmembrane pressure of 2 bar was selected to accelerate fouling kinetics and to ensure a steady state flux above the lower limit of the flow meter. During processing, the yeast suspension had a pH of 4.8 and there was no measurable loss of viability.

Rinsing

After fouling, the membrane was given a primary rinse to remove loose cake, concentration polarisation, and all traces of the yeast suspension from the system. After cleaning, a secondary rinse was required to remove debris and cleaning chemicals.

In both cases, rinsing was carried out at a temperature of 23°C and a cross-flow velocity of 0.74 $m.s^{-1}$ (Re = 2956) for 1 minute with the permeate side closed and the retentate sent to drain. The flow rate and temperature chosen ensures turbulent flow with minimum energy input. To avoid cross contamination, the permeate side, pump by-pass and recycle valves were closed.

Cleaning

Four possible methods of operation during chemical cleaning were considered:

1) Permeate side open with single pass.
2) Permeate side open with recycle.
3) Permeate side closed with single pass.
4) Permeate side closed with recycle.

Methods 1 and 2 generate flux data, allowing calculation of membrane resistance during the cleaning period. However, cleaning efficiency with the permeate side open was found lower than when closed[28]. In this study, cleaning efficiency with the permeate side open was as much as 30% less than when closed.

Method 3 was found unnecessary when compared to method 4. Under recycle conditions with the permeate side closed no measurable re-deposition of foulants was detected.

Methods 3 and 4 achieved the greatest cleaning efficiency but provide little data for collection. Single experimental runs with no permeate collected during cleaning provide just the overall flux recovery. In order to determine the fouling resistance as a function of time, it was necessary to carry out numerous experiments, taking incremental 'snap shots' of the permeability.

Method 4 is used in this study, due to its industrial relevance, despite the problem of data generation.

Foulant Visualisation

Low temperature scanning electron microscopy (LTSEM) was used (JEOL 6310) to view the hydrated, biological samples in a pseudo-natural state[41]. LTSEM ensures that possible artefacts of drying procedures such as shrinkage and collapse are avoided.

Immediately following experimentation, the membrane was removed from the module and cut to size. Sample preparation involved immersion in liquid nitrogen slush at -180°C, surface frost removal at -90°C and gold sputtering at -180°C, all under vacuum.

RESULTS AND DISCUSSION

Fouling Analysis

A typical flux decline profile measured during CFMF of the isotonic yeast suspension is shown in Figure 4. The average starting flux was 4245±309 $L.m^{-2}.h^{-1}$ and the average steady state flux was 99±54 $L.m^{-2}.h^{-1}$. When the steady state flux is viewed relative to the initial flux, the average percentage flux decline was 98±1%.

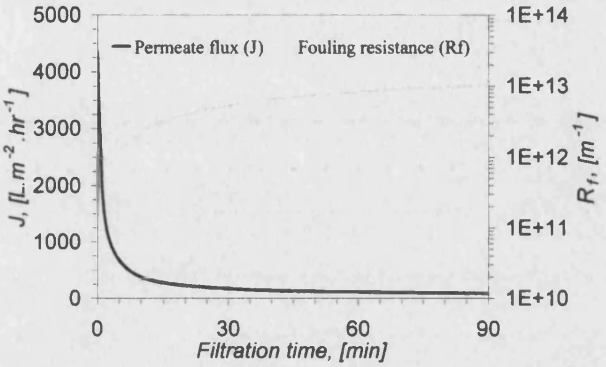

Figure 4: Experimental plot of permeate flux J and fouling resistance R_f (logarithmic scale) versus filtration time.

At steady state the average fouling resistance was $\approx 10^{13}$ m^{-1}; three orders of magnitude greater than the average membrane resistance of $\approx 10^{10}$ m^{-1}. However, rinsing reduced the fouling resistance by two orders of magnitude to $\approx 10^{11}$ m^{-1}, defined here as the irreversible fouling resistance. LTSEM analysis of the membrane surface before and after rinsing revealed that the majority of the cellular cake had been removed. After rinsing, the surface deposit was comprised of randomly scattered cells and a non-cellular matrix, as shown in Figure 5. Impressions of the original cell sites within the non-cellular matrix were well preserved. From the known average cell diameter, the non-cellular matrix height can be estimated at ≈ 1 µm at its thickest. Cells can be seen to be turgid due to hydration, rather than flaccid and dry. This suggests that lysis is unlikely to account for the existence of the non-cellular deposit.

The irreversibly fouled layer has been analysed independently by Reading Scientific Services Ltd. using Fourier transform infrared (FT-IR) microspectroscopy. The apparatus used was a Perkin-Elmer 1725 X FT-IR spectrometer with a Spectra-Tech IR-PLAN™ research microscope attachment. The wavelength range was 4000 to 600 cm^{-1} with a resolution of 8 cm^{-1}. Samples were flattened between two diamonds in an anvil before

analysis. Absorbance peeks were reported at wavelengths of 3781, 3313, 2930, 1652, 1536, 1455, 1395, 1238, 1074, and 702 cm^{-1}. Significant peeks exist at 1652 and 1536 cm^{-1}, which correspond well to the amide I and amide II peeks assigned to proteins. The majority of the other wavelengths were assigned to the hydrocarbon chain. In conclusion, spectra of the deposited material suggest it is predominantly proteinaceous.

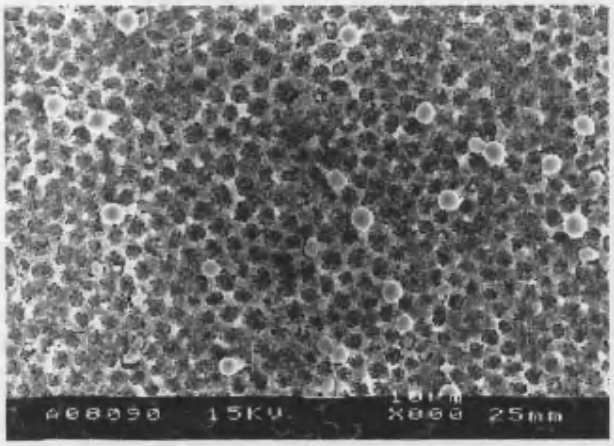

Figure 5: Supor 100 surface prior to cleaning.

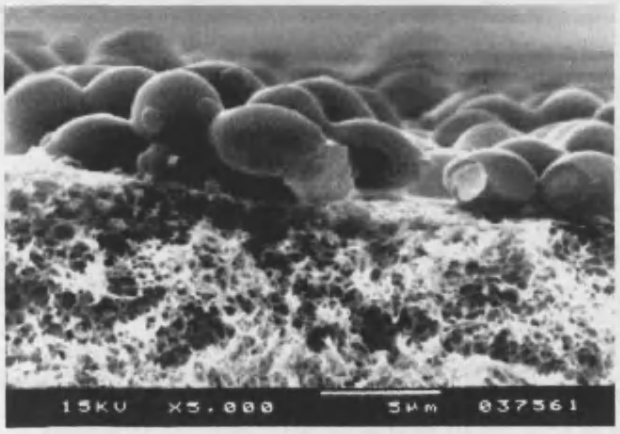

Figure 6: Cross section of fouled membrane.

Figure 6 indicates that cellular material is not visible inside the membrane structure. In addition, non-cellular material has yet to be identified within the membrane structure.

Analysis of the foulant clearly defined the cleaning requirement allowing preliminary selection of appropriate detergents and strategies.

Hydraulic and Mechanical Cleaning

The water temperature used for rinsing was relatively low, at 23°C. Therefore the cleaning efficiency of water at higher temperatures was also investigated.

Figure 7 shows the cleaning effect of water at the temperatures 30, 40, 50 and 60°C. An increase from 23°C to 30°C did not significantly reduce fouling resistance. However, at 40°C fouling resistance was progressively reduced over a 30 minute period. Fouling resistance was removed more rapidly at temperatures of 50°C and 60°C, reaching a minimum at approximately 10 minutes.

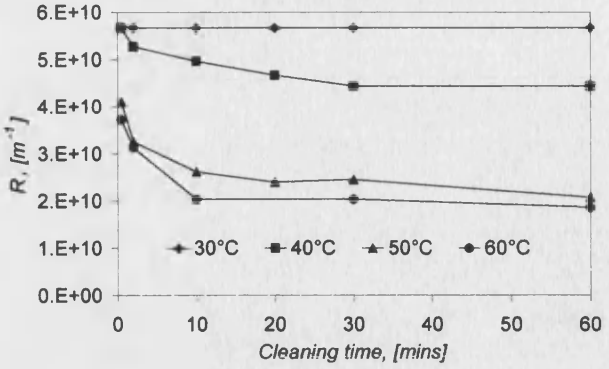

Figure 7: Cleaning effect of water between 30 and 60°C at a cross-flow velocity of 0.74 $m.s^{-1}$.

Although the Reynolds number increases from 3450 to 5834 when the temperature is increased by 30°C, it is thought more likely that thermal energy, rather than kinetic energy, was responsible for deposit removal.

Mechanical cleaning was attempted by scouring the fouled membrane surface vigorously with a sponge. This created very high shear but resulted in low permeate flux recovery equal to water cleaning at 40°C after 60 minutes.

Sodium Hydroxide Cleaning

Sodium hydroxide greatly improved foulant removal, even at low temperatures, but was unable to fully restore permeability. Figure 8 shows a typical profile of flux recovery versus sodium hydroxide concentration. An optimal sodium hydroxide concentration of 0.01 wt% produced a flux recovery of 93±3% independent of cleaning temperature (30 - 60°C) and flow regime ($1380 \leq Re \leq 8071$). When compared to values reported for other systems, an optimal concentration of 0.01 wt% seems low. For example, Bartlett *et al*[28] reported sodium hydroxide concentration optima of 0.2 wt% and 0.4 wt% for removal of whey proteins from sintered stainless steel and ceramic membranes respectively. However, the deposit generated in this study was relatively thin, possibly explaining the relatively small energy requirement for removal.

LTSEM was applied after cleaning at the optimal sodium hydroxide concentration and showed that the flux increase was primarily due to complete removal of the non-cellular matrix. A new deposit was also visible with a smaller, regular crystalline structure. X-ray microanalysis (Link Systems, AN10000) of the remaining deposit has identified the presence of inorganic material including sodium, silicon and chlorine. Chlorine was associated with the cell deposits, while sodium and silicon were associated with the new deposits. It was postulated that the presence of sodium and chlorine was directly related to the presence of salt in the filtrate. Therefore, a non-isotonic yeast suspension was filtered and the resulting deposit was cleaned with 0.01 wt% sodium hydroxide. For each of three repetitions, flux recovery was successfully restored. Thus, the required presence of salt in the yeast suspension

is thought to greatly complicate the cleaning process.

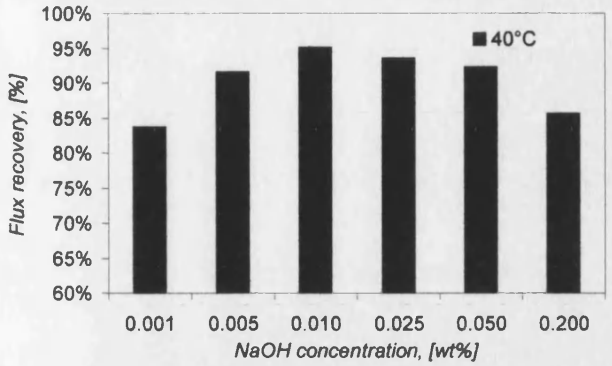

Figure 8: Percentage clean water flux recovery versus sodium hydroxide concentration at 40°C (Re ≈ 3160)

Nitric Acid Cleaning

Nitric acid cleaning was investigated due to the discovery of inorganic deposits. When 0.064 M was applied to the initial deposit at 50°C, the flux recovery obtained was just 88%, comparable to water cleaning. However, when the membrane was first cleaned with 0.01 wt% sodium hydroxide for 2 minutes at 40°C, a subsequent clean with 0.064 M nitric acid completed flux recovery, as shown in Figure 9.

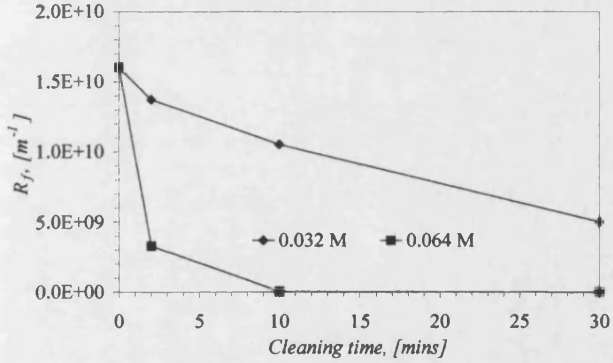

Figure 9: Two-stage cleaning. Sodium hydroxide followed by nitric acid at 50°C.

Nagata *et al*[42] reported that cleaning with 1 M sodium hydroxide for 4 hours and then 1 M nitric acid for 1 hour was effective for the removal of *Bacillus polymyxa* deposits from ceramic, stainless steel, and polypropylene membranes. For yeast deposit removal in this system, the required sodium hydroxide and nitric acid concentrations are far less, 0.002 M and 0.064 M respectively. Either *Bacillus polymyxa* pose a greater cleaning problem than *Saccharomyces cerevisiae*, which could be related to the bacterial extracellular matrix[43], or there is further scope for optimisation.

With respect to cleaning, results suggest that the yeast deposit essentially comprises two species: organic and inorganic in nature.

P3 Ultrasil 11 Cleaning

P3 Ultrasil 11 was able to completely restore membrane permeability in a single-stage clean. LTSEM also shows that all visible traces of foulant were removed.

The initial fouling resistance, after fouling and rinsing, had an average value of $6x10^{10}\pm5x10^{9}$ m^{-1}. Concentrations of *P3 Ultrasil 11* were selected to give equivalent sodium hydroxide alkalinity. Titration with hydrochloric acid and phenolphthalein indicator showed the ratio of alkaline strength between sodium hydroxide and *P3 Ultrasil 11* to be 1.96:1.

Figure 10 shows fouling resistance versus *P3 Ultrasil 11* concentration after cleaning for 1 hour. At 30°C, the investigated treatment combinations did not fully restore membrane permeability. However, at 60°C concentrations of 0.049 wt% and 0.098 wt% *P3 Ultrasil 11* achieved complete flux recovery.

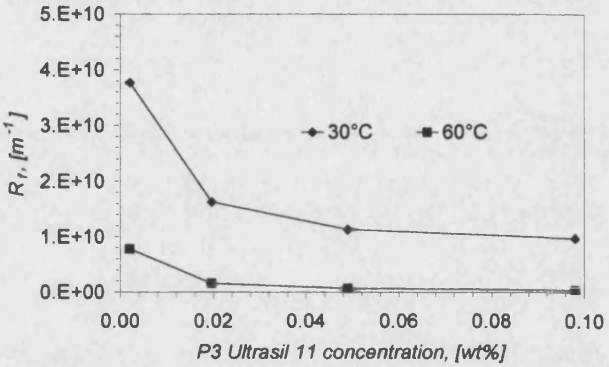

Figure 10: P3 Ultrasil 11 cleaning for 60 minutes at temperatures of 30°C and 60°C.

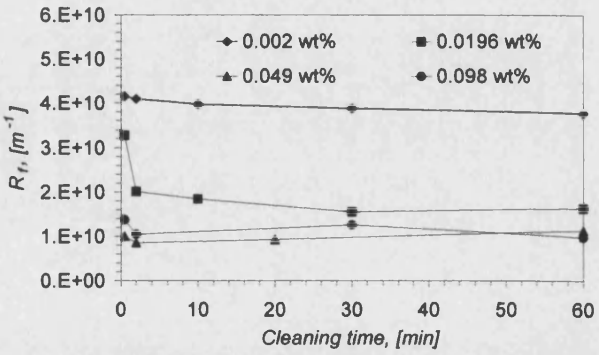

Figure 11: Cleaning with P3 Ultrasil 11 at 30°C.

Figure 11 shows that at 30°C, increased solution concentration has a positive effect upon flux recovery. However, at concentrations of 0.049 wt% and 0.098 wt% flux recovery appears to have reached a maximum. Much of the cleaning occurs within the first 2 minutes. Figure 12 shows that at the higher temperature of 60°C, *P3 Ultrasil 11* cleaning efficiency is improved. At concentrations greater than 0.002 wt%, complete recovery of membrane permeability was achieved after 10 - 20 minutes.

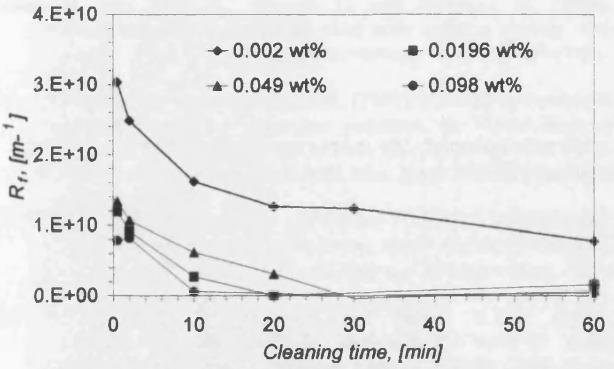

Figure 12: Cleaning with P3 Ultrasil 11 at 60°C.

Although the effects of individual ingredients can be estimated in isolation, combined effects can only be speculated. The sodium hydroxide content of *P3 Ultrasil 11* is thought to be responsible for the majority of the flux recovery. However, complete flux recovery could be equally attributable to the wetting action of the surfactants or the detergency of the EDTA, which is known to reduce the retention characteristics of certain bacterial biofilms due to modification of the extracellular matrix[27].

CONCLUSIONS

A reproducible fouling and cleaning protocol has been established for yeast microfiltration. The morphology of the irreversible fouling layer has been characterised as a complex arrangement of organic and inorganic material. Cleaning mechanisms have been identified over a wide range of detergent temperatures and concentrations. An optimal sodium hydroxide concentration of 0.01 wt% maximised flux recovery. However, sodium hydroxide alone was not sufficient to ensure complete flux recovery.

Two effective cleaning strategies are suggested for restoring membrane permeability following micro-organism fouling. The first is a two-stage cleaning protocol involving the sequential application of dilute sodium hydroxide and nitric acid. The second is the use of a dilute formulated detergent (*P3 Ultrasil 11*) in a single-stage clean. In both cases it is recommended that cleaning is most efficient with the permeate side closed.

NOMENCLATURE

J	Permeate flux, [$m^3.m^{-2}.s^{-1}$]
L	Litre, [10^{-3} m^3]
$P1$	Feed pressure, [$N.m^{-2}$]
$P2$	Retentate pressure, [$N.m^{-2}$]
$P3$	Permeate pressure, [$N.m^{-2}$]
Re	Reynolds number, [dimensionless]
R_f	Hydrodynamic fouling resistance, [m^{-1}]
R_m	Hydrodynamic membrane resistance, [m^{-1}]
R_T	Total hydrodynamic resistance, [m^{-1}]

Greek Symbols

ΔP_{TM}	Applied pressure difference across the membrane, [$N.m^{-2}$]
$\Delta\Pi$	Difference in osmotic pressure across the membrane, [$N.m^{-2}$]
μ_p	Permeate viscosity, [$kg.m^{-1}.s^{-1}$]

Abbreviations

CFMF	Cross-flow microfiltration
LTSEM	Low temperature scanning electron microscopy
PIR	Pressure indicator and recorder
TIR	Temperature indicator and recorder
CIP	Cleaning in-place
PVDF	Polyvinylidenfluoride
NYL	Nylon
PES	Polyethersulphone
PS	Polysulphone

REFERENCES

1. Coulson, J.M. and Richardson, J.F. (1991). *Chemical Engineering.* **2.** 4th Ed. Oxford: Pergammon Press Plc
2. Scott, K. (1995). *Handbook of industrial membranes.* 1st Ed. Oxford: Elsevier Advanced Technology
3. Mackay, D. and Salusbury, T. (1988). Choosing between centrifugation and cross-flow microfiltration. *The Chemical Engineer.* **477**, pp. 45 - 50
4. van der Horst, H.C. and Hanemaaijer, J.H. (1990). Cross-flow microfiltration in the food industry: state of the art. *Desalination.* **77**, pp. 235-258
5. Belfort, G., Davis, R.H. and Zydney, A.L. (1994). The behaviour of suspensions and macromolecular solutions in crossflow microfiltration. *J. Membrane Science.* **96**, pp. 1-58
6. Mulder, M. (1991). *Basic principles of membrane technology.* Dordrecht: Kluwer Academic Publishers
7. Romney, A.J.D. (1990). Principles of cleaning. In: *CIP: cleaning in place* (A.J.D. Romney, ed). 2nd Ed. Huntingdon: The Society of Dairy Technology
8. Plett, E. (1985). Cleaning of fouled surfaces. In: *Fouling and cleaning in food processing.* (D. Lund, E. Plett and C. Sandu, eds), p. 286. Wisconsin: University of Wisconsin-Madison Ext. Dup.
9. Field, R.W., Wu, D., Howell, J.A. and Gupta, B.B. (1995). Critical flux concept for micro-filtration fouling. *J. Membrane Science.* **100**, pp. 259-272
10. Lojkine, M.H., Field, R.W. and Howell, J.A. (1992). Crossflow microfiltration of cell suspensions: A review of models with emphasis on particle size effects. *Trans IChemE.* **70**(C), pp. 149-164
11. Schluep, T. and Widmer, F. (1996). Initial transient effects during cross flow microfiltration of yeast suspensions. *J. Membrane Science.* **115**. pp. 133-145
12. Biatt, W.F., Dravid, A., Michaels, A.S. and Nelson, L. (1970). Solute polarization and cake formation in membrane ultrafiltration: causes, consequences and control techniques. In: *Membrane science and technology* (J.E. Flinn, ed), pp. 47-97. New York: Plenum Press
13. Green, G. and Belfort, G. (1980). Fouling of ultrafiltration membranes: lateral migration and the particle trajectory model. *Desalination.* **35**, pp. 129-147
14. Belfort, G. (1989). Fluid mechanics in membrane filtration: recent developments. *J. Membrane Science.* **40**, pp. 123-147
15. Zydney, A.L. and Colton, C.K. (1986). A concentration polarisation model for the filtration flux in crossflow microfiltration of particulate suspensions. *Chem. Eng. Communications* **47**, pp. 1-21
16. Romero, C.A. and Davis, R.H. (1988). Global model of crossflow microfiltration based on hydrodynamic particle diffusion. *J. Membrane Science.* **39**, pp. 157-185
17. Romero, C.A. and Davis, R.H. (1991). Experimental verification of the shear-induced hydrodynamic diffusion model of crossflow microfiltration. *J. Membrane Science.* **62**, pp. 249-273
18. Arora, N. and Davis, R.H. (1994). Yeast cake layers as secondary membranes in dead-end microfiltration of bovine serum albumin. *J. Membrane Science.* **92**, pp. 247-256
19. Defrise, D. and Gekas, V. (1988). Microfiltration membranes and the problem of microbial adhesion: A literature survey. *Process Biochemistry.* **23**, pp. 105 - 116
20. Trägårdh, G. (1989). Membrane cleaning. *Desalination.* **71**, pp. 325-335
21. Redkar, S.G and Davis, R.H. (1995). Cross-flow microfiltration with high-frequency reverse filtration. *AIChemE Journal.* **41**(3), pp. 501-508